

**Intrusion Detection System for Attacks in Wi-Fi Networks: A
Discrete Event System Approach**

*Thesis submitted in partial fulfilment of the requirements
for the award of the degree of*

Doctor of Philosophy

in

Computer Science and Engineering

by

Mayank Agarwal

Under the supervision of

**Dr. Santosh Biswas
Prof. Sukumar Nandi**



**Department of Computer Science and Engineering
Indian Institute of Technology Guwahati
Guwahati - 781039, India**

NOVEMBER, 2016

Copyright © Mayank Agarwal 2016. All Rights Reserved.

Dedicated to

Parents, elder brother Nitin, cousin Anshul and friends !

Whose love, blessings, constant inspiration and love made my path
of success

People are often unreasonable, illogical, and self-centered.

Forgive them anyway.

If you are kind,
people may accuse you of selfish ulterior motives.

Be kind anyway.

If you are successful,
you will win some false friends and some true enemies.

Succeed anyway.

If you are honest and frank,
people may cheat you.

Be honest and frank anyway.

What you spend years building,
someone could destroy overnight.

Build anyway.

If you find serenity and happiness,
they may be jealous.

Be happy anyway.

The good you do today,
people will often forget tomorrow.

Do good anyway.

Give the world the best you have,
and it may never be enough.

Give the best you've got anyway.

You see, in the final analysis it is between you and God;

It was never between you and them anyway.

~ Mother Teresa

Acknowledgements

This thesis is a result of combination of efforts of so many people who have helped me directly or indirectly during my exciting journey of PhD.

First and foremost I would like to profusely thank my supervisors Dr. Santosh Biswas and Prof. Sukumar Nandi. For Dr. Santosh Biswas I would like to say that I am so fortunate to have him as my supervisor. He has given me a free hand and allowed me sufficient time to think on my own. He never forced me or chained me with deadlines, albeit he always made me aware of the clock ticking away! The biggest quality that I found in him is that he allows a student to evolve as per their potential. The amount of patience and perseverance he possess is simply amazing. It is said that “In pursuit of perfection you achieve excellence”. During my journal revisions, at times I used to get bored due to the monotonous nature of review, but he always had the energy, enthusiasm to read it another time and improve the manuscript. He is just a call away whenever I felt like discussing my research with him. Apart from technical discussion related to PhD, we had many candid discussions on various topics which I would always cherish.

For Prof. Sukumar Nandi, I can say he is reservoir of knowledge and has ample of experience. During my PhD journey, many times I used to feel that I have reached a dead end in pursuit of my goal. So many negative thoughts flashed my mind making me feel that my entire effort and energy might prove to be futile. At that time, I have poured out my anxiety and feelings to him. He has always provided me with a new direction and given a ray of hope. Suddenly from all the negative thoughts, I used to come out with a new vigor to explore the new directions suggested by him. Apart from this, he has helped me improve my technical writing. His suggestions on the editing of manuscript, the flow between paragraph, grammar etc., have been invaluable. He also provided me with various opportunities to organize workshop and conferences during my PhD. His backing and support has allowed me to grow as a person and acquire many skills that have shaped my personality. I also thank him for allowing me to be a part of the Information Security Education and Awareness (ISEA) program - an ambitious program by the government of India to promote information security education and training across India. Thanks to the ISEA project, I got the learn many things while at the same time helping me financially after my scholarship period ended.

It is an extreme delight to have Prof. Diganta Goswami, Dr. Sanasam Ranbir Singh and Dr. Partha Sarathi Mandal as the honourable members of my thesis doctoral committee. I would like to express my earnest gratitude to all of them for their invaluable time in evaluating the work progress and fruitful advices towards improving the work quality. It is a matter of great pride and honour to be a student of IIT Guwahati. I express my sincere gratitude to all persons whose persistent efforts have ensured that this place remained conducive for research and academic development. I owe my sincere thanks to Prof. Purandar Bhaduri (former Head, Deptt. of CSE), Prof. Shivashankar B. Nair (former Head, Deptt. of CSE), Prof. Diganta Goswami (Current Head, Deptt. of CSE), Prof. Gautam Barua (former Director), and Prof. Gautam Biswas (present Director), all the Deans and administrative staffs of the institute. I also express my sincere regards to all respected faculties and staffs of the department of CSE for their extended help and support. I feel privileged to have received the prestigious Tata Consultancy Services (TCS) research fellowship for pursuing my doctoral research. I would like to acknowledge the support granted to me by TCS. It ensured me that I could present my research work at both national and international platforms and meet fellow researchers as well as experts in my field. I would like to thank Mr. Rahul Pandey, the former program manager and Mr. Sachin Parkhi, the present program manager for helping us with various queries from time to time and ensuring that all things executed systematically and smoothly. I am grateful to Mr. Sunil Kumar Barua, Deputy Registrar of Academic Affairs. He has skilfully handled all our queries related to TCS in a friendly manner despite his heavy workload. Many thanks to Mr. Rijumoni Dutta from academic affairs and Mr. Sunil Sarma, Ms. Kajal Lata from finance section for handling our TCS related matters. Thank you TCS for your wonderful initiative for promoting research in India.

The office staffs at the Department of CSE were always cordial and supportive. I would like to thank Mr. Souvik, Mr. Prashanta, Mr. Monojit Bhattacharjee, Ms. Gauri and Mr. Prabhin Bharali for handling our office related matters with a smile. I would like to acknowledge the support and assistance provided to us by the scientific officers Mr. Nanu Alan Kachari, Mr. Bhuriguraj Borah and Mr. Raktajit Pathak. They have always strived very hard to ensure that we do not face any issues related to network, printer etc. At a personal level, I must say that it is pleasure to have learnt many things from them.

A special thanks must go to all security guards, janitors, housekeeping staffs, mess staff, canteen staffs, hostel caretaker, wardens, doctors, medical staff, and drivers for making our life so easy in IITG. These people form the lifeline of our stay at IIT Guwahati and are really the unsung heroes. When you stay at such extended periods in a residential campus, your friends and colleagues becomes your family. You share your happiness, sorrows, grief, festivals, moments to remember, birthdays with them! This acknowledgment would be

incomplete without mentioning their names.

Among friends, I would first like to thank my dear friend Vikas Kumar. Right from my initial days at IIT Guwahati he has always been there for me. In fact, our numerous discussions in wireless security helped me choose the same topic for my doctoral research.

No amount of thanks and appreciation would be enough to acknowledge the support and learning provided to me by Shirshendu Das and Vishal Deshpande. Shirshendu Das has been like an elder brother, mentor, friend and a teacher. Shirshendu Das has been the most versatile person I have met at IIT Guwahati. I must admit that during my initial phase I used to fear coding long lines of code. His tips and guidance helped me overcome the fear which later proved to be instrumental for me in my doctoral research. My interactions with him have helped me evolve as a better person. Whenever I have sought advice from him with regards to any matter, he has always been there to guide me. Amidst all my joys, sorrows, turmoil, hardships and frustrations Vishal Deshpande has been like a shadow throughout my PhD journey. I thank him for walking along with me in my journey. There has been so much to learn from Vishal. His ability to remain patient and calm amidst success, disappointments without getting flustered is noteworthy. Thank you Vishal for your unwavering support and friendship. The company of Mahesh Patel made the journey more rich and entertaining. Very few people can offer help as whole heartedly as Mahesh does. I would always value the lovely moments Mahesh, Vishal and I shared on the mess table. Thank You Mahesh.

I am thankful to Shashi Shekar Jha for the numerous discussion on the various topics (both technical and non-technical) we had together. His insights and ideas about things are quite worthy. For Nilkanta, let me thank him for generating interest in watching other sports too :). The outings with Nilkanta, Shashi and Shirshendu Das will remain etched into my memory for life! Thank you Shilpa for being such a good friend in my PhD journey. The library sittings, long walks, lab hours spent out together, lengthy chats would always be cherished in my memory. Thank you Basant for the proof reads I gave to you from time to time and the wonderful moments over evening tea. Thank you Dipika for the innocence filled conversations that made the mood lighter and brighter!

Smrati has always been very caring and helpful despite her heavy workload. At troubled times, she is just a call away. For Jayshree, I would say that one can learn from her that how can we balance our passion and PhD together. Her amazing talent in art, music and dance added thrill to our PhD journey. I would also like to thank my friend Isha Vishan for the various candid conversations and satires together. Thank you Smrati, Jayshree and Isha.

During my doctoral research I got to interact a lot students few of which deserve an acknowledgment. First, a big thankyou to Mohit Kumar for preparing this wonderful ~~TEX~~

template for thesis writing! Thankyou Hema for the wonderful moments at tea, your suggestion, thoughts and honest opinions regarding various matters. Never change ! I would like to acknowledge Dilip Pasumarthi, Sanketh Purwar, Argha Sen and Prabal Ghosh for their research inputs and the technical discussions we had together. Thanks to each one of you. It was a nice feeling to be associated with Sambhav Kothari and Nitish Garg, whom I had mentored to create few in-house projects at IITGuwahati. There is no surreal feeling than contributing to your institution! Thank you Sambhav Kothari and Nitish Garg.

I am thankful to Gurudutt Rao and Nilesh Jha with whom I always had endless discussion on academic related activities right from my BTech days. Thank you guys. My school friends Niraj, Prashant, Srijoy and Souvik always cheered me up during my difficult times of my PhD. Although we met infrequently, having group interactions with them always had a lasting memory. Thank you Mahendra Mehra and Ashish Mangal for retaining the same energy in our friendship though we were separated by distance. Thank you both of you for always being there. Amrita Banerjee deserves a special mention in my thesis for her constant support and companionship throughout my PhD despite being miles away. Thanks Amrita. Thank you Anasree Chatterjee for your kind friendship and the small pep-talks we used to share. Thank you Subarna Chatterjee for the wonderful moments at the TaCTiCS conference. It's very rare to have met people at conferences with such great energy and enthusiasm. I am indebted to one of the most talented guy I met at IIT Guwahati - Ashish Namdeo for his support during the course of my PhD. I am particularly thankful to Ankur Jain and Ankan Shrivastava who were my wall mates during my stay at the hostel for the fun filled moments we spent together.

I am grateful to all the teachers that have taught me right from my school days till my college life. Only because of their toil and efforts I could reach this place. This acknowledgment would be incomplete without mentioning the names of two ladies - Mrs. Sandhya Sundarkar and Mrs. Shibani Ray. Both of them have loved me like their own son right from my school days and they continue to do so. I feel so honoured to have lived under the umbrella of their love and blessings. Thank you Mrs. Chaitali Biswas Dutta for the delicious homemade food you served me on various occasions. I am grateful to Mr. Dipul who used to iron my clothes. While traveling to conferences, I used to give my clothes at the eleventh hour and he ensured that they are ironed perfectly on time. Thank you to the guys at Bani Mandir, Core 3, IIT Guwahati, for always being so helpful with regards to our printing and photocopy needs.

I wish to acknowledge Dr. Arnab Sarkar for the off topics discussions we had. It is rare for a faculty to be so open to the thoughts of students. I wish to thank Dr. Vijaya Saradhi for helping me take interest in Linux Scripting which eventually proved very useful

in simplifying my tasks. I would like to acknowledge Dr. T. Venkatesh for suggesting me CRAWDAD – ‘A Community Resource for Archiving Wireless Data’ which eventually helped me learn to analyze network traces. Thank you Dr. Kalpesh Kapoor for reaching out to me in my initial days. Your tips, discussions on things, life, PhD have always been handy. The first Diwali that was away from home made me feel homesick. Dr. Hemangee Kapoor called us to her house for Diwali celebrations. It was a very sweet gesture on her part. Thank you Madam for those wonderful memories.

Among other notable mentions include Debanjan, Sibaji, Mamata Di, Mr. Shrinivasa Naika, Mrs. Amrita Bose Paul, Mrs. Maushumi Barooah, Jaideep, Achyut Mani Tripathi, Deepak, Saptarshi, Piyoosh, Sandip Chakraborty, Sukarn, Rakesh Pandey, Nayantara, Sujata Kulkarni, Swarup, Shuvendu Rana, Nidhi and Sangita Roy whom I need to acknowledge for being a part of this wonderful journey of doctoral research. And thank you to all the wonderful people who have helped me in my pursuit whom I did not mention here. I sincerely acknowledge your efforts too! I would like to acknowledge those anonymous users, bloggers, forum moderators whose answers to various queries have helped me when I got stuck. A big thanks also goes out to Google, Wikipedia and online cloud storage providers like Dropbox, Copy.com, MEGA which ensured that our data remained safe and secure. I express my gratitude to my AMD and Acer Vertion Desktop, HP laptops and who have stood by me in all my experiments. I must acknowledge my cell phone and bicycle. Both of them have been used so roughly and yet they have always remained my faithful partners. Many thanks to my hostel room A-117, Barak Hostel, which has been my second home for last 6 years.

Without having an adequate support from your family members, traveling the doctoral journey could only remain a dream. I would like to thank my uncle, Mr. Rajendra Agrawal who motivated me to opt for doctoral research. If he had not motivated me, I would have certainly missed the exciting journey one goes through in a doctoral research. I would also like to acknowledge my uncle, Mr. Ajay Agarwal, who has always been a source of inspiration right from my early days of PhD. Whenever I used to feel low and disheartened with regards to my PhD research, he has always re-kindled a ray of optimism inside me. My elder brother Nitin Agarwal has always been caring and supportive. His guidance on various matters with regards to career, both personal and professionalism has helped me immensely. A special thanks goes to my cousin Anshul Agarwal. I have admired his presence in my life. He has also been a source of motivation to me in my doctoral research and always given me hope. His work ethics are a source of inspiration to me. I am grateful to my sister-in-law Ms. Priya for the warm welcome and care she has taken whenever we have met. Thank you Priya! The laughter and cuteness of my little niece Aarohi has always bought smiles on my face :). Thanks Aarohi. I would also like to thank Mrs. Arti Agarwal, my aunt for her love

and affection! Many thanks to my aunt Mrs. Vandana Agrawal for her care too!

The highest amount of acknowledgment goes out to my parents. I was always a difficult child to handle right from my childhood. Their sacrifices ensured that no obstacles could hinder the pace of my journey. Thank you Mother (Mrs. Ramlata Agarwal) and Father (Mr. Naresh Kumar Agarwal) for being so very kind, supportive, caring and for all your love. This thesis is a culmination of your blessings! Last, but not the least I would like to thank Almighty for his grace.

May 3, 2017

Mayank Agarwal

Declaration

I certify that

- The work contained in this thesis is original and has been done by myself and under the general supervision of my supervisor(s).
- The work reported herein has not been submitted to any other Institute for any degree or diploma.
- Whenever I have used materials (concepts, ideas, text, expressions, data, graphs, diagrams, theoretical analysis, results, etc.) from other sources, I have given due credit by citing them in the text of the thesis and giving their details in the references. Elaborate sentences used verbatim from published work have been clearly identified and quoted.
- I also affirm that no part of this thesis can be considered plagiarism to the best of my knowledge and understanding and take complete responsibility if any complaint arises.
- I am fully aware that my thesis supervisor(s) are not in a position to check for any possible instance of plagiarism within this submitted work.

May 3, 2017

Mayank Agarwal



Department of Computer Science and Engineering
Indian Institute of Technology Guwahati
Guwahati - 781039, India

Dr. Santosh Biswas

Associate Professor

Email : santosh_biswas@iitg.ernet.in

Phone : +91-361-258-2364

Prof. Sukumar Nandi

Professor

Email : sukumar@iitg.ernet.in

Phone : +91-361-258-2357

Certificate

This is to certify that this thesis entitled "**Intrusion Detection System for Attacks in Wi-Fi Networks: A Discrete Event System Approach**" submitted by **Mayank Agarwal**, in partial fulfilment of the requirements for the award of the degree of Doctor of Philosophy, to the Indian Institute of Technology Guwahati, Assam, India, is a record of the bonafide research work carried out by him under my guidance and supervision at the Department of Computer Science and Engineering, Indian Institute of Technology Guwahati, Assam, India. To the best of my knowledge, no part of the work reported in this thesis has been presented for the award of any degree at any other institution.

Date: May 3, 2017

Place: IIT Guwahati

Dr. Santosh Biswas

Prof. Sukumar Nandi

Publications Related to Thesis

Journals

1. **Agarwal, M.**, Biswas, S. and Nandi, S. “Advanced Stealth Man in The Middle Attack in WPA2 Encrypted Wi-Fi Networks”, *IEEE Communications Letters*, Vol. 19, No. 4, Pages: 581–584, April 2015.
2. **Agarwal, M.**, Biswas, S. and Nandi, S. “Intrusion Detection System for PS-Poll DoS Attack in 802.11 Networks using Real Time DES”, *IEEE/CAA Journal of Automatica Sinica*, 2015. (Accepted)
3. **Agarwal, M.**, Biswas, S. and Nandi, S. “DES Framework for Fault Diagnosis with Measurement Inconsistency: IDS for DHCP Attack ”, *IEEE/CAA Journal of Automatica Sinica*, 2016. (Accepted)

Communicated

- **Agarwal, M.**, D., Biswas, S. and Nandi, S. “Intrusion Detection System for Evil Twin Attack in Wi-Fi networks using Discrete Event System Framework”, *WPC Springer*, March 2016, (Under Review).

Conferences

1. **Agarwal, M.**, Biswas, S. and Nandi, S. “Detection of De-authentication DoS attacks in Wi-Fi Networks: A Machine Learning Approach”, “Detection of De-authentication DoS attacks in Wi-Fi Networks: A Machine Learning Approach”, *IEEE SMC 2015 Conference*, Pages: 246–251, October 2015, Hong Kong.
2. **Agarwal, M.**, Biswas, S. and Nandi, S. “I²-diagnosability framework for detection of Advanced Stealth Man in the Middle attack in Wi-Fi networks ”, *23rd Mediterranean Conference on Control and Automation*, Pages: 349–356, June 2015, Spain.
3. **Agarwal, M.**, Biswas, S. and Nandi, S. “Detection of De-authentication Denial of Service attack in 802.11 networks” In: *Annual IEEE India Conference (INDICON)*, Pages: 1–6, December 2013. Mumbai, India.

Other Publications

1. Barbhuiya, F., **Agarwal, M.**, Purwar, S., Biswas, S. and Nandi, S. “Application of stochastic discrete event system framework for detection of induced low rate TCP attack”, *ISA Transactions*, Elsevier, Vol. 58, Pages: 474–492, September 2015.
2. **Agarwal, M.**, Pasumarthi, D., Biswas, S. and Nandi, S. “Machine learning approach for detection of flooding DoS attacks in 802.11 networks and attacker localization”, *International Journal of Machine Learning and Cybernetics*, Springer, Pages: 1–17, November 2014.
3. A. Bhandari, **M., Agarwal, M.**, Biswas, S. and Nandi, S. “Intrusion Detection System for Identification of Throughput Degradation Attack on TCP”, “Intrusion Detection System for Identification of Throughput Degradation Attack on TCP”, *NCC*, Pages: 1–6, March 2016.

Abstract

Wireless Fidelity (Wi-Fi) has brought about a paradigm shift in the area of communication. Recent advances in Wi-Fi technology have made it possible to achieve gigabit speeds on wireless medium making them a cost effective solution as compared to wired deployment. However, all these benefits comes at the price of security. As wireless communication is inherently broadcast, any user within the wireless range of the communicating devices can eavesdrop on the traffic exchange between the Wi-Fi clients without their knowledge. In addition, a poorly configured Wi-Fi network is vulnerable to misuse and various types of network attacks. In order to detect these attacks, the network administrator usually deploys Intrusion Detection System (IDS), which is primarily a hardware device and (or) software program that monitors the Wi-Fi network or host activities for malicious behavior. Among the two widely used IDS design techniques, signature based IDS checks for fixed patterns to identify attacks whereas anomaly based IDS uses statistical features to detect attacks.

Although signature and anomaly based IDSs detect most classes of attacks, there exists a class of attacks in Wi-Fi network like evil twin attack, Stealth Man-in-the-Middle (SMiTM) attack, power save Denial of Service (DoS) attack, rogue Dynamic Host Control Protocol (DHCP) attack etc., that do not differ in semantics or statistics under normal and attack circumstances. As a result, signature and anomaly based IDSs are unable to detect such attacks. The objective of this thesis is to design and develop wireless IDSs for such class of attacks which are not detectable by signature and anomaly based IDSs.

In the first contribution of this thesis, we propose an IDS for detecting evil twin attack in Wi-Fi network. In evil twin attack, an attacker mimics a genuine Access Point (AP) by spoofing its Service Set Identifier (SSID) and MAC address. If a client connects to evil twin AP, an attacker can re-direct it to phishing websites, steal sensitive information, capture client's credentials etc. In the second contribution of this thesis, we propose a novel insider attack termed as 'Advanced Stealth Man-in-the-Middle (ASMiTM)' attack which enables an attacker to launch a Man-in-the-Middle attack in WPA2 encrypted Wi-Fi network. We also propose an IDS for detecting the proposed ASMiTM attack. In the third contribution of this thesis, we propose an IDS for detecting Power Save DoS (PS-DoS) attack in Wi-Fi network. In PS-DoS attack, an attacker spoofs as a genuine client and fetches the buffered frames at the AP while the client is in power save state thereby causing frame losses to the client. In the final contribution of this thesis, we propose an IDS for detecting rogue DHCP server

attack in Wi-Fi network. In rogue DHCP server attack, an attacker sets up a rogue DHCP server and sends fictitious IP address, DNS and gateway address (or a combination of these) to the client requesting DHCP services. By supplying false information, an attacker can re-direct client's traffic via its terminal thereby sniffing client's information, re-directing clients to phishing websites, install malware into the client's machine etc.

The hallmark of each of the IDSs proposed for the above attacks is that they do not require any sort of protocol modifications, encryptions, certificate management etc., and can be readily deployed on both legacy as well as modern network. In addition, all of the proposed IDSs are developed using the Failure Detection and Diagnosis (FDD) theory of Discrete Event System (DES). Developing of the proposed IDSs using the DES framework helps to prove the correctness and completeness of the IDS which ensures that the attacker does not escape detection under any circumstances. A DES is characterized by a discrete state space and event driven dynamics. For FDD, DES models are designed for the system (network) under normal and failure (attack) conditions. Following that, a state estimator called diagnoser (or detector, if only detection of failure is required) is designed which observes sequence of events generated by the system to decide whether the states through which the system traverses correspond to normal or faulty DES model. In the proposed DES based IDSs, attacks are mapped to failures and the diagnoser is implemented as the IDS engine.

For each of the DES framework used in IDS for detection of the attack, we first show how the same DES framework can be used for fault detection in a benchmark process of two/three tank system. This illustrates how the DES theory mainly developed for fault detection of large systems like chemical, mechanical etc., is also applicable for intrusion detection in wireless network. Furthermore, all attacks discussed earlier have been implemented on practical testbed and the results are shown in terms of accuracy and detection rate of the IDS. In summary, this thesis provides an insight into design of IDS for various MAC layer attacks in 802.11 Wi-Fi network that cannot be detected using standard signature or anomaly based IDSs.

Contents

Abstract	xix
List of Figures	xxvii
List of Tables	xxxix
List of Algorithms	xxxiii
List of Symbols	xxxv
List of Abbreviations	xxxvii
1 Introduction	1
1.1 Motivation and Contribution	5
1.1.1 802.11 Terminologies	6
1.1.2 Failure Detection and Diagnosis (FDD) of Discrete Event System (DES) and IDS	7
1.1.3 Evil Twin Attack	8
1.1.4 Advanced Stealth Man-in-the-Middle (ASMiTM) Attack	10
1.1.5 Power Save Denial of Service (PS-DoS) Attack	14
1.1.6 Rogue Dynamic Host Control Protocol (DHCP) Attack	16
1.2 Organization of the Thesis	19
2 IDS for Evil Twin Attack in Wi-Fi networks using DES Framework	21
2.1 Introduction	21
2.2 Background and Motivation	25

2.2.1	Vulnerabilities of Management and Control Frames in 802.11 Wi-Fi networks	25
2.2.2	Evil Twin Attack	26
2.2.3	Existing Approaches to Detect or Prevent Evil Twin Attack	28
2.3	Proposed Scheme for the Detection of Evil Twin Attack	32
2.3.1	Working Principle of the IDS for Detecting Evil Twin Attack	33
2.3.2	IDS Components	35
2.3.3	Attacker and IDS Assumptions	36
2.4	FDD Theory of DES: Three Tank System	37
2.4.1	DES Modeling: Measurement Limitations and Failure Diagnosis	38
2.4.2	Application of Failure Detection and Diagnosis Theory of DES on Three Tank System	40
2.4.3	Diagnosability	46
2.4.4	DES Diagnoser Construction and Fault Detection in Three Tank System	47
2.5	DES Model of Evil Twin Attack	51
2.5.1	An Example of Evil Twin Attack Detection Using DES Diagnoser	58
2.6	Results and Discussions	58
2.6.1	Network Setup for Evil Twin	58
2.6.2	Detection Rate and Accuracy of the Proposed DES Based IDS	59
2.6.3	Correctness of the DES Diagnoser	60
2.6.4	Discussion	61
2.7	Conclusion	62
3	IDS for ASMiTM Attack in Wi-Fi Networks using I²-DES	65
3.1	Introduction	65
3.2	Background and Proposed ASMiTM Attack	68
3.2.1	ARP Spoofing Attack	68
3.2.2	Hole 196	70
3.2.3	Stealth Man in the Middle (SMiTM) Attack	70
3.2.4	Wireless Denial of Service (WDoS) Attack	72

3.2.5	Proposed ASMiTM Attack	73
3.2.6	Existing Approaches to Detect or Prevent ASMiTM attack	75
3.3	Proposed Scheme for the Detection of ASMiTM Attack	76
3.3.1	ARP Probe as Indicator Event and Importance of Updation of PAC- NUM value	78
3.3.2	IDS Components	79
3.3.3	Attacker and IDS Assumptions	80
3.4	FDD Theory of I ² -DES: Two Tank System	80
3.4.1	Need for I ² -DES Framework	81
3.4.2	I ² -DES Model: Measurement Limitations and Failure Diagnosis	82
3.4.3	Application of Failure Detection and Diagnosis Theory of I ² -DES on Two Tank System	84
3.4.4	Diagnosability	90
3.4.5	I ² -Diagnoser Construction and Failure Diagnosis in I-Diagnosability vs I ² -Diagnosability Framework for the Two Tank System	92
3.5	I ² -DES Model for ASMiTM attack	96
3.5.1	An Example of ASMiTM attack Detection Using I ² -DES Diagnoser	100
3.6	Results and Discussion	101
3.6.1	Network Setup for Evil Twin	101
3.6.2	Detection Rate and Accuracy of the Proposed I ² -DES Based IDS	103
3.6.3	Correctness of the I ² -DES Diagnoser	104
3.6.4	Discussion	105
3.7	Conclusion	105
4	IDS for PS-Poll DoS Attack in Wi-Fi Networks using RTDES Framework	107
4.1	Introduction	107
4.2	Background and Motivation	110
4.2.1	Power Save Feature of 802.11 Standard	110
4.2.2	Vulnerabilities in Power Save Feature of 802.11 Standard	111
4.2.3	Existing Approaches to Detect or Prevent PS-DoS Attack	112
4.3	Proposed Scheme for the Detection of PS-DoS Attack	114

4.3.1	Working Principle of the IDS for Detecting PS-DoS Attack	115
4.3.2	IDS Components	116
4.3.3	Attacker and IDS Assumptions	118
4.4	FDD Theory of RTDES: Three Tank System	120
4.4.1	RTDES Modeling: Measurement Limitations and Failure Diagnosis .	121
4.4.2	Application of Failure Detection and Diagnosis Theory of RTDES on Three Tank System	123
4.4.3	Diagnosability	129
4.4.4	RTDES Diagnoser Construction Fault Detection in Three Tank System	130
4.5	RTDES Model for PS-DoS Attack	134
4.5.1	An Example of PS-DoS Attack Detection Using RTDES Diagnoser . .	139
4.6	Results and Discussions	141
4.6.1	Network Setup for PS-DoS	141
4.6.2	Detection Rate and Accuracy of the Proposed RTDES Based IDS . . .	141
4.6.3	Network Load because of Power Save Probes	143
4.6.4	Correctness of the RTDES Diagnoser	144
4.6.5	Discussion	147
4.7	Conclusion	147
5	IDS for Rogue DHCP Server Attack in Wi-Fi Networks using MIDES Framework	149
5.1	Introduction	149
5.2	Background and Motivation	153
5.2.1	Basic Operation of DHCP	153
5.2.2	Vulnerabilities in DHCP Message Exchange	155
5.2.3	Existing Approaches to Detect or Prevent Rogue DHCP Server Attack	156
5.3	Proposed Scheme for the Detection of Rogue DHCP Server Attack	157
5.3.1	Working Principle of the IDS for Detecting Rogue DHCP Server Attack	158
5.3.2	IDS Components	159
5.3.3	Attacker and IDS Assumptions	160
5.4	FDD Theory of MIDES: Two Tank System	161

5.4.1	Need for MIDES Framework	162
5.4.2	MIDES Model: Measurement Limitations and Failure Diagnosis . . .	164
5.4.3	MIDES Model: Measurement Inconsistency	165
5.4.4	Application of Failure Detection and Diagnosis Theory of MIDES on Two Tank System	166
5.4.5	Diagnosability	172
5.4.6	MIDES Diagnoser Construction and Inconsistency Handling in MLDES vs MIDES Framework for the Two Tank System	173
5.5	MIDES Model for Rogue DHCP Server Attack	182
5.5.1	An Example of Rogue DHCP Server Attack Detection Using MIDES Diagnoser	187
5.6	Results and Discussions	188
5.6.1	Network Setup for Rogue DHCP Server Attack	188
5.6.2	Detection Rate and Accuracy of the Proposed MIDES Based IDS . . .	189
5.6.3	Network Load because of DHCP Probes	190
5.6.4	Correctness of the MIDES Diagnoser	191
5.6.5	Discussion	192
5.7	Conclusion	192
6	Conclusions and Future Work	195
6.1	Summary of Contribution of the Thesis	196
6.2	Scope of Future Work	198

List of Figures

1.1	Basic components of 802.11 Wi-Fi network	6
1.2	Four-way handshake between a client and access point.	8
2.1	Normal and evil twin setup	23
2.2	Four-way handshake between a client and access point	25
2.3	Evil twin setup	26
2.4	Timeline for launching evil twin attack	26
2.5	Association response frame format	27
2.6	Flowchart of detection of evil twin attack	33
2.7	Timeline of detection of evil twin attack	34
2.8	Components of the proposed IDS for detection of evil twin attack	35
2.9	The three tank system	40
2.10	DES of the three tank system shown in Fig. 2.9	43
2.11	Diagnoser obtained for the DES model of the three tank system shown in Fig. 2.10	50
2.12	Normal and attack DES model for evil twin attack	51
2.13	Diagnoser for evil twin attack	57
2.14	Experimental setup for evil twin attack	59
2.15	Size of database growth of the IDS	60
2.16	Memory usage of the IDS	60
2.17	CPU utilization of the proposed IDS	61
3.1	ARP cache mappings under normal and spoofing conditions	69
3.2	SMiTM Attack	71

3.3	Cipher-block chaining Message authentication code Protocol (CCMP) encapsulation	71
3.4	WDoS Attack	72
3.5	ASMiTM attack	73
3.6	Experimental setup for ASMiTM attack	77
3.7	Components of the proposed IDS for detection of ASMiTM attack	79
3.8	The two tank system	84
3.9	DES of the Two Tank System Shown in Fig. 3.8	86
3.10	I ² -DES Diagnoser of the Two Tank System Shown in Fig. 3.8	95
3.11	Normal and Attack I ² -DES Model of ASMiTM Attack	97
3.12	Diagnoser for ASMiTM Attack	99
3.13	FromDS frame	102
3.14	A ToDS Frame. Converting a ToDS frame to FromDS requires the cyclic shifts as shown	102
4.1	Frame format of null data frame	110
4.2	Timeline for launching PS-DoS attack	111
4.3	Timeline for detecting the PS-DoS attack	116
4.4	Components of the proposed IDS for detection of PS-DoS attack	117
4.5	The three tank system	124
4.6	RTDES of the three tank system shown in Fig. 4.5	126
4.7	Diagnoser obtained from Fig. 4.6	134
4.8	DES model for PS-DoS attack	135
4.9	Diagnoser for PS-DoS attack.	139
4.10	Experimental setup	141
4.11	Network traffic with and without use of IDS	143
4.12	Six possible cases of arrival of null data frames	145
5.1	Four way DHCP handshake	153
5.2	Rogue DHCP setup	154
5.3	Timeline of the rogue DHCP server attack	154

5.4	Timeline of the rogue DHCP server attack detection methodology.	159
5.5	Components of the proposed IDS for detection of rogue DHCP server attack	159
5.6	The two tank system	167
5.7	MIDES of the Two Tank System Shown in Fig. 5.6	169
5.8	Case 1: MLDES diagnoser assuming no measurement inconsistent transition is observed	177
5.9	Case 2: MLDES diagnoser considering measurement inconsistent transition as unmeasurable.	178
5.10	Case 3: MIDES diagnoser considering measurement inconsistent transition as measurable and tries to predict the possible O -node(s).	179
5.11	Normal and attack model in rogue DHCP server attack	183
5.12	Diagnoser for rogue DHCP server attack	186
5.13	Experimental setup for rogue DHCP server attack	188
5.14	Network load with and without IDS	190

List of Tables

2.1	Types of rogue access point	22
2.2	Differentiating parameters of the second association response	34
2.3	Sensor map for three tank system	41
2.4	Transitions along with their representation. Events, sensor conditions, controller commands of the DES model of the three tank system shown in Fig. 2.10	44
2.5	Model variables and their domains	51
2.6	Transition table for DES model shown in Fig. 2.12	53
2.7	Detection rate statistics using the proposed IDS	59
2.8	All possible attack cases for proving the correctness of the DES diagnoser . .	62
2.9	Comparison of existing mitigation solutions for Evil Twin attack	62
3.1	ASMiTM Detection Table	78
3.2	Sensor map for two tank system	85
3.3	Transitions along with their representation. Events, Sensor Conditions, Controller Commands of the I ² -DES model of the two Tank System shown in Fig. 3.9	87
3.4	Duration (in mins) of SMiTM vs ASMiTM attack.	102
3.5	Comparison of SMiTM, WDoS and ASMiTM Attacks	103
3.6	ASMiTM Attack Detection and Accuracy Statistics	104
4.1	Sensor map for three tank system	125
4.2	Transitions along with their representation. Events, sensor conditions, controller commands of the RTDES model of the three tank system shown in Fig. 4.6	127
4.3	Transition table for Fig. 4.8	138

4.4	Parameters values for beacon interval and listen intervals	140
4.5	PS-DoS attack detection and accuracy statistics	142
4.6	Comparison of existing mitigation solutions for PS-DoS attack	147
5.1	Sensor map for two tank system	168
5.2	Transitions along with their representation. Events, sensor conditions, controller commands of the MIDES model of the two tank system shown in Fig. 5.7	170
5.3	Notations used in DES modeling for rogue DHCP server	183
5.4	Transition table for DES Model shown in Fig. 5.11. Assumption: 2 Genuine DHCP Servers and 1 Rogue DHCP Server	184
5.5	Detection rate statistics with and without the use of measurement inconsistent based IDS	189
5.6	Comparison of existing mitigation solutions for Rogue DHCP Server attack	192

List of Algorithms

1	Algorithm for construction of diagnoser O for an DES model G	48
2	Algorithm for construction of diagnoser O for an I ² -DES model G	93
3	Algorithm for construction of diagnoser O for an RTDES model G	131
4	Algorithm for construction of diagnoser O for an MIDES model G	174
5	Estimator diagnoser for the MIDES framework	180

List of Symbols

<u>Symbols</u>	<u>Description</u>
G	MIDES model
Σ	Set of events of the MIDES model G
V	Set of model variables of the MIDES model G ,
\mathfrak{S}	Set of transitions of the MIDES model G ,
τ	A transition $\tau \in \mathfrak{S}$
X	Finite set of states of the MIDES model G
X_0	Initial state of the MIDES model G
σ	Event on which the transition τ is enabled
$check(V)$	Condition(s) on a subset of the model variables for τ .
$assign(V)$	Assignment(s) on a subset of the model variables for τ .
$L(G)$	Set of all traces <i>generated by</i> G
X_N	Set of all normal states of the MIDES model G .
X_{F_i}	Set of all faulty states of the MIDES model G .
F_i	i^{th} failure
σ_{F_i}	Event related to causing failure F_i
O	Diagnoser of the MIDES model G
Z	Set of diagnoser nodes called <i>O-nodes</i>
Z_0	Initial state of the diagnoser
A	Set of diagnoser transitions called <i>O-transitions</i>
τ_{ub}	Measurement Inconsistent G -transition
z_{ub}	Measurement inconsistent O -node.

List of Abbreviations

<u>Terms</u>	<u>Abbreviations</u>
AAA	Authentication Authorization and Accounting
ACK	Acknowledgment
AID	Association ID
AP	Access Point
ARP	Address Resolution Protocol
ARR	Analytical Redundancy
BI	Beacon Interval
BSS	Basic Service Set
BSSID	Basic Service Set Identifier
CA	Certification Authority
CPU	Central Processing Unit
CTS	Clear to Send
CVE	Common Vulnerability Exposure
DB	Database
DEAUTH	Deauthentication
DES	Discrete Event System
DHCP	Dynamic Host Configuration Protocol
DIFS	Distributed Inter Frame Spacing
DNS	Domain Name System
DoS	Denial of Service
DST	Destination
FCS	Frame Check Sequence

FDD	Failure Detection and Diagnosis
FN	False Negative
FP	False Positive
FSM	Finite State Automata
GTK	Group Temporal Key
HIDS	Host Intrusion Detection System
HTTP	Hypertext Transfer Protocol
HVAC	Heating Ventilation Air-Conditioning
IAT	Inter Arrival Time
IBSS	Independent Basic Service Set
ICMP	Internet Control Message Protocol
ID	IDentifier
IDS	Intrusion Detection System
IEEE	Institute of Electrical and Electronics Engineers
IP	Internet Protocol
LAN	Local Area Network
LI	Listen Interval
MAC	Media Access Control
MD5	Message Digest 5
MIDES	Measurement Inconsistent Discrete Event System
MITM	Man-in-the-Middle
MLDES	Measurement Limitation Discrete Event System
NIC	Network Interface Controller
NIDS	Network Intrusion Detection System
OS	Operating System
PACNUM	Packet Number
PCA	Principal Component Approach
PHY	Physical
PMK	Pairwise Master Key

PTK	Pairwise Transient Key
RAP	Rogue Access Point
RFC	Request for Comment
RSSI	Received Signal Strength Indicator
RST	Reset
RTDES	Real Time Discrete Event System
RTS	Request to Send
RTT	Round Trip Time
SIFS	Short Inter Frame Spacing
SRC	Source
SSID	Service Set Identifier
SVM	Support Vector Machine
TCP	Transmission Control Protocol
TIM	Traffic Indication Message
TP	True Positive
TSF	Timing Synchronization Function
USB	Universal Serial Bus
VPN	Virtual Private Network
WEP	Wired Equivalent Privacy
Wi-Fi	Wireless Fidelity
WLAN	Wireless Local Area Network
WPA	Wi-Fi Protected Access
WPA2	Wi-Fi Protected Access II
WPA-PSK	Wi-Fi Protected Access-Pre-Shared Key

“If you spend more on coffee than on IT security, you will be hacked. What’s more, you deserve to be hacked.”

Richard Clarke
White House Cybersecurity Advisor

1

Introduction

Wi-Fi has brought about a paradigm shift in the way people communicate. Rapid deployment of Wi-Fi networks across colleges, libraries, offices, malls, airports, food courts etc., has made it possible for people to stay connected while on the move. Portable devices such as laptops, cellphones, Personal Digital Assistants (PDAs), tablets, phablets etc., have Wi-Fi chip-set pre-built into them. Furthermore, the price of wireless networking equipment have dropped significantly over the years. Wireless Network Interface Cards (NICs) are nearing the price of their wired counterparts.

Wireless Local Area Network (WLAN) technology has progressed at a rapid pace. The initial Institute of Electrical and Electronic Engineers (IEEE) 802.11 standard which was released in the year 1997 supported data rates up to 2 Mbps. In subsequent years, devices capable of supporting data rates upto 54 Mbps became a commonplace. Furthermore, with the release of 802.11n standard, that utilizes Multiple Input Multiple Output (MIMO) technology, data rates up to 300 Mbps is possible. The latest 802.11ac standard breaks the gigabit barrier for Wi-Fi networks and supports data rates upto 1300 Mbps! There are many reasons why organizations are fast moving towards deploying wireless LANs over wired LANs. Few of those reasons are listed below:

- Increased productivity because of increased mobility.
- Lower infrastructure cost compared to wired networks.
- Rapid deployment and expansion schedules.
- Aesthetically unobtrusive.
- Provides support to a large number of Wi-Fi compatible devices.

Unfortunately, wireless networking is a double-edged sword. The initial developers of Wi-Fi technology primarily focused on the ease of access with little regards to the security aspect. Although, wireless users are presented with lot of opportunities in terms of flexibility and ease of usage, there is no denying the fact that these users are subject to greater security risks as compared to their wired counterparts. Throughout the entire process, the integrity and confidentiality of the information traveling through the air has always been a matter of concern as communication over a wireless medium is always susceptible to eavesdropping. In contrast, wired networks are difficult (not impossible) to eavesdrop as the wired infrastructure are relatively secured. With wireless networking, there is no physical security. An attacker just needs to be in the vicinity of the target network in order to sniff the network's traffic. Such promiscuous eavesdropping of the network traffic by an attacker can never be prevented in wireless network because of its broadcast nature.

An attacker armed with a Wi-Fi device and a penetration Operating Systems (OSs) like BackTrack (now Kali Linux) [1], BackBox Linux [2] can easily launch a myriad of attacks on a Wi-Fi network. These penetrating OSs come pre-installed with various packet crafting and hacking tools like aircrack-ng suite [3], scapy [4], Airpwn [5], AirJack [6], WifiCopper [7] etc., which ease the process of launching various attacks even for novice attackers. Given the rapid deployment of Wi-Fi networks, it is imperative that adequate security arrangements are put in place to ensure protection of these networks against various security threats. The increased number of networked machines has led to a rise in unauthorized activity [8], not only from external attackers, but also from internal sources such as disgruntled employees and people abusing their privileges for personal gain [9]. Moreover, because of lack of proper authentication of the communicating parties, inherent protocol weakness, bugs in Wi-Fi router software, drivers etc., Wi-Fi networks are prone to various attacks like Man-in-the-Middle (MiTM), unauthorized access, spoofing, Denial of Service (DoS), privacy threats [10, 11, 12, 13] etc. This mandates the requirement for a suitable intrusion detection system for detecting various attacks in a Wi-Fi network.

Network administrators deploy a number of security measures like access control list, anti-malware, anti-spyware, anti-virus, biometric authentication, disabling insecure services and ports, encryption, firewalls, honeypots, honeynets, Intrusion Prevention System (IPS), Intrusion Detection System (IDS), proxy servers, smart cards, Virtual Private Network (VPN) etc., in order to protect the network assets and resources. Three primary goals of network security are:

- **Confidentiality:** It ensures that the precious business data is available only to the intended and the authorized persons. Individuals who are not authorized to use the data are not permitted to use the same.

-
- **Integrity:** It ensures that the data is accurate and consistent. The function of integrity is to make sure that the data is accurate and is in its original form and has not been altered in any form by noise, hackers etc.
 - **Availability:** It ensures that the data, resources or services are available to the genuine users, whenever they require it.

Intrusion is any set of actions that attempt to compromise the confidentiality, integrity or availability of a network or host resource [14]. An Intrusion Detection System (IDS) monitors the network or host activities in real-time and alerts for potential vulnerabilities and attacks. IDS is a vital security component of an organization these days. IDS helps to detect an attack before it inflicts widespread damage. IDS has received a considerable attention in recent years. Depending on their deployment and characteristic features, IDSs can be classified into 6 major categories:

1. **Passive IDS:** A passive IDS works by monitoring and analyzing the network traffic and raising an alert to the administrator if potential vulnerabilities or attacks are observed. A passive IDS cannot take any action on its own. Although these IDSs are easier to deploy, it may generate too many alerts for the administrator if they are improperly configured. As an example, if the attack traffic and genuine traffic is not defined properly, an administrator may receive too many false alerts.
2. **Active IDS:** Unlike passive IDS, an active IDS can be configured to take necessary action without the intervention of an administrator. An active IDS provides real time network protection against potential security breaches. However, when an active IDS is configured improperly, it results in denial of access to genuine users or services.
3. **Network Based IDS (NIDS):** A NIDS is deployed to monitor the network activities of an organization. It is generally placed along the network boundary. A NIDS typically consists of a NIC operating in promiscuous mode which monitors all the network traffic traveling through it.
4. **Host Based IDS (HIDS):** A host-based IDS is deployed on individual hosts that needs to be monitored. Unlike NIDS, the HIDS monitors the activities of only the host system on which it is installed. The HIDS monitors the operating system and network activities of the host on which it is installed and triggers an alarm whenever any suspicious activities are observed.
5. **Signature Based IDS or Knowledge Based IDS:** A signature-based IDS refers to a database of known intrusion patterns typically known as signatures for detecting intrusions. It monitors the host or network activities by correlating the traffic generated

using the attack signatures and raising an alarm whenever there is a match. The advantages of signature-based IDS is the fast and accurate detection of known attacks, low false alarm rate etc. On the other hand, the major drawback of a signature-based IDS is that it needs a regular update of its attack signatures for detecting new attacks. If an attack signature is not present in its database, a signature-based IDS ignores the threat. Therefore, these IDS perform poorly when it comes to detecting zero-day attacks and latest threats whose signatures are not present in the database. Snort [15] and EMERALD [16] are some of the prominently used signature-based IDSs.

A simple example of a Snort signature for “*land*” attack is as follows.

```
alert ip any any -> any any (msg : “BAD TRAFFIC sameSRC/DST”;  
sameip; reference : cve,CVE – 1999 – 0016;  
reference : url,www.cert.org/advisories/CA – 1997 – 28.html;  
classtype : bad – unknown; sid : 527; rev : 3;)
```

This signature raises an alarm whenever an Internet Protocol (IP) packet having same source and destination address is observed.

- 6. Anomaly Based IDS:** Unlike signature-based IDSs, anomaly-based IDSs have the capability to detect both known and unknown attacks. An anomaly-based IDS builds a normal profile of a host or network based on statistical evaluation. The normal profile is built by observing statistics like CPU usage, memory utilization, disk activity, processor usage, network bandwidth usage, number of users logged in, count of failed logins, amount of mails sent and received etc. Anomaly-based IDS marks any deviation from the normal activity as suspicious and raises an alarm. Although anomaly-based IDS can detect new attacks, it suffers from high false alarm rate, i.e., it marks normal activities as suspicious. For example, suppose that an anomaly based system reports 3 failed login attempts as an intrusion attempt. Therefore, if a genuine user, forgets his password and enters a wrong password 3 times, the activity is marked as suspicious by the anomaly-based IDS. A review of various anomaly-based IDSs can be found in [17, 18].

A signature or anomaly-based IDS can be deployed as a host-based or network-based IDS. Rest of this thesis mainly deals with wireless NIDS and henceforth unless explicitly mentioned, the term IDS refers to wireless NIDS.

1.1 Motivation and Contribution

In signature-based IDSs, a set of known attack patterns or signatures are stored in a database and the system or network activity is compared with these signatures. If a match is found, an alert is raised signaling the detection of malicious activity. Although signature-based IDSs can detect known attacks accurately, they require constant signature updates in order to make them effective to detect new attacks. Many signature detectors are designed to use tightly defined signatures that prevents them from detecting variants of common attacks. Anomaly-based IDS makes use of statistical features of traffic and behavior in order to detect malicious activities. As anomaly-based IDS uses statistical inferences it is capable to detect new attacks as well. However, they usually produce a large number of false alarms because of the unpredictable and dynamic behavior of users, systems and networks. Further, they require extensive “training sets” of system or network event records in order to characterize normal and attack behavior, which is a difficult task. If such tasks of characterizing the normal and attack behavior are assigned to security experts, it may lead to conflicting opinions as different security experts consider different factors for marking a host or network activity as normal or attack. Therefore, designing an anomaly based IDS is always a challenging task.

There are certain class of attacks which cannot be effectively detected by signature or anomaly-based IDSs as the semantics of the network remain the same during normal and attack conditions. Some of them are:

1. Evil Twin attack.
2. Advanced Stealth Man-in-the-Middle (ASMiTM) attack.
3. Power Save Denial of Service (PS-DoS) attack.
4. Rogue Dynamic Host Control Protocol (DHCP) attack.

These attacks are detailed next. Each of these attacks have the following two properties which makes them subtle:

1. They can be launched by injecting very few frames in the network, typically one or two while leaving all other statistical properties of network traffic intact. So, no anomaly is noticed in the network when such attack occurs.
2. The sequence of frame exchange under normal and attack scenarios is same. So, developing a signature or anomaly pattern is quite difficult and may result in high false alarm rate.

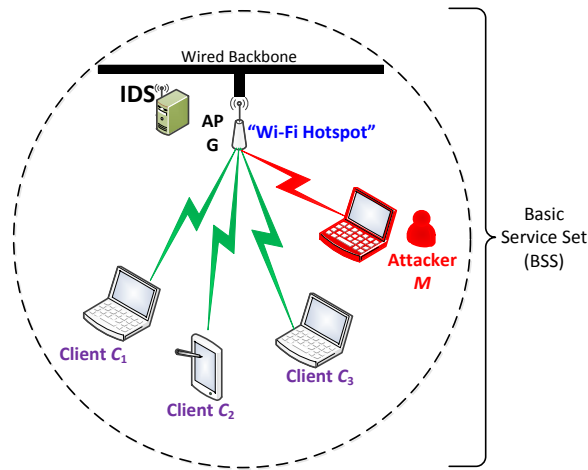


Figure 1.1: Basic components of 802.11 Wi-Fi network

1.1.1 802.11 Terminologies

In this subsection, we look at the basic terminologies and components of a 802.11 Wi-Fi network. These are explained using Fig. 1.1. The symbols shown in Fig. 1.1 are used throughout the thesis for consistency and readability purposes e.g., Clients C_1 , C_2 , C_3 , attacker M and Access Point G etc.

1. **Basic Service Set (BSS):** The core unit of an 802.11 network is called a Basic Service Set (BSS). A BSS consists of a central Access Point (AP) and a set of client(s). In Fig. 1.1 the circle consisting of AP and the clients C_1 , C_2 and C_3 together constitute a BSS.
2. **Access Point (AP):** The AP coordinates all the activities within the BSS. All the clients within a BSS communicate via the AP. The AP acts as a central arbiter. If the client C_1 wants to communicate with client C_2 , C_1 first sends message to the AP which in turn forwards the message to client C_2 . Due to this centralized control, BSS networks are also known as infrastructure networks. We denote the AP using the symbol G ($G \rightarrow$ Genuine).
3. **Clients:** The clients are Wi-Fi devices that connect to the AP in order to access the services provided by the AP. In Fig. 1.1, the clients C_1 , C_2 and C_3 are associated with the AP G .
4. **Service-Set Identifier (SSID):** A BSS is identified by a Service-Set Identifier (SSID). This can generally be thought of as the name of the wireless network. In Fig. 1.1, the SSID of the network is 'WiFi-Hotspot'.
5. **Authentication:** Authentication is the process by which a client establishes its identity

with the AP.

6. Association: Association is the process by which a client officially joins an 802.11 network and becomes eligible to access the services provided by the AP. Only after a successful authentication a client is allowed to associate.
7. De-authentication: De-authentication is the process by which a client terminates its connection with the AP.
8. Attacker: The attacker is an intruder who has the capability to launch various attacks such as Man-in-the-Middle (MiTM), Denial of Service (DoS), unauthorized access, spoofing attacks etc. We denote the attacker using the symbol M ($M \rightarrow$ Malicious). The attacker M may or may not be associated with the AP.

1.1.2 Failure Detection and Diagnosis (FDD) of Discrete Event System (DES) and IDS

The theory of Failure Detection and Diagnosis (FDD) of Discrete Event System (DES) has been mainly applied for large systems like chemical reaction chambers, HVAC (Heating, Ventilating, and Air Conditioning) plants, hybrid systems [19, 20, 21, 22, 23, 24, 25, 26, 27] etc. An overview of FDD using DES is discussed in [28, 29]. DES based FDD have various frameworks depending on the system under consideration. For example, in distributed systems Petri Net-based frameworks are preferred [30, 31, 32, 33], while in a system involving stochastic process, a stochastic DES based framework is recommended [34, 35]. In cases where the underlying system involves incomplete or partial observation, frameworks based on partial observation and learning needs to be used [36]. For faults related to timing of events, a Real Time DES (RTDES) [37, 38, 39, 40] based framework proves to be beneficial. The central idea of DES modeling is to develop the normal and failure model corresponding to normal and failure scenarios. Subsequently, a diagnoser which is a state estimator is built using the states traversed in the normal and fault models. The diagnoser determines whether the system is operating under faulty, non-faulty or un-certain conditions.

DES based IDSs have been found to be effective in detecting security attacks in wired networks [41, 42]. To the best of our knowledge, we have shown for the first time that this framework can also be applied to detect attacks in Wi-Fi networks. The motivation behind using DES based IDS is the similarity between the attacks occurring in networks and faults¹ in DES. Under normal condition (when no attacker is present), the sequence of frame exchange can be captured as the normal DES model of the network. An attack

¹In this thesis, the terms attack, fault and failure are used interchangeably.

leads to deviation from the normal network activity. This deviation is captured as a faulty (attack) DES model. Using the information of the normal model, faulty (attack) model and the observable frames, the diagnoser is constructed that serves as an IDS engine. Diagnostoser have the capability to capture the difference between the normal and the fault models aiding in attack (fault) detection thereby having the capability of behaving as an IDS.

Throughout this thesis, we have adapted different DES paradigms for developing IDS for detection of MAC layer attacks in Wi-Fi networks. Irrespective of the paradigm used, the core DES philosophy remains the same. DES based IDS basically comprises 3 simple steps: 1) Design the normal DES model using the system behavior under normal network condition. 2) Design the faulty DES model using the system behavior under attack condition. 3) Design a diagnoser which basically serves as an IDS engine using the normal model and faulty model. The diagnoser is basically a state estimator that determines whether the system is moving as per the normal or faulty model using the observed system values (i.e., network features, characteristics, sequence of frame exchange etc.). An added advantage of using a DES based IDS is that it is formally verifiable, which ascertains whether all possible attack cases are detected, thereby making the detection scheme robust.

We now look into the evil twin attack, ASMiTM attack, PS-DoS attack and rogue DHCP attacks briefly. We also describe briefly the literature survey for the prevention/detection of these attacks and the issues associated with them. We also show how DES based IDS can prove to be an effective mechanism for detecting such attacks without any need for protocol modification, encryption or installation of proprietary hardware.

1.1.3 Evil Twin Attack

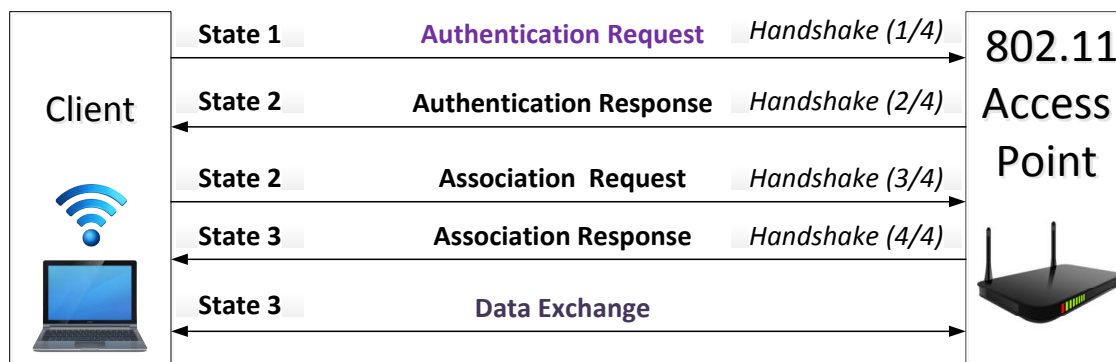


Figure 1.2: Four-way handshake between a client and access point.

When a client connects to a Wi-Fi network it first needs to establish a connection with the wireless Access Point (AP). This connection is established using a four way handshake

that occurs between client and AP as shown in Fig. 1.2. Once this handshake is successful, the client can access services offered by the AP. The AP acts a central arbiter between the client and the outside world. Once the client is connected to the AP all its communication is managed by the AP. An attacker can easily create a Rogue AP (RAP) in order to lure the client(s) into connecting them. A RAP is a software based AP that can provide all the services of the genuine AP. Usually, an attacker sets up such RAP at public places like malls, libraries, coffee shops etc. If a client connects to a RAP setup by an attacker, the attacker can gain complete control over client's activity.

Evil twin is a special form of RAP wherein an attacker spoofs the Media Access Control (MAC) address and the Service-Set Identifier (SSID) i.e., the network name of the genuine AP². When a client sees the list of available Wi-Fi APs, it sees only one AP instead of two APs as the evil twin AP spoofs both the MAC address and the SSID of the genuine AP. Modern operating systems choose the AP with a higher signal strength in-case of multiple APs configured with the same name. In presence of an evil twin AP, if the signal strength of the evil twin AP exceeds the signal strength of the genuine AP, the client(s) get associated with the evil twin AP. The attacker setting up the evil twin AP must provide a working Internet connection to the clients connecting into it else they would switch to other APs citing lack of internet connectivity.

Various solutions have been suggested in the literature to detect/prevent the evil twin attack. Few solutions propose deployment of expensive hardware in order to detect the presence of evil twin [43, 44, 45]. However, deploying such hardware increases the operational as well as maintenance costs. Authors in [43, 46] suggest protocol modifications in order to detect the evil twin attack. Though the methods suggested in [43, 46] are effective, they require software as well as hardware upgrades making the deployment cumbersome. Few methods suggested in [47, 48, 49, 50, 51, 52, 53] etc., are based on frame measurement characteristics. Since these methods are based on a similar philosophy we look into few generic methods suggested by these authors. In [50], the authors use the response time of a DNS query. They assume that the evil twin AP uses the services of the genuine AP to provide Internet services. As a result of the additional hop (Client \rightleftharpoons Evil twin AP \rightleftharpoons Genuine AP), this delay can be seen on the client as well as the genuine AP side. For example, the technique in [51] uses the inter-arrival time of the frames as a frame measure. Again, it assumes that the additional hop leads to delay in the arrival of DNS response. Technique in [52] collects various frame statistics on the core switch assuming that the evil twin uses the genuine AP for Internet services and consequently the frames from the client reach the core switch. However, all these techniques fail, if the evil twin provides its own private Internet

²Genuine AP implies an AP setup by network administrator.

connection. Few methods suggest use of encryption and digital certificates for ensuring the genuine AP identity [54, 55, 56, 57]. The usage of digital certificate introduces additional issues like certificate renewal, revocation and other certificate management issues which increases the complexity of such schemes.

From the review, it may be stated that an evil twin attack detection scheme needs to have the following features

- No modification of 802.11 protocol.
- Easy deployment to existing as well as new networks.
- Hardware costs should not be prohibitive.
- Should not require patching of underlying operating system or installation of new software.
- Scheme should have low overhead.

As a part of the first contribution, we have applied the DES framework for developing an IDS to detect the evil twin attack. It has been shown that the proposed scheme is scalable, does not require modification in the 802.11 protocol, does not require encryption and is formally verifiable. The summary of our contributions are:

1. We propose a DES based IDS that detects the evil twin AP in Wi-Fi networks. We augment the DES based IDS with *model variables* to overcome the state explosion problem.
2. The only hardware requirement is a sensor capable of sniffing the wireless data. So the cost of scheme is low and can be readily applied to legacy as well as existing networks.

1.1.4 Advanced Stealth Man-in-the-Middle (ASMiTM) Attack

An attacker launches a MiTM attack in order to place itself between two communicating parties. By establishing a MiTM, an attacker can sniff the entire communication taking place between them. Traditionally MiTM has been achieved via Address Resolution Protocol (ARP) spoofing. When two hosts want to communicate with each other, they need to know the MAC address of each other. Given the IP address of a host, the ARP is used to determine its MAC or physical address. If the sender does not know the MAC address of

the destination, it sends a broadcast ARP request asking for the MAC address corresponding to the destination host's IP address. All the hosts receiving this broadcast ARP request frame check the IP address whose MAC address is requested. Only the destination host identifies that the ARP request is meant for its IP address and sends back its corresponding MAC address in a unicast ARP reply frame. The ARP request/response frame exchange is unauthenticated. The IP-MAC mapping in the request/response frame is sent in plain text and hence is susceptible to attacks. As ARP has no mechanism for checking the authenticity of the information being sent, a host receiving an ARP frame directly updates the ARP cache entry without verifying the genuineness of the source. In addition, hosts also cache all ARP replies sent to them even if no explicit ARP request is initiated by the host

In ARP spoofing attack [58, 59, 60], an attacker crafts and sends spoofed ARP frames (i.e., ARP frames having wrong IP:MAC mapping) to victim host thereby poisoning victim's ARP cache. This is called ARP spoofing. ARP spoofing leads to many other attacks. In the ARP based Man-in-the-Middle Attack, the attacker spoofs ARP frames and inserts itself between the communication path of two target systems. This allows the attacker to sniff all the frames transferred between the target systems and paves way for the attacker to alter the messages (if it desires). An attacker can also use the ARP spoofing methods to launch DoS attack, MAC Flooding attacks etc.

ARP spoofing is still possible in open Wi-Fi networks. However, it was presumed that ARP spoofing would not be possible in Wi-Fi Protected Access II (WPA2) encrypted Wi-Fi networks. In WPA2 encrypted Wi-Fi network, two different set of keys are used for encryption purposes. A 'Pairwise Transient Key' (PVTKY) and a 'Group Transient Key' (GRPKY). All unicast messages are encrypted using the PVTKY. Both clients and the AP can encrypt as well as decrypt frames using PVTKY. The PVTKY is unique for every client that is associated with the AP. A client gets a fresh PVTKY for every new association with the same AP. The GRPKY can only be used by the AP for encryption purposes while the clients use it for decryption purposes. GRPKY cannot be used by clients for encryption purposes and is common among all clients associated with the same AP.

We propose a novel attack termed as 'ASMiTM attack' that exploits the Hole 196 vulnerability [61] and in addition breaks the replay counter synchronization between the genuine AP and the client. The combination of exploiting the Hole 196 vulnerability and breaking the replay counter (hence 'advanced'), results in MiTM attack and a prolonged ARP cache poisoning without the knowledge of genuine AP (hence 'stealth'). To prevent replay attacks in the WPA2 encrypted Wi-Fi networks, each frame contains a packet number which is monotonically increasing. Frames received with lesser packet number than the current packet number are dropped by the client assuming them to be replay frame(s).

As the spoofed ARP frame does not reach the genuine AP because of exploitation of Hole 196 vulnerability, the AP continues to send frame(s) with the old packet number which are dropped by the client. Thus, in ASMiTM attack the attacker not only is able to sniff the frames between two communicating parties but also causes frame losses between the client and the AP due to out of sync packet number value. Currently, WPA2 is the best known and widely used encryption algorithm for Wi-Fi networks. As ASMiTM attack makes it possible to launch an insider attack in a WPA2 enabled Wi-Fi network, it possesses serious security concerns for organizations. Surveys have shown that insider threats have caused more damage to an organization than outsider threats [62, 63, 64, 65]. Keeping this in mind, ASMiTM attack is a serious threat in WPA2 enabled Wi-Fi networks.

In ASMiTM attack, if ARP spoofing can be prevented/detected, the ASMiTM attack cannot take place. We now see various measures that have been suggested in the literature to defend against the ARP spoofing attacks. The best way to prevent ARP attacks is to manually assign static IPs to all the systems and maintain static IP-MAC pairings at all the systems [66]. As Wi-Fi networks are mostly deployed in dynamic environments, this scheme is not suitable. It is quite cumbersome to physically go to every new machine and perform its IP configuration. For wired networks, port based solutions have been suggested to counter ARP spoofing [67]. In this approach, each port of the switch is tied to a fixed MAC address. A change in the transmitter's MAC address can result in port shutdown or ignoring the change. The problem with this approach is that if the first sent packet itself has a spoofed MAC address then the whole system fails. In Wi-Fi networks, the clients connect to AP over the air rather than switches. Software based solutions like ARPWATCH [68], COLASOFT-CAPSA [69] keep a watch on changes in the IP-MAC pairs on the switch and report for changes in IP-MAC mapping. If any ambiguity is observed in the IP-MAC mapping it is reported to the administrator. These software solutions are inexpensive as compared to the switches having advanced port security features. However, their response time is slow making them ineffective. Several cryptography based techniques have been suggested to prevent ARP attacks namely S-ARP [70], TARP [71]. Addition of cryptographic features in ARP lead to various issues like performance penalty, faster battery draining and changes in basic ARP protocol.

Signature-based IDSs like Snort [15] can be used to detect ARP attacks and inform the administrator with an alarm. However, if signature-based IDSs are used for detection of ARP attacks it leads to large number of false positives. Only one ARP request/response frame is needed to poison the ARP cache. So, ARP spoofing does not induce any sort of anomaly in terms of frame injection, bandwidth utilization etc. So using anomaly-based IDS might prove in-effective in detecting the ARP spoofing attacks. One obvious solution for ASMiTM

attack is to never use GRPKY and always use PVTKY even for broadcast messages. However, if PVTKY is used for broadcast message, the AP has to send the same message encrypted using the PVTKY of every client that is associated with the AP. This not only adds a huge burden on the AP but also necessitates protocol changes in WPA2.

From the earlier observations it can be concluded that detecting or preventing ARP spoofing attack is difficult. As ASMiTM attack is based on ARP spoofing, detection of ASMiTM attack is a challenging task. For the evil twin attack, the system is found to be diagnosable using a simple DES framework. This means that if an evil twin attack occurs it is possible to confirm its occurrence by analyzing frame sequence and frame characteristics within finite amount of time after the evil twin attack takes place. ASMiTM attack is detectable under certain network conditions while non-detectable under other network conditions. In certain circumstances it is not possible to detect the occurrence of ASMiTM attack within finite time after the ASMiTM attack occurs. This attack can be detected using active probing. Here an IDS (actively) sends specially crafted ‘probe’ frames to ascertain the presence of an attacker. A ‘probe’ frame is a normal network frame injected with special parameters. Crafting of the ‘probe’ frame is vital as improper crafting may lead to an attacker escaping detection. The design philosophy of active probing is that, after the injection of ‘probe’ frame, both the attacker and the genuine client/server are forced to reply to the ‘probe’ frame. Based on the ‘probe’ response, the presence/absence of the attacker is ascertained.

In [72], authors have given a DES framework called I-diagnosability for partial diagnosis problems. Here some indicator events are defined and failure diagnosis (attack detection) is tested only in those paths where a fault (attack) is followed by an indicator event. The paths where there are no indicator events, may contain some (fault or normal) uncertain states, but that does hinder diagnosis of the system as a whole. For ASMiTM attack, the paths where smaller packet number is sent in the ‘probe’ frame than the current packet number synchronized at the AP and client, no indicator event is available. The I-diagnosability cannot be directly applied for the detection of ASMiTM attack as I-diagnosability requires that the fault (attack) must be diagnosable whenever the fault is followed by an indicator event. However, if a probe is sent with a smaller packet number than the current packet number synchronized at the AP and client, ASMiTM attack cannot be ascertained as the genuine client drops the frame having smaller packet number assuming it to be replay frame. So, the ‘probe’ response from the genuine client is not possible, hampering fault diagnosis (attack detection). As a result, the I-diagnosability framework fails to detect the ASMiTM attack. Hence, we propose an I^2 -diagnosability (Induced I-diagnosability) DES framework that improves over I-diagnosability framework [72] and is adopted for modeling and designing IDS for the detection of ASMiTM attack. The proposed IDS detects ASMiTM

attack and does not require any sort of encryption, protocol changes, software or hardware upgrades etc. The contributions of this scheme are enumerated below:

1. An new DES paradigm termed as I²-diagnosability (Induced I-diagnosability) framework based IDS has been designed to detect the ASMiTM attack. Like the previous DES framework, we have made use of DES model state variables in order to deal with very large size of the domains of the variables.
2. The I²-diagnosability framework based IDS has a high detection rate and accuracy while at the same time adds minimal overhead in terms of probes injected.

1.1.5 Power Save Denial of Service (PS-DoS) Attack

Wi-Fi devices like smart-phones, laptops, PDAs etc., have limited battery life owing to which conserving battery life is important. In order to preserve the battery life, the 802.11 Wi-Fi standard provides power management feature that allows clients to enter into sleep state to preserve energy without any frame losses. A client uses null data or PS-Poll frame³ to inform the AP whether it is in sleep state or wake-up state. A client sends a null data frame with PwrMgmt bit set to 1 (0) to the AP to inform that it is in sleep (wake-up) state. Null data frame does not contain any data. Encryption schemes like Wired Equivalent Privacy (WEP), WPA, WPA2, etc., only encrypt the data payload but leaves the MAC header in plain-text. So, the null data frames(s) are sent in the plain text and no authentication option is available to check for their genuineness. As a result, an attacker can send spoofed null data frames on behalf of the genuine client and falsely inform the AP that the client has woken up. Due to lack of authentication, the AP believes that the client has woken up and transmits all the buffered frames to the attacker. The attacker acknowledges the buffered frames on behalf of the sleeping client. When the genuine client actually wakes up, there are no buffered frames available for it (as they have already been retrieved by the attacker) causing Power Save Denial of Service (PS-DoS) attack. An attacker can repeat this procedure with multiple clients causing severe frame losses for the clients under attack.

Current approaches to prevent or detect the PS-DoS attack require encryption, change in protocol or installation of proprietary hardware. In Wi-Fi networks, only the data frames are encrypted. The management and control frames are unencrypted. Null data does not contain any data payload (hence the name 'null data'). So this frame is sent in clear text even on encrypted networks. Bellardo et al. in [73] suggests that all management and control frames should also be encrypted in addition to the data frames. Although, encryption

³Null data and PS-Poll frame have the same functionality. So, in this thesis, we explain the concepts using null data frame only. In case of exceptions, a clear distinction is made.

does prevent spoofing, thereby alleviating the PS-DoS attack, encryption of management and control frames require firmware upgrades on both client and AP which leads to increased deployment costs. If all the frames are encrypted, decryption of these encrypted frames result in extra CPU cycles leading to faster draining of batteries.

Qureshi et al. [74] propose an encryption based scheme to prevent the PS-DoS attack by encrypting the Association ID (AID) portion of the PS-Poll frame using pre-established Pairwise Transient Key (PVTKY). As PVTKY is only available in WPA2 encryption technique, this method is not useful for detection of PS-DoS attack on those Wi-Fi networks that are either open or use WEP based encryption. Null data frame also does not contain the AID field, which limits this method to those clients which use PS-Poll frames to inform whether they are entering sleep state or not. Leandro Meiners [75] proposes that the clients must use non-empty data frame like ICMP/ARP for reporting the change in power save mode. The motive behind this solution is to eliminate all possible frame candidates that are vulnerable to the PS-DoS attack. As ICMP/ARP frame contains data, the encryption of the data portion, prevents possible spoofing by an adversary. However, this solution has fundamental drawbacks. First, it breaks the AP compatibility with those clients that use traditional frames like null data frames, PS-Poll frames to inform about the change in power save mode. The null data frames are used by NICs for managing power, scanning channel and keeping the association awake [76]. Eliminating the processing of such frames would prevent the client from performing these functions.

Faria et al. [77] use the AP(s) as sensors and obtain the Received Signal Strength Indicator (RSSI) values for each client within its range. They have shown that the signalprints of a client and its physical location are closely correlated. Azimi et al. [78] and Chen et al. [79] also make use of physical layer countermeasures like RSSI values and Radio Frequency (RF) signal print to detect and localize the attacker. In RSSI based techniques, the approximate location of the sender is determined. Then the location of the source MAC address in the received null data frame is determined. If the difference in the location exceeds a certain threshold, the frame is not processed and tagged as spoofed. Though physical layer countermeasures are effective, they require specialized hardware and firmware changes in 802.11 which are costly. If the clients are located close to each other, their physical characteristics are similar, which may result in false positives, since a genuine client might be classified as an attacker. For PS-DoS attack, writing a signature or generating an anomaly pattern is not possible as the syntax and sequence of network traffic under normal and attack situations do not differ. So, it is not possible to detect these attacks using signature/anomaly-based IDS. These drawbacks in the existing techniques motivated us to propose a novel approach for detecting the PS-DoS attack.

The simple (untimed) DES framework and the I^2 -diagnosability framework discussed earlier cannot be used to detect the PS-DoS attack. Both DES and I^2 -diagnosability framework do not incorporate timing information in their modeling scheme. PS-DoS attack manifests itself with respect to timing information associated with transmitted frames. Hence, for detecting PS-DoS attack, we use the delay-deadline based diagnosability framework known as Real Time Discrete Event System (RTDES) framework [80]. In the RTDES framework, while modeling the system, the timing information of the events is also specified. Faults (attacks) are manifested in terms of variation of timing (delay-deadline). The contributions of this scheme are enumerated below:

1. A RTDES framework based IDS has been designed to deal with PS-DoS attack. To deal with the state explosion problem in DES modeling, model variables are used.
2. The RTDES framework based IDS has minimal resource overhead and has high attack detection rate and accuracy.

1.1.6 Rogue Dynamic Host Control Protocol (DHCP) Attack

As seen earlier, a client performs a four-way handshake in order to authenticate and associate with the AP. Following the successful four-way handshake, the client solicits the AP for its IP configuration. Most wireless APs do provide an interface for a Dynamic Host Configuration Protocol (DHCP) service. The DHCP service provides a pool of IP addresses that can be allocated when a client requests for an IP address. The primary function of a DHCP server is to allocate IP address and other vital information like subnet mask, default gateway, DNS address to the clients requesting it. The client does a four-way handshake with the DHCP server in order to obtain its IP configuration. On open Wi-Fi networks the information exchange between the client and the DHCP server is done in plain text making it susceptible to spoofing. It is also possible for a Wi-Fi network to have multiple DHCP servers. Multiple DHCP servers are usually deployed for fault tolerance and management of IP addresses in case one of the DHCP server fails.

The DHCP does not have any means to authenticate the frame exchange between the client and the DHCP server. As a result, it is possible for an attacker to set up a rogue DHCP server by spoofing the IP and MAC address of the genuine DHCP server and send fictitious IP address, DNS and gateway address (or a combination of these) to the client(s) requesting DHCP services. If a client receives multiple DHCP OFFER(s) from different DHCP server(s) (one from the genuine and other from the rogue DHCP server) it is free to choose the offer of its choice. If the client accepts the IP configuration from the rogue DHCP server then

it may lead to serious security concerns. By supplying wrong default gateway and DNS server address an attacker setting up the rogue DHCP server can re-direct client's traffic via its terminal thereby sniffing client's information, re-directing clients to phishing websites, install malware into the client's machine etc. Thus, a rogue DHCP server is a serious threat to a Wi-Fi network.

Various approaches have been suggested in the literature to detect or prevent the rogue DHCP server attack. In DHCP snooping feature [81], an administrator can configure individual switch ports to be trusted or not trusted. Only trusted ports are allowed to serve DHCP OFFER and 'DHCP Acknowledgment' (DHCPACK) frames. If a non trusted port is generating DHCP OFFER or DHCPACK frame, it is blocked at the switch level itself. The clients in Wi-Fi networks are connected over the air to the AP and not via switches. So, DHCP snooping technique might not work in the case of Wi-Fi networks. Some security experts postulate for network wide scanning for studying the IP-MAC mappings of all the clients in the network. As the IP address of the genuine DHCP server(s) is known beforehand, those IP addresses providing DHCP service but not in the white-list of genuine DHCP server(s) list can be marked as rogue [82]. However network wide scanning leads to generation of too much traffic and white-list based methods can be defeated by spoofing the IP and MAC address of the genuine DHCP server.

As DHCP lacks authentication mechanism, the RFC 3118 [83] provided the authentication option with an aim to resolve the security related issues associated with DHCP. The authors in [84] suggest the use of RSA signatures for authentication purposes. Although RSA provides a significant level of security, it is computationally expensive which may further lead to faster draining of the batteries of hand-held Wi-Fi devices like smart-phones, laptops, PDAs etc. The major issue in the adoption of the authentication option in Wi-Fi network is because of handling of key management for the large number of clients [85]. Xu et al. [86], Glazer et al. [87], Demerjian et al. [88] propose various methods that make use of digital certificates for both entity authentication as well as message authentication and is based on RFC 3118. The usage of digital certificate provides sufficient authentication and protects against the rogue DHCP server attacks. However, the usage of digital signature brings in issues like certificate management, revocation, overhead between client and DHCP server, trust issues etc.

Graaf et al. [89] in their patent describe a method that makes use of special Authentication, Authorization and Accounting (AAA) server that achieves authentication using shared secret between client and AAA server. Similar to this method, the authors in [90] make use of Kerberos V for mutual authentication of the DHCP server and the client, and for the DHCP message authentication. The main disadvantage of these schemes is the additional

communication overhead between the Kerberos, AAA server and the DHCP server. Also, The sequence of frame exchange in the four-way handshake remains the same under normal and rogue DHCP server conditions. Somers et al. [91] describe a method where in they calculate trustworthiness scores based on the DHCP offers received from the DHCP server(s) present in the network. However, the method is prone to large number of false positives because of its scoring methodology. From the various methods discussed above, it can be concluded that rogue DHCP server cannot be effectively detected by simply observing the frame exchange between the client and the DHCP server. A rogue DHCP server does not bring about a significant change in the network traffic. As a result, generation of signature or statistics from this four way frame exchange is difficult and may result in high amounts of false positives [92]. In brief, the drawbacks of the existing schemes to detect or prevent the rogue DHCP server attack are: 1) Require Digital Certificates. 2) Use of specialized servers like AAA, Kerberos. 3) Requires extensive key management strategies.

Rogue DHCP attack is similar to an evil twin attack and clearly lacks signature or anomaly. However, in all the DES frameworks discussed till now, we have assumed that the diagnoser/IDS always receives frames from the genuine client as well as the attacker reliably under normal, attack and probing conditions. However, many times the IDS fails to capture few frame(s) because of frame losses, capturing errors etc., leading to inconsistent measurement. The DES based fault detection framework handles measurement inconsistency rather strictly. DES framework assumes measurement inconsistent transitions as permanently unmeasurable and never uses them for fault diagnosis. These inconsistent transitions are inherently measurable, so considering them as permanently unmeasurable may lead to weak diagnosis.

In order to overcome this problem, we propose a Measurement Inconsistent Discrete Event System (MIDES) framework which does not assume measurement inconsistent transitions as permanently unmeasurable; albeit if a transition is measured then it is used for fault diagnosis and if the same transition leads to measurement inconsistency the possible system state(s) are predicted using an estimator diagnoser. We have used the MIDES based Intrusion Detection System (IDS) for rogue DHCP server attack detection. The steps to model is same as those of the previous DES frameworks i.e., to construct the normal and fault model followed by diagnoser construction. The MIDES diagnoser proceeds in exactly the same manner as the previously discussed DES frameworks (simple (untimed) DES, I^2 -DES, RTDES) unless a measurement inconsistency occurs. If a measurement inconsistency occurs (because of frame loss), the estimator diagnoser predicts the possible system states and continues fault diagnosis. The contributions of the scheme are enumerated below:

1. We propose a modified DES based FDD scheme called Measurement Inconsistency

DES (MIDES), which is capable of diagnosing the faults even when measurement inconsistency occurs. In contrast to traditional DES, the MIDES scheme handles the measurement inconsistency in a flexible manner, instead of assuming them as permanently unmeasurable. To handle the state explosion problem, the MIDES framework is augmented with model variables.

2. We develop an MIDES based IDS in order to detect rogue DHCP server in Wi-Fi networks and demonstrate its efficacy. The IDS designed using MIDES based framework does not require change in protocol, generates minimal extra traffic overhead and does not require patching in individual hosts.

1.2 Organization of the Thesis

The aim of this thesis is to provide a DES based IDS for detection of those attacks which does not have signature pattern or anomaly profile. A variety of MAC layer attacks are considered like evil twin attack, power-save DoS (PS-DoS) attack and rogue DHCP attack. In all of these attacks, the frame exchange sequence during normal and attack scenarios do not differ significantly. As a result, generation of signature or observation of anomaly is difficult. Even if a signature or anomaly-based IDS is developed, it may result in high amounts of false positives. This has enabled the study of feasibility of the basic idea of the thesis i.e., “use of DES paradigm for developing IDS” for different MAC layer attacks in 802.11 Wi-Fi networks. Though we have considered attacks taking place at the MAC layer, each attack requires a different DES philosophy for the development of the IDS. This shows that even though all the attacks exists at MAC layer, their characteristic features and detection philosophy differs significantly. The chapter wise organization of the thesis is given below:

Chapter 2: In this chapter, a DES based IDS for evil twin attack detection has been proposed.

Chapter 3: In this chapter, we propose a novel attack termed as ASMiTM attack. In addition, we propose a new DES framework known as I²-DES framework which is an improvement over I-DES framework. Using the I²-DES framework, we also propose an I²-DES based IDS to detect the ASMiTM attack.

Chapter 4: This chapter presents a novel technique for detecting Power Save DoS attack using RTDES framework.

Chapter 5: This chapter proposes MIDES based DES for designing an IDS to detect rogue DHCP server attack in Wi-Fi networks. In order to handle measurement inconsistency, we

propose the MIDES framework. The normal DES diagnosability considers measurement inconsistency as permanently unmeasurable leading to weak diagnosis.

Chapter 6: This final chapter highlights the conclusions arrived at and also summarizes the contributions made. New avenues for future research have also been described.



“People often represent the weakest link in the security chain and are chronically responsible for the failure of security systems.”

Bruce Schneier
American cryptographer

2

Intrusion Detection System for Evil Twin Attack in Wi-Fi networks using Discrete Event System Framework

2.1 Introduction

The IEEE 802.11 standard [93] consists of a Medium Access Control (MAC) and Physical Layer (PHY) specification for wireless connectivity for fixed, portable and moving clients within a Local Area Network (LAN). The 802.11 MAC layer is common to all 802.11 PHY layer specifications like Frequency Hopping Spread Spectrum (FHSS), Direct Sequence Spread Spectrum (DSSS), Orthogonal Frequency Division Multiplexing (OFDM), Infrared Medium etc. The 802.11 MAC performs important functions like: scanning for available Wi-Fi networks, authentication and association with a Wi-Fi network, fragmentation to deliver large sized frames, power save operations, managing the frame delivery etc. The initial IEEE 802.11 standard released in the year 1997 supported a maximum data rate of just 2 Mbps. So, the initial development was more focused on increasing the performance rather than security. As a result, the 802.11 MAC layer remained susceptible to many attacks which exploit their design weakness, features, loopholes etc.

Over the years as the technology improved, the Wi-Fi devices became more advanced supporting higher data transfer rates and encryption schemes like Wi-Fi Protected Access (WPA), Wi-Fi Protected Access II (WPA2) etc. However, in order to maintain the backward compatibility and the existence of a large number of legacy devices, the MAC layer vulner-

abilities that exist in the initial standard continued to stay even in recent standards that are released. The existence of a large number of free and unsecured Wi-Fi APs across the world make it difficult to prevent the occurrence of security threats in a Wi-Fi network. Information traveling in an open Wi-Fi network can be easily spoofed, hijacked or altered. Even if strong encryption schemes like WPA2 is used, because of the inherent protocol weakness, attacks like deauthentication/deassociation, duration inflation, attacks against 802.11i, probe request flood, authentication or association request flood, rogue access point, evil twin etc., can be launched on a Wi-Fi network by an attacker.

In this chapter, we focus on the evil twin attack which is a special form of a rogue access point. Rogue Access Point (RAP) are APs installed without an explicit authorization from a network administrator [94] or created by an attacker in order to lure the clients into connecting to them. By setting up a RAP, an attacker can re-direct clients to fake login portal(s), steal passwords, access credit card information by eavesdropping on communication links, launch Man-in-the-Middle attack etc. [95, 96]. Ma et al. [97] have provided a comprehensive taxonomy of different classes of RAP as shown in Table 2.1.

Table 2.1: Types of rogue access point

Type of Rogue Access Point (RAP)	How it is Exploited
Improperly Configured AP	Administrators setting default/weak passwords or unknowingly installing faulty/buggy device driver making AP vulnerable
Unauthorized AP	Setup without the prior permission of the network administrator
Compromised AP	Attacker cracks the encryption key using key cracking tools to evade security
Evil Twin (Phishing) AP	Clone (mimic) a genuine Wi-Fi AP by spoofing its MAC address and Service-Set Identifier (SSID) i.e., the network name of the genuine AP

In evil twin attack, an attacker creates a software based AP by spoofing the MAC address and Service-Set Identifier (SSID) i.e., the network name of the genuine AP¹. If the client connects to the evil twin AP, an attacker can gain complete control over client's activity. When a client sees the list of available Wi-Fi APs, it sees only one AP instead of two APs as the evil twin AP spoofs both the MAC address and the SSID of the genuine AP. Modern operating systems choose the AP with a higher signal strength in-case there are multiple APs configured with the same name. If the signal strength of the evil twin AP exceeds the signal strength of the genuine AP, the client(s) get associated with the evil twin AP. Higher signal strength leads to higher throughput and lesser frame loss. Hence a client always prefers to opt for APs offering higher signal strength. All modern operating systems display the list of available APs in order of their signal strengths offered.

¹Genuine AP implies an AP setup by an authorized network administrator.

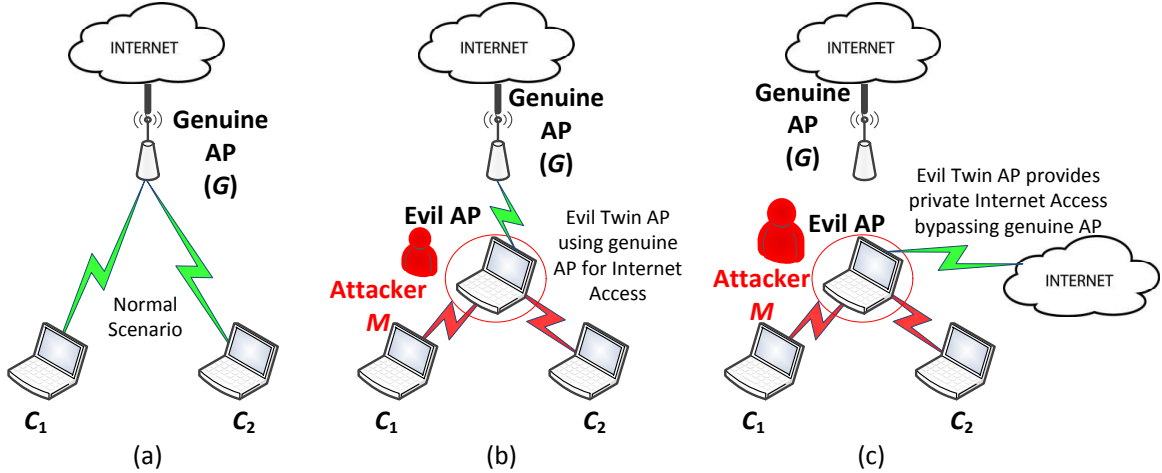


Figure 2.1: Normal and evil twin setup

It must be noted that the evil twin must provide Internet connection to the clients connecting into it. Under normal circumstances, the AP provides the Internet connection as shown in Fig. 2.1 (a). If the evil twin does not provide Internet, the clients will disconnect from the evil twin AP and switch to other APs available. For providing Internet, the evil twin can bridge the connection using the genuine AP as shown in Fig. 2.1 (b) (as genuine AP is already configured to provide Internet services) or the evil twin may provide a private Internet connection all by itself as shown in Fig. 2.1 (c). A private connection by the attacker helps it to overcome many rogue AP detection methodologies that might be configured on the genuine AP or on the core switch as explained in the later section. In our work, we assume that the attacker setting up the evil twin provides private Internet connection. Our detection methodology is capable to detect the presence of evil twin irrespective of the type of Internet access provided by the attacker.

Existing solutions to detect the presence of evil twin require installation of proprietary hardware [43, 44, 45], protocol and client side modifications such as modifications to drivers [98], operating system [99], patching client software [100], encryption [43, 101, 102] etc., measuring frame features characteristics like Round Trip Time (RTT) [50], Inter Arrival Time (IAT) [47], response time for Domain Name Server (DNS) query [49] etc., [48, 51, 53, 103, 104] etc. However these methods are either too expensive, require protocol modifications, encryption, suffer from high false positive rate, lack formalism and have scalability issues. The frame exchange sequence under normal and evil twin circumstances shows no significant difference. Only few frames need to be injected in the Wi-Fi network to launch the evil twin attack. As a result, generation of signature for evil twin is very difficult, and usage of anomaly-based IDS might result in high false positive rate. Hence, we propose a Discrete Event System (DES) based Intrusion Detection System (IDS) that helps

to overcome the drawbacks listed above and detect the evil twin AP with high detection rate and accuracy.

DES based IDS have been found to be effective in detecting security attacks in wired networks [41, 42], where attacks are mapped to failures and the diagnoser is implemented as the IDS engine. The central idea of DES modeling is to develop the normal and failure model corresponding to normal and failure scenarios. Subsequently, a diagnoser which is a state estimator is built using the states traversed in the normal and fault models. The diagnoser determines whether the system is operating under normal or failure (attack) conditions. In order to show that DES framework basically developed for industrial process systems can also be applied to detect evil twin attack, we first show how the DES framework can be used to detect failures a benchmark process of three-tank system.

However, the classical DES theory cannot be directly applied for developing an IDS for detection of evil twin attack for the following reason: Evil twin frame exchange involves many parameters like source and destination MAC address, retry bit, sequence numbers and Association IDentifier (AID) that need to be modeled. As the range of these parameters is very large, the DES model may have extremely large number of states. Throughout this thesis, we augment the DES framework with model variables, which preserve the advantages of the DES modeling framework and at the same time address the issue of state explosion. The proposed scheme is scalable, does not require modification in the 802.11 protocol, encryption, maintenance of white-list etc. and is formally verifiable. The summary of our contributions are:

1. We propose a DES based IDS that detects the evil twin AP in Wi-Fi networks. The developed IDS adheres to the 802.11 standard and does not require protocol modifications.
2. The only hardware requirement is a sensor capable of sniffing the wireless data. So the cost of scheme is low and can be readily applied to legacy as well as existing networks.
3. As DES is a formal paradigm, the correctness of the proposed scheme is verified by considering all possible attack scenarios. We augment the proposed DES based IDS with *model variables* to overcome the state explosion problem.

The rest of the chapter is organized as follows. In Section 2.2 we discuss the basics of 802.11 authentication and association mechanism followed by the evil twin attack. A detailed study of the existing approaches to tackle the evil twin attack is also presented in this section. In Section 2.3 we describe the proposed methodology to detect evil twin attack. In Section

2.4, we consider the Fault Detection and Diagnosis (FDD) of pump valve system using DES. Section 2.5 describes the DES modeling and the diagnoser construction for the evil twin attack. The correctness of the IDS along with its detection rate, accuracy and network load of the IDS are described in Section 2.6. Section 2.7 concludes the chapter.

2.2 Background and Motivation

In this section, we look into authentication and association process of 802.11 Wi-Fi networks and the vulnerabilities associated with them. The evil twin attack is elaborated next. We also discuss the existing approaches to mitigate the evil twin attack and discuss their drawbacks.

Figure 2.2 shows the four-way handshake that takes place between a client and the AP [105]. It also shows the various states a client traverses before it can start exchanging data with the AP. A Wi-Fi client can be in one of the three states (State 1, State 2, State 3) at any given time. Only after the four way handshake is successful a client can access the services offered by the AP.

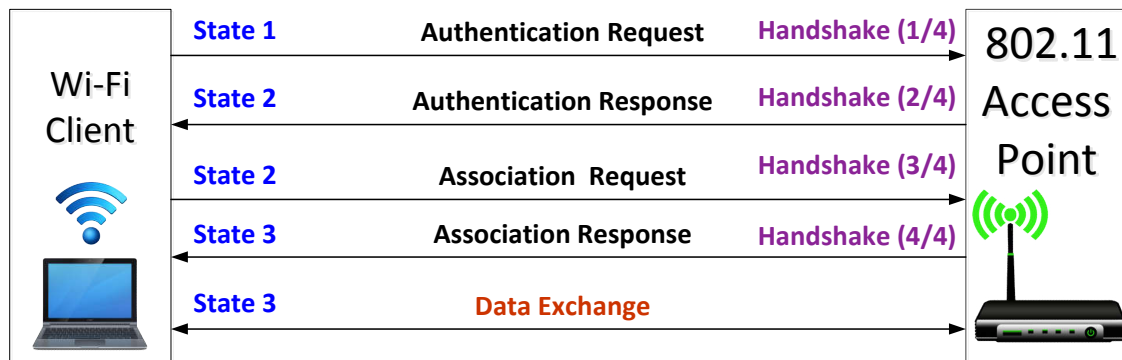


Figure 2.2: Four-way handshake between a client and access point

2.2.1 Vulnerabilities of Management and Control Frames in 802.11 Wi-Fi networks

802.11 frames are divided into three categories: Management, Control and Data frames. The management and control frames are important frames which facilitates client's connection establishment, maintenance and termination. The data frames contain the data payload to be exchanged with the AP. The various encryption schemes of 802.11 Wi-Fi networks like WEP, WPA and WPA2 encrypt only data frames. The management and control frames travel in plain text even on encrypted Wi-Fi networks making them vulnerable to

spoofing. All the frames exchanged in the four-way handshake are management frames making them vulnerable to spoofing. We now describe the evil twin attack in detail.

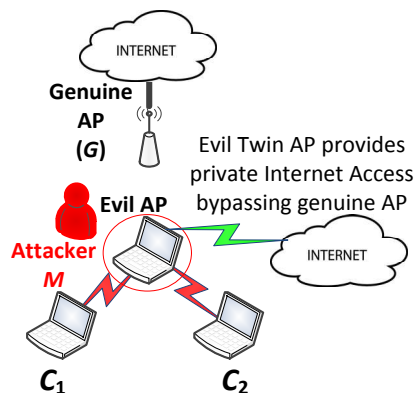


Figure 2.3: Evil twin setup

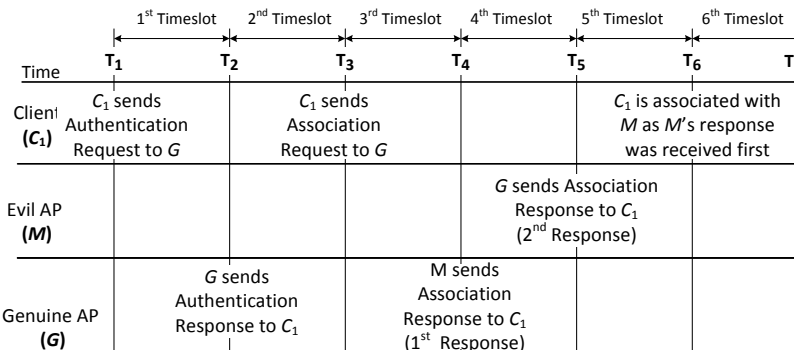


Figure 2.4: Timeline for launching evil twin attack

2.2.2 Evil Twin Attack

The evil twin attack is explained using the network setup shown in Fig. 2.3 and the timeline in Fig. 2.4. We assume an open Wi-Fi network. G is the genuine AP, M is the evil twin AP, C_1 is a client that wishes to connect to G which is unaware of the existence of M . From Fig. 2.2, it can be seen that the attacker needs to do the following to launch the evil twin attack:

1. Spoof Authentication Response Frame [Handshake (2/4)].
2. Spoof Association Response Frame [Handshake (4/4)].

We now explain how the attacker achieves these goals using the timeline shown in Fig. 2.4. Each of the distinct time-slots shown in above timeline are explained as follows:

1. [1st Timeslot (T_1) – Handshake(1/4)] : C_1 sends authentication request frame to G . M sniffs the authentication request from C_1 .
2. [2nd Timeslot (T_2) – Handshake(2/4)] : G replies to C_1 with a successful authentication response². C_1 is now authenticated to G . Authentication process in an open Wi-Fi network does not involve any sort of key exchange. It involves a simple frame exchange between the client and the AP. Sending an authentication response by M might expose M to be detected by an IDS. M does not explicitly authenticate C_1 as G

²Henceforth in this thesis, an authentication response would mean a successful authentication response.

2.2. Background and Motivation

would anyway authenticate C_1 . M maintains a list of clients authenticated to G . M also keeps a record of the parameters sent by G to C_1 when G sends an authentication response to C_1 . M then readies itself expecting a possible association request from C_1 .

3. [3rd Timeslot (T_3) – Handshake(3/4)] : C_1 sends an association request frame to G .
4. [4th Timeslot (T_4) – Handshake(4/4)] : (**Spoofed Association Response Frame**) M sends a successful association response³ to C_1 .
5. [5th Timeslot (T_5)] : G too sniffs an association request frame from C_1 sent in time-slot (T_3). So, G also sends an association response to C_1 .

Here the important point to note is that the client C_1 associates with the AP whose association response it receives first (M in this case). The first response can be either from the genuine AP (G) or evil twin AP (M) depending on their proximity to the client C_1 .

Frame Control	Duration ID	Address 1 Client MAC	Address 2 BSSID (AP MAC)	Address 3 AP MAC	Sequence Control	Address 4 Unused	Network Data	FCS Checksum		
Protocol Version	Type 0	Sub-Type 1	ToDS	FromDS	More Frag	Retry	Power Mgmt	More Data	WEP	Order

Figure 2.5: Association response frame format

For concealing identity, M needs to manipulate few fields of an association response frame shown in **bold** in Fig. 2.5.

- **Type and Sub-Type fields:** The **Type** field has its bit set to 0 while the **Subtype** field has its bit set to 1 indicating that the frame is of association response type.
- **Address 1, Address 2 and Address 3 Fields:** In an association response, the Address 1 contains the client's MAC address, Address 2 is Basic Service Set Identifier (BSSID) address and Address 3 fields contains the AP's MAC address. The attacker sets the MAC address of the genuine AP in the Address 2 and Address 3 fields so that frames appear to come from the genuine AP.
- **Sequence Control Field:** This is a 12 bit field that increments by 1 for every frame that is transmitted. As it is a 12 bit field, it can take any of the possible $2^{12} = 4096$ [0 –

³Henceforth in this thesis, an association response would mean a successful association response.

4095] values. When a client associates with an AP the association response frame contains the sequence number. The start value varies with the implementation.

- **FCS - Frame Check Sequence:** This field computes the checksum of the frame which is useful for the checking its integrity. So the checksum value varies depending on the values of various fields of the frame.

It can be observed that the above parameters of the association response frame can be manipulated easily by an attacker. For example, setting the Type-Subtype, MAC address and computing checksum is trivial. The sequence number increments by 1 for every frame. So, given an initial sequence number the future sequence numbers can be predicted. Keeping these factors in mind, it can be observed that the attacker can tweak these parameters in order to escape detection. Due to these reasons evil twin is a stealthy attack.

2.2.3 Existing Approaches to Detect or Prevent Evil Twin Attack

Now we look into the existing schemes for detection and prevention of evil twin attack. These can be broadly classified into **four** categories.

Monitoring Wireless and Wired Traffic

Most of the wireless-side solutions try to deploy sniffers throughout the network to gather vital information statistics like Service Set Identifier (SSID), MAC Address of AP, Received Signal Strength Indicator (RSSI) values etc. SSID is basically the name assigned to a Wi-Fi hotspot. The information collected using these sniffers can help the network administrators to detect RAPs. Many enterprise level wireless sniffers such as Motorola AirDefence [44], AirMagnet Wi-Fi Analyzer PRO [106] and Airwave [45] are available today which can automate the process of evil twin detection. However the solutions offered here are proprietary and the products are very expensive.

Maintaining White-list of Authorized AP(s)

In this technique white-lists of authorized MAC addresses of the APs are maintained and an alert is raised whenever a new AP with a MAC address not in the authorized list is found. Kao et al. [52] and Whelan et al. [107] detect the presence of rogue AP by maintaining a white-list of the authorized MAC address of the genuine APs in the Wi-Fi networks. The sniffer monitors the wireless traffic continuously and if an AP is found whose MAC address is not in the white-list, it is marked as rogue AP. Sriram et al. [108] and Chirumamilla et

al. [109] suggested an agent based IDS for finding out RAP(s). The task of the agent is to monitor the network and detect the presence of new APs. New APs not listed in authorized lists are marked as RAP. Shrestha et al. [110] propose a method to maintain a centralised server called AP registration centre (APRC) that maintains a list of authorised APs with their MAC address. A wireless user can check if a specific AP is genuine by querying APRC about its legitimacy in a secure way using the concept of voting and signal strength-based authentication. In evil twin AP, both the SSID and MAC address are spoofed. As a result, the above techniques fails as evil twin's MAC address matches with the MAC address of the authorized AP. Thus maintenance of white-list of authorized APs is not sufficient for detection of evil twin AP.

In [111], the authors describe a technique known as Dense Array of Inexpensive Radios (DAIR), in which they make use of the organization's desktop computers by equipping them with inexpensive USB-based wireless adapters. These wireless adapters continuously monitor the network and summarize all SSID's and BSSID's (Access Point MAC addresses) that it overhears to a database server every 90 seconds and report for anomalies. However there are two problems associated with this approach. First, the performance of the desktop computers is degraded because of the presence of wireless adapters on it. Second, the centralized database server cannot differentiate between the genuine AP and evil twin as evil twin AP has the same SSID and BSSID as that of genuine AP.

Frame Feature Extraction and Timing Based Methods

In frame feature extraction technique, the system first aggregates/logs all the packets using the mirror port of a core switch or by using the packets received from the wireless sensors deployed throughout the network segments. Using the information from the collected packets, various frame features are extracted to gain vital information regarding the presence or absence of rouge AP. The choice of the appropriate feature plays an important role in determining the success of the algorithm.

Some authors assume that evil twin AP forms a bridge between genuine AP and the client to provide Internet services to the clients. Han et al. [49] have suggested a method in which they measure the round trip time (RTT) for a DNS query. Similarly Mano et al. [50] have also made use of a local RTT metric and a frame payload slicing technique to detect rogue APs. The authors propose that the additional hop because of the evil twin induces extra delay which can be seen in the RTT. Kim et al. [112] also use the RTT measurements without relying on information from authorized lists of APs or users. Yimin et al. [51] have suggested the use of Inter-arrival time (IAT) to capture the additional delay induced by

evil twin. Aggarwal et al. [113] propose a method that computes the expected processing delay of the wireless access point by analyzing the measured RTT delay and the expected processing delay, and validating the Wi-Fi APs based upon the analysis. Based on this analysis it is determined if the AP is genuine or rogue. These schemes fail when evil twin AP provides its own private connection circumventing the effect because of additional hop.

The feature extraction and timing based solutions listed above suffer from the following drawbacks. First, it results in an additional load on the core switch. Second, the approach may result in lot of false positives in case the packets are queued by a busy router. Third, if the attacker provides its own private connection, the traffic does not even reach the core switch, leaving the attack undetected. Fourth, an attacker can simply send a spoofed response to the client, so as to avoid the time delay that may incur because of an additional hop [49] thereby circumventing the timing based detection techniques. To elaborate, the rogue AP can simply forge a response to the client, thus avoiding the time penalty of the additional wireless link. Fifth, these techniques involve wireless Network Interface Card (NIC) driver modifications which may not be practically feasible due to severe limitations [114]. Finally timing based solution are strictly technology dependent. With the rapid increase in wireless transmission rates (e.g. 802.11 ac) the differences in delay between the wired and wireless medium is slowly fading out [115]. As a result a distinct separation of wired and wireless terminals using timing based scheme becomes difficult.

Agrawal [116] have suggested an anomaly-based solution by maintaining an authenticated list and by comparing the traffic generated against this list. If any discrepancy is found in the traffic pattern, it rejects the frames coming to the AP assuming it to be coming from the evil AP. However, the method to profile the authenticated traffic is cumbersome and is susceptible to errors. Yu et al. [117] propose the use of TCP profiling for identifying the wired and wireless traffic. Using this information and the fact that the evil AP uses the genuine AP for Internet services, the delay incurred in the additional hop can be seen in the profiling. Kohno et al. [118] have shown that clock skews can be used to generate a reliable fingerprint of a device. Jana et al. [53] and Lanze et al. [119] have used the clock skew to detect unauthorized APs present in the network. They calculate the clock skews of various APs present using the IEEE 802.11 Time Synchronization Function (TSF) timestamps sent out in the beacon/probe response frames. If the clock skew calculated for a device differs from the existing clock skews maintained in master database, it is termed as rogue AP. Bratus et al. [120] showed that it is possible for an attacker to synchronize the timestamp of its rogue AP with that of the genuine AP's TSF in-order to pass the clock skew test thereby circumventing the detection procedure. An attacker can choose not to send beacons or probe response frame in order to avoid its clock skew calculation. Beacon finger-

printing based methods are suggested in [121, 122]. A beacon frame is sent by the genuine AP every 100ms in order to inform the clients about its presence. However, the attacker setting up the evil twin can configure itself and disable beacon sending circumventing the said method.

Proprietary Hardware or Software Patching

Pradip et al. [43] propose the presence of a special probing unit to detect the rouge APs. The special probing unit sends a pre-detection message with a proprietary information bit to an associated AP in the communication network. This message indicates the associated APs the beginning of the rogue AP detection mode and informs them not to respond to any probe requests. Further the special probing unit broadcasts a probe request message in the communication network. Any AP which responds to this request is marked as rogue. This technique suffers from two drawbacks. Not responding to 802.11 probe requests results in violation of the 802.11 standards. Second, an attacker may not respond to probe request to remain hidden. As a result, this method cannot detect those rogue AP(s) which do not respond to probe request sent by the special probing unit. In addition to this, the system makes use of proprietary bit and a probing unit. Many legacy system may not be able to support the proprietary bit and hence this system is not scalable.

The method in [98] uses an apparatus for passively identifying the Angle-of-Arrival (AoA) of a received Wi-Fi signal, using a standard off-the-shelf Wi-Fi receiver. Based on the AoA of the frames, the position of the rogue AP is determined and is compared with the location of the genuine AP. If a discrepancy is found, then the presence of rogue AP is ascertained. Although AoA based methods do provide promising results, the main concern is the deployment of special hardware and the effort involved for training and calibrating these systems. Ahmad et al. [99] propose a client centric solution using the RSSI values measured over time between client and APs. In their method, the AP piggybacks AP-sensitive information in IEEE 802.11 beacon frame. As a result of piggybacking, a client can manipulate the information in the beacon frame along with the measured RSSI values in order to detect the rogue AP without authentication and association to any AP.

A client centric solution is proposed in [101] to detect the evil twin AP by monitoring the Wi-Fi frames traveling in the air. Kumar et al. [46] propose a method to detect the evil twin AP which requires modifications to the Operating System, Probe Response frame, and Access Point. Mustafa et al. [102] propose a CETAD mechanism which leverages the public servers to detect evil twin attacks. CETAD requires installing an app at the client device and does not require to change the hotspot APs. In order to detect an evil twin AP, the CETAD

technique analyzes the traffic patterns and explores the similarities between the genuine APs and discrepancies between evil twin APs and genuine ones. Client centric solutions requires patching the client software, modifications to operating system and hence are not scalable.

To summarize the drawbacks of the current approaches to tackle the evil twin AP attack are as follows:

- Expensive Deployment.
- Requires change in 802.11 protocol.
- Requires proprietary hardware.
- Patching client software.
- Result in large number of false positives and false negatives.

So a scheme for detecting evil twin AP is required having the following features.

- No modification of 802.11 protocol.
- Easy deployment to existing as well as new networks.
- Hardware costs should not be prohibitive.
- Should not require patching of underlying operating system or installation of new software.
- Scheme should have low overhead.

The semantics and network behavior seen under normal and the presence of evil twin is similar. Hence generation of appropriate signatures or statistics for anomaly-based detection may lead to a lot of false positives. In such cases, a DES based IDS have proven to be an effective mechanism for detection of network attacks without any need for protocol modification, encryption or installation of proprietary hardware. A DES based IDS can be formally proved to be correct. In this chapter, we propose a DES based IDS for detecting evil twin AP that incorporates the features listed above and overcomes the drawbacks of the existing approaches.

2.3 Proposed Scheme for the Detection of Evil Twin Attack

This section describes the working principle of the proposed IDS, its components and the assumptions of IDS and attacker.

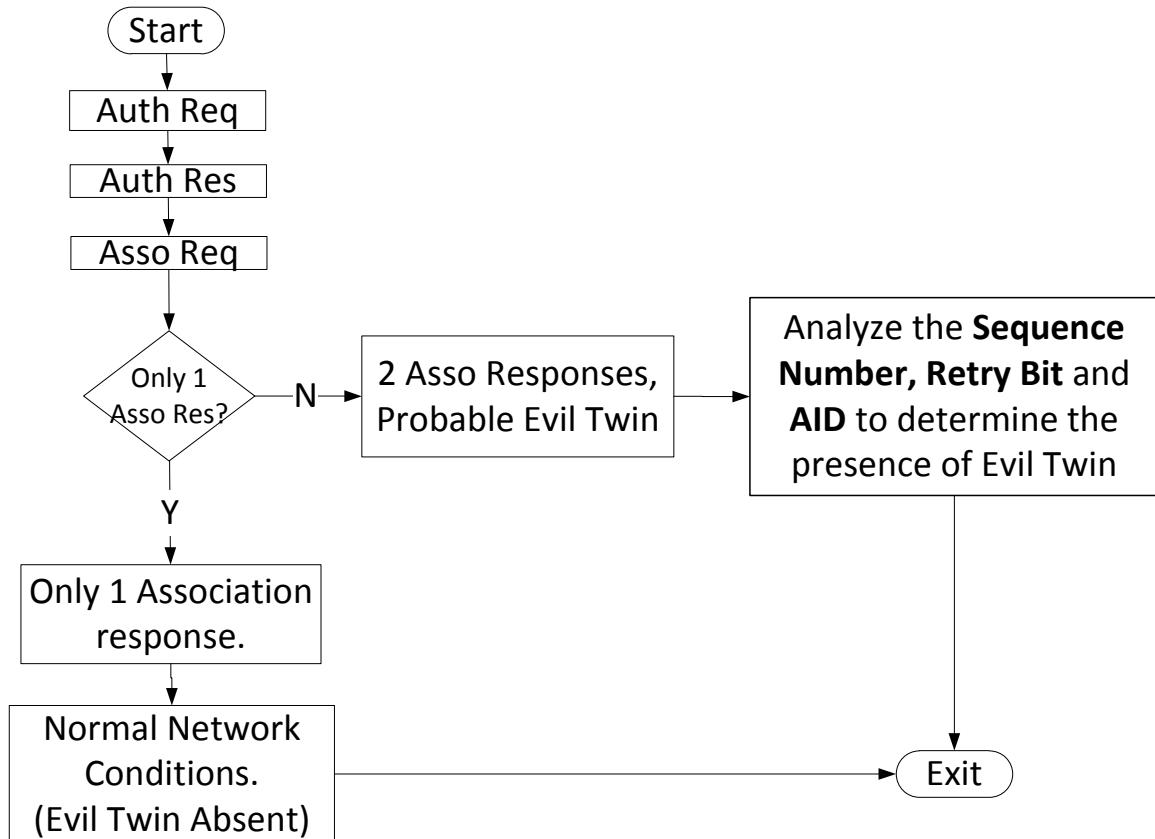


Figure 2.6: Flowchart of detection of evil twin attack

2.3.1 Working Principle of the IDS for Detecting Evil Twin Attack

The working principle of the IDS for the detection of evil attack is explained using the flowchart shown in Fig. 2.6. Initially the authentication request (Auth Req) and authentication response (Auth Res) frames are observed by the IDS for the client. After the IDS sniffs the association request (Asso Req) frame it checks whether the client receives one or two association responses. If only one association response is obtained then the network is under normal circumstances. However, if two association responses are obtained then the activity is marked as suspicious and further analysis is done for determining the presence of evil twin. It must be noted that if two association responses are received, it cannot be directly marked as an attack activity as two association responses can also be obtained under normal circumstances (For example, in case the acknowledgment for the first response is not obtained by the AP, the AP retransmits the association response making it a genuine second response). The retry bits, sequence number and AID of both responses are analyzed for concluding if evil twin AP is present. The characteristics features of these parameters that help in detection of evil twin are shown in Table 2.2

Table 2.2: Differentiating parameters of the second association response

Parameter	Normal Conditions	Evil Twin Conditions
Sequence Number	Has same sequence number as the first response.	Has different sequence number as compared to the first response.
Retry Bit	Has Retry Bit set to 1.	Has Retry Bit set to 0.
Association ID (AID)	Has same AID as the first response.	Has different AID as compared to the first response.

Out of the eight possible attack cases, six cases can be directly detected using the combination of the values of sequence number and retry bit obtained using the two association responses. Only two cases require the checking of the AID. So the evil twin AP escapes detection only when it does not send an association response at the first place. If the evil twin AP does not send an association response, the client connects to genuine AP making the evil twin dormant entity. Hence an evil twin AP tries to send a successful association response to every client requesting association with the AP. However sending of association response leads to the detection of evil twin AP by the IDS.

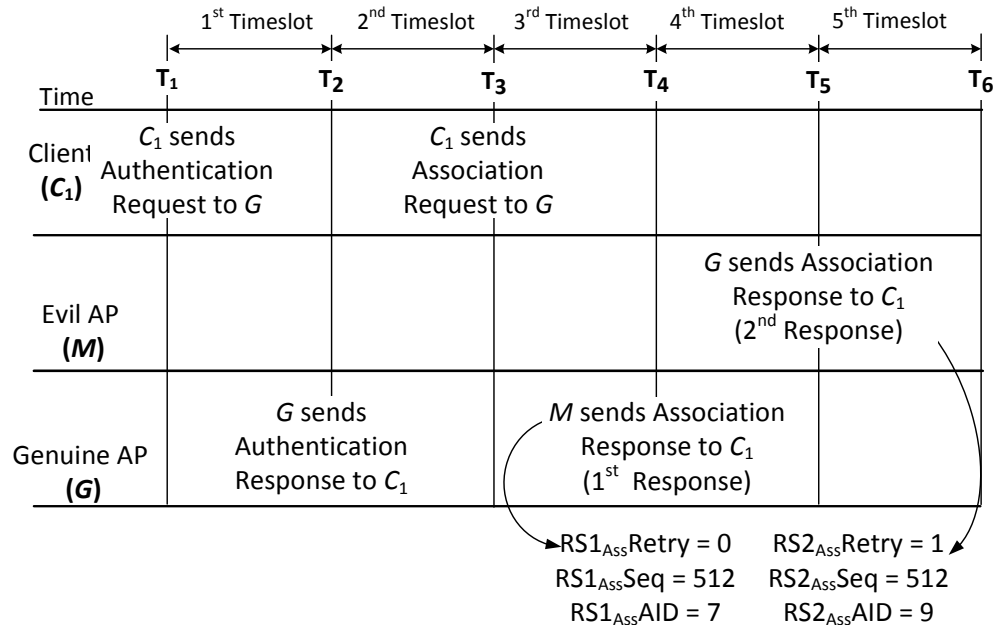


Figure 2.7: Timeline of detection of evil twin attack

Using the above explanation we show an example of evil twin attack detection technique with the help of the timeline shown in Fig. 2.7. We denote G as the genuine AP, M as the evil twin AP, C_1 as the client that wishes to connect to G who is unaware of the existence of M . We assume that the evil AP sends the first response. The first four timeslots are

same as those explained in Subsection 2.2.2. In brief, they indicate the four-way handshake which includes the first association response. In the 5th timeslot the IDS sniffs the second association response sent to the client C_1 . The second response has the same sequence number, retry bit set to 1 but has a different AID as compared to the first response. As the AID differs in the second response despite the retry bit being set, the response must have been sent by the evil twin AP leading to its detection. The same scenario is explained using the timeline shown in Fig. 2.7.

- [5th Timeslot (T_5)] : IDS sniffs the second association response. IDS checks that first and second association response have retry bit set to 0 and 1 respectively while both the responses have identical sequence number (512) and but different AID (7 & 9). An AP assign only a single AID to a particular client. Here, as both the responses contain different AIDs (despite the second response being a retransmitted one), one of the association response must be sent by the attacker setting up the evil twin AP. So, the presence of evil twin attack is detected.

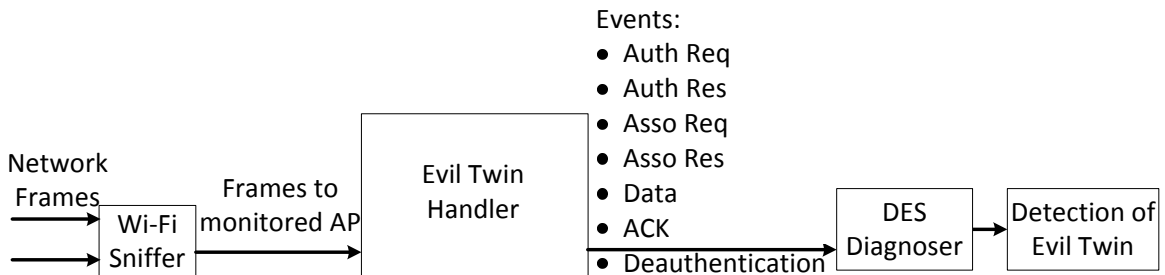


Figure 2.8: Components of the proposed IDS for detection of evil twin attack

2.3.2 IDS Components

The components of the IDS are shown in Fig. 2.8 and explained as follows:

- **Wi-Fi Sniffer:** The Wi-Fi sniffer works in promiscuous mode and captures all Wi-Fi frames traveling in the network. Only those frames destined to and from the monitored AP are sniffed. Frames destined to non-monitored APs are dropped. The Wi-Fi sniffer forwards the captured frames to the “Evil Twin Handler”.
- **Evil Twin Handler:** The “Evil Twin Handler” is responsible for extracting vital information like retry bit, sequence number, AID from the association response frames. The “Evil Twin Handler” component is also responsible for the generation of events

like *Auth Req*, *Auth Res*, *Asso Req*, *Asso Res*, *Data*, *ACK*, *Deauthentication* and forwarding them to the DES Diagnoser. The DES diagnoser determines if the evil twin attack has occurred or not based on the sequence of events captured.

- **DES Diagnoser:** The DES diagnoser is actually implemented as a software module and used as attack detector. The DES diagnoser forms the crux of the detection methodology and is constructed from the DES model under normal and attack conditions. The construction of the diagnoser is described in Subsection 2.4.4.

2.3.3 Attacker and IDS Assumptions

In this sub-section, we look at the attacker and IDS assumptions along with the motivation behind each assumption.

Attacker Assumptions

- **Attacker (evil twin AP) does not send beacon frames neither replies to probe request.**

Beacon frames are sent by an AP periodically to inform about its presence. The transmission of beacon frame by the attacker may lead to its detection since beacon frame consists of vital information about the network. Methods like [53, 118, 123] use the beacon frame information to detect evil twin AP. By not sending beacons, the attacker overcomes the methods suggested in [53, 118, 123] and also conceals its identity.

- **Attacker does not depend on the genuine AP to provide Internet to the client and uses its own private connection.**

Most of the rogue AP/evil twin AP setup studied in the literature assume that the attacker is connected to the genuine AP, to provide Internet services to the client. We assume that the attacker provides private connection for each client connected to it. Many techniques [49, 50, 51] use the additional delay induced (because of the additional hop traversed to connect to the genuine AP to provide Internet connection) for detecting the evil twin AP.

- **Only one evil twin AP is present.**

We consider the presence of a single evil twin AP in the network for simplicity of illustration. Our proposed scheme works even if multiple evil twin APs are present.

- **Attacker aims to associate maximum clients to it to cause maximum damage**

The attacker always sends an association response to an association request. This en-

ables the attacker to cause maximum damage to the connected clients by re-directing them to phishing websites, steal credentials etc.

IDS Assumptions

- **Monitoring of authorized APs only.**

The IDS maintains a white-list of the MAC address of the AP that need to protected. Only the frames destined to and from these APs are monitored. Frames destined to other APs are discarded.

- **Genuine AP always replies to client's request.**

We assume that the genuine AP always replies to client's request i.e., there is no instance of DoS attack on genuine AP.

- **Proposed IDS has sniffing capabilities.**

The IDS has the ability to promiscuously sniff the Wi-Fi frames traveling in the air.

2.4 Fault Detection and Diagnosis Theory of Discrete Event System (DES): Three Tank System

In this section we present the DES framework augmented with *model variables*. The *DES model G* is defined as:

$$G = \langle X, X_0, \Sigma, \mathfrak{S}, V \rangle \quad (2.1)$$

- X is the finite set of states.
- X_0 is the initial state.
- Σ is the set of events. Note that an event can be measurable or unmeasurable.
- \mathfrak{S} is the set of transitions.
- V is the set of model variables. Each element v_i of V can take values from a domain Dom_i .

A transition $\tau \in \mathfrak{S}$ is defined as a five-valued tuple $\langle x, x^+, \sigma, check(v), assign(v) \rangle$, where

- x is the initial state of the transition denoted as $initial(\tau)$.
- x^+ is the final state of the transition denoted as $final(\tau)$.

- $\sigma \in \{\Sigma \cup \epsilon\}$ is an event on which the transition τ is enabled.
- $check(V)$ represents the conditions on a subset of the model variables. For firing τ , along with the enabling event σ , $check(V)$ should hold true.
- $assign(V)$ represents a subset of the model variables and assignment of the values from their corresponding domain, when τ fires.

A *trace* of the model G is a sequence of transitions generated by G denoted as $s = \langle \tau_1, \tau_2, \dots, \tau_f \rangle$, where $initial(\tau_{i+1}) = final(\tau_i)$, for $i = 1$ to $(f - 1)$. We denote $initial(\tau_1)$ as $initial(s)$ and $final(\tau_f)$ as $final(s)$. The set of all traces generated by G is the language of G , denoted as $L(G)$. Naturally, $L(G)$ is a subset of \mathfrak{S}^w , where \mathfrak{S}^w is the set of all infinite sequences of \mathfrak{S} . Any finite member of $L(G)$ is in \mathfrak{S}^* , the Kleene closure of \mathfrak{S} . The post language of G after a trace s is denoted as $L(G)/s = \{t \in \mathfrak{S}^* \mid st \in L(G)\}$. $L_f(G)/s \subset L(G)/s$ comprises finite prefixes of the infinite traces of $L(G)/s$.

2.4.1 DES Modeling: Measurement Limitations and Failure Diagnosis

Limitations of measurement give rise to uncertainty in transitions in the observed dynamics of the model. In this sub-section the notion of measurement limitation in the DES framework is formally introduced and the consequent uncertainty in transitions in G is characterized. In order to explain the definitions in a more clear and concise way we take help of the three tank system explained in Subsection 2.4.2. Very briefly, the three tank system involves filling of tank T_1 followed by filling of tank T_2 . Both the tanks are drained into tank T_3 . After tank T_3 gets full, the mixture in tank T_3 is drained off. We have reproduced few standard definitions available in the DES literature [72, 124, 125] for the sake of completeness and simplicity of explanation.

Definition 1. Measurable and unmeasurable events/transitions: Any event that can (cannot) be measured using sensors are measurable (unmeasurable) events. A **transition** $\tau_i = \langle x, x^+, \sigma, check(V), assign(V) \rangle$ is said to be a measurable (unmeasurable) transition if σ is a measurable (unmeasurable) event. \mathfrak{S}_m and \mathfrak{S}_u denote the set of measurable and unmeasurable transitions. In Fig. 2.10 the event “ T_1 Filling” is a measurable event so the transition τ_1 associated with the event “ T_1 Filling” is also measurable.

Definition 2. Measurement equivalent transitions and states: Two transitions $\langle x_1, x_1^+, \sigma_1, check_1(V), assign_1(V) \rangle$ and $\langle x_2, x_2^+, \sigma_2, check_2(V), assign_2(V) \rangle$ are equivalent if $\sigma_1 = \sigma_2$ (same event), $check_1(V) \equiv check_2(V)$ (same equalities over the same subset of variables in V), and $assign_1(V) \equiv assign_2(V)$ (same subset of model variables with same

assignment). If $\tau_1 \equiv \tau_2$ then the source states of the transitions are equivalent and so are the destination states, i.e., $x_1 \equiv x_2$ and $x_1^+ \equiv x_2^+$. In Fig. 2.10, upon comparing the transitions τ_1 and τ'_1 we observe that the same event (T_1 Filling) is associated with both the transitions. So, $\tau_1 \equiv \tau'_1$ which implies $s_0 \equiv s'_0$ and $s_1 \equiv s'_1$. As a result when the event “ T_1 Filling” occurs, it cannot be said with certainty whether the system has taken the transition τ_1 or τ'_1 . So, the transitions τ_1 and τ'_1 are said to be measurement equivalent transitions.

Definition 3. Projection and Inverse Projection Operator: A **projection** operator $P : \mathfrak{S}^* \rightarrow \mathfrak{S}_m^*$ is defined as: $P(\epsilon) = \epsilon$ (null string); $P(\tau) = \tau$ if $\tau \in \mathfrak{S}_m$; $P(\tau) = \epsilon$ if $\tau \in \mathfrak{S}_u$; $P(s\tau) = P(s)P(\tau)$, where $s \in L_f(G), \tau \in \mathfrak{S}$. The function P erases the unmeasurable transitions from the argument finite trace. $P(s)$ is termed as the *measurable finite trace* corresponding to the finite trace s . An **inverse projection** operator $P^{-1} : \mathfrak{S}_m^* \rightarrow 2^{\mathfrak{S}^*}$ is defined as: $P^{-1}(s) = \{s' \in L_f(G) \mid sEs'\}$. Thus, $P^{-1}(s)$ encompasses all possible sequences of transitions that are equivalent to the finite trace s . The projection function P , the inverse function P^{-1} and the measurement equivalence E of finite traces can be extended to traces $\in \mathfrak{S}^w$, in a natural way.

Definition 4. Measurable Equivalent Traces: Two finite traces s and s' are said to be measurement equivalent if the following relation holds: $P(s) = \langle \tau_1, \tau_2, \dots, \tau_n \rangle$, $P(s') = \langle \tau'_1, \tau'_2, \dots, \tau'_n \rangle$ and $\tau_i E \tau'_i, 1 \leq i \leq n$.

We use the symbol E to denote measurement equivalence of finite traces as well as that of transitions, with slight abuse of notation. The equivalence of finite traces s and s' implies that if measurable transitions are extracted from s and s' by use of the operator P , then all the transitions are measurement equivalent. Following Definition 2, it can be seen that the trace $\langle \tau_1, \tau_2, \tau_3 \rangle$ in Fig. 2.10, is measurement equivalent to the trace $\langle \tau'_1, \tau'_2, \tau'_3 \rangle$.

Definition 5. Normal G -state/ G -transition and Failure G -state/ G -transition: States that are traversed by the system when operating without any faults (attack) are known as **normal G -state**. X_N denotes the set of all normal states. A G -transition $\langle x, x^+ \rangle$ is called a *normal G -transition* if $x, x^+ \in X_N$. States that are traversed by the system when operating under **failure** circumstances are known as Failure G -state. X_{F_i} denotes the set of all failure states. A G -transition $\langle x, x^+ \rangle$ is called a *failure G -transition* if $x, x^+ \in X_{F_i}$. In Fig. 2.10, the states s_0, s_1, s_2 are normal G -states. The transitions associated with these states viz. τ_1, τ_2 are normal G -transitions. The states s'_0, s'_1, s'_2 are failure G -states. The transitions associated with these states viz. τ'_1, τ'_2 are failure G -transitions.

Definition 6. Failure causing G -transition: A transition $\langle x, x^+ \rangle$, where $x \in X_N$ and $x^+ \in X_{F_i}$, is called a *failure causing G -transition* indicating the occurrence of some failure. Since failures are assumed to be *permanent*, there is no transition from any $x \in X_{F_i}$

to $x^+ \in X_N$. In Fig. 2.10, the transition τ_{0F1} is the failure causing G -transition as it moves the model from normal to the failure state. All failure causing G -transition are inherently unmeasurable.

The objective of the failure diagnosis problem is to determine the occurrence of a failure F_i . If the event (σ) corresponding to τ_{F_i} is measurable, failure diagnosis is trivial. So the failure causing transitions are assumed to be unmeasurable. For such failure causing transitions, σ is unmeasurable. As σ is unmeasurable, there are no checks or assignment for model variables. As failures are assumed to be *permanent*, there is no transition from any state in x_{F_i} to any state in X_N . The event related to causing F_i is denoted as σ_{F_i} .

2.4.2 Application of Failure Detection and Diagnosis Theory of DES on Three Tank System

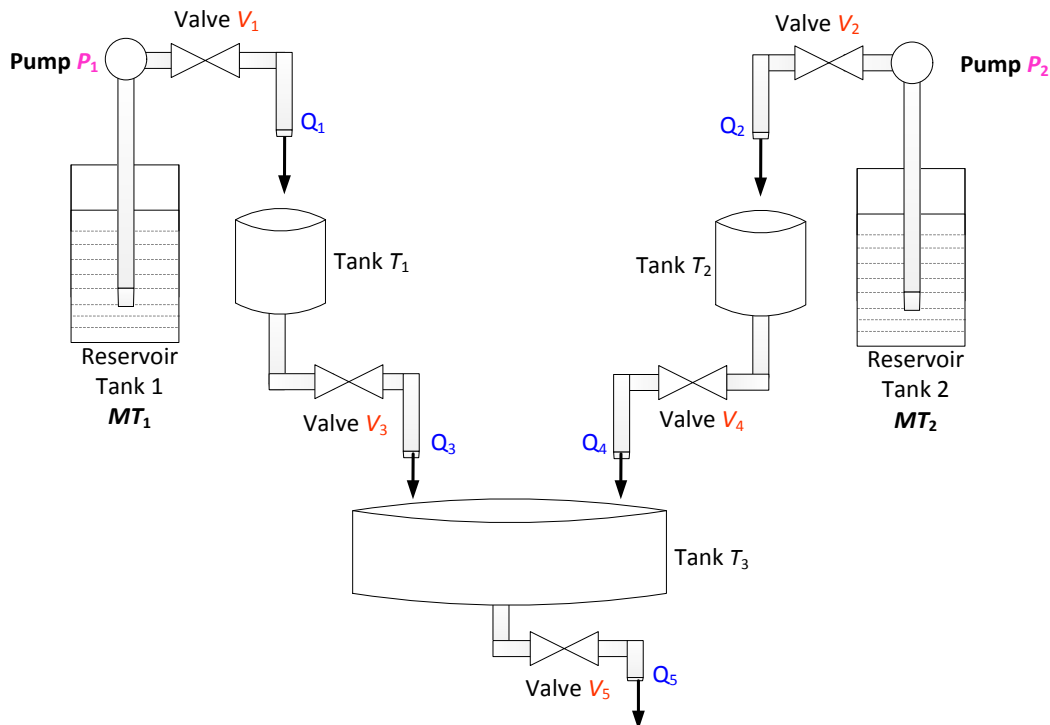


Figure 2.9: The three tank system

We demonstrate the Failure Detection and Diagnosis (FDD) theory of the DES using an example of three connected tanks [126] viz. T_1 , T_2 and T_3 as shown in Fig. 2.9. Tanks T_1 and T_2 are supplied substances from reservoir tanks MT_1 and MT_2 using pumps P_1 and P_2 , respectively. The flow through pumps P_1 and P_2 are controlled using valves V_1 and V_2 , respectively. Tanks T_3 and T_1 are connected by means of valve V_3 . Tanks T_3 and T_2 are connected by means of valve V_4 . This broad arrangement of three tanks is used in many

industrial process e.g., which require mixing of two substances in a predetermined ratio (β , say). To elaborate, MT_1 and MT_2 contain the substances that are to be mixed and the ratio of the volume of tank T_1 to T_2 is $\beta : 1$. For this example, we assume $\beta = 1$ (so 1 unit of substance is added from each tank). First the substance from MT_1 is filled in the tank T_1 followed by filling of T_2 from MT_2 . Then the substances from T_1 and T_2 are drained into the tank T_3 . The substance in T_3 is stirred to ensure that the mixture is homogeneous. Once T_1 and T_2 are emptied, they are refilled again and the process repeats. When T_3 is full the homogenous mixture is drained out for usage.

The control of flows in the system is done by opening and closing of the valves by a controller which in turn depends on the two types of sensor outputs viz. (i) level sensors of the tanks and (ii) flow sensors of the valves. The tanks are equipped with two level sensors each in order to determine whether the level of the substance in the tank is low or high. For example, in the tank T_1 if the level of substance is at the lowest (highest) point, the low (high) level sensor indicated by $T_1\text{Low}$ ($T_1\text{High}$) gives output 1. There is a flow sensor (indicated as Q_1, \dots, Q_5) beside every valve that indicates whether substance is flowing through the adjoining pipe or not. For example, $Q_3 = 1$ (0) if substance is flowing (not flowing) through the pipe corresponding to Q_3 which connects T_1 to T_3 . Table 2.3 shows the details of the sensors, their possible outputs and their interpretations.

Table 2.3: Sensor map for three tank system

Sensor	Possible Outputs	Interpretation
$T_i\text{Low}$ ($i = 1, 2, 3$)	0	$T_i\text{Low} = 0$ implies substance in the tank T_i is NOT at the lowest level.
	1	$T_i\text{Low} = 1$ implies substance in the tank T_i IS at the lowest level.
$T_i\text{High}$ ($i = 1, 2, 3$)	0	$T_i\text{High} = 0$ implies substance in the tank T_i is NOT at the highest level.
	1	$T_i\text{High} = 1$ implies substance in the tank T_i IS at the highest level.
Q_i ($i = 1, 2, 3, 4, 5$)	0	NO Flow measured by Flow sensor Q_i
	1	POSITIVE Flow measured by Flow sensor Q_i

Now we elaborate the working of the three tank system in terms of sensor outputs and controller commands to open/close the valves. Initially, all the tanks have their substances at the lowest levels, indicated by $T_1\text{Low} = T_2\text{Low} = T_3\text{Low} = 1$ (and obviously $T_1\text{High} = T_2\text{High} = T_3\text{High} = 0$). As all the valves are closed there is no flow in any of the pipes, so flow sensor outputs: $Q_1 = 0, \dots, Q_5 = 0$. First T_1 is to be filled which is initiated by the controller issuing the command $CV_1 = 1$. This results in opening of the valve V_1 to allow the flow of substance into T_1 . Once the substance starts flowing into T_1 from MT_1 , Q_1 becomes 1 and $T_1\text{Low}$ becomes 0. After the tank T_1 is full $T_1\text{High}$ becomes 1 and the controller issues the command $CV_1 = 0$ to close the valve V_1 . Flow to T_1 stops and Q_1 becomes 0.

Next, in a similar manner, valve V_2 is opened ($Q_2 = 1$ and $T_2\text{Low} = 0$) in order to fill the tank T_2 . After T_2 gets full, $T_2\text{High} = 1$ and controller makes $CV_2 = 0$ which stops the flow to T_2 making $Q_2 = 0$. After both T_1 and T_2 are full the controller issues the command $CV_3 = 1$ and $CV_4 = 1$ which open the valves V_3, V_4 simultaneously and substances from T_1 and T_2 are allowed to fall into the tank T_3 ; $Q_3 = 1, Q_4 = 1$ and $T_3\text{Low} = 0$. We have assumed that $\beta = 1$ and the flow rate from T_1 and T_2 to T_3 are same. So T_1 and T_2 get emptied at the same time (sensor outputs $T_2\text{Low} = 1$ and $T_2\text{Low} = 1$). Tanks T_1 and T_2 are refilled again and the process continues till T_3 becomes full. In the current system it is assumed that the volume of the tank T_3 is ' h ' times the volume of the tanks T_1 and T_2 taken together. So after ' h ' iterations of dropping of the substances from T_1 and T_2 , T_3 gets full (indicated by $T_3\text{High} = 1$). Controller opens the valve V_5 by the command $CV_5 = 1$ and the mixture is drained out for usage. When T_3 becomes empty (indicated by $T_3\text{Low} = 1$) the whole process is repeated.

We consider the 'stuck-closed' fault of valve V_5 (denoted as $F1$) for the three connected tank system. Due to the 'stuck-closed' fault of valve V_5 , the mixture does not drain out of the tank T_3 (i.e., $Q_5 = 0$) even when the controller issues the command $CV_5 = 1$. The 'stuck-closed' fault results in stalling of the system. Such catastrophic faults can be detected by DES models without needing to resort to any complex frameworks like hybrid systems that employ continuous dynamics [72].

Now we discuss the modeling of the three tank system using the DES framework. The DES model G used to represent three tank system under normal and fault scenarios is shown in Fig. 2.10. The various components of G are as follows:

$$X = \{s_0, s_1, s_2, s_3, s_4, s_5, s_6, s_7, s_8, s_9, s'_0, s'_1, s'_2, s'_3, s'_4, s'_5, s'_6, s'_7, s'_9\}$$

$$X_0 = \{s_0\}$$

$$\Sigma = \{T_1\text{Empty}, T_1\text{Filling}, T_1\text{Full}, T_2\text{Empty}, T_2\text{Filling}, T_2\text{Full}, T_3\text{Empty}, T_3\text{Filling}, T_3\text{Full_Drain}, T_1 \& T_2\text{Refill}, T_3\text{Full}\}$$

$$\mathfrak{S} = \{\tau_0, \tau_1, \tau_2, \tau_3, \tau_4, \tau_5, \tau_6, \tau_7, \tau_8, \tau_9, \tau_{11}, \tau_{0F1}, \tau'_1, \tau'_2, \tau'_3, \tau'_4, \tau'_5, \tau'_6, \tau'_7, \tau'_8, \tau'_{10}, \tau'_{12}\}$$

$$V = \{\epsilon\}^4$$

States and transitions belonging to normal (attack) model are denoted by the non-primed (primed) notations. The occurrence of fault is modeled by the failure causing transition τ_{0F1} . For simplicity of illustration, we assume that fault can occur only from state s_0 .

⁴As the number of states in the three tank system are not large, model variables are not used. So corresponding to each transition of the three tank system both $check(V)$ and $assign(V)$ are set to $\langle -, - \rangle$. However the model variables are used in the proposed IDS for detection of the evil twin attack in order to avoid the state explosion problem. The details are elaborated later while discussing the DES model of evil twin attack in later sections.

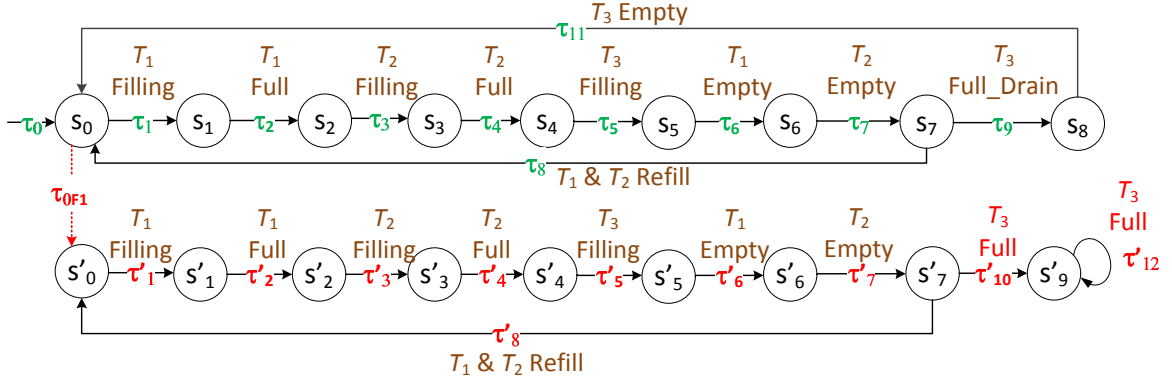


Figure 2.10: DES of the three tank system shown in Fig. 2.9

In Fig. 2.10, the transitions are not explicitly detailed as their six tuples, however, the corresponding event is shown. Table 2.4 illustrates the events corresponding to the sensor outputs and control commands. The transitions which are enabled by these events are shown in Table 2.4. For explanation of the modeling we discuss the details of a normal G -transition (τ_1) and an F_i - G -transition (τ'_{10}).

τ_1 has the event T_1 Filling. When the sensor outputs for the tank T_1 are $-T_1$ Low = 1 and T_1 High = 0, the controller issues the command $CV_1 = 1$ which opens the valve V_1 . This allows flowing of the substance to T_1 and the flow sensor output $Q_1 = 1$. These sensor outputs and the controller command are represented by the event T_1 Filling that corresponds to the transition τ_1 .

From s_0 there is another transition τ_{0F1} . τ_{0F1} indicates occurrence of a failure. Let us consider the F_i - G -transition τ'_{10} which has the event T_3 Full associated with it. When the system is in state s'_7 (if F_i has occurred), the sensor outputs for the T_3 are $-T_3$ Low = 0 and T_3 High = 1, indicating that T_3 is full and the mixture must be drained out. Upon reading the sensor outputs, the controller issues the command $CV_5 = 1$ which should open the valve V_5 leading to draining out of the mixture. However, because of failure F_i , the valve remains stuck-closed and as the mixture does not flow out, resulting in the sensor Q_5 outputting 0.

If the fault has occurred the controller maintains the command $CV_5 = 1$ perpetually because T_3 does not become empty and the sensor output T_3 Low = 1, which makes $CV_5 = 0$, never occurs. As a result the system moves from state s'_7 to s'_9 and continues to remain there forever, which is modeled as the self loop τ'_{12} (and the event is T_3 Full). On the other hand, if the system is normal, T_3 becomes empty and it is modeled by the transition τ_{11} . In a similar manner, referring to Table 2.4 and the discussion on the working of the three tank system, the whole modeling given in Fig. 2.10 can be explained.

In the three tank system under consideration, we have assumed that the volume of the

Table 2.4: Transitions along with their representation. Events, sensor conditions, controller commands of the DES model of the three tank system shown in Fig. 2.10

Transition	What it Represents	Event	Sensor Conditions	Controller Commands
τ_0	All Tanks are Empty	Start	$T_1\text{Low} = 1, T_2\text{Low} = 1, T_3\text{Low} = 1,$ $T_1\text{High} = 0, T_2\text{High} = 0, T_3\text{High} = 0,$ $Q_1 = 0, Q_2 = 0, Q_3 = 0, Q_4 = 0, Q_5 = 0.$	$CV_1 = 0, CV_2 = 0, CV_3 = 0,$ $CV_4 = 0, CV_5 = 0,$
$\tau_1 \ \& \ \tau'_1$	Tank T_1 Filling	T_1 Filling	$T_1\text{Low} = 0, T_2\text{Low} = 1, T_3\text{Low} = 1,$ $T_1\text{High} = 0, T_2\text{High} = 0, T_3\text{High} = 0,$ $Q_1 = 1, Q_2 = 0, Q_3 = 0, Q_4 = 0, Q_5 = 0.$	$CV_1 = 1, CV_2 = 0, CV_3 = 0,$ $CV_4 = 0, CV_5 = 0,$
$\tau_2 \ \& \ \tau'_2$	Tank T_1 Full	T_1 Full	$T_1\text{Low} = 0, T_2\text{Low} = 1, T_3\text{Low} = 1,$ $T_1\text{High} = 1, T_2\text{High} = 0, T_3\text{High} = 0,$ $Q_1 = 0, Q_2 = 0, Q_3 = 0, Q_4 = 0, Q_5 = 0.$	$CV_1 = 0, CV_2 = 0, CV_3 = 0,$ $CV_4 = 0, CV_5 = 0,$
$\tau_3 \ \& \ \tau'_3$	Tank T_2 Filling	T_2 Filling	$T_1\text{Low} = 0, T_2\text{Low} = 0, T_3\text{Low} = 1,$ $T_1\text{High} = 1, T_2\text{High} = 0, T_3\text{High} = 0,$ $Q_1 = 0, Q_2 = 1, Q_3 = 0, Q_4 = 0, Q_5 = 0.$	$CV_1 = 0, CV_2 = 1, CV_3 = 0,$ $CV_4 = 0, CV_5 = 0,$
$\tau_4 \ \& \ \tau'_4$	Tank T_2 Full	T_2 Full	$T_1\text{Low} = 0, T_2\text{Low} = 0, T_3\text{Low} = 1,$ $T_1\text{High} = 1, T_2\text{High} = 1, T_3\text{High} = 0,$ $Q_1 = 0, Q_2 = 0, Q_3 = 0, Q_4 = 0, Q_5 = 0.$	$CV_1 = 0, CV_2 = 0, CV_3 = 0,$ $CV_4 = 0, CV_5 = 0,$
$\tau_5 \ \& \ \tau'_5$	Tank T_3 Filling, T_1 and T_2 Draining	T_3 Filling	$T_1\text{Low} = 0, T_2\text{Low} = 0, T_3\text{Low} = 0,$ $T_1\text{High} = 0, T_2\text{High} = 0, T_3\text{High} = 0,$ $Q_1 = 0, Q_2 = 0, Q_3 = 1, Q_4 = 1, Q_5 = 0.$	$CV_1 = 0, CV_2 = 0, CV_3 = 1,$ $CV_4 = 1, CV_5 = 0,$
$\tau_6 \ \& \ \tau'_6$	Tank T_1 Empty	T_1 Empty	$T_1\text{Low} = 1, T_2\text{Low} = 0, T_3\text{Low} = 0,$ $T_1\text{High} = 0, T_2\text{High} = 0, T_3\text{High} = 0,$ $Q_1 = 0, Q_2 = 0, Q_3 = 0, Q_4 = 0, Q_5 = 0.$	$CV_1 = 0, CV_2 = 0, CV_3 = 0,$ $CV_4 = 0, CV_5 = 0,$
$\tau_7 \ \& \ \tau'_7$	Tank T_2 Empty	T_2 Empty	$T_1\text{Low} = 1, T_2\text{Low} = 1, T_3\text{Low} = 0,$ $T_1\text{High} = 0, T_2\text{High} = 0, T_3\text{High} = 0,$ $Q_1 = 0, Q_2 = 0, Q_3 = 0, Q_4 = 0, Q_5 = 0.$	$CV_1 = 0, CV_2 = 0, CV_3 = 0,$ $CV_4 = 0, CV_5 = 0,$
$\tau_8 \ \& \ \tau'_8$	Tank T_1 & T_2 Re-Filling	T_1 & T_2 Refill	$T_1\text{Low} = 1, T_2\text{Low} = 1, T_3\text{Low} = 0,$ $T_1\text{High} = 0, T_2\text{High} = 0, T_3\text{High} = 0,$ $Q_1 = 0, Q_2 = 0, Q_3 = 0, Q_4 = 0, Q_5 = 0.$	$CV_1 = 0, CV_2 = 0, CV_3 = 0,$ $CV_4 = 0, CV_5 = 0,$
τ_9	Tank T_3 Full and Draining	T_3 Full_Drain	$T_1\text{Low} = 1, T_2\text{Low} = 1, T_3\text{Low} = 0,$ $T_1\text{High} = 0, T_2\text{High} = 0, T_3\text{High} = 1,$ $Q_1 = 0, Q_2 = 0, Q_3 = 0, Q_4 = 0, Q_5 = 1.$	$CV_1 = 0, CV_2 = 0, CV_3 = 0,$ $CV_4 = 0, CV_5 = 1,$
τ_{0F1}	Failure Causing	Fault	$T_1\text{Low} = 1, T_2\text{Low} = 1, T_3\text{Low} = 1,$ $T_1\text{High} = 0, T_2\text{High} = 0, T_3\text{High} = 0,$ $Q_1 = 0, Q_2 = 0, Q_3 = 0, Q_4 = 0, Q_5 = 0.$	$CV_1 = 0, CV_2 = 0, CV_3 = 0,$ $CV_4 = 0, CV_5 = 0,$
$\tau_{11} \ \& \ \tau'_{11}$	Tank T_3 Empty	T_3 Empty	$T_1\text{Low} = 1, T_2\text{Low} = 1, T_3\text{Low} = 1,$ $T_1\text{High} = 0, T_2\text{High} = 0, T_3\text{High} = 0,$ $Q_1 = 1, Q_2 = 0, Q_3 = 0, Q_4 = 0, Q_5 = 0.$	$CV_1 = 1, CV_2 = 0, CV_3 = 0,$ $CV_4 = 0, CV_5 = 0,$
τ'_{10}, τ'_{12}	Tank T_3 Full	T_3 Full	$T_1\text{Low} = 1, T_2\text{Low} = 1, T_3\text{Low} = 0,$ $T_1\text{High} = 0, T_2\text{High} = 0, T_3\text{High} = 1,$ $Q_1 = 1, Q_2 = 0, Q_3 = 0, Q_4 = 0, Q_5 = 0.$	$CV_1 = 0, CV_2 = 0, CV_3 = 0,$ $CV_4 = 0, CV_5 = 1,$

tank T_3 is $h = 4$ times the volume of tank T_1 and T_2 taken together. This implies that after four iterations of draining of the substance from both T_1 and T_2 the tank T_3 gets full. So, from the DES model in Fig. 2.10 it can be observed that in order for T_3 to get full, the system moves in the trace containing transitions $\langle \tau_1, \tau_2, \tau_3, \tau_4, \tau_5, \tau_6, \tau_7, \tau_8 \rangle$ for three times and during the fourth iteration the system takes the trace $\langle \tau_1, \tau_2, \tau_3, \tau_4, \tau_5, \tau_6, \tau_7, \tau_9 \rangle$ which breaks out of the loop and the tank T_3 gets filled. Thus, the trace containing the transition τ_8 is traversed three times while the transition τ_9 is traversed only once out of four times.

Now we discuss measurable/unmeasurable transitions of the model and consequently the equivalent states and transitions are identified. In this system all the sensor outputs are

measurable and so are the controller commands. So any transition whose enabling event is based on the change in some sensor output or controller command, is measurable. For example, in case of τ_2 the event is $T_1\text{Full}$, whose corresponding change in sensor outputs are $T_1\text{Low} = 0$ (from 1), $T_1\text{High} = 1$ (from 0), $Q_1 = 0$ (from 1) and controller command is $CV_1 = 0$ (from 1). So τ_2 is a measurable transition. In a similar way it can be shown that all transitions except τ_{0F1} are measurable. τ_{0F1} is the failure causing transition and is unmeasurable because it is not caused by a change of any sensor output or controller command.

Two transitions are measurement equivalent if the corresponding changes in the sensor outputs and the controller commands are same. Events associated with equivalent transitions are also same. For example, transitions τ_2 and τ'_2 are measurement equivalent because they are caused by same changes in sensor outputs and controller commands i.e., $T_1\text{Low} = 0$, $T_1\text{High} = 1$, $Q_1 = 0$ and controller command is $CV_1 = 0$. Also the event associated with both these transitions is $T_1\text{Full}$. As per the Definition 2, $s_0Es'_0$ and $s_1Es'_1$, because the source states and also the destination states of equivalent transitions are equivalent. In a similar way it can be verified that $\tau_iE\tau'_i$, $1 \leq i \leq 8$. It may be noted that in case of F_i -transitions τ'_i , $1 \leq i \leq 8$ there is an equivalent normal transition e.g., $\tau_1E\tau'_1$. So, after the failure as long as the system moves through F_i -transitions τ'_i , $1 \leq i \leq 8$, the fault cannot be diagnosed because there is no transition that distinguishes the faulty behavior from the normal condition. To elaborate, F_i -transitions τ'_i , $1 \leq i \leq 8$ do not capture failure manifestation (in terms of distinguishing sensor outputs and controller commands) and hence cannot detect the fault.

Now let us consider the transitions τ_9 and τ'_{10} . The sensor outputs and the controller command for the transition τ_9 are $T_3\text{Low} = 0$, $T_3\text{High} = 1$, $CV_5 = 1$ and $Q_5 = 1$. In case of the transition τ'_{10} the sensor outputs and controller command are $T_3\text{Low} = 0$, $T_3\text{High} = 1$, $CV_5 = 1$ and $Q_5 = 0$. It may be noted that for both the transitions, the controller issues the command $CV_5 = 1$ after detecting that T_3 is full (by sensor outputs $T_3\text{Low} = 0$, $T_3\text{High} = 1$). In case of τ_9 , as the system is normal the valve V_5 opens and the substance is drained out, which is captured by sensor output $Q_5 = 1$. However, in case of τ'_{10} , as the system is faulty, even when the controller issues the command $CV_5 = 1$ there is no flow out of T_3 and $Q_5 = 0$. So transition τ'_{10} captures the fault manifestation i.e., the valve V_5 does not open after T_3 is full ($T_3\text{Low} = 0$, $T_3\text{High} = 1$) and controller issues the command $CV_5 = 1$. As F_i -transition τ'_{10} captures failure manifestation its occurrence is required for detection of F_i . In a similar way it can be verified that τ'_{12} can also detect the fault.

2.4.3 Diagnosability

The objective of the failure diagnosis problem is to determine the occurrence of a failure F_i . If the event (σ) corresponding to τ_{F_i} is measurable, failure diagnosis is trivial. So the failure causing transitions are assumed to be unmeasurable. For such failure causing transitions, σ is unmeasurable. As σ is unmeasurable, there are no checks or assignment for model variables. As failures are assumed to be *permanent*, there is no transition from any state in x_{F_i} to any state in X_N . The event related to causing F_i is denoted as σ_{F_i} .

Informally, an DES G is diagnosable if it is always possible to determine the failure status of the states beyond a certain point along all the possible traces of G after the occurrence of a failure, using the sequence of measurements. A few terms are introduced before formally defining diagnosability.

Let $\psi(X_{F_i}) = \{s | s \in L_f(G) \text{ and } final(s) \in X_{F_i} \text{ and } s \text{ ends in a measurable transition} \}$.

Definition 7. F_i -Diagnosability: An DES model G (under a given measurement limitation) is said to be diagnosable for failure F_i iff the following holds.

$$(\exists n_j \in \mathbb{N})[\forall s \in \Psi(X_{F_i})](\forall t \in L_f(G)/s)[|t| \geq n_j \Rightarrow D] \quad (2.2)$$

where the condition D is $\forall y \in \{P^{-1}[P(st)]\}$, $final(y) \in X_{F_i}$

The above definition means the following. Let s be any finite prefix of a trace of G that ends in an F_i -state and let t be any sufficiently long continuation of s . Condition D then requires that every sequence of transitions, measurement indistinguishable with st , should end into an F_i -state. This implies that, along every continuation t of s , one can detect the occurrence of failure F_i with a finite delay, specifically in at most n_j transitions of the system after s .

The fault diagnosis problem is to determine if the fault F_i has occurred within finite number n_{F_i} (where $n_{F_i} \in \mathbb{N}$) say, of transitions after the occurrence of the failure causing transition τ_{F_i} . Let us consider a trace of the DES model of the three tank system; $s = \langle \tau_0, \tau_{0F1}, \tau'_1 \rangle$; obviously $s \in \Psi(X_{F_i})$. For diagnosing F_i , any sufficiently long but finite extension t of s of length n_{F_i} must ascertain that fault has occurred. In this case, if we extend $s = \langle \tau_0, \tau_{1F_i}, \tau'_1 \rangle$ as $t = \langle (\tau'_2, \tau'_3, \tau'_4, \tau'_5, \tau'_6, \tau'_7, \tau'_8, \tau'_1)^k \rangle$, where k is arbitrarily large, we get $\exists y = \langle \tau_0, \tau_1, (\tau_2, \tau_3, \tau_4, \tau_5, \tau_6, \tau_7, \tau_8, \tau_1)^k \rangle \in P^{-1}(P(st)) \wedge final(y) = x_1 \notin X_{F_i}$. In other words, as the F_i - G -trace $\langle \tau'_1, (\tau'_2, \tau'_3, \tau'_4, \tau'_5, \tau'_6, \tau'_7, \tau'_8, \tau'_1)^k \rangle$ is equivalent to $\langle \tau_1, (\tau_2, \tau_3, \tau_4, \tau_5, \tau_6, \tau_7, \tau_8, \tau_1)^k \rangle$ (normal condition), so this F_i - G -trace cannot detect the fault. As already discussed, as none of the transitions involved in the F_i - G -trace under question captures failure manifestation, it is not helpful in fault detection.

In this example there is only one more way of extending s , namely, $t1$ is $\langle \tau'_1, \dots, \tau'_7, \tau'_{10}, (\tau'_{12})^k \rangle$. It may be noted that $\nexists y \in P^{-1}(P(st1))$ such that $final(y) \notin X_{F_i}$. So the fault is diagnosable. In other words, the transitions τ'_{10} and τ'_{12} capture failure manifestation. So the trace $st1$ detects the fault making the fault diagnosable.

2.4.4 DES Diagnoser Construction and Fault Detection in Three Tank System

The diagnoser is a directed graph represented by $O = \langle Z, A \rangle$; where Z is the set of diagnoser nodes, called O -nodes, and $A \subseteq Z \times Z$ is the set of diagnoser transitions, called O -transitions. Each O -node $z \in Z$ corresponds to a set of G -states representing the uncertainty about the actual state. Similarly, each O -transition $a \in A$ of the form $\langle z_i, z_f \rangle$ is a set of measurement equivalent transitions representing the uncertainty about the actual measurable transition that occurs. The *unmeasurable successor* (set) of a set Y of states is defined as $\mathcal{U}(Y) = \bigcup_{x \in Y} \{x^+ | \tau = \langle x, x^+ \rangle \in \mathfrak{S}_u\}$. The *unmeasurable reach* of a set Y of states, denoted as $\mathcal{U}^*(Y)$, is the reflexive-transitive closure of unmeasurable successors of Y .

Diagnoser Construction: The states in X_0 are partitioned into equivalent subsets denoted as $X_{01}, X_{02}, \dots, X_{0m}$. For all i , $1 \leq i \leq m$, an initial O -node z_{0i} is obtained as the unmeasurable reach of X_{0i} , i.e., $z_{0i} = \mathcal{U}^*(X_{0i})$. The set of all initial O -nodes is denoted as $Z_0 = z_{01} \cup \dots \cup z_{0m}$. The initial O -nodes capture the fact that the diagnoser can infer a set z_{0i} of possible initial system states (or their unmeasurable reach) by measuring the variables without waiting for the first measurable transition. Given any O -node z , the O -transitions emanating from z are obtained as follows. Let \mathfrak{S}_{mz} denote the set of measurable G -transitions from the states $x \in z$. Let A_z be the set of all equivalence classes of \mathfrak{S}_{mz} under E . For each $a \in A_z$, a successor O -node z^+ of z such that $z^+ = final(a)$ can be created as follows. Let $z_a^+ = \{final(\tau) | \tau \in a\}$; then $z^+ = \mathcal{U}^*(z_a^+)$ and a is designated as: $\langle z, z^+ \rangle$. The set of the diagnoser transitions is augmented as: $A \leftarrow A \cup \{a\}$, and the set of O -nodes is augmented as: $Z \leftarrow Z \cup \{z^+\}$. Each $a \in A$ is an ordered pair $\langle z, z^+ \rangle$, where $z = initial(a)$ and $z^+ = final(a)$. Thus, each O -node contains equivalent states. The detailed algorithm for diagnoser construction is shown in Algorithm 1

Henceforth, we refer to states, transitions, and traces of G as G -states, G -transitions and G -traces, respectively. Similarly, for the diagnoser nodes and transitions, we use O -nodes, O -transitions and O -traces respectively. Now, we look into few definitions and properties related to the diagnoser.

Definition 8. (Embedding of G -traces in O -traces): Given a O -trace $\gamma = \langle a_1, a_2, \dots, a_k \rangle$, a G -trace s , where $P(s) = \langle \tau_1, \tau_2, \dots, \tau_k \rangle$, is said to be embedded in γ , if $\tau_i \in a_i$, $1 \leq i \leq k$. The set of all G -traces embedded in a O -trace γ is represented as $A_D(\gamma)$.

Algorithm 1: Algorithm for construction of diagnoser O for an DES model G

Input: DES model G
Output: DES Diagnoser

- 1 Partition X_0 into equivalent subsets $X_{01}, X_{02}, \dots, X_{0m}$
- 2 **for all** $i, 1 \leq i \leq m$ **do**
- 3 $z_{0i} = \mathcal{U}^*(X_{0i})$
- 4 **end**
- 5 $Z_0 \leftarrow z_{01} \cup \dots \cup z_{0m}$
- 6 $Z \leftarrow Z_0$
- 7 $A \leftarrow \phi$
- 8 **for all** $z \in Z$ **do**
- 9 /* Find the set of measurable G -transitions (\mathfrak{S}_{mz}) outgoing from z */
 $\mathfrak{S}_{mz} \leftarrow \{\tau \mid \tau \in \mathfrak{S}_m \wedge \text{initial}(\tau) \in z\}$
- 10 /* Find the set of all measurement equivalent classes A_z , of \mathfrak{S}_{mz} */
- 11 **for all** $a \in A_z$ **do**
- 12 $z_a^+ = \{\text{final}(\tau) \mid \tau \in a\}$
- 13 $z^+ = \mathcal{U}^*(z_a^+)$
- 14 $Z = Z \cup \{z^+\}$
- 15 $A = A \cup \{a\}$
- 15 **end**
- 16 **end**

Property 1. If two traces $t, y \in A_D(\gamma)$, where t is F_i - G -trace and y is non- F_i - G -trace, then the O -nodes traversed by γ are F_i -uncertain.

Proof. The property also follows from the diagnoser construction. As any O -transition $a \in \gamma$ has an non- F_i - G -transition and a F_i - G -transition (which are equivalent), so source and destination O -nodes of a are F_i -uncertain. \square

Definition 9. F_i - O -node: An O -node, which contains an F_i - G state, is called an F_i - O -node, denoted as z_{F_i} . The set of all F_i - O -nodes is denoted as Z_{F_i} . In Fig. 2.11 the O -nodes z_0, \dots, z_7, z_9 are F_i - O -nodes as each O -node contains an F_i - G -state.

Definition 10. F_i -certain O -node and F_i -uncertain O -node: An F_i - O -node z is called an F_i -certain O -node if $z \subseteq X_{F_i}$. In Fig. 2.11 the O -node z_9 are F_i -certain O -node as it contains only failure G -states. An F_i - O -node which is not F_i -certain is called F_i -uncertain- O -node. In Fig. 2.11 the O -nodes z_0, \dots, z_7 are F_i -uncertain O -nodes as they contain both normal G -states as well as failure G -states.

In words, F_i -certain O -node comprises only F_i - G states, while F_i -uncertain O -node comprises some F_i - G states and some non F_i - G -states. So, if the diagnoser reaches any F_i -certain O -node failure is diagnosed. By Property 1 and Definition 8, if there is a O -trace γ

which moves in F_i -uncertain O -nodes, there is a F_i - G -trace t which is embedded in γ . After failure, diagnoser moves in γ by virtue of t . However, as there is another non- F_i - G -trace y say, equivalent to t , fault cannot be diagnosed till γ is exited.

Definition 11. F_i - O -path (γ_{F_i}): A path of the diagnoser O is a sequence of O -transitions $\gamma = \langle a_1, a_2, \dots \rangle$, with the consecution property $initial(a_{i+1}) = final(a_i), i \geq 1$. An F_i - O -path γ is an O -path in which every O -node is an F_i - O -node.

Definition 12. F_i -uncertain cycle: An F_i -uncertain cycle is an F_i - O -cycle in which there is no F_i -certain O -node. In Fig. 2.11, the O -transitions sequence $\langle a_1, a_2, a_3, a_4, a_5, a_6, a_7, a_8 \rangle$ associated with the diagnoser state sequence is $\langle z_0, z_1, z_2, z_3, z_4, z_5, z_6, z_7, z_0 \rangle$ represents an F_i -uncertain cycle. This is because, none of the O -nodes $(z_0, z_1, z_2, z_3, z_4, z_5, z_6, z_7, z_0)$ is an F_i -certain O -node.

Definition 13. F_i -indeterminate cycle: An F_i -uncertain cycle γ in which the F_i -states contained in the O -nodes of γ form a cycle in G comprising transitions from γ , is called an F_i -indeterminate cycle. Consider a sequence $\langle x_1, x_2, x_3, \dots, x_k \rangle$ that corresponds to a normal cycle and measurement equivalent failure cycle $\langle x'_1, x'_2, x'_3, \dots, x'_k \rangle$. If the system is under normal conditions, the diagnoser moves into normal cycle and once a failure occurs it moves in the failure cycle. As both the normal and attack cycles are measurement equivalent, the normal and failure cycles are indistinguishable from one another. As a result of the presence of the indeterminate cycle it is not possible to predict whether the diagnoser is moving under normal or failure cycle leading to non-diagnosability. Thus, an F_i -indeterminate cycle is an F_i -uncertain cycle with the special property as stated below:

“There is also a cycle involving F_i -states of the composite model that corresponds to the F_i -uncertain diagnoser cycle.” In simple words, the existence of an F_i -indeterminate cycle in the diagnoser implies that there are at least two measurement indistinguishable *syntactic* cycles in G , one comprising only non- F_i -states and the other comprising F_i -states. This implies that if the system moves in an F_i -indeterminate cycle, then the measurable variables are observed to be similar in both non- F_i and F_i conditions. Thus, if the diagnostic estimate moves along such an F_i -indeterminate cycle, then the fault F_i cannot be diagnosed, because, at each point in the cycle there exists uncertainty regarding the occurrence of F_i and as faults are assumed to be permanent, the system may not exit from such a cycle. The existence of an F_i -indeterminate cycle thwarts diagnosability. The equivalence between F_i -diagnosability and the absence of F_i -indeterminate cycles has been formally established for DES models [72].

We highlight the significance of the presence and absence of F_i -indeterminate cycle on fault diagnosis. The diagnoser for the DES model of Fig. 2.10 is shown in Fig. 2.11. Some

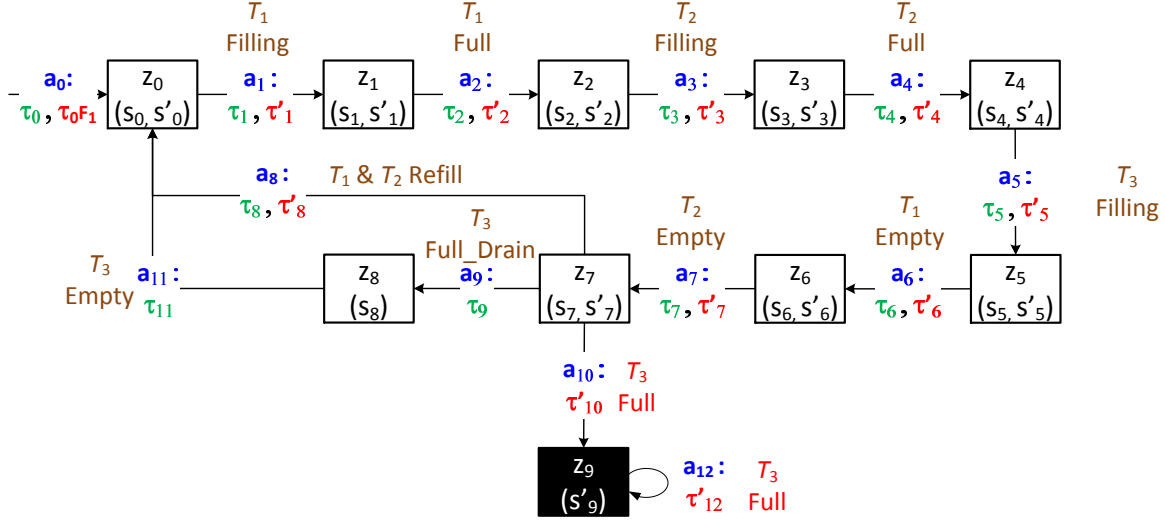


Figure 2.11: Diagnoser obtained for the DES model of the three tank system shown in Fig. 2.10

of the initial steps for this example are as follows:

- The initial state of the diagnoser i.e., z_0 is obtained as follows. First, $s_0 \in X_0$ is inserted in z_0 . Now, all states in $\mathcal{U}^*(s_0)$ are inserted in z_0 ; s'_0 is within unmeasurable reach of s_0 and is inserted in z_0 . So, $z_0 = \langle s_0, s'_0 \rangle$.
- The outgoing O -transitions from z_0 are obtained as follows. Here, $\mathfrak{S}_{mz_0} = \{\tau_1, \tau'_1\}$ which are all the outgoing measurable transitions from G -states in z_0 . Now, $A_{z_1} = \{\{\tau_1, \tau'_1\}\}$ as $\tau_1 E \tau'_1$. Corresponding to $\{\tau_1, \tau'_1\}$ there is a O -transition a_1 .
- The destination O -node corresponding to a_1 is obtained as follows. $z_1 a_1^+ = \{\langle s_1, s'_1 \rangle\}$ as a_1 comprises O -transitions τ_1, τ'_1 and $final(\tau_1) = s_1$ and $final(\tau'_1) = s'_1$. Further, $z_1^+ = \{s_1, s'_1\}$ as $\mathcal{U}^*(\{s_1\}) = \{s_1, s'_1\}$ and $\mathcal{U}^*(\{s'_1\}) = \{s'_1\}$. Thus, the destination O -node of the O -transition a_1 is $z_1 : \{\langle s_1, s'_1 \rangle\}$.

There is no F_i -indeterminate cycle present in the diagnoser for the benchmark process of two-tank system shown in Fig. 2.11. Hence the fault is diagnosable. Referring to the diagnoser the F_i -certain O -node z_9 comprises the F_i - G -state s'_9 . The state s'_9 corresponds to controller command 'Valve_{OPEN}' but flowmeter outputs ($Q_5 = 0$ i.e., no-flow). As discussed earlier, the combination "Valve_{OPEN} but $Q_5 = 0$ " detects the fault.

In the next section, we propose a DES based IDS for the detection of the evil twin attack which is based on the application of the adapted DES framework presented in this section.

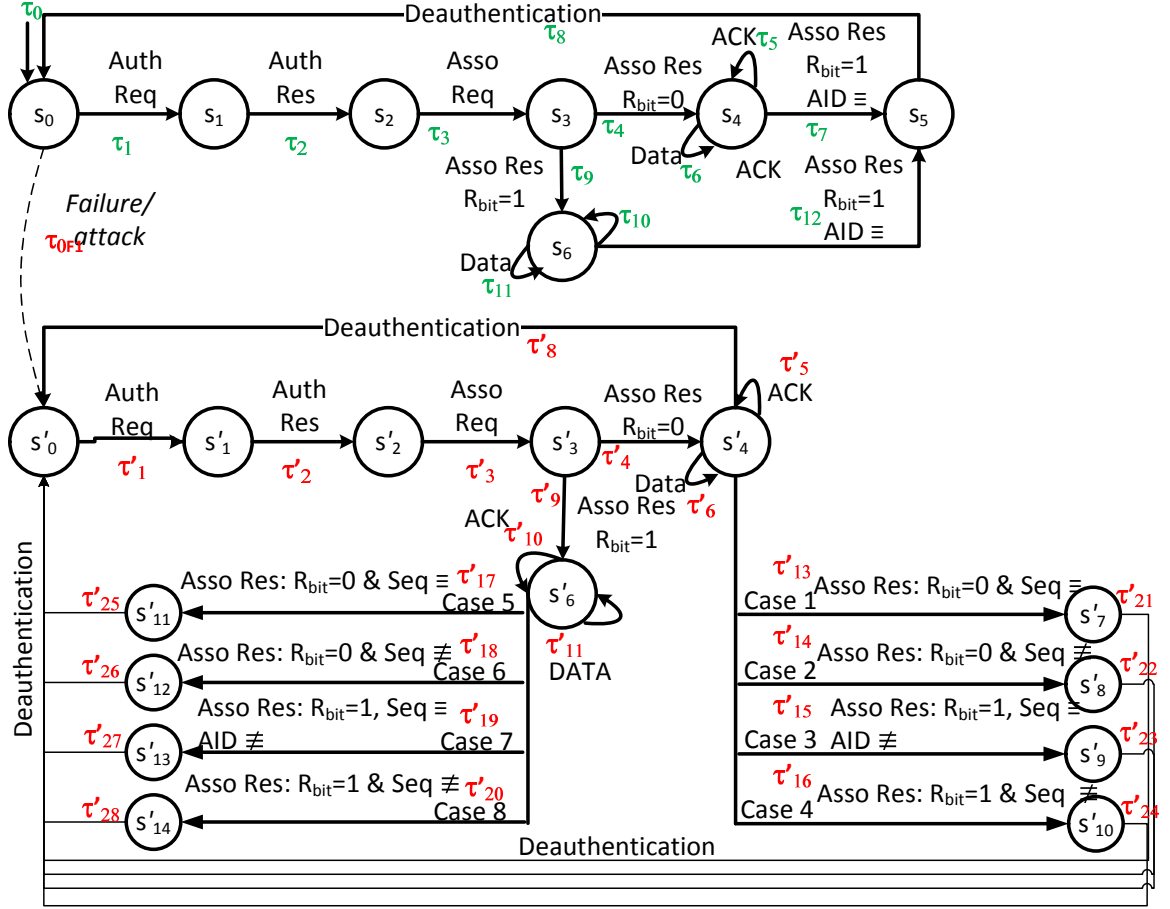


Figure 2.12: Normal and attack DES model for evil twin attack

Table 2.5: Model variables and their domains

Model Variable	Domain	What it holds
mac_{src}, mac_{dst}	$\{xx : xx : xx : xx : xx : xx \mid x \in [0 - F]\}$	Source and destination MAC address.
$RS1_{Ass}Seq, RS2_{Ass}Seq$	$\{0, \dots, 4095\}$	Sequence number of the first and the second association response frame
$RS1_{Ass}Retry, RS2_{Ass}Retry$	$\{0, 1\}$	Retry bit value of the first and the second association response frame
$RS1_{Ass}AID, RS2_{Ass}AID$	$\{0, \dots, 2007\}$	Association ID(AID) of the first and the second association response frame

2.5 DES Model of Evil Twin Attack

The DES model G under normal and evil twin attack scenarios is shown in Fig. 2.12. For readability purposes Fig. 2.12 is annotated with transition number τ_i and the event because of which the transition τ_i is enabled. The transitions of the DES model G shown in Fig. 2.12 are explained in Table 2.6. States and transitions belonging to normal (attack) model

are denoted by the non-primed (primed) notations. The various components of G are as follows:

$$X = \{s_0, s_1, s_2, s_3, s_4, s_5, s_6, s'_0, s'_1, s'_2, s'_3, s'_4, s'_6, s'_7, s'_8, s'_9, s'_{10}, s'_{11}, s'_{12}, s'_{13}, s'_{14}\}$$

$$\Sigma = \{\text{Auth Req, Auth Res, Asso Req, Asso Res, Data, ACK, Deauthentication}\}$$

$$\mathfrak{S} = \{\tau_1, \tau_2, \tau_3, \tau_4, \tau_5, \tau_6, \tau_7, \tau_8, \tau_9, \tau_{10}, \tau_{11}, \tau_{12}, \tau'_1, \tau'_2, \tau'_3, \tau'_4, \tau'_5, \tau'_6, \tau'_8, \tau'_9, \tau'_{10}, \tau'_{11}, \tau'_{13}, \tau'_{14}, \tau'_{15}, \tau'_{16}, \tau'_{17}, \tau'_{18}, \tau'_{19}, \tau'_{20}, \tau'_{21}, \tau'_{22}, \tau'_{23}, \tau'_{24}, \tau'_{25}, \tau'_{26}, \tau'_{27}, \tau'_{28}\}$$

$V = \{mac_{src}, mac_{dst}, RS1_{Ass}Seq, RS2_{Ass}Seq, RS1_{Ass}Retry, RS2_{Ass}Retry, RS1_{Ass}AID, RS2_{Ass}AID\}$ is the set of model variables. Their domains are shown in Table 2.5. Here $RS1_{Ass}Seq, RS2_{Ass}Seq$ represents the sequence number of first and second association response respectively. $RS1_{Ass}Retry, RS2_{Ass}Retry$ represents the value of the retry bit of first and second association response respectively. $RS1_{Ass}AID, RS2_{Ass}AID$ represents the value of the AID bit of first and second association response respectively.

—**Behavior Under Normal Conditions and its DES Model:** Under normal conditions (evil twin absent), either one or two association responses are received. In case only one response is received no checks are required to be performed on the sequence number and retry bit. However, it is possible that two association responses are obtained under normal circumstances for a single association request. If the first association response is lost the AP retransmits the association response making it the genuine second association response. In such a case, even though both the responses are sent by the genuine AP, the IDS checks for the sequence number, retry bit and the AID to verify that the second association response was from genuine AP.

States $\{s_0, s_1, s_2, s_3, s_4, s_5, s_6\}$ and transitions $\{\tau_1, \tau_2, \tau_3, \tau_4, \tau_5, \tau_6, \tau_7, \tau_8, \tau_9, \tau_{10}, \tau_{11}, \tau_{12}\}$ represent the DES model of the system under **normal** conditions.

- s_0 : The model starts at state s_0 . In state s_0 , the client is about to send an authentication request (“Auth Req”) frame to the AP.
- $\tau_1(s_0 \rightarrow s_1)$: Step 1 of the four-way handshake between client and the AP. Here the client sends an authentication request (“Auth Request”) to the AP. As this is the first frame from client to the AP, there are no checks made for this frame. So, $check(V) = \{--\}^5$ as no checks are made here and $assign(V) = \{mac_{src} \leftarrow mac_{client}, mac_{dst} \leftarrow mac_{AP}\}$. $mac_{src} \leftarrow mac_{client}$ is the assignment of SRC MAC (client MAC address in this case) address to model variable mac_{src} . $mac_{dst} \leftarrow mac_{AP}$ is the assignment of DST MAC (AP’s MAC address in this case) to model variable⁶ mac_{dst} . The assignment

⁵Henceforth, we concentrate more on the check(V) and assign(V) parameters. If either of check(V) and assign(V) are $\{--\}$ the corresponding explanation is skipped. The values of $check(V)$ and $assign(V)$ are shown in Table 2.6

⁶If model variables (V) are not used then there would be $2^{48} * 2^{48}$ transitions (and states) from s_0 , each

2.5. DES Model of Evil Twin Attack

Table 2.6: Transition table for DES model shown in Fig. 2.12

Transition	Initial State	Final State	Event	check(V)	assign(V)	Remarks
$\tau_1 (\tau'_1)$	$s_0 (s'_0)$	$s_1 (s'_1)$	Auth Req	---	$mac_{SRC} \leftarrow mac_{client},$ $mac_{DST} \leftarrow mac_{AP}$	Step 1 of four way handshake. Authentication Request
$\tau_2 (\tau'_2)$	$s_1 (s'_1)$	$s_2 (s'_2)$	Auth Res	$mac_{SRC} \equiv mac_{AP},$ $mac_{DST} \equiv mac_{client}$	---	Step 2 of four way handshake. Authentication Response.
$\tau_3 (\tau'_3)$	$s_2 (s'_2)$	$s_3 (s'_3)$	Asso Req	$mac_{SRC} \equiv mac_{client},$ $mac_{DST} \equiv mac_{AP}$	---	Step 3 of four way handshake. Association Request.
$\tau_4 (\tau'_4)$	$s_3 (s'_3)$	$s_4 (s'_4)$	Asso Res	$mac_{SRC} \equiv mac_{AP},$ $mac_{DST} \equiv mac_{client}$	$RS1_{Ass}Retry \leftarrow 0,$ $RS1_{Ass}Seq \leftarrow seq_no,$ $RS1_{Ass}AID \leftarrow AID,$	Step 4 of four way handshake. Association Response.
$\tau_9 (\tau'_9)$	$s_3 (s'_3)$	$s_6 (s'_6)$	Asso Res	$mac_{SRC} \equiv mac_{AP},$ $mac_{DST} \equiv mac_{client}$	$RS1_{Ass}Retry \leftarrow 1,$ $RS1_{Ass}Seq \leftarrow seq_no,$ $RS1_{Ass}AID \leftarrow AID,$	Step 4 of four way handshake. Association Response. (Re-transmitted)
$\tau_6 (\tau'_6)$ $\tau_{11} (\tau'_{11})$	$s_4 (s'_4)$ $s_6 (s'_6)$	$s_4 (s'_4)$ $s_6 (s'_6)$	Data	$mac_{SRC} \equiv mac_{AP},$ $mac_{DST} \equiv mac_{client}$	---	Data Exchange
$\tau_5 (\tau'_5)$ $\tau_{10} (\tau'_{10})$	$s_4 (s'_4)$ $s_6 (s'_6)$	$s_4 (s'_4)$ $s_6 (s'_6)$	ACK	$mac_{SRC} \equiv mac_{client},$ $mac_{DST} \equiv mac_{AP}$	---	Acknowledgments from the AP
τ_7 τ_{12}	s_4 s_6	s_5 s_5	Asso Res	$mac_{SRC} \equiv mac_{AP},$ $mac_{DST} \equiv mac_{client},$ $RS2_{Ass}Seq \equiv RS1_{Ass}Seq,$ $RS2_{Ass}Retry \equiv 1,$ $RS2_{Ass}AID \equiv RS1_{Ass}AID,$	---	Second Association Response. AID Same
τ'_{13}	s'_4	s'_7	Asso Res (Case 1)	$mac_{SRC} \equiv mac_{AP},$ $mac_{DST} \equiv mac_{client},$ $RS1_{Ass}Retry \equiv 0, RS2_{Ass}Retry \equiv 0,$ $RS2_{Ass}Seq \equiv RS1_{Ass}Seq$	---	Second Association Response must have R = 1. Evil Twin Present.
τ'_{14}	s'_4	s'_8	Asso Res (Case 2)	$mac_{SRC} \equiv mac_{AP},$ $mac_{DST} \equiv mac_{client},$ $RS1_{Ass}Retry \equiv 0, RS2_{Ass}Retry \equiv 0,$ $RS2_{Ass}Seq \neq RS1_{Ass}Seq$	---	Second Association Response must have R = 1 and same sequence number. Evil Twin Present.
τ'_{15}	s'_4	s'_9	Asso Res (Case 3)	$mac_{SRC} \equiv mac_{AP},$ $mac_{DST} \equiv mac_{client},$ $RS1_{Ass}Retry \equiv 0, RS2_{Ass}Retry \equiv 1,$ $RS2_{Ass}Seq \equiv RS1_{Ass}Seq,$ $RS2_{Ass}AID \neq RS1_{Ass}AID,$	---	Second Association Response is re-transmitted. Must have same AID. Evil Twin Present.
τ'_{16}	s'_4	s'_{10}	Asso Res (Case 4)	$mac_{SRC} \equiv mac_{AP},$ $mac_{DST} \equiv mac_{client},$ $RS1_{Ass}Retry \equiv 0, RS2_{Ass}Retry \equiv 1,$ $RS2_{Ass}Seq \neq RS1_{Ass}Seq$	---	Second Association Response must have sequence number if R = 1. Evil Twin Present.
τ'_{17}	s'_6	s'_{11}	Asso Res (Case 5)	$mac_{SRC} \equiv mac_{AP},$ $mac_{DST} \equiv mac_{client},$ $RS1_{Ass}Retry \equiv 1, RS2_{Ass}Retry \equiv 0,$ $RS2_{Ass}Seq \equiv RS1_{Ass}Seq$	---	Second Association Response must have R = 1 if 1 st Response has R = 1. Evil Twin Present.
τ'_{18}	s'_6	s'_{12}	Asso Res (Case 6)	$mac_{SRC} \equiv mac_{AP},$ $mac_{DST} \equiv mac_{client},$ $RS1_{Ass}Retry \equiv 1, RS2_{Ass}Retry \equiv 0,$ $RS2_{Ass}Seq \neq RS1_{Ass}Seq$	---	Second Association Response must have R = 1 if 1 st Response has R = 1. Evil Twin Present.
τ'_{19}	s'_6	s'_{13}	Asso Res (Case 7)	$mac_{SRC} \equiv mac_{AP},$ $mac_{DST} \equiv mac_{client},$ $RS1_{Ass}Retry \equiv 1, RS2_{Ass}Retry \equiv 1,$ $RS2_{Ass}Seq \equiv RS1_{Ass}Seq,$ $RS2_{Ass}AID \neq RS1_{Ass}AID,$	---	Similar to Case 3. Second Association Response must have same AID. Evil Twin Present.
τ'_{20}	s'_6	s'_{14}	Asso Res (Case 8)	$mac_{SRC} \equiv mac_{AP},$ $mac_{DST} \equiv mac_{client},$ $RS1_{Ass}Retry \equiv 1, RS2_{Ass}Retry \equiv 1,$ $RS2_{Ass}Seq \neq RS1_{Ass}Seq$	---	Second Association Response cannot have different sequence number if R = 1. Evil Twin Present.
τ_8 τ'_8 τ'_{21} τ'_{22} τ'_{23} τ'_{24} τ'_{25} τ'_{26} τ'_{27} τ'_{28}	s_5 s'_4 s'_7 s'_8 s'_9 s'_{10} s'_{11} s'_{12} s'_{13} s'_{14}	s_0 s'_0 s'_0 s'_0 s'_0 s'_0 s'_0 s'_0 s'_0 s'_0	Deauthentication	$mac_{SRC} \equiv mac_{client},$ $mac_{DST} \equiv mac_{AP},$	---	Deauthentication Frame

done in this step helps to identify a client uniquely. The corresponding mapping for the same can be seen in the transition τ_2 which is explained next.

- $\tau_2(s_1 \rightarrow s_2)$: Step 2 of the four-way handshake between client and the AP. After receiving the “Auth Req” frame from the client the AP sends an authentication response (“Auth Res”) frame to the client. Here, a check needs to be done to ensure whether the client which solicits the “Auth Res” has sent an “Auth Req” previously or not. So, when sending an “Auth Res” a check is done on the source MAC and destination MAC addresses. A rule of thumb for the networks is that the source and destination address of a request frame get reversed in its corresponding response frame i.e., the source MAC address of the “Auth Req” frame becomes the destination MAC address of the “Auth Res” frame. As the AP sends the “Auth Res” to the client the $check(V) = \{mac_{src} \equiv mac_{AP}\}$ and $\{mac_{dst} \equiv mac_{client}\}$. The $check(V)$ checks whether the “Auth Res” belongs to the “Auth Req” frame sent in the previous step and does not belong to any other client and the source and destination MAC address are properly set.
- $\tau_3(s_2 \rightarrow s_3)$: Step 3 of the four-way handshake between client and the AP. After successful authentication, the client sends an association request (“Asso Req”) frame. Here, $check(V)$ checks that the client which has successfully authenticated in the previous step is sending the “Asso Req” frame. Here $check(V)$ is same as τ_1 .
- $\tau_4(s_3 \rightarrow s_4)$: Step 4 of the four-way handshake between client and the AP. It represents the association response (“Asso Res”) frame sent by the AP to the client. Here $check(V)$ checks that the “Asso Res” belongs the “Asso Req” frame received in the previous step and does not belong to any other client. In $assign(V)$, $RS1_{Ass}Retry$, $RS1_{Ass}Seq$, $RS1_{Ass}AID$ stores the value of the retry bit, sequence number and the AID of the first association response received by the client. Here $RS1_{Ass}Retry$ is set to 0 implying that this is the first association response from the AP. Here $check(V)$ is same as τ_2 .
- $\tau_5(s_4 \rightleftharpoons s_4)$: This represents the ACK frames sent by the AP to the client for the data frames sent in the previous step. Here $check(V)$ is reversed as compared to τ_6 since the direction of frame travel is reversed.
- $\tau_6(s_4 \rightleftharpoons s_4)$: This represents the data frames sent by the client to the AP. Here $check(V)$ checks whether the data frames are sent by the same client which associated in τ_4 .

representing the possible source and destination MAC address (as MAC address are 48 bit) sent in the request frame leading to state explosion problem.

- $\tau_7(s_4 \rightarrow s_5)$: The transition τ_7 represents the second association response. In case the first association response is lost, the AP retransmits the second association response with exactly the same parameters except that it has retry bit ($RS1_{Ass}Retry$) set to 1. It may happen that the client has already processed the first association response frame but the acknowledgment (ACK) sent by the client for the first association response is lost. As a result the AP assumes that the first association response is lost and sends the second association response. Here $check(V)$ checks that “Asso Res” is a re-transmitted frame of the previously sent first association response.
- $\tau_8(s_5 \rightarrow s_0)$: Here the client sends deauthentication to the AP and ends its association with the AP. The $check(V)$ checks whether the deauthentication frame is received from the client that was associated previously. The DES model returns to start state s_0 via the transition τ_8 .
- $\tau_9(s_3 \rightarrow s_6)$: This is similar to τ_4 except for $RS1_{Ass}Retry$ set to 1 in the $assign(V)$. As Wi-Fi is a lossy medium, it is possible that the client might not receive the “Asso Res” with $RS1_{Ass}Retry$ is set to 0 and receive the “Asso Res” with $RS1_{Ass}Retry$ set to 1 as its first association response.
- $\tau_{10}(s_6 \rightleftharpoons s_6)$: Similar to transition τ_5 .
- $\tau_{11}(s_6 \rightleftharpoons s_6)$: Similar to transition τ_6 .
- $\tau_{12}(s_6 \rightarrow s_5)$: Similar to transition τ_7 .

—**Behavior Under Attack Conditions and its DES Model:** Under attack conditions (evil twin present), two association responses are always received. One response is from the genuine AP while the other is from the evil twin AP. The order of receipt of response depends on the network conditions. Here, the three parameters viz. retry bit, sequence number and the AID are compared to determine the presence of evil twin. Only few cases require comparing the AIDs of both the association responses obtained else the retry bit and sequence number are enough to detect the presence of evil twin.

States $\{s'_0, s'_1, s'_2, s'_3, s'_4, s'_6, s'_7, s'_8, s'_9, s'_{10}, s'_{11}, s'_{12}, s'_{13}, s'_{14}\}$ and transitions $\{\tau'_1, \tau'_2, \tau'_3, \tau'_4, \tau'_5, \tau'_6, \tau'_8, \tau'_9, \tau'_{10}, \tau'_{11}, \tau'_{13}, \tau'_{14}, \tau'_{15}, \tau'_{16}, \tau'_{17}, \tau'_{18}, \tau'_{19}, \tau'_{20}, \tau'_{21}, \tau'_{22}, \tau'_{23}, \tau'_{24}, \tau'_{25}, \tau'_{26}, \tau'_{27}, \tau'_{28}\}$ represent the DES model of the system under **attack** conditions.

For the attack model we analyze the characteristics of second association response as the first four steps ($\tau'_1, \tau'_2, \tau'_3, \tau'_4$) are same as those under normal conditions. For each transition representing the second response, $check(V)$ checks whether the second response

has the same source and destination MAC address as the first association response. Next, the various characteristics of the second response is shown below.

- $\tau'_{13}(s'_4 \rightarrow s'_7)$: [Case 1 of Table 2.6, $RS1_{Ass}Retry \equiv 0, RS2_{Ass}Retry \equiv 0, RS2_{Ass}Seq \equiv RS1_{Ass}Seq$] Here the second association response has an identical sequence number as that of first association response. However the retry bit of the second association response is set to 0.
- $\tau'_{14}(s'_4 \rightarrow s'_8)$: [Case 2 of Table 2.6, $RS1_{Ass}Retry \equiv 0, RS2_{Ass}Retry \equiv 0, RS2_{Ass}Seq \neq RS1_{Ass}Seq$] Here, the first association response and second association response have different sequence number but both have retry bit set to 0.
- $\tau'_{15}(s'_4 \rightarrow s'_9)$: [Case 3 of Table 2.6, $RS1_{Ass}Retry \equiv 0, RS2_{Ass}Retry \equiv 1, RS2_{Ass}Seq \equiv RS1_{Ass}Seq, RS2_{Ass}AID \neq RS1_{Ass}AID$]. Here the sequence number of second association response is same as that of first association response. The retry bit of second association response is set to 1. For this case, Association ID (AID) needs to be taken into account as analyzing only retry bit and sequence numbers leads to inconclusive results. In this case, the AID of second association response is different from that of first association response.
- $\tau'_{16}(s'_4 \rightarrow s'_{10})$: [Case 4 of Table 2.6, $RS1_{Ass}Retry \equiv 0, RS2_{Ass}Retry \equiv 1, RS2_{Ass}Seq \neq RS1_{Ass}Seq$] Here the second association response has retry bit 1 and has a different sequence number than the first association response.
- $\tau'_{17}(s'_6 \rightarrow s'_{11})$: [Case 5 of Table 2.6, $RS1_{Ass}Retry \equiv 1, RS2_{Ass}Retry \equiv 0, RS2_{Ass}Seq \equiv RS1_{Ass}Seq$] Here the second association response has retry bit 0. Also the sequence number of both responses are equivalent.
- $\tau'_{18}(s'_6 \rightarrow s'_{12})$: [Case 6 of Table 2.6, $RS1_{Ass}Retry \equiv 1, RS2_{Ass}Retry \equiv 0, RS2_{Ass}Seq \neq RS1_{Ass}Seq$] Here the retry bit of second association response is set to 1 but the sequence number of second association response is different than that of the first association response.
- $\tau'_{19}(s'_6 \rightarrow s'_{13})$: [Case 7 of Table 2.6, $RS1_{Ass}Retry \equiv 1, RS2_{Ass}Retry \equiv 1, RS2_{Ass}Seq \equiv RS1_{Ass}Seq, RS2_{Ass}AID \neq RS1_{Ass}AID$] Similar to Case 3. For this case too, AID needs to be taken into account.
- $\tau'_{20}(s'_6 \rightarrow s'_{14})$: [Case 8 of Table 2.6, $RS1_{Ass}Retry \equiv 1, RS2_{Ass}Retry \equiv 1, RS2_{Ass}Seq \neq RS1_{Ass}Seq$] Here the second association response has retry bit 1. Also the sequence number of both responses are not equivalent.
- $\tau'_{21}, \dots, \tau'_{28}$: Deauthentication frame sent by the client to the AP. Similar to τ_8 .

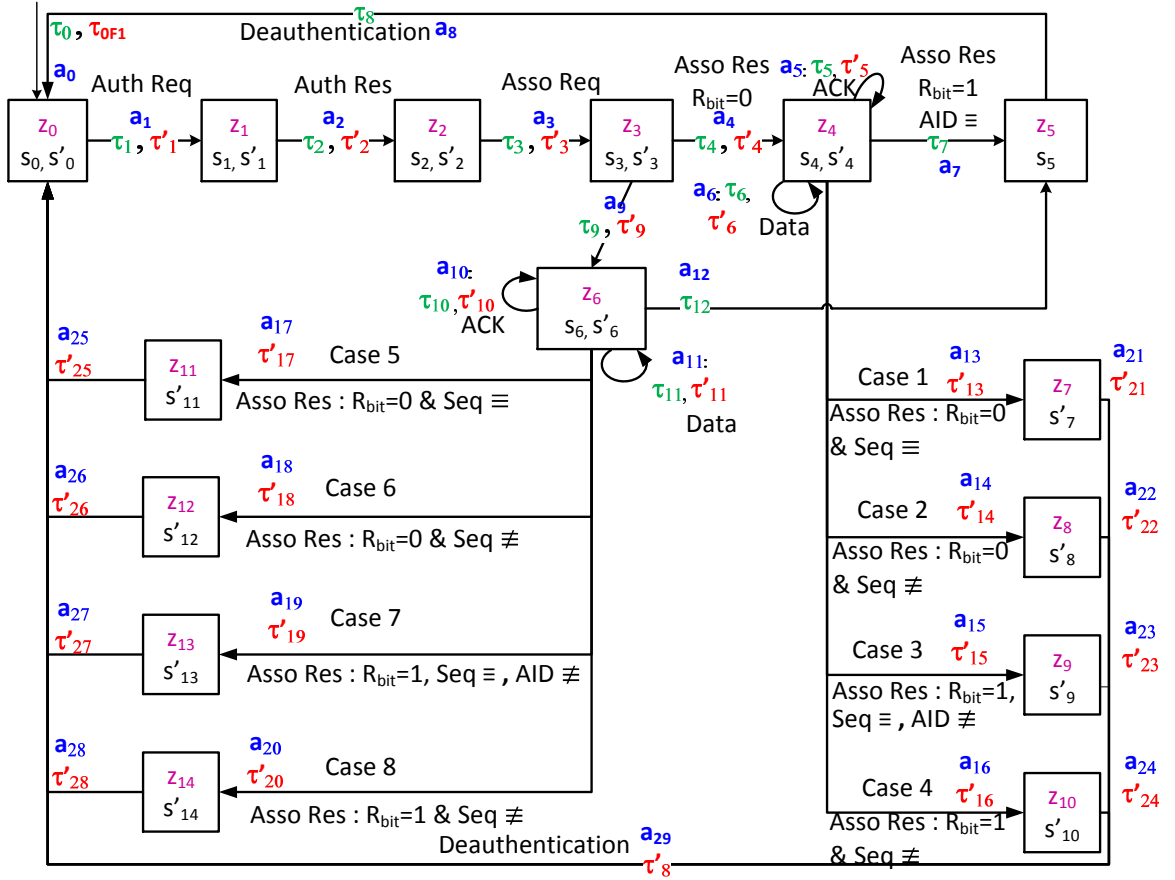
Diagnoser construction for Evil Twin attack


Figure 2.13: Diagnoser for evil twin attack

Figure 2.13 is the diagnoser for the DES model G shown in Fig. 2.12. The diagnoser is built following the Algorithm 1. In order to detect evil twin attack, the diagnoser should reach any of the F_i -certain O -nodes (attack certain O -node) $\langle z_7, z_8, z_9, z_{10}, z_{11}, z_{12}, z_{13}, z_{14} \rangle$. The equivalence between F_i -diagnosability and the absence of F_i -indeterminate cycles has been formally established for DES models [72]. F_i -uncertain O -nodes comprise some normal O -nodes and some F_i -certain- O -nodes. So, F_i -uncertain O -nodes cannot detect whether the system is under normal or faulty (attack) conditions. On the other hand, F_i -certain O -nodes can detect that a fault (attack) has occurred because the F_i -certain states comprise only F_i - O -nodes. Presence of F_i -indeterminate cycles imply that after failure F_i , the system can move indefinitely in F_i -uncertain O -nodes making the fault (attack) non-diagnosable. Upon observing the diagnoser shown in Fig. 2.13, there exists no F_i -indeterminate cycles. As no F_i -indeterminate cycles exists in the diagnoser, the fault (attack) is diagnosable. So, the DES diagnoser which is implemented as an IDS engine detects all possible cases of evil twin attack.

2.5.1 An Example of Evil Twin Attack Detection Using DES Diagnoser

We consider the Case 3 of Table 2.6 for the example. In Case 3, the first association response has retry bit 0, the second response has retry bit 1, both the responses have identical sequence number and different AID. The O -trace $\langle a_1, a_2, a_3, a_4 \rangle$ represents the four way handshake between the client and the AP taking the diagnoser to O -node z_4 . Next, the IDS sniffs a second response for the association request sent. As two association responses are received for one association request, IDS treats this as suspicious activity. “Evil Twin Handler” generates the event “Asso Res” and the diagnoser reaches state z_9 . The diagnoser O -node z_9 corresponds to the second association response having retry bit 1, identical sequence number as the first association response and different AID. Under normal circumstances, the AID of the second association response must be same as that of the first association response. The diagnoser reaches O -node z_9 which is an F_i -certain O -node. So the diagnoser successfully determines the presence of evil twin AP. In a similar manner all the evil twin attack scenarios shown in Table 2.8 can be shown to be detected by the diagnoser.

2.6 Results and Discussions

This section describes the statistics related to detection rate, accuracy, and the impact of the IDS on the system resources.

2.6.1 Network Setup for Evil Twin

The network setup for the evil twin attack is shown in Fig. 2.14. We denote C_1, C_2 as the clients, G as the genuine AP with SSID as “FreeWiFi” having the MAC address as 00:19:D2:AC:B6:23 running on channel 6 and M as the evil twin AP. The evil twin AP is setup using the *airbase-ng* utility of the *aircrack-ng* suite [3]. To obtain the MAC address, SSID and the channel number on which the genuine AP is running the attacker analyzes the information sent in the beacon frames by the genuine AP. The SSID, MAC address and the channel on which the evil twin runs is identical to that of the genuine AP. The evil twin AP is configured on a machine having Backtrack 5R3 operating system with kernel version 3.2.6. The IDS is located close to the genuine AP so that frames traveling to and from the genuine AP are not lost. The IDS is implemented in C language running on a machine with Ubuntu 12.04 (kernel 3.2.0) installed. We used smartphones, laptops and desktops equipped with wireless cards as clients for testing the the IDS. The vital information required for detecting the presence of evil twin are extracted from the authentication request, authentication response, association request, and association response are stored in the MySQL database.

Table 2.7: Detection rate statistics using the proposed IDS

Run #	Attack Instances launched	Instances detected using proposed IDS	Detection Rate %	Run #	Attack Instances launched	Instances detected using proposed IDS	Detection Rate %
1	120	111	92.50	6	120	119	99.17
2	120	113	94.13	7	120	114	95.00
3	120	115	95.83	8	120	120	100.00
4	120	118	98.33	9	120	117	97.50
5	120	114	95.00	10	120	114	95.00

The experiments lasted for a period of 24 hours which is later divided into ten runs as shown in Table 2.7.

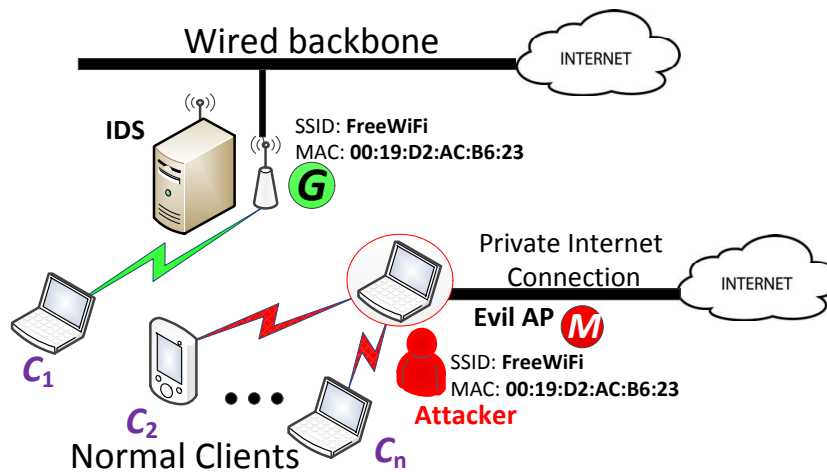


Figure 2.14: Experimental setup for evil twin attack

2.6.2 Detection Rate and Accuracy of the Proposed DES Based IDS

The metrics used for measuring the performance of IDS are detection rate and accuracy. Detection Rate is defined as the number of attacks detected by the IDS to the total number of attacks actually present. $Detection\ Rate = TP / (TP + FN)$. Accuracy is the proportion of the total number of attacks that are correctly detected. $Accuracy = TP / (TP + FP)$. Here, TP is True Positive, FP is False Positive, and FN is False Negative. A TP is an instance, which is actually an attack and is classified as attack by the IDS. A $FP(FN)$ is a case when an IDS classifies a normal(attack) activity as attack(normal) activity.

Table 2.7 shows the detection rate and accuracy for the proposed IDS. As seen, the detection rate is in the range of 92-100% mark. During our experiments the evil twin terminal is always kept active. So the detection ratio under ideal circumstances should had been 100%. However, it falls below that mark in certain runs. Our scheme works on the assumption of receipt of two association responses in lieu of one association request frame. As wireless

is a noisy medium, it is observed that in certain cases the IDS fails to capture one of the two association responses. As a result, it treats the evil twin scenario as normal network scenario (since it receives only one association response frame). On the other hand, the accuracy touches 100% in all the runs. It is because once the IDS receives multiple association responses, presence of evil twin is accurately determined (i.e., no false positives).

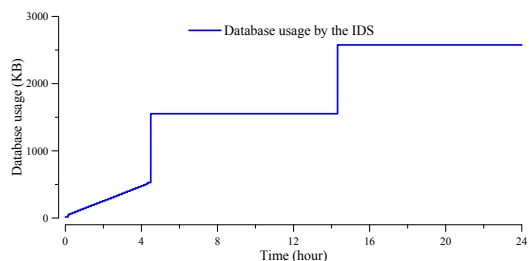


Figure 2.15: Size of database growth of the IDS

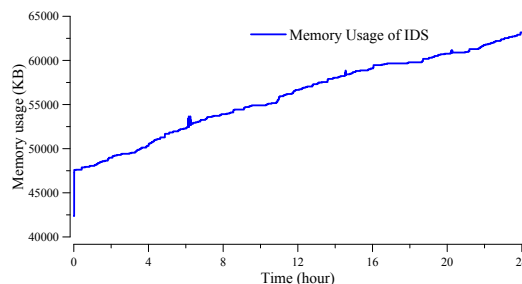


Figure 2.16: Memory usage of the IDS

Fig. 2.15, Fig. 2.16 and Fig. 2.17 represent the database size growth, memory usage, and CPU usage respectively of the IDS over a period of 24 hours. As seen in Fig. 2.15, database occupies a maximum space of **2750** KB over 24 hours usage. We also flush our DB every 24 hours so that, the size of DB does not grow over the period of time. From Fig. 2.16, we see that the memory utilization of the IDS reaches a peak value of mere 62 MB when it runs continuously for a period of 24 hours. We also observe that the proposed IDS is lightweight and does not consume excessive amounts of memory. Similar observations can be made for the CPU utilizations. During the four runs of the IDS, we can see the average CPU utilization by the IDS is just 1-2% as seen in Fig. 2.17. Some spikes can be seen in the CPU utilization graph, but they do not exceed 3% usage. Hence the proposed IDS is CPU friendly.

2.6.3 Correctness of the DES Diagnoser

There are a number of ways in which the evil twin attack can be launched. In order to ensure that all possible cases are detected by the proposed DES based IDS, the correctness of the DES diagnoser is must. The correctness ensures that all possible cases are detectable by the proposed DES based IDS. In order to prove the correctness of the diagnoser shown in Fig. 2.13 we consider 10 possible cases enumerated in Table 2.8. We explain only Case 1 of Table 2.8. Case 1 has the following characteristics: $RS1_{Ass}Retry \equiv 0$, $RS2_{Ass}Retry \equiv 0$, $RS2_{Ass}Seq \equiv RS1_{Ass}Seq$ i.e., the first and the second response have retry bit set to 0 and both have the same sequence number. From a networking point of view as the retry bit of second association response is 0, its sequence number cannot be the same as the first

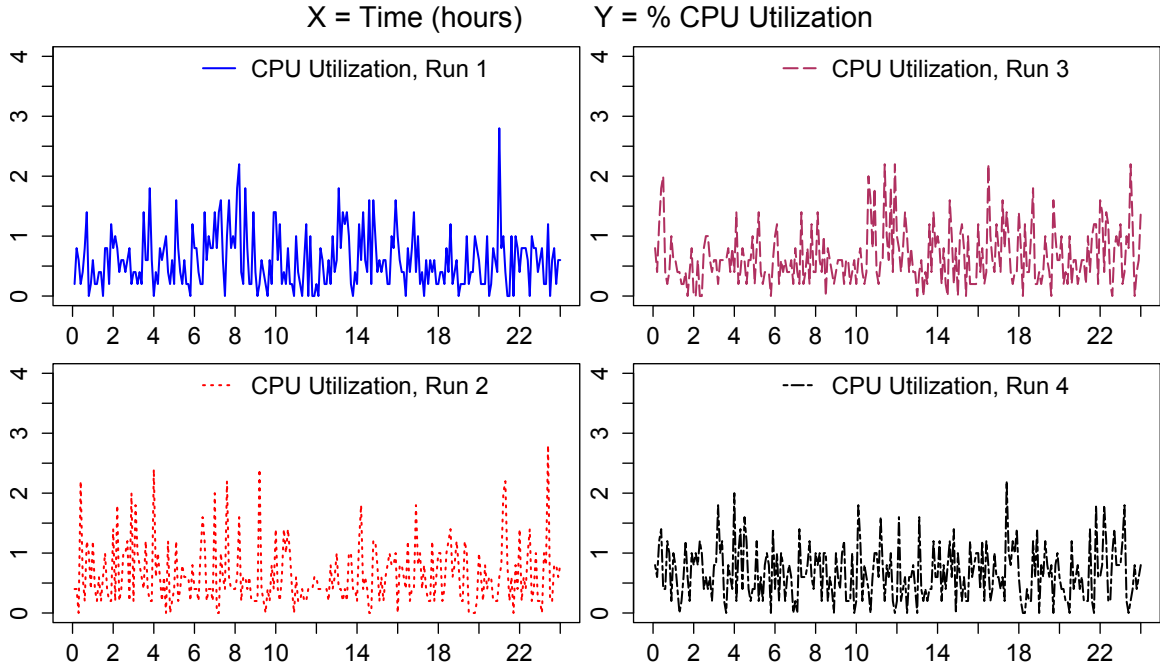


Figure 2.17: CPU utilization of the proposed IDS

response (hence, the second association response must be sent by the evil twin AP).

As shown in Fig. 2.13, trace $\langle a_1, a_2, a_3, a_4 \rangle$ represents the four-way handshake explained earlier. The transition a_{13} is the second association response received by client. It has retry bit ($RS2_{Ass}Retry$) is set to 0 and has identical sequence number as the first association response. It takes the diagnoser to state z_7 which is F_i -certain (attack) state. As F_i -certain (attack) state is reached the diagnoser detects the presence of evil twin in the network. In a similar manner all the 10 cases shown in Table 2.8 are correctly identified by the diagnoser. This proves that the proposed DES based IDS can detect all possible attack cases for evil twin AP ensuring that the attacker does not escape detection.

2.6.4 Discussion

Table 2.9 compares the various existing mitigation techniques for the evil twin attack. The other features that we compare are the requirements of maintaining white list of authorized APs, timing based methods, collecting frame features, proprietary hardware and resource overhead. The remarks column of Table 2.9 describes the pros and cons of the techniques discussed.

The proposed method depends highly on the ability of the IDS to capture the association response frames correctly. If the IDS misses one of the association response frames, the IDS considers the network to be under normal conditions. The environment considered is an

2. IDS for Evil Twin Attack in Wi-Fi networks using DES Framework

Table 2.8: All possible attack cases for proving the correctness of the DES diagnoser

Case #	O-transition Traversed	F_i -certain state Reached?	Actual Activity	Diag. Conclusion.	Remarks
1	$a_1, a_2, a_3, a_4, \mathbf{a13}$	Y, z_7	A	A	Second Association Response must have R = 1
2	$a_1, a_2, a_3, a_4, \mathbf{a14}$	Y, z_8	A	A	Second Association Response must have R = 1 and identical sequence number.
3	$a_1, a_2, a_3, a_4, \mathbf{a15}$	Y, z_9	A	A	Second Association Response must have same AID.
4	$a_1, a_2, a_3, a_4, \mathbf{a16}$	Y, z_{10}	A	A	Second Association Response cannot have different sequence number if R = 1.
5	$a_1, a_2, a_3, a_9, \mathbf{a17}$	Y, z_{11}	A	A	Second Association Response must have R = 1.
6	$a_1, a_2, a_3, a_9, \mathbf{a18}$	Y, z_{12}	A	A	Second Association Response must have R = 1.
7	$a_1, a_2, a_3, a_9, \mathbf{a19}$	Y, z_{13}	A	A	Similar to Case 3
8	$a_1, a_2, a_3, a_9, \mathbf{a20}$	Y, z_{14}	A	A	Second Association Response cannot have different sequence number if R = 1.
9	$a_1, a_2, a_3, \mathbf{a4}$	N, z_4	N	N	Normal Case as only one Response obtained).
10	$a_1, a_2, a_3, \mathbf{a4}$	N, z_4	N	N	Similar to Case 9.
Cases Correctly Identified by the Diagnoser					10/10

NOTE: Case 1-8: Attacker Present And Active. Case 9: Attacker Present But Passive. Case 10: Attacker Absent. A denotes ‘Attack’. N denotes ‘Normal’ conditions.

Table 2.9: Comparison of existing mitigation solutions for Evil Twin attack

Method	Detects Evil Twin attack	Maintaining White-list of Authorized AP(s)	Requires Timing Characteristics	Requires Traffic Profiling	Requires Specialized hardware	Overhead	Remarks
Maintaining White-list [52, 107]	N	Y	N	N	N	N	Does not detect evil twin AP.
Maintaining RTT, IAT [49, 50, 51, 113]	Y	N	Y	Y	Y	High	Requires precise timing characteristics.
Frame Feature Extraction [117, 118, 121]	Y	N	Y	Y	Y	High	Require precision in measurements of traffic. Prone to false positives
Proposed Scheme	Y	N	N	N	N	Low	Easy to deploy. Encryption Free. Low resource overhead. Formally verifiable. No protocol modification required.

open Wi-Fi network, but the methods can be extended to encrypted Wi-Fi networks also.

2.7 Conclusion

In this chapter, the DES framework has been adapted and used for building an IDS for the evil twin attack. In evil twin attack, an attacker creates a rogue AP by cloning the genuine AP’s MAC address and SSID (network name) in order to eavesdrop on client’s communication, re-direct clients to malicious websites, steal credentials of the clients connecting to it

etc. Existing schemes for evil twin attack detection and prevention suffer from expensive setup, deployment issues, maintenance, scalability and lack formal frameworks for design of the attack detector etc. The DES based IDS addresses all these issues associated with the existing approaches. It is also shown that the DES framework needs to be augmented with model variables to make it capable of modeling and detecting the evil twin attack. The IDS is verified on a test bed and the results illustrate detection rate exceeding 92% mark and 100% accuracy.

In the next chapter, we propose Advanced Stealth Man-in-the-Middle (ASMiTM) attack that makes use of ARP spoofing in order to establish a Man-in-the-Middle environment on WPA2 encrypted Wi-Fi networks. WPA2 encryption is currently the best available encryption method and the fact that ASMiTM attack can be launched on WPA2 encrypted networks, ASMiTM attack poses a serious security threat. We also propose an I²-diagnosability (Induced I-diagnosability) DES framework that improves over I-diagnosability framework [72] and is adopted for modeling and designing IDS for the detection of ASMiTM attack.



*“The man who trades freedom for security does not deserve
nor will he ever receive either.”*

Benjamin Franklin
American Statesman, Scientist, Philosopher

3

Advanced Stealth MiTM Attack in Wi-Fi Networks and its Detection using I²-Discrete Event System based IDS

3.1 Introduction

A Man-in-the-Middle (MiTM) attack is a type of attack where an attacker inserts itself between two communicating parties in order to intercept the communication between them. In this chapter, we propose a new insider attack termed as “Advanced Stealth Man-in-the-Middle” (ASMiTM) that combines Stealth Man-in-the-Middle (SMiTM) [61] and Wireless Denial of Service (WDoS) [61] attacks. Both SMiTM and WDoS attacks exploit the Hole 196 vulnerability in the Wi-Fi Protected Access II (WPA2) encrypted Wi-Fi networks.

WPA2 is currently the best encryption method and is widely used these days. WPA2 uses two different keys for encryption purposes: Group Transient Key (GRPKY) and Pairwise Transient Key (PVTKY). The broadcast messages are protected using the GRPKY. The GRPKY is a one-way key shared between all clients that are associated with the AP. The GRPKY is used by the AP for encryption while the clients use it for decryption of broadcast/multicast traffic. The unicast messages are protected using the PVTKY. The PVTKY is a two-way key and is unique to every client. This key is used by both the AP and the client for encryption and decryption of unicast (one-to-one) traffic. For every new association a new PVTKY is generated for the client. However, malicious insiders¹ can launch ASMiTM attack exploiting

¹ASMiTM attack is an example of insider attack. For simplicity of explanation we refer malicious insider as ‘attacker’ in the thesis to maintain uniformity of the terminology used.

the Hole 196 vulnerability and spoof as AP to inject broadcast/multicast frames encrypted with the GRPKY.

In a SMiTM attack, an attacker poisons the Address Resolution Protocol (ARP) cache of a client to setup a Man-in-the-Middle (MiTM) environment to intercept the client's traffic. However, SMiTM attack is usually short lived because a fresh ARP update replaces the poisoned ARP cache entries with genuine ones. Regular insertion of spoofed ARP frames is required to sustain the attack but such regularity may lead to SMiTM attack detection. Technique suggested in [127] can detect SMiTM attack using ARP probing.

To prevent replay attacks in WPA2 encrypted networks, each frame contains a packet number which is monotonically increasing. Frames having lesser packet number than the expected packet number value are dropped by the AP/client assuming them to be replay frame(s). In a WDoS attack, an attacker inflates the broadcast packet number value of a client to a higher value. This results in genuine broadcast/multicast frames sent to the clients with lower packet number values being dropped by the clients assuming them to be replay frame(s).

In this chapter, we propose an ASMiTM attack that prolongs the effects of the individual SMiTM and WDoS attacks while preserving stealthiness. Furthermore, the proposed ASMiTM attack causes dropping of broadcast/multicast frames leading to tougher detection as compared to the detection of the individual SMiTM and WDoS attacks. The probing technique suggested in [127] for detecting SMiTM attack fails to detect ASMiTM attack. ASMiTM attack enables an attacker to steal intellectual property, client's credentials etc., without involving any brute force or key cracking. Our findings are significant as various surveys [63, 64, 65] reveal that insider attacks have caused more losses to an organization than outsider attacks. As WPA2 is one of the most advanced and widely used encryption techniques for securing Wi-Fi networks, ASMiTM attack is a major security threat with virtually no quick fix.

As seen in the previous chapter, DES based IDS can prove to be effective in detection of network attacks. The network attacks are mapped to failures and the diagnoser is implemented as the IDS engine. A DES model is said to be diagnosable, if there exists no failure indeterminate cycle in the DES diagnoser for all the failure types. This property is termed as diagnosability condition. DES diagnosability (analysis) has been comprehensively studied in the literature [72, 128, 124, 129, 80, 130, 131]. The DES framework offers numerous advantages in terms of modeling the system and studying the associated failure diagnosis problem. This stringent requirement of DES diagnosability requiring absence of F_i -indeterminate cycle renders many systems non-diagnosable. The DES framework used in evil twin attack cannot be used for the detection of ASMiTM attack directly. In evil twin

attack, the responses from the attacker and the genuine AP could be differentiated on the basis of frame features like sequence number, retry bit, and AID. This helped to identify the presence of evil twin in the network. However, in ASMiTM attack such differentiation is not possible because of the very nature of ASMiTM attack.

Hence, we require an active DES based IDS, that has the capability to inject frames (called ‘probes’) into the network in order to create differences between the normal and attack scenario, so that ASMiTM attack can be detected. For such attacks, where only partial diagnosis is possible (since attack detection directly depends on sending of properly crafted probe frames), I-diagnosability provides a weaker and a relaxed notion for diagnosability by associating indicator events with the failures (attacks) [72], [124]. A DES model is said to be I-diagnosable if there exists an observable indicator event following the failure and the occurrence of the failure can be detected within finite time after the indicator event has occurred. Some system failures are rendered non-diagnosable by the I-Diagnosability framework even in the presence of observable indicator events following the failure. The I-diagnosability DES framework fails to detect the ASMiTM attack. For detection of ASMiTM attack it is important that ‘probe’ frame is crafted appropriately. If frame features of ‘probe’ frame is incorrectly crafted or supplied with inappropriate values, it may lead to wrong conclusion regarding the state of the network (an attack case concluded as normal).

In order to diagnose ASMiTM attack reliably, we propose a new diagnosability framework known as **Induced I-Diagnosability** (I^2 -Diagnosability). Under this framework, given a DES model and an indicator event, an empowering event² ensures that the indicator event sensitizes the failure (attack). The I^2 -DES modeling framework first develops normal and fault model corresponding to normal and fault scenarios. Subsequently, an I^2 diagnoser is built and implemented as an IDS engine which determines whether the system is operating under normal failure (attack) conditions. We first show how the proposed I^2 -DES modeling framework can be used to detect the faults in a benchmark process of two-tank system system. Following that we propose an I^2 -DES based IDS for detection of the ASMiTM attack. The summary of our contributions are:

1. We propose a new DES diagnosability framework termed as I^2 -diagnosability framework that overcomes the drawbacks of I-diagnosability framework.
2. We propose an I^2 -diagnosability based IDS for detecting ASMiTM attack in 802.11 Wi-Fi networks. We also show that I-Diagnosability framework based IDS fails to diagnose

²For example, to check whether a bulb is working or not, we need to turn ON the switch and check for illumination. The turning ON of the switch is the indicator event. The indicator event helps to sensitize the failure (whether the bulb is working or not). The presence of main power supply empowers the indicator event and hence the main supply becomes empowering event.

the ASMiTM attack whereas the I²-Diagnosability framework based IDS successfully diagnoses the ASMiTM attack.

3. We augment the I²-diagnosability based IDS with *model variables* to overcome the state explosion problem. It has been shown that the proposed scheme is scalable, does not require alteration in the 802.11 protocol stack, nor injects too much traffic into the network on account of probes and is formally verifiable.

The rest of the chapter is organized as follows. Section 3.2 elaborates the 802.11 basics and ASMiTM attack. The detection methodology for ASMiTM attack is discussed in Section 3.3. Section 3.4 describes the I²-Discrete Event System and the terminology associated with it. We consider the Fault Detection and Diagnosis (FDD) of pump valve system to illustrate the proposed I²-Diagnosability framework. In Section 3.5, the proposed I²-Diagnosability framework for ASMiTM attack is illustrated. We also show how I-Diagnosability framework fails to detect the ASMiTM attack and proposed I²-Diagnosability framework successfully detects it. The results obtained using the proposed approach are shown in Section 3.6. Section 3.7 concludes the chapter.

3.2 Background and Proposed ASMiTM Attack

In this section, we look into the ARP spoofing attack, Hole 196 vulnerability, SMiTM attack and WDoS attack. We then propose the ASMiTM attack that combines SMiTM and WDoS attacks.

3.2.1 ARP Spoofing Attack

ARP protocol is used for getting the MAC address of a client when its IP address is already known. We consider the example depicted in Fig. 3.1. C_1 , C_2 , M are three Wi-Fi clients connected to an AP. The IP-MAC mapping of these three client is shown in Fig. 3.1. If C_1 wishes to send data to C_2 , it needs to know the MAC address of C_2 . For obtaining the MAC address of C_2 , C_1 sends an ARP request with source (SRC) IP address set to C_1 's IP address, source MAC address set to C_1 's MAC address, destination IP address set to C_2 's IP address and destination MAC address set to broadcast address (FF:FF:FF:FF:FF:FF). Since ARP request is a broadcast frame it is received by both C_2 and M but only C_2 responds to the ARP request since the destination IP address in ARP request frame is of C_2 . C_2 stores the IP-MAC mapping of C_1 received in ARP request message without any authentication in its ARP cache table. C_2 responds with an ARP reply frame consisting of the source IP address

3.2. Background and Proposed ASMiTM Attack

set to C_2 's IP address, source MAC address set to C_2 's MAC address, destination IP address set to C_1 's IP address and destination MAC address set to C_1 's MAC address. Thus C_1 and C_2 both have the IP-MAC mapping of each other and can communicate. Their mappings are shown in Fig. 3.1 in the row containing 'ARP Cache under normal conditions'. In a similar manner other IP-MAC mappings are obtained. This describes the working of ARP protocol.

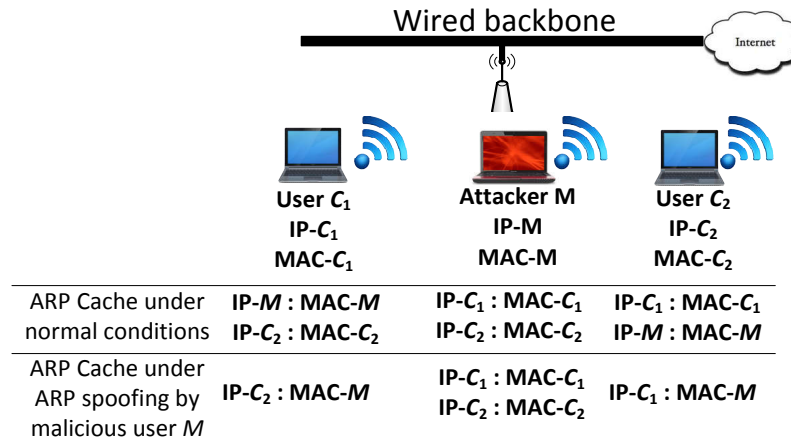


Figure 3.1: ARP cache mappings under normal and spoofing conditions

However, ARP protocol is vulnerable. The vulnerability of the ARP protocol lies in the non-verification of IP:MAC mappings in the ARP request and ARP response frames. The protocol is designed to trust the information contained in the ARP request and response frames. Referring to the previous example, let M be an attacker. M sends a spoofed ARP request with source IP address set to C_1 's IP address, source MAC address set to M 's MAC address, destination IP address set to C_2 's IP address and destination MAC address set to broadcast address ($FF:FF:FF:FF:FF:FF$). The mapping of source IP address and source MAC address in the ARP request frame is wrong (IP: C_1 -MAC: M). The attacker M maps the source IP address of C_1 's with it MAC address. When C_2 receives the spoofed ARP request frame, it stores the IP-MAC mapping of C_1 as IP- C_1 :MAC- M in ARP cache without verification. This phenomenon of invalidating the ARP cache is known as ARP poisoning and the attack is termed as ARP spoofing. Thus, because of ARP spoofing C_2 's ARP cache is poisoned and C_1 's IP is mapped to M 's MAC address in the ARP cache of C_2 . So when C_2 sends data to C_1 , it actually reaches M because of in-correct IP-MAC mapping of C_1 in C_2 's ARP cache. On similar lines, M can poison the cache of C_1 . This enables M to intercept data between C_1 and C_2 thereby becoming a Man-in-the-Middle for clients C_1 and C_2 .

3.2.2 Hole 196

“Hole 196” vulnerability can lead to a potentially fatal insider attack (i.e., must be performed within the network.), where an insider can bypass the WPA2 PVTKY encryption and authentication to scan the authorized devices for vulnerabilities, install malware/spyware on these and steal personal or confidential corporate information from the devices. Although specifically mentioned for WPA2, the vulnerability applies to the WPA version also, irrespective of the authentication method used (TKIP/AES).

The Hole 196 vulnerability exposes authorized client(s) of a WPA2 secured Wi-Fi network to insider attacks. SRC MAC spoofing is not possible in WPA2 networks as client’s MAC address is used for the computation of its PVTKY. If an attacker creates a MAC frame with spoofed SRC MAC address, then the decapsulation procedure at the receiver generates an error. However, GRPKYs do not have this property [93]. Clients cannot use the GRPKY for encryption as per the 802.11 standard. However, by exploiting the Hole 196 vulnerability, an attacker can spoof as AP and inject broadcast/multicast frames by encrypting them using the GRPKY. This vulnerability of GRPKY is known as “Hole 196” [61]. “Hole 196” is the name of WPA2 vulnerability that was showcased by AirTight Networks researchers at the Black Hat and Defcon security conferences in Las Vegas. The vulnerability is so named because it is buried on the page 196 of the of the 1232-page IEEE 802.11 Standard (Revision, 2007). The “Hole 196” vulnerability affects Wi-Fi networks of all sorts, including those using robust Enterprise encryption.

It is easy to exploit the “Hole 196” vulnerability. Hence, the vulnerability can lead to practical insider attacks (launched by disgruntled employees or Cyberspies) when compared with the WPA TKIP vulnerability, which was largely of theoretical interest in nature and difficult to exploit for launching any practical attacks.

3.2.3 Stealth Man in the Middle (SMiTM) Attack

SMiTM attack exploits the Hole 196 vulnerability to set up a Man-in-the-Middle environment by injecting spoofed ARP frames to poison the ARP cache of the client(s) in the network. By poisoning the ARP cache of a client, an attacker re-directs traffic coming from the client to a different target. In this attack, an attacker spoofs as the AP and injects falsified ARP frames encrypted with the GRPKY. A small network setup demonstrating the SMiTM attack is shown in Fig. 3.2. M is the attacker, C_1 is the victim client connected to the same AP and $GTWY$ is the gateway. GRPKY denotes the group transient key, $PVTKY_{C_1}$ and $PVTKY_M$ represent pairwise transient key of C_1 and M , respectively.

3.2. Background and Proposed ASMiTM Attack

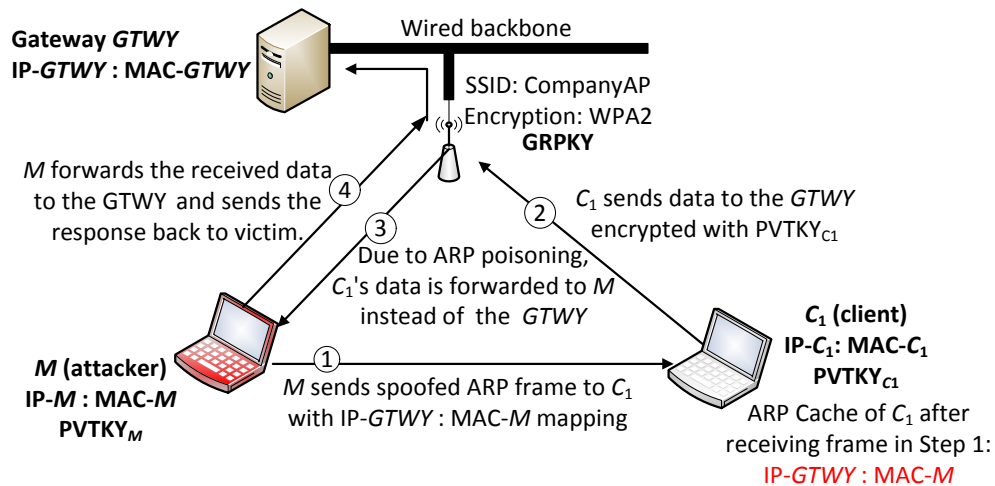


Figure 3.2: SMiTM Attack

M crafts a spoofed ARP request frame with source IP-MAC mapping set to IP-GTWY:MAC- M (i.e., spoofing gateway's IP address with the attacker's MAC address) and destination IP-MAC mapping set to IP-C $_1$:Broadcast MAC (FF:FF:FF:FF:FF:FF). M spoofs as AP and encrypts the ARP frame with the GRPKY. When the client C_1 processes this frame, it updates its ARP cache with IP-GTWY:MAC- M (poisoned) mapping. As M spoofs the MAC address of the AP and encrypts the ARP frame using the GRPKY, the client C_1 assumes that the frame came from genuine AP and updates its ARP cache. Due to ARP cache poisoning of the client C_1 , frames sent by C_1 to the $GTWY$ first reach M . In order to escape detection, M forwards the frame to the $GTWY$. After receiving the corresponding response from the $GTWY$, M forwards the response back to the client C_1 so that M 's identity as Man-in-the-Middle is concealed. Thus, in SMiTM attack, an attacker is successful in establishing MiTM on a WPA2 encrypted Wi-Fi network. However, a fresh ARP update from the $GTWY$ or resetting of the ARP cache by the host OS refreshes the ARP cache of C_1 thereby clearing the poisoned ARP entries.

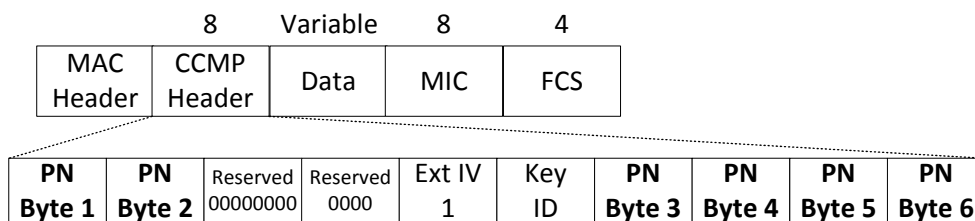


Figure 3.3: Cipher-block chaining Message authentication code Protocol (CCMP) encapsulation

3.2.4 Wireless Denial of Service (WDoS) Attack

The WPA2 encryption technique prevents replay attacks by using a replay counter known as packet number (PACNUM henceforth) in every frame. Fig. 3.3 shows the frame format of Cipher-block chaining Message authentication code (CCMP) Protocol encapsulation. The PACNUM is a 48-bit (6 octets shown in **bold** in Fig. 3.3) monotonically incrementing non-negative integer, initialized to 1 when the corresponding transient key is initialized. The client and its associated AP maintain a separate 48 bit replay counter for unicast and broadcast traffic. The PACNUM value at the AP and the client are always in sync. A client discards any frame that it receives with the broadcast PACNUM value less than or equal to its current PACNUM value.

We explain the WDoS attack using an example shown in Fig. 3.4. The locally cached broadcast PACNUM value at the client C_1 and the AP is 780. M spoofs as the AP and sends a broadcast frame encrypted with the GRPKY having high PACNUM value (say, 1500). In this frame the FromDS bit is set to 1 and the ToDS bit is set to 0 to make the frame appear to be coming from the AP. All clients (including the client C_1) update their broadcast PACNUM value to 1500. As the AP did not send this frame, it is unaware of the change (being a broadcast frame, it reaches the AP, but the setting of FromDS bit to 1 makes the AP drop the frame) in the broadcast PACNUM value of the client C_1 . As a result, it sends the successive broadcast/multicast frames with old PACNUM values – 781, 782 and so on. The client C_1 drops all broadcast/multicast frames having PACNUM value less than 1500, resulting in a loss of frames because of WDoS attack.

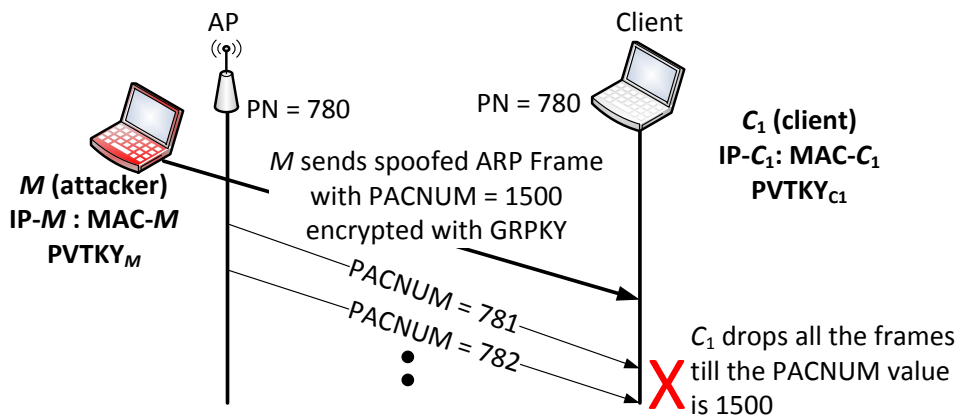


Figure 3.4: WDoS Attack

3.2.5 Proposed ASMiTM Attack

ASMiTM attack exploits the Hole 196 vulnerability to launch a more powerful version of Man-in-the-Middle attack. Very briefly, an attacker spoofs as AP, crafts an ARP request frame containing forged IP-MAC mapping for the gateway, encrypts it using GRPKY along with a high PACNUM value in order to poison the ARP cache for a longer duration. The forged ARP information reaches the clients, who update their ARP cache with the spoofed IP-MAC mapping of the gateway address. The basic network setup used for illustrating the ASMiTM attack is shown in Fig. 3.5. Some details of the network like keys and the IP:MAC mapping of the M , C_1 and $GTWY$ are also shown.

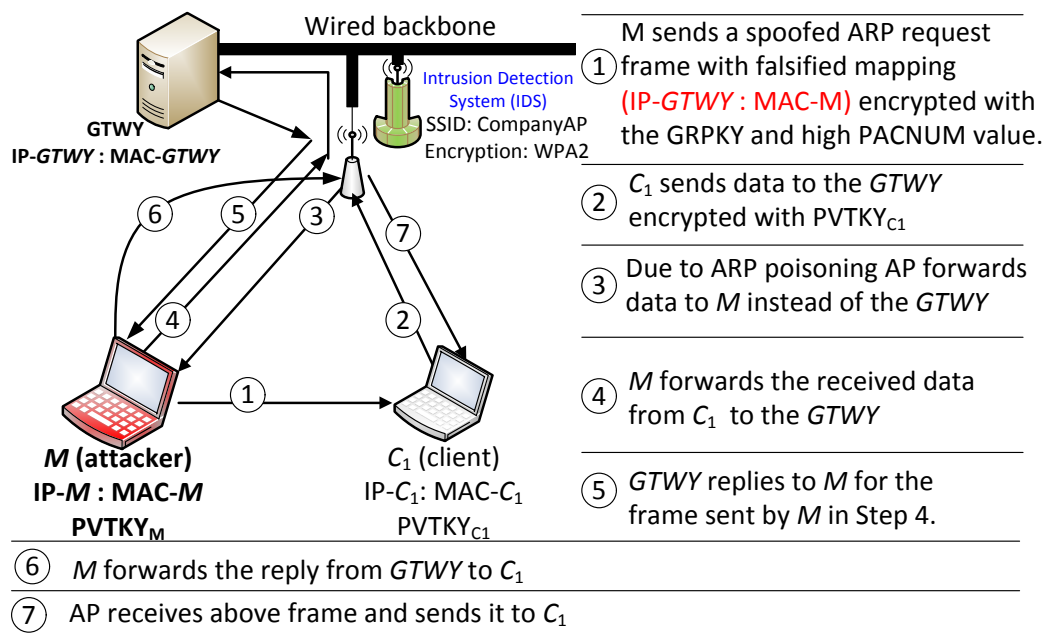


Figure 3.5: ASMiTM attack

Step 1: M needs to perform the following four tasks to launch ASMiTM attack:

- 1. ARP Poisoning:** M crafts a spoofed ARP request frame with source IP address set to $GTWY$'s IP address, source MAC address set to M 's MAC address, destination IP address set to C_1 's IP address and destination MAC address set to broadcast MAC address. By spoofing the $GTWY$'s IP address with its own MAC address, traffic traveling to $GTWY$ first arrives at M 's terminal.
- 2. Reset ToDS and set FromDS bit:** M resets the ToDS bit and sets the FromDS bit to make the ARP request frame appear to be coming from the AP. ToDS and FromDS bits are instrumental in determining the direction in which the frame is traveling. The frame travels from client (AP) to AP (client) if the ToDS (FromDS) bit is set.

3. **Set high PACNUM value:** In order to make the attack more potent, the PACNUM value in the ARP request frame is advanced. As a result the broadcast PACNUM value of the client C_1 is set to a higher value. The increase in PACNUM value ensures that ARP cache of C_1 does not get the genuine IP:MAC mapping via a fresh ARP update, resulting in longer attack duration. Under plain MiTM and SMiTM attack PACNUM is *not* altered.
4. **Transmit the ARP request frame:** M encrypts the ARP request frame with the GRPKY and transmits it.

When the client C_1 receives this spoofed ARP frame, its ARP cache is poisoned and its broadcast PACNUM value is advanced to the value received in the frame. As a result of ARP poisoning, the client C_1 's ARP cache has IP-MAC mapping for the $GTWY$ as IP- $GTWY:MAC-M$. Now, for C_1 , M is the gateway. So traffic sent to $GTWY$ by C_1 now arrives at M 's terminal first.

Step 2: To send (unicast) data to the $GTWY$, C_1 encrypts the frame using $PVTKY_{C_1}$ and transmits it. AP decrypts the frame sent by the client C_1 and finds that the frame needs to be forwarded to M .

Step 3: In Step 2, the client C_1 intended to send the frame to the $GTWY$. However, because of ARP poisoning of C_1 (in Step 1) the frame is sent to M instead of the $GTWY$. In order to send data to M , the AP encrypts the received frame from C_1 with $PVTKY_M$ and forwards it. So the frame sent by the client C_1 to the $GTWY$ is intercepted by M before reaching the $GTWY$. This results in M becoming the Man-in-the-Middle for the client C_1 and the $GTWY$.

Step 4: To escape detection, M must behave like an intermediary. So it forwards the received frame from C_1 to the $GTWY$ by encrypting it using $PVTKY_M$.

Step 5: The AP forwards the response obtained from the $GTWY$ back to M . In case the ARP cache had not been poisoned in Step 1, this response would have come to C_1 directly. To evade detection, M must forward this frame back to the client C_1 . This is important since M needs to hide its identity.

Step 6: M encrypts the received frame in the previous step using $PVTKY_M$, sets the destination MAC address to C_1 's MAC address and transmits the frame.

Step 7: Upon receiving the frame sent in the previous step, the AP encrypts it using $PVTKY_{C_1}$ and forwards it to the client C_1 . So, the client C_1 is unaware about the presence of M behaving as Man-in-the-Middle.

The AP is unaware about the change in the PACNUM value of the client C_1 . So, the AP continues to send broadcast frames with old PACNUM which are eventually dropped by client. C_1 , thus becomes a victim of ASMiTM attack. In the following section we propose a

probing based solution to detect the presence of ASMiTM attack in the Wi-Fi network.

3.2.6 Existing Approaches to Detect or Prevent ASMiTM attack

As the ASMiTM attack is very recent, to the best of author's knowledge no practical solutions exist for its detection. The 802.11 standard does not provide any mechanism to detect the source MAC forgery of the frames encrypted using the GRPKY. This leaves the client with no option but to accept forged frames encrypted with the GRPKY that has correct semantics, as seen in the case of ASMiTM attack. The sequence and semantics of the ARP operations under normal and ASMiTM attack are the same. As a result, detecting ASMiTM attack using signature-based attack detection schemes is difficult. As explained earlier, anomaly-based schemes leads to high false alarm rate. One possible solution is to upgrade the WPA2 protocol while maintaining backward compatibility to prevent misuse of the GRPKY. Technique proposed in [127] can detect SMiTM attack using ARP probing but not ASMiTM attack as it increases the PACNUM in order to nullify the effect of ARP probe proposed in [127].

APs can be configured to enable client isolation. Client isolation [132, 59] does not allow communication between users associated with the same AP. Client isolation is not a part of 802.11 standard. As a result, its implementation varies across vendors. If client isolation is enabled, it might not stop an attacker from injecting spoofed GRPKY frames, but the responses from the attacker are not forwarded to the client. To circumvent client isolation, an attacker can setup a fake wired side gateway, and send a spoofed GRPKY to poison the ARP cache so that all traffic is forwarded to the fake gateway. Client isolation also prevents sharing data between users which may render this technique as not so feasible approach on networks which require sharing [133]. ARP spoofing detection utilities like arpwatch, DecaffeintID [134] can be useful to detect ARP spoofing, however installing these utilities on all endpoints is often cumbersome. Most of the utilities do not support all available platforms (e.g., iPads, iPhones, MacOS, Android Phones, Blackberry, Windows Mobile, Symbian, Windows 7, 8.1, 10 etc.).

Nam et al. [135] propose a voting based mechanism for identifying the attacker poisoning the ARP cache of the clients as long as there are more genuine clients in the network than non-genuine ones. However, providing fairness in voting among the various heterogeneous devices like laptops, smartphones, PDAs and other Wi-Fi devices which possess differential computing capabilities is quite a challenge. The proposed method requires extensive maintenance of tables by the clients and mapping of genuine IP-MAC mappings in a long-term table. Its also sends ten ARP requests in order to check the IP-MAC mapping mapping before

entering the mapping to the long term table. This leads to a huge addition to the network traffic.

Abraham et al. [136] propose a method to verify the ARP request frames using digital signatures encrypted using asymmetric cryptography. However, this methods requires additional administrative overhead like key maintenance, key revocation etc. In addition, this method requires protocol modifications which is cumbersome. One possible solution is to change the GRPKY periodically. However, an attacker can obtain the fresh GRPKY using tools like `wpa_supplicant` [137]. Another solution is to completely disable the use of GRPKY and use PVTKY even for broadcast traffic by individually sending the broadcast frame to every associated client using its PVTKY. However, this solution adds a huge burden on the AP in terms of the number of frames to be transmitted, which defeats the purpose of group communications in the first place [138]. The footprint of the ASMiTM attack is limited to air, which renders wired side solutions useless. So currently no fool-proof methods are available to mitigate ASMiTM attack. ASMiTM attack requires installation of a wireless IDS that actively monitors the Wi-Fi communication between the users.

3.3 Proposed Scheme for the Detection of ASMiTM Attack

In this section, we look into the principle to detect the ASMiTM attack, architecture of the proposed IDS followed by the list of attacker and IDS assumptions.

The ASMiTM attack poisons the ARP cache, so it is essential to verify IP-MAC mapping sent in the ARP request frame. To verify these mapping we make use of ARP probes. ARP probe are ARP request frames that are crafted and injected by the IDS. The source IP and source MAC address in the ARP probe frame is set to IP and MAC address of the IDS respectively. The destination IP is set to IP address being verified and destination MAC address is the broadcast MAC address. A client receiving ARP probe treats it like a normal ARP request. The client whose MAC address is being queried in the ARP probe replies to the ARP probe. Depending on the response received for the ARP probe the IDS determines whether ASMiTM attack has occurred or not.

Figure 3.6 shows a simplified block diagram of the network setup for ASMiTM attack and its detection. M is the attacker, C_1 is the victim client and $GTWY$ is the gateway of the network. IDS monitors the activities of the network and raises an alarm if ASMiTM attack is detected. The attack conditions are same as explained in the earlier section i.e., the attacker spoofs the $GTWY$ IP with its own MAC address in an ARP request frame and sets high PACNUM value. We now see how ARP probe helps the IDS to create difference in the

3.3. Proposed Scheme for the Detection of ASMiTM Attack

ARP sequence under normal and ASMiTM attack conditions. For every step shown in Fig. 3.6, a row is added in Table 3.1. Assume the current value of PACNUM for *GTWY* synced at AP is 780 and the PACNUM value set by the attacker in ARP request frame be 1500.

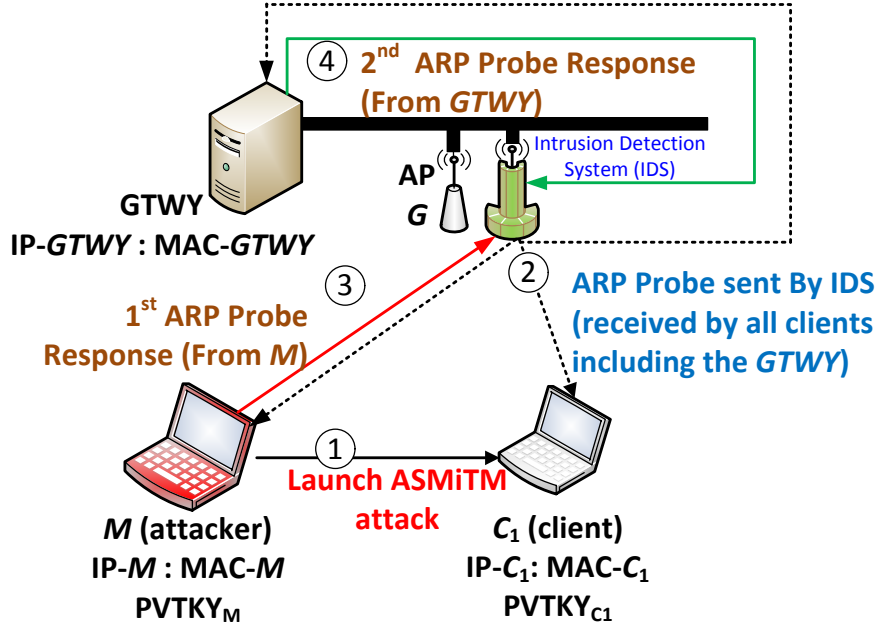


Figure 3.6: Experimental setup for ASMiTM attack

Step 1: Here *M* launches the ASMiTM attack on *C₁*. Row 1 of Table 3.1 is updated.

Step 2: To verify the genuineness of IP-MAC mapping in the ARP request frame sent in Step 1, IDS sends ARP probe with IP-MAC mapping shown in row 2 of Table 3.1. The IDS also updates the *PACNUM* value in the ARP probe to 1501 so that the *PACNUM* value for *GTWY* and AP are in sync.

Step 3: In order to evade detection, *M* re-sends the same IP-MAC mapping i.e., IP-*GTWY*:MAC-*M*, in response to the ARP probe sent by the IDS. This is shown in the row 3 of Table 3.1. Referring the mapping of the *GTWY* in Step 1 and 3, it is evident that both are same. At this point, it cannot be determined whether an ASMiTM attack has occurred or not.

Step 4: The *GTWY* replies with its IP-MAC mapping i.e., IP-*GTWY*:MAC-*GTWY* and sends it to the IDS. This populates the row 4 of Table 3.1. As can be seen, there is a mismatch in the IP-MAC mapping for the *GTWY* in row 3 and row 4 of Table 3.1. The same IP (IP-*GTWY*) is mapped to two different MAC addresses (MAC-*M*) and (MAC-*GTWY*) which is not possible. This ambiguity of IP-MAC mapping provides enough evidence of the presence of an attacker performing ASMiTM attack.

Table 3.1: ASMiTM Detection Table

Step #	Action	SRC IP	SRC MAC	DST IP	DST MAC	Value of Frame PACNUM
Step 1	Forged ARP Frame with high PACNUM encrypted with GRPKY	IP <i>GTWY</i>	MAC <i>M</i>	IP <i>C₁</i>	FF-FF-FF-FF-FF-FF	1500
Step 2	ARP Probe by IDS	IP IDS	MAC IDS	IP <i>GTWY</i>	FF-FF-FF-FF-FF-FF	1501
Step 3	ARP probe response by <i>M</i>	IP <i>GTWY</i>	MAC <i>M</i>	IP IDS	MAC IDS	1502
Step 4	ARP probe response by <i>GTWY</i>	IP <i>GTWY</i>	MAC <i>GTWY</i>	IP IDS	MAC IDS	1503

In this example, we have assumed that *M* responds first to the ARP probe and then the *GTWY* responds. This order depends on the network circumstances. If the *GTWY* responds first, the presence of the attacker is determined in row 3 of Table 3.1. Thus ARP probe helps to detect ASMiTM attack.

3.3.1 ARP Probe as Indicator Event and Importance of Updation of PACNUM value

Under normal circumstances, when ARP probe is sent only one response is obtained. This probe response has the same IP-MAC mapping as the one sent in the initial ARP request frame for which the probe frame is sent. In case an attacker is present in the network, there are two possibilities: a) getting two ARP responses and both having different IP-MAC mapping for the same IP address queried in the ARP probe. b) single ARP response but containing a different IP-MAC mapping when compared to the IP-MAC mapping received in the earlier ARP request frame for which the probe is sent. The receiving of multiple responses or mis-matching responses for the same IP in response to the ARP probe sent by the IDS, helps in the detection of ASMiTM attack. So, the ARP probes have the capability to differentiate between the normal and attack scenarios leading to the detection of ASMiTM attack. As a result, ARP probe is designated as an indicator event in the I²-DES model for ASMiTM attack.

In order to understand the importance of updating the PACNUM, we once again visit the Table 3.1. If the IDS did not update the PACNUM value to 1501 in Step 2, it would have sent the ARP probe with a PACNUM value 781. As *C₁*'s PACNUM value is updated to 1500 in Step 1 by the attacker, *C₁* on receiving the ARP probe with PACNUM value 781 drops it assuming it to be a replay frame. So only one response (the one obtained in row 3 of Table 3.1) to the ARP probe is obtained. Since the IP-MAC mapping obtained in response to the ARP probe matches with the IP-MAC mapping that is sent in original ARP request frame (the one obtained in Step 1), the IDS in-correctly concludes that the network is under normal conditions.

So simply sending ARP probes is not sufficient. The ARP probe must be sent with an updated PACNUM value so that the genuine host (gateway in our case) always responds. As the IDS monitors the communication promiscuously, it updates the PACNUM value of C_1 to 1500 before sending ARP probe. The sending of ARP probe with an updated PACNUM value is instrumental for the detection of ASMiTM attack. In the proposed I²-DES based IDS the sending of the ARP probe is designated as the indicator event while updating the PACNUM is designated as the empowering event. In the following section, we demonstrate the application of I²-Diagnosability framework for the detection of ASMiTM attack.

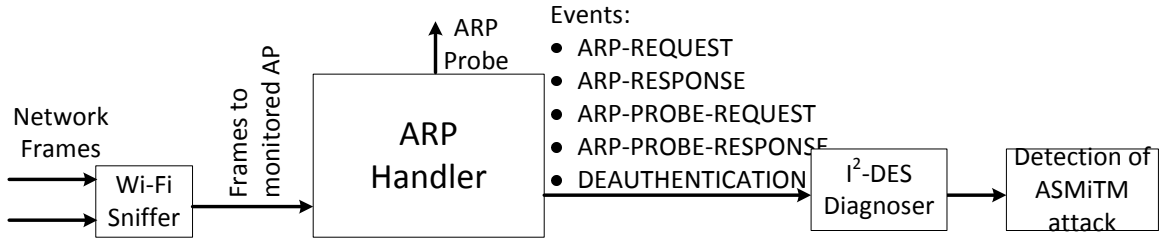


Figure 3.7: Components of the proposed IDS for detection of ASMiTM attack

3.3.2 IDS Components

The block diagram for the IDS used for detection of the ASMiTM attack is shown in Fig. 3.7. The different components are described as follows:

- **Wi-Fi Sniffer:** A Wi-Fi sniffer is capable of capturing all the Wi-Fi frame(s) traveling in the network. However, in our proposed scheme, only the frames destined to and from the monitored APs are captured. Frame(s) to other APs are ignored. The Wi-Fi sniffer forwards the captured frame(s) to ‘ARP Handler’.
- **ARP Handler:** The ARP Handler is responsible for extracting vital information like SRC IP and MAC address from the frame headers. The ARP Handler component is responsible for the generation of events like ARP-REQUEST, ARP-RESPONSE, ARP-PROBE-REQUEST, APR-PROBE-RESPONSE, DEAUTHENTICATION. The ARP Handler also makes use of the value of the attributes like source MAC address (MACS), source IP address (IPS), destination MAC address (MACD) and destination IP address (IPD) contained in these network frames (events). The ARP Handler forwards these event(s) and attribute(s) to the I² diagnoser which determines if ASMiTM attack has occurred or not.
- **I² Diagnoser:** The I² diagnoser is implemented as a software module and used for attack detection purposes. The I² diagnoser is constructed from the DES model under normal

and attack conditions and is the principle component of the detection methodology. The construction and uses of the I² diagnoser are described in Subsection 3.4.5.

3.3.3 Attacker and IDS Assumptions

- **Attacker spoofs the gateway IP address with its own MAC .:** This is done by the attacker to cause maximum damage. This ensures that all the frames traveling to the gateway, first reaches the attacker's terminal.
- **Attacker knows GRPKY of the Wi-Fi network:** As ASMiTM attack is an insider attack, the attacker knows the GRPKY of the network.
- **IDS has sniffing and injection capabilities:** The IDS needs to sniff the frames traveling to and from the monitored AP while it needs injection capabilities to send ARP probe frames.

So, from the above discussion it is clear that capturing of various frames and sending of ARP probes (events) is necessary for the detection of ASMiTM attack. However, it is vital to craft the ARP probes correctly. If the ARP probe is not crafted with suitable parameters, the ASMiTM attack cannot be detected. We now look how the I² DES framework is capable of detecting the ASMiTM attack in all cases and the I-diagnosability framework fails to detect the presence of ASMiTM attack.

3.4 Fault Detection and Diagnosis Theory of I²-Discrete Event System: Two Tank System

In this section we present the proposed the I²-DES framework augmented with *model variables*. The I²-DES model G is defined as:

$$G = \langle X, X_0, \Sigma, \mathfrak{S}, V \rangle \quad (3.1)$$

- X is the finite set of states.
- X_0 is the initial state.
- Σ is the set of events. Note that an event can be measurable or unmeasurable.
- \mathfrak{S} is the set of transitions.

- V is the set of model variables. Each element v_i of V can take values from a domain Dom_i .

A transition $\tau \in \mathfrak{S}$ is defined as a five-valued tuple $\langle x, x^+, \sigma, check(v), assign(v) \rangle$, where

- x is the initial state of the transition denoted as $initial(\tau)$.
- x^+ is the final state of the transition denoted as $final(\tau)$.
- $\sigma \in \{\Sigma \cup \epsilon\}$ is an event on which the transition τ is enabled.
- $check(V)$ represents the conditions on a subset of the model variables. For firing τ , along with the enabling event σ , $check(V)$ should hold true.
- $assign(V)$ represents a subset of the model variables and assignment of the values from their corresponding domain, when τ fires.

A *trace* of the model G is a sequence of transitions generated by G denoted as $s = \langle \tau_1, \tau_2, \dots, \tau_f \rangle$, where $initial(\tau_{i+1}) = final(\tau_i)$, for $i = 1$ to $(f - 1)$. We denote $initial(\tau_1)$ as $initial(s)$ and $final(\tau_f)$ as $final(s)$. The set of all traces generated by G is the language of G , denoted as $L(G)$. Naturally, $L(G)$ is a subset of \mathfrak{S}^w , where \mathfrak{S}^w is the set of all infinite sequences of \mathfrak{S} . Any finite member of $L(G)$ is in \mathfrak{S}^* , the Kleene closure of \mathfrak{S} . The post language of G after a trace s is denoted as $L(G)/s = \{t \in \mathfrak{S}^* \mid st \in L(G)\}$. $L_f(G)/s \subset L(G)/s$ comprises finite prefixes of the infinite traces of $L(G)/s$.

3.4.1 Need for I²-DES Framework

Discrete Event Systems (DES) approach has been extensively used for failure detection and diagnosis. A DES model is said to be diagnosable if after the occurrence of a fault, the model can accurately predict whether the system is in normal or failure state using a subset of measurable state variables. A common approach used for such purposes is to build a diagnoser which is a state estimator of the DES model. Using the diagnoser it can be ascertained within finite time whether the system is in failure state after the occurrence of a failure event. A DES model is said to be diagnosable, if there exists no failure indeterminate cycle in the DES diagnoser for all the failure types. This property is termed as *diagnosability condition*. DES diagnosability (analysis) has been comprehensively studied in the literature [72], [80], [124], [128], [129], [130], and [131]. The DES framework offers numerous advantages in terms of modeling the system and studying the associated failure diagnosis problem.

This stringent requirement of DES diagnosability requiring absence of F_i -indeterminate cycle renders many systems non-diagnosable. To overcome this stringent requirement, I-diagnosability provides a weaker and a relaxed notion for diagnosability by associating indicator events with the failures [72], [124]. A DES model is said to be I-diagnosable if there exists an observable indicator event following the failure and the occurrence of the failure can be detected within finite time after the indicator event has occurred following the failure. Some systems failures are rendered non-diagnosable by the I-diagnosability framework even in the presence of observable indicator events following the failure. In order to diagnose such systems, we propose a new diagnosability framework known as Induced I-Diagnosability (I²-Diagnosability). Under this framework, given a DES Model G and an indicator event, an empowering event ensures that the indicator event sensitizes the failure.

3.4.2 I²-DES Model: Measurement Limitations and Failure Diagnosis

Limitations of measurement give rise to uncertainty in transitions in the observed dynamics of the model. In this sub-section the notion of measurement limitation in the I²-DES framework is formally introduced and the consequent uncertainty in transitions in G is characterized. In order to explain the definitions in a more clear and concise way we take help of the two tank system explained in Subsection 3.4.3. Very briefly, the two tank system involves filling of tank T_1 , followed by filling of tank T_2 . After tank T_2 gets full, the mixture in tank T_2 is drained off. We have reproduced few standard definitions available in the DES literature [72, 124, 125] for the sake of completeness and simplicity of explanation.

Definition 14. Measurable and unmeasurable events/transitions: Any event that can (cannot) be measured using sensors are measurable (unmeasurable) events. A **transition** $\tau_i = \langle x, x^+, \sigma, check(V), assign(V) \rangle$ is said to be a measurable (unmeasurable) transition if σ is a measurable (unmeasurable) event. \mathfrak{S}_m and \mathfrak{S}_u denote the set of measurable and unmeasurable transitions. In Fig. 3.9 the event “ T_1 Filling” is a measurable event so the transition τ_1 associated with the event “ T_1 Filling” is also measurable.

Definition 15. Measurement equivalent transitions and states: Two transitions $\langle x_1, x_1^+, \sigma_1, check_1(V), assign_1(V) \rangle$ and $\langle x_2, x_2^+, \sigma_2, check_2(V), assign_2(V) \rangle$ are equivalent if $\sigma_1 = \sigma_2$ (same event), $check_1(V) \equiv check_2(V)$ (same equalities over the same subset of variables in V), and $assign_1(V) \equiv assign_2(V)$ (same subset of model variables with same assignment). If $\tau_1 \equiv \tau_2$ then the source states of the transitions are equivalent and so are the destination states, i.e., $x_1 \equiv x_2$ and $x_1^+ \equiv x_2^+$. In Fig. 3.9, upon comparing the transitions τ_1 and τ'_1 we observe that the same event (T_1 Filling) is associated with both the transitions.

So, $\tau_1 \equiv \tau'_1$ which implies $s_0 \equiv s'_0$ and $s_1 \equiv s'_1$. As a result when the event “ T_1 Filling” occurs, it cannot be said with certainty whether the system has taken the transition τ_1 or τ'_1 . So, the transitions τ_1 and τ'_1 are said to be measurement equivalent transitions.

Definition 16. Projection and Inverse Projection Operator: A **projection** operator $P : \mathfrak{S}^* \rightarrow \mathfrak{S}_m^*$ is defined as: $P(\epsilon) = \epsilon$ (null string); $P(\tau) = \tau$ if $\tau \in \mathfrak{S}_m$; $P(\tau) = \epsilon$ if $\tau \in \mathfrak{S}_u$; $P(s\tau) = P(s)P(\tau)$, where $s \in L_f(G)$, $\tau \in \mathfrak{S}$. The function P erases the unmeasurable transitions from the argument finite trace. $P(s)$ is termed as the *measurable finite trace* corresponding to the finite trace s . An **inverse projection** operator $P^{-1} : \mathfrak{S}_m^* \rightarrow 2^{\mathfrak{S}^*}$ is defined as: $P^{-1}(s) = \{s' \in L_f(G) \mid sEs'\}$. Thus, $P^{-1}(s)$ encompasses all possible sequences of transitions that are equivalent to the finite trace s . The projection function P , the inverse function P^{-1} and the measurement equivalence E of finite traces can be extended to traces $\in \mathfrak{S}^w$, in a natural way.

Definition 17. Measurable Equivalent Traces: Two finite traces s and s' are said to be measurement equivalent if the following relation holds: $P(s) = \langle \tau_1, \tau_2, \dots, \tau_n \rangle$, $P(s') = \langle \tau'_1, \tau'_2, \dots, \tau'_n \rangle$ and $\tau_i E \tau'_i$, $1 \leq i \leq n$.

We use the symbol E to denote measurement equivalence of finite traces as well as that of transitions, with slight abuse of notation. The equivalence of finite traces s and s' implies that if measurable transitions are extracted from s and s' by use of the operator P , then all the transitions are measurement equivalent. Following Definition 15, it can be seen that the trace $\langle \tau_1, \tau_2, \tau_3 \rangle$ in Fig. 3.9, is measurement equivalent to the trace $\langle \tau'_1, \tau'_2, \tau'_3 \rangle$.

Definition 18. Normal G -state/ G -transition and Failure G -state/ G -transition: States that are traversed by the system when operating without any faults (attack) are known as **normal G -state**. X_N denotes the set of all normal states. A G -transition $\langle x, x^+ \rangle$ is called a *normal G -transition* if $x, x^+ \in X_N$. States that are traversed by the system when operating under **failure** circumstances are known as **Failure G -state**. X_{F_i} denotes the set of all failure states. A G -transition $\langle x, x^+ \rangle$ is called a *failure G -transition* if $x, x^+ \in X_{F_i}$. In Fig. 3.9, the states s_0, s_1, s_2 are normal G -states. The transitions associated with these states viz. τ_1, τ_2 are normal G -transitions. The states s'_0, s'_1, s'_2 are failure G -states. The transitions associated with these states viz. τ'_1, τ'_2 are failure G -transitions.

Definition 19. Failure causing G -transition: A transition $\langle x, x^+ \rangle$, where $x \in X_N$ and $x^+ \in X_{F_i}$, is called a *failure causing G -transition* indicating the occurrence of some failure. Since failures are assumed to be *permanent*, there is no transition from any $x \in X_{F_i}$ to $x^+ \in X_N$. In Fig. 3.9, the transition τ_{0F1} is the failure causing G -transition as it moves the model from normal to the failure state. All failure causing G -transition are inherently unmeasurable.

The objective of the failure diagnosis problem is to determine the occurrence of a failure F_i . If the event (σ) corresponding to τ_{F_i} is measurable, failure diagnosis is trivial. So the failure causing transitions are assumed to be unmeasurable. For such failure causing transitions, σ is unmeasurable. As σ is unmeasurable, there are no checks or assignment for model variables. As failures are assumed to be *permanent*, there is no transition from any state in x_{F_i} to any state in X_N . The event related to causing F_i is denoted as σ_{F_i} .

3.4.3 Application of Failure Detection and Diagnosis Theory of I²-DES on Two Tank System

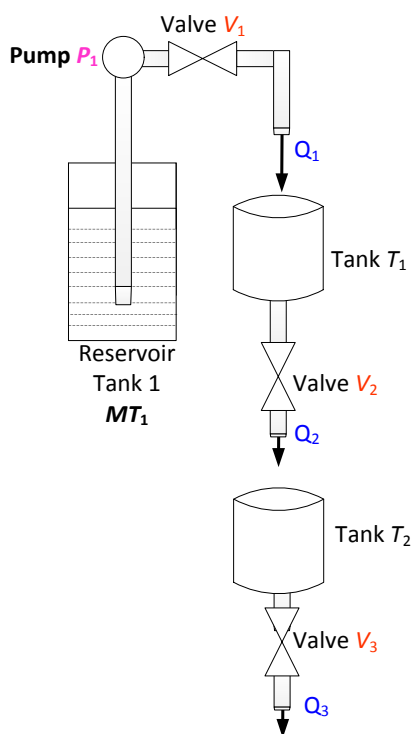


Figure 3.8: The two tank system

We demonstrate the Failure Detection and Diagnosis (FDD) theory of the DES using an example of two connected tanks viz. T_1 and T_2 as shown in Fig. 3.8. Tank T_1 is supplied substance from reservoir tank MT_1 using pump P_1 . The flow through pump P_1 is controlled using valve V_1 . Tanks T_1 and T_2 are connected by means of valve V_2 . Tank T_2 has an outlet pipe whose flow is controlled by means of valve V_3 . This broad arrangement of two tanks is used in many industrial process which require mixing of two substances in a predetermined ratio. First the substance from MT_1 is filled in the tank T_1 . The volume of T_2 is same as that of volume of tank T_1 . When T_1 is full, the valve V_2 is opened which drains out the substance from tank T_1 into tank T_2 . As the volume of both the tanks is same, the emptying of tank

T_1 implies that the tank T_2 is full. The substances in tank T_1 and T_2 are stirred to ensure that the mixture is homogeneous. Later, when T_2 becomes full the valve V_3 is opened and substance from tank T_2 is drained out for usage. Once T_1 and T_2 are emptied, they are refilled again and the process repeats.

The control of flows in the system is done by opening and closing of the valves by a controller which in turn depends on the two types of sensor outputs viz. (i) level sensors of the tanks and (ii) flow sensors of the valves. The tanks are equipped with two level sensors each in order to determine whether the level of the substance in the tank is low or high. For example, in the tank T_1 if the level of substance is at the lowest (highest) point the low (high) level sensor, indicated by $T_1\text{Low}$ ($T_1\text{High}$), gives output 1. There is a flow sensor (indicated as Q_1, Q_2, Q_3) beside every valve that indicates whether substance is flowing through the adjoining pipe or not. For example, $Q_1 = 1$ (0) if substance is flowing (not flowing) through the pipe corresponding to Q_1 which connects MT_1 to T_1 . Table 3.2 shows the details of the sensors, their possible outputs and their interpretations.

Table 3.2: Sensor map for two tank system

Sensor	Possible Outputs	Interpretation
$T_i\text{Low}$ ($i = 1, 2$)	0	$T_i\text{Low} = 0$ implies substance in the tank T_i is NOT at the lowest level.
	1	$T_i\text{Low} = 1$ implies substance in the tank T_i IS at the lowest level.
$T_i\text{High}$ ($i = 1, 2$)	0	$T_i\text{High} = 0$ implies substance in the tank T_i is NOT at the highest level.
	1	$T_i\text{High} = 1$ implies substance in the tank T_i IS at the highest level.
Q_i ($i = 1, 2, 3$)	0	NO Flow measured by Flow sensor Q_i
	1	POSITIVE Flow measured by Flow sensor Q_i

Now we elaborate the working of the two tank system in terms of sensor outputs and controller commands to open/close the valves. Initially, all the tanks have their substances at the lowest levels, indicated by $T_1\text{Low} = T_2\text{Low} = 1$ (and obviously $T_1\text{High} = T_2\text{High} = 0$). As all the valves are closed there is no flow in any of the pipes, so flow sensor outputs: $Q_1 = Q_2 = Q_3 = 0$. First T_1 is to be filled which is initiated by the controller issuing the command $CV_1 = 1$. This results in opening of the valve V_1 to allow the flow of substance into T_1 . Once the substance starts flowing into T_1 from MT_1 , Q_1 becomes 1 and $T_1\text{Low}$ becomes 0. After the tank T_1 is full $T_1\text{High}$ becomes 1 and the controller issues the command $CV_1 = 0$ to close the valve V_1 . Flow to T_1 stops and Q_1 becomes 0. After T_1 becomes full the controller issues the command $CV_2 = 1$ which opens the valves V_2 and substance from T_1 is allowed to fall into the tank T_2 ; $Q_2 = 1$ and $T_2\text{Low} = 0$. As the volume of T_2 is same as the volume of T_1 , the emptying of tank T_1 (i.e., $T_1\text{Low} = 1$) implies that the tank T_2 gets full (i.e., $T_2\text{High} = 1$).

We consider the fault of the flow sensor Q_3 for the current system. Due to the fault in the

flow sensor Q_3 , it always reports a positive flow even if there is no flow measured on the pipe where the sensor Q_3 is placed. So, even when the valve V_3 remains in a closed position (which ensures that there should not be any flow seen from flow sensor Q_3), the flow sensor Q_3 still reports positive flow. Due to the faulty flow sensor Q_3 , incorrect conclusions are obtained for the two tank system.

Now we discuss the modeling of the two tank system using the I²-DES framework. The I²-DES model G used to represent two tank system under normal and fault scenarios is shown in Fig. 3.9. The various components of G are as follows:

$$X = \{s_0, s_1, s_2, s_3, s_4, s_5, s_6, s_7, s'_0, s'_1, s'_2, s'_3, s'_4, s'_5, s'_6, s'_7, s'_8\}$$

$$X_0 = \{s_0\}$$

$$\Sigma = \{T_1 \text{ Filling}, T_1 \text{ Full}, V_2 \text{ Open}, T_2 \text{ Filling}, T_2 \text{ Full}, T_2 \text{ Drain}, V_3 \text{ Open}, T_2 \text{ Intermediate}\}$$

$$\mathfrak{S} = \{\tau_0, \tau_1, \tau_2, \tau_3, \tau_4, \tau_5, \tau_6, \tau_7, \tau_8, \tau_9, \tau_{0F1}, \tau'_1, \tau'_2, \tau'_3, \tau'_4, \tau'_5, \tau'_6, \tau'_7, \tau'_8, \tau'_9, \tau'_{10}\}$$

$$V = \{\epsilon\}^3$$

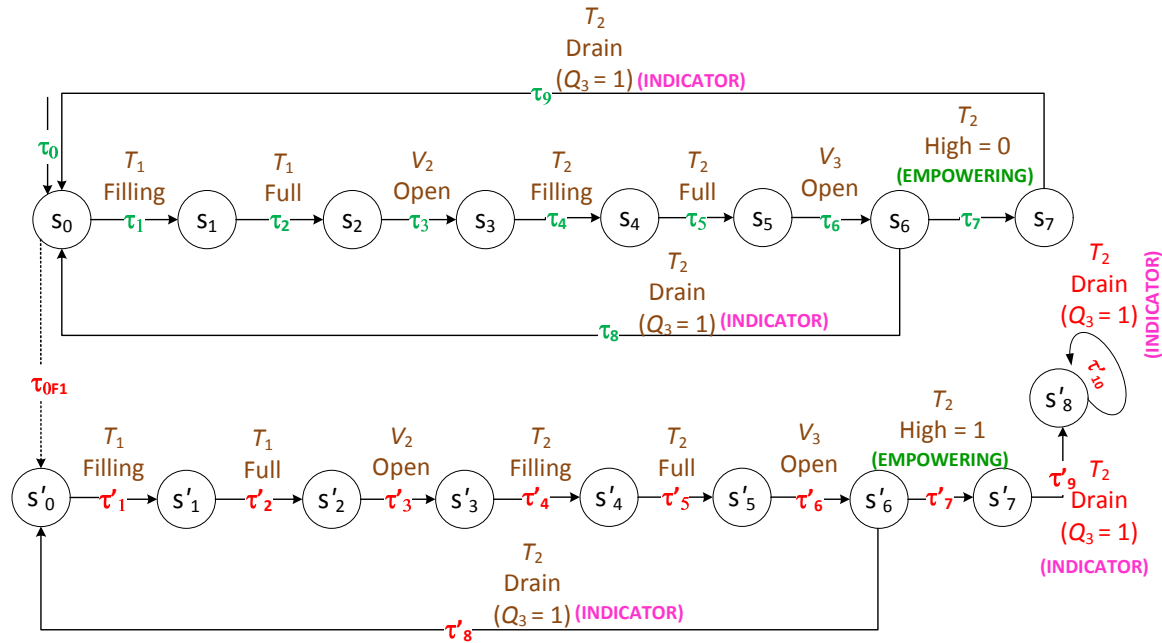


Figure 3.9: DES of the Two Tank System Shown in Fig. 3.8

States and transitions belonging to normal (fault) model are denoted by the non-primed (primed) notations. The occurrence of fault is modeled by the failure causing transition τ_{0F1} . For simplicity of illustration, we assume that fault can occur only from state s_0 . In Fig. 3.9, the transitions are not explicitly detailed as their six tuples, however, the corresponding

³As the number of states in the two tank system are not large, model variables are NOT used as explained in earlier chapter.

3.4. FDD Theory of I²-DES: Two Tank System

Table 3.3: Transitions along with their representation. Events, Sensor Conditions, Controller Commands of the I²-DES model of the two Tank System shown in Fig. 3.9

Transition	What it Represents	Event	Sensor Conditions	Controller Commands
τ_0	All Tanks are Empty	Start	$T_1Low = 1, T_2Low = 1,$ $T_1High = 0, T_2High = 0,$ $Q_1 = 0, Q_2 = 0, Q_3 = 0.$	$CV_1 = 0, CV_2 = 0, CV_3 = 0.$
τ_1 & τ'_1	Tank T_1 Filling	$T_1Filling$	$T_1Low = 0, T_2Low = 1,$ $T_1High = 0, T_2High = 0,$ $Q_1 = 1, Q_2 = 0, Q_3 = 0.$	$CV_1 = 1, CV_2 = 0, CV_3 = 0.$
τ_2 & τ'_2	Tank T_1 Full	T_1Full	$T_1Low = 0, T_2Low = 1,$ $T_1High = 1, T_2High = 0,$ $Q_1 = 0, Q_2 = 0, Q_3 = 0.$	$CV_1 = 0, CV_2 = 0, CV_3 = 0.$
τ_3 & τ'_3	Valve V_2 Open	V_2Open	$T_1Low = 0, T_2Low = 1,$ $T_1High = 1, T_2High = 0,$ $Q_1 = 0, Q_2 = 1, Q_3 = 0.$	$CV_1 = 0, CV_2 = 1, CV_3 = 0.$
τ_4 & τ'_4	Tank T_2 Filling	$T_2Filling$	$T_1Low = 0, T_2Low = 0,$ $T_1High = 0, T_2High = 0,$ $Q_1 = 0, Q_2 = 1, Q_3 = 0.$	$CV_1 = 0, CV_2 = 1, CV_3 = 0.$
τ_5 & τ'_5	Tank T_2 Full	T_2Full	$T_1Low = 1, T_2Low = 0,$ $T_1High = 0, T_2High = 1,$ $Q_1 = 0, Q_2 = 0, Q_3 = 0.$	$CV_1 = 0, CV_2 = 0, CV_3 = 0.$
τ_6 & τ'_6	Valve V_3 Open	V_3Open	$T_1Low = 1, T_2Low = 0,$ $T_1High = 0, T_2High = 1,$ $Q_1 = 0, Q_2 = 0, Q_3 = 1.$	$CV_1 = 0, CV_2 = 0, CV_3 = 1.$
τ_7	Tank T_2 Intermediate	$T_2Intermediate$	$T_1Low = 1, T_2Low = 0,$ $T_1High = 0, T_2High = 0,$ $Q_1 = 0, Q_2 = 0, Q_3 = 1.$	$CV_1 = 0, CV_2 = 0, CV_3 = 1.$
τ_8 & τ'_8	Tank T_2 Drain	T_2Drain	$T_1Low = 1, T_2Low = 0,$ $T_1High = 0, T_2High = 0,$ $Q_1 = 0, Q_2 = 0, Q_3 = 1.$	$CV_1 = 0, CV_2 = 0, CV_3 = 1.$
τ_9	Tank T_2 Drain	T_2Drain	$T_1Low = 1, T_2Low = 0,$ $T_1High = 0, T_2High = 0,$ $Q_1 = 0, Q_2 = 0, Q_3 = 1.$	$CV_1 = 0, CV_2 = 0, CV_3 = 1.$
τ'_7	Tank T_2 Intermediate	$T_2Intermediate$	$T_1Low = 1, T_2Low = 0,$ $T_1High = 0, T_2High = 1,$ $Q_1 = 0, Q_2 = 0, Q_3 = 1.$	$CV_1 = 0, CV_2 = 0, CV_3 = 1.$
τ'_9 & τ'_{10}	Tank T_2 Drain	T_2Drain	$T_1Low = 1, T_2Low = 0,$ $T_1High = 0, T_2High = 1,$ $Q_1 = 0, Q_2 = 0, Q_3 = 1.$	$CV_1 = 0, CV_2 = 0, CV_3 = 1.$
τ_{0F1}	Failure Causing	Fault	$T_1Low = 1, T_2Low = 1,$ $T_1High = 0, T_2High = 0,$ $Q_1 = 0, Q_2 = 0, Q_3 = 0.$	$CV_1 = 0, CV_2 = 0, CV_3 = 0.$

event is shown. Table 3.3 illustrates the events corresponding to the sensor outputs and control commands. The transitions which are enabled by these events are shown in the Table 3.3. For explanation of the modeling we discuss the details of a normal G -transition (τ_1) and an F_i - G -transition (τ'_9).

τ_1 has the event $T_1Filling$. When the sensor outputs for the tank T_1 are – $T_1Low = 1$

and $T_1\text{High} = 0$, the controller issues the command $CV_1 = 1$ which opens the valve V_1 . This allows flowing of the substance to T_1 and the flow sensor output $Q_1 = 1$. These sensor outputs and the controller command are represented by the event $T_1\text{Filling}$ that corresponds to the transition τ_1 .

From s_0 there is another transition τ_{0F1} which indicates the occurrence of a failure. Let us consider the F_i - G -transition τ'_9 which has the event $T_2\text{Drain}$ associated with it. When the system is in state s'_5 (if F_i has occurred), the sensor outputs for the T_2 are $-T_2\text{Low} = 0$ and $T_2\text{High} = 1$, indicating that T_2 is full. Now the controller issues the command to open the valve V_3 so that tank T_2 can be emptied. After the command to open valve V_3 is issued, the system reaches the state s'_6 . As the valve V_3 is opened, the substance in tank T_2 should drain out. While the substance in tank T_2 drains out, the level of substance in the tank T_2 (which was full before the valve V_3 was opened) begins to fall gradually. However, at state s'_7 when the sensor outputs that the level of substance in tank T_2 is still at the highest level despite the controller command to open valve V_3 ($CV_3 = 1$). Next, the flow sensor also outputs positive flow (transition τ'_9) while the level of substance in tank T_2 continues to remain at the highest level (indicated by the sensor outputs: $T_2\text{Low} = 0$ and $T_2\text{High} = 1$). Such conflicting scenario is not possible in the normal operations (indication of positive by the flow sensor Q_3 and the substance in tank T_2 being at the highest level). As we have assumed that the level sensors report correct readings, it can be ascertained that the flow sensor Q_3 incorrectly reported that a positive flow was observed.

If the fault has occurred the controller maintains the command $CV_3 = 1$ perpetually because T_2 does not become empty and the sensor output $T_2\text{Low} = 1$, which makes $CV_3 = 0$, never occurs. As a result the system moves from state s'_7 to s'_8 and continues to remain there forever, which is modeled as the self loop τ'_{10} (and the event is $T_2\text{Drain}$). On the other hand, if the system is normal, T_2 becomes empty and it is modeled by the transition τ_9 . In a similar manner, referring to Table 3.3 and the discussion on the working of the two tank system, the whole modeling given in Fig. 3.9 can be explained.

Now we discuss measurable/unmeasurable transitions of the model and consequently the equivalent states and transitions are identified. In this system all the sensor outputs are measurable and so are the controller commands. So any transition whose enabling event is based on the change in some sensor output or controller command, is measurable. For example, in case of τ_2 the event is $T_1\text{Full}$, whose corresponding change in sensor outputs are $T_1\text{Low} = 0$ (from 1), $T_1\text{High} = 1$ (from 0), $Q_1 = 0$ (from 1) and controller command is $CV_1 = 0$ (from 1). So τ_2 is a measurable transition. In a similar way it can be shown that all transitions except τ_{0F1} are measurable. τ_{0F1} is the failure causing transition and is unmeasurable because it is not caused by a change of any sensor output or controller

command.

Two transitions are measurement equivalent if the corresponding changes in the sensor outputs and the controller commands are same. Events associated with equivalent transitions are also same. For example, transitions τ_2 and τ'_2 are measurement equivalent because they are caused by same changes in sensor outputs and controller commands i.e., $T_1\text{Low} = 0$, $T_1\text{High} = 1$, $Q_1 = 0$ and controller command is $CV_1 = 0$. Also the event associated with both these transitions is $T_1\text{Full}$. As per the Definition 15, $s_0Es'_0$ and $s_1Es'_1$, because the source states and also the destination states of equivalent transitions are equivalent. In a similar way it can be verified that $\tau_iE\tau'_i$, $1 \leq i \leq 6$ and $\tau_8E\tau'_8$ are measurement equivalent transitions. It may be noted that in case of F_i -transitions τ'_i , $1 \leq i \leq 6$ and τ'_8 , there is an equivalent normal transition e.g., $\tau_1E\tau'_1$. So, after the failure as long as the system moves through F_i -transitions τ'_i , $1 \leq i \leq 6$ and $\tau_8E\tau'_8$, the fault cannot be diagnosed because there is no transition that distinguishes the faulty behavior from the normal condition. To elaborate, F_i -transitions τ'_i , $1 \leq i \leq 6$ and τ'_8 do not capture failure manifestation (in terms of distinguishing sensor outputs and controller commands) and hence cannot detect the fault.

Now let us consider the transitions τ_7 , τ_9 and τ'_7 , τ'_9 . The sensor outputs and the controller command for the transition τ_7 are $T_2\text{Low} = 0$, $T_2\text{High} = 0$, $CV_3 = 1$ and $Q_3 = 1$. It indicates that once the valve V_3 was opened, the level of liquid from tank T_2 started to reduce gradually (indicated by $T_2\text{Low} = 0$, $T_2\text{High} = 0$). The sensor outputs and the controller command for the transition τ_9 are $T_2\text{Low} = 1$, $T_2\text{High} = 0$, $CV_3 = 1$ and $Q_3 = 1$. The ' T_2 Drain' event empties the tank completely (indicated by $T_2\text{Low} = 1$, $T_2\text{High} = 0$).

In case of the transition τ'_7 the sensor outputs and controller command are $T_2\text{Low} = 0$, $T_2\text{High} = 1$, $CV_3 = 1$ and $Q_3 = 1$. It may be noted that the controller issues the command $CV_3 = 1$ after detecting that T_2 is full (by sensor outputs $T_2\text{Low} = 0$, $T_2\text{High} = 1$). However, despite the command $CV_3 = 1$ the substance in the tank T_2 continues to remain at the highest level ($T_2\text{High} = 1$). In addition, the flow sensor Q_3 reports positive flow i.e., $Q_3 = 1$. As we have assumed that the level sensors are reliable, the reporting of positive flow by the flow sensor Q_3 despite the fact that the level of substance in tank T_2 remained at the highest level after the controller issued the command to open the valve V_3 , the failure of the flow sensor Q_3 is ascertained. So transition τ'_7 , τ'_9 captures the fault manifestation. As F_i -transition τ'_7 , τ'_9 captures failure manifestation its occurrence is required for detection of F_i .

3.4.4 Diagnosability

The objective of the failure diagnosis problem is to determine the occurrence of a failure F_i . If the event (σ) corresponding to τ_{F_i} is measurable, failure diagnosis is trivial. So the failure causing transitions are assumed to be unmeasurable. For such failure causing transitions, σ is unmeasurable. As σ is unmeasurable, there are no checks or assignment for model variables. As failures are assumed to be *permanent*, there is no transition from any state in x_{F_i} to any state in X_N . The event related to causing F_i is denoted as σ_{F_i} .

Informally, an DES G is diagnosable if it is always possible to determine the failure status of the states beyond a certain point along all the possible traces of G after the occurrence of a failure, using the sequence of measurements. A few terms are introduced before formally defining diagnosability.

Let $\psi(X_{F_i}) = \{s | s \in L_f(G) \text{ and } final(s) \in X_{F_i} \text{ and } s \text{ ends in a measurable transition} \}$.

Definition 20. F_i -Diagnosability: An DES model G (under a given measurement limitation) is said to be diagnosable for failure F_i iff the following holds.

$$(\exists n_j \in \mathbb{N})[\forall s \in \Psi(X_{F_i})](\forall t \in L_f(G)/s)[|t| \geq n_j \Rightarrow D] \quad (3.2)$$

where the condition D is $\forall y \in \{P^{-1}[P(st)]\}$, $final(y) \in X_{F_i}$

The above definition means the following. Let s be any finite prefix of a trace of G that ends in an F_i -state and let t be any sufficiently long continuation of s . Condition D then requires that every sequence of transitions, measurement indistinguishable with st , should end into an F_i -state. This implies that, along every continuation t of s , one can detect the occurrence of failure F_i with a finite delay, specifically in at most n_j transitions of the system after s .

Definition 21. Indicator transitions: An indicator transition is a measurable event that sensitize a failure. A system can have multiple transitions that can qualify to be indicator transition. \mathfrak{S}_I denotes the set of indicator transitions.

The following definition, suggested in [72], which formalizes the notion of diagnosability (of the failure F_i) for DES models is adopted for I²-DES models. Let $\Psi(X_{F_i}) = \{s \in L_f(G) | \text{the last transition of } s \text{ is measurable and } final(s) \in X_{F_i}\}$.

Definition 22. I-Diagnosability: An I-DES model G is said to be I-diagnosable for a failure F_i under a measurement limitation if the following holds:

$$\begin{aligned} & \exists n \in \mathbb{N}[\forall s \in \Psi(X_{F_i})\{(\forall it \in L_f(G)/s)(|t| \geq n \Rightarrow D)\}], \\ & \text{where } D \text{ is } \forall u \in P^{-1}[P(sit)], final(u) \in X_{F_i}. \end{aligned}$$

Definition 22 means the following. Let s be any finite trace of G that contains an F_i -state and let it be any sufficiently long continuation of trace s . Event i is an indicator event and t is any sufficiently long continuation of trace si . Condition D then requires that every sequence of transitions, measurement equivalent with sit (i.e., belonging to $P^{-1}(P(sit))$), should end into an F_i -state. This implies that, along every continuation it of s , one can detect the occurrence of failure corresponding to F_i within a finite delay, specifically in at most n transitions of the system after si . However, there is a possibility $\exists u \in P^{-1}[P(sit)], final(u) \notin X_{F_i}$ in which case the system is non-I-diagnosable.

Definition 23. I²-Diagnosability: An I²-DES model G is said to be I²-diagnosable for a failure F_i under a measurement limitation if the following holds:

$$\exists n \in \mathbb{N} [\forall s \in \Psi(X_{F_i}) \{(\forall ejit \in L_f(G)/s)(|t| \geq n \Rightarrow D)\}],$$

where D is $\forall u \in P^{-1}[P(sejit)], final(u) \in X_{F_i}$.

The I²-diagnosability condition D consists of the empowering event ‘ e ’ and the optional trace j that executes between the empowering event ‘ e ’ and the indicator event i . The notations s, i, t have the same implication as those in I-diagnosability definition. The empowering event ‘ e ’ ensures that the indicator event ‘ i ’ sensitizes the occurrence of failure corresponding to F_i within a finite delay, specifically in at most n transitions of the system after $seji$. Thus it can be seen that the definitions of I-Diagnosability and I²-Diagnosability differ in terms of the empowering event ‘ e ’ and the trace ‘ j ’ that executes between the empowering event ‘ e ’ and indicator event i . The trace ‘ j ’ can be null also.

The fault diagnosis problem is to determine if the fault F_i has occurred within finite number n_{F_i} (where $n_{F_i} \in \mathbb{N}$) say, of transitions after the occurrence of the failure causing transition τ_{F_i} . Let us consider a trace of the DES model of the two tank system; $s = \langle \tau_0, \tau_{0F1}, \tau'_1 \rangle$; obviously $s \in \Psi(X_{F_i})$. For diagnosing F_i , any sufficiently long but finite extension t of s of length n_{F_i} must ascertain that fault has occurred. In this case, if we extend $s = \langle \tau_0, \tau_{0F1}, \tau'_1 \rangle$ as $t = \langle (\tau'_2, \tau'_3, \tau'_4, \tau'_5, \tau'_6, \tau'_8, \tau'_1)^k \rangle$, where k is arbitrarily large, we get $\exists y = \langle \tau_0, \tau_1, (\tau_2, \tau_3, \tau_4, \tau_5, \tau_6, \tau_8, \tau_1)^k \rangle \in P^{-1}(P(st)) \wedge final(y) = x_1 \notin X_{F_i}$. In other words, as the F_i - G -trace $\langle \tau'_1, (\tau'_2, \tau'_3, \tau'_4, \tau'_5, \tau'_6, \tau'_8, \tau'_1)^k \rangle$ is equivalent to $\langle \tau_1, (\tau_2, \tau_3, \tau_4, \tau_5, \tau_6, \tau_8, \tau_1)^k \rangle$ (normal condition), so this F_i - G -trace cannot detect the fault. As already discussed, as none of the transitions involved in the F_i - G -trace under question captures failure manifestation, it is not helpful in fault detection.

In this example there is only one more way of extending s , namely, $t1$ is $\langle \tau'_1, \dots, \tau'_6, \tau'_7, \tau'_9, (\tau'_{10})^k \rangle$. It may be noted that $\exists y \in P^{-1}(P(st1))$ such that $final(y) \notin X_{F_i}$. So the fault is diagnosable. In other words, the transitions τ'_7, τ'_9 and τ'_{10} capture failure manifestation. So the trace $st1$ detects the fault making the fault diagnosable.

3.4.5 I²-Diagnoser Construction and Failure Diagnosis in I-Diagnosability vs I²-Diagnosability Framework for the Two Tank System

The diagnoser is a directed graph represented by $O = \langle Z, A \rangle$; where Z is the set of diagnoser O -nodes, called O -nodes, and $A \subseteq Z \times Z$ is the set of diagnoser transitions, called O -transitions. Each O -node $z \in Z$ corresponds to a set of G -states representing the uncertainty about the actual state. Similarly, each O -transition $a \in A$ of the form $\langle z_i, z_f \rangle$ is a set of measurement equivalent transitions representing the uncertainty about the actual measurable transition that occurs. The *unmeasurable successor* (set) of a set Y of states is defined as $U(Y) = \bigcup_{x \in Y} \{x^+ | \tau = \langle x, x^+ \rangle \in \mathfrak{S}_u\}$. The *unmeasurable reach* of a set Y of states, denoted as $U^*(Y)$, is the reflexive-transitive closure of unmeasurable successors of Y .

Diagnoser Construction: The states in X_0 are partitioned into equivalent subsets denoted as $X_{01}, X_{02}, \dots, X_{0m}$. For all i , $1 \leq i \leq m$, an initial O -node z_{0i} is obtained as the unmeasurable reach of X_{0i} , i.e., $z_{0i} = U^*(X_{0i})$. The set of all initial O -nodes is denoted as $Z_0 = z_{01} \cup \dots \cup z_{0m}$. The initial O -nodes capture the fact that the diagnoser can infer a set z_{0i} of possible initial system states (or their unmeasurable reach) by measuring the variables without waiting for the first measurable transition. Given any O -node z , the O -transitions emanating from z are obtained as follows. Let \mathfrak{S}_{mz} denote the set of measurable G -transitions from the states $x \in z$. Let A_z be the set of all equivalence classes of \mathfrak{S}_{mz} under E . For each $a \in A_z$, a successor O -node z^+ of z such that $z^+ = final(a)$ can be created as follows. Let $z_a^+ = \{final(\tau) | \tau \in a\}$; then $z^+ = U^*(z_a^+)$ and a is designated as: $\langle z, z^+ \rangle$. The set of the diagnoser transitions is augmented as: $A \leftarrow A \cup \{a\}$, and the set of O -nodes is augmented as: $Z \leftarrow Z \cup \{z^+\}$. Each $a \in A$ is an ordered pair $\langle z, z^+ \rangle$, where $z = initial(a)$ and $z^+ = final(a)$. Thus, each O -node contains equivalent states. The detailed algorithm for diagnoser construction is shown in Algorithm 2

Henceforth, we refer to states, transitions, and traces of G as G -states, G -transitions and G -traces, respectively. Similarly, for the diagnoser nodes and transitions, we use O -nodes, O -transitions and O -traces respectively. Now, we look into few definitions and properties related to diagnoser.

Definition 24. (Embedding of G -traces in O -traces): Given a O -trace $\gamma = \langle a_1, a_2, \dots, a_k \rangle$, a G -trace s , where $P(s) = \langle \tau_1, \tau_2, \dots, \tau_k \rangle$, is said to be embedded in γ , if $\tau_i \in a_i$, $1 \leq i \leq k$. The set of all G -traces embedded in a O -trace γ is represented as $A_D(\gamma)$.

Property 2. If two traces $t, y \in A_D(\gamma)$, where t is F_i - G -trace and y is non- F_i - G -trace, then the O -nodes traversed by γ are F_i -uncertain.

Algorithm 2: Algorithm for construction of diagnoser O for an I²-DES model G

```

Input: I2-DES model  $G$ 
Output: I2-DES Diagnoser
1 Partition  $X_0$  into equivalent subsets  $X_{01}, X_{02}, \dots, X_{0m}$ 
2 for all  $i, 1 \leq i \leq m$  do
3    $z_{0i} = \mathcal{U}^*(X_{0i})$ 
4 end
5  $Z_0 \leftarrow z_{01} \cup \dots \cup z_{0m}$ 
6  $Z \leftarrow Z_0$ 
7  $A \leftarrow \phi$ 
8 for all  $z \in Z$  do
9   /* Find the set of measurable  $G$ -transitions ( $\mathfrak{S}_{mz}$ ) outgoing from  $z$  */
    $\mathfrak{S}_{mz} \leftarrow \{\tau \mid \tau \in \mathfrak{S}_m \wedge \text{initial}(\tau) \in z\}$ 
   /* Find the set of all measurement equivalent classes  $A_z$ , of  $\mathfrak{S}_{mz}$  */
10  for all  $a \in A_z$  do
11     $z_a^+ = \{\text{final}(\tau) \mid \tau \in a\}$ 
12     $z^+ = \mathcal{U}^*(z_a^+)$ 
13     $Z = Z \cup \{z^+\}$ 
14     $A = A \cup \{a\}$ 
15  end
16 end

```

Proof. The property also follows from the diagnoser construction. As any O -transition $a \in \gamma$ has an non- F_i - G -transition and a F_i - G -transition (which are equivalent), so source and destination O -nodes of a are F_i -uncertain. \square

Definition 25. F_i - O -node: An O -node, which contains an F_i - G state, is called an F_i - O -node, denoted as z_{F_i} . The set of all F_i - O -nodes is denoted as Z_{F_i} . In Fig. 3.10 the O -nodes $z_0, \dots, z_6, z_8, z_9$ are F_i - O -nodes as each O -node contains an F_i - G -state.

Definition 26. F_i -certain O -node and F_i -uncertain O -node: An F_i - O -node z is called an F_i -certain O -node if $z \subseteq X_{F_i}$. In Fig. 3.10 the O -node z_9 are F_i -certain O -node as it contains only failure G -states. An F_i - O -node which is not F_i -certain is called F_i -uncertain- O -node. In Fig. 3.10 the O -nodes z_0, z_1, z_2 are F_i -uncertain O -nodes as they contain both normal G -states as well as failure G -states.

In words, F_i -certain O -node comprises only F_i - G states, while F_i -uncertain O -node comprises some F_i - G states and some non F_i - G -states. So, if the diagnoser reaches any F_i -certain O -node failure is diagnosed. By Property 2 and Definition 24, if there is a O -trace γ which moves in F_i -uncertain O -nodes, there is a F_i - G -trace t which is embedded in γ . After failure, diagnoser moves in γ by virtue of t . However, as there is another non- F_i - G -trace y say, equivalent to t , fault cannot be diagnosed till γ is exited.

Definition 27. *F_i-O-path* (γ_{F_i}): A path of the diagnoser O is a sequence of O -transitions $\gamma = \langle a_1, a_2, \dots \rangle$, with the consecution property $initial(a_{i+1}) = final(a_i), i \geq 1$. An F_i - O -path γ is an O -path in which every O -node is an F_i - O -node.

Definition 28. *F_i-uncertain cycle*: An F_i -uncertain cycle is an F_i - O -cycle in which there is no F_i -certain O -node. In Fig. 3.10, the O -transitions sequence $\langle a_1, a_2, a_3, a_4, a_5, a_6, a_8 \rangle$ associated with the diagnoser state sequence $\langle z_0, z_1, z_2, z_3, z_4, z_5, z_6, z_0 \rangle$ represents an F_i -uncertain cycle. This is because, none of the O -nodes $(z_0, z_1, z_2, z_3, z_4, z_5, z_6, z_0)$ is an F_i -certain O -node.

Definition 29. *F_i-indeterminate cycle*: An F_i -uncertain cycle γ in which the F_i -states contained in the O -nodes of γ form a cycle in G comprising transitions from γ , is called an *F_i-indeterminate cycle*. Consider a sequence $\langle x_1, x_2, x_3, \dots, x_k \rangle$ that corresponds to a normal cycle and measurement equivalent failure cycle $\langle x'_1, x'_2, x'_3, \dots, x'_k \rangle$. If the system is under normal conditions, the diagnoser moves into normal cycle and once a failure occurs it moves in the failure cycle. As both the normal and attack cycles are measurement equivalent, the normal and failure cycles are indistinguishable from one another. As a result of the presence of the indeterminate cycle it is not possible to predict whether the diagnoser is moving under normal or failure cycle leading to non-diagnosability. Thus, an F_i -indeterminate cycle is an F_i -uncertain cycle with the special property as stated below:

“There is also a cycle involving F_i -states of the composite model that corresponds to the F_i -uncertain diagnoser cycle.” In simple words, the existence of an F_i -indeterminate cycle in the diagnoser implies that there are at least two measurement indistinguishable *syntactic* cycles in G , one comprising only non- F_i -states and the other comprising F_i -states. This implies that if the system moves in an F_i -indeterminate cycle, then the measurable variables are observed to be similar in both non- F_i and F_i conditions. Thus, if the diagnostic estimate moves along such an F_i -indeterminate cycle, then the fault F_i cannot be diagnosed, because, at each point in the cycle there exists uncertainty regarding the occurrence of F_i and as faults are assumed to be permanent, the system may not exit from such a cycle. The existence of an F_i -indeterminate cycle thwarts diagnosability. The equivalence between F_i -diagnosability and the absence of F_i -indeterminate cycles has been formally established for DES models [72].

Definition 30. *F_i-I-indeterminate cycle*: An F_i -indeterminate cycle having an indicator transition embedded inside it is called an *F_i-I-indeterminate cycle*. A diagnoser having F_i -I-indeterminate cycle is non-diagnosable w.r.t to I-diagnosability framework.

Definition 31. *F_i-I²-indeterminate cycle*: An F_i -I-indeterminate cycle having an empowering transition embedded inside it is called an *F_i-I²-indeterminate cycle*. For a system to be I²-

diagnosable it is essential that the I²-diagnoser should not contain any F_i -I²-indeterminate cycle.

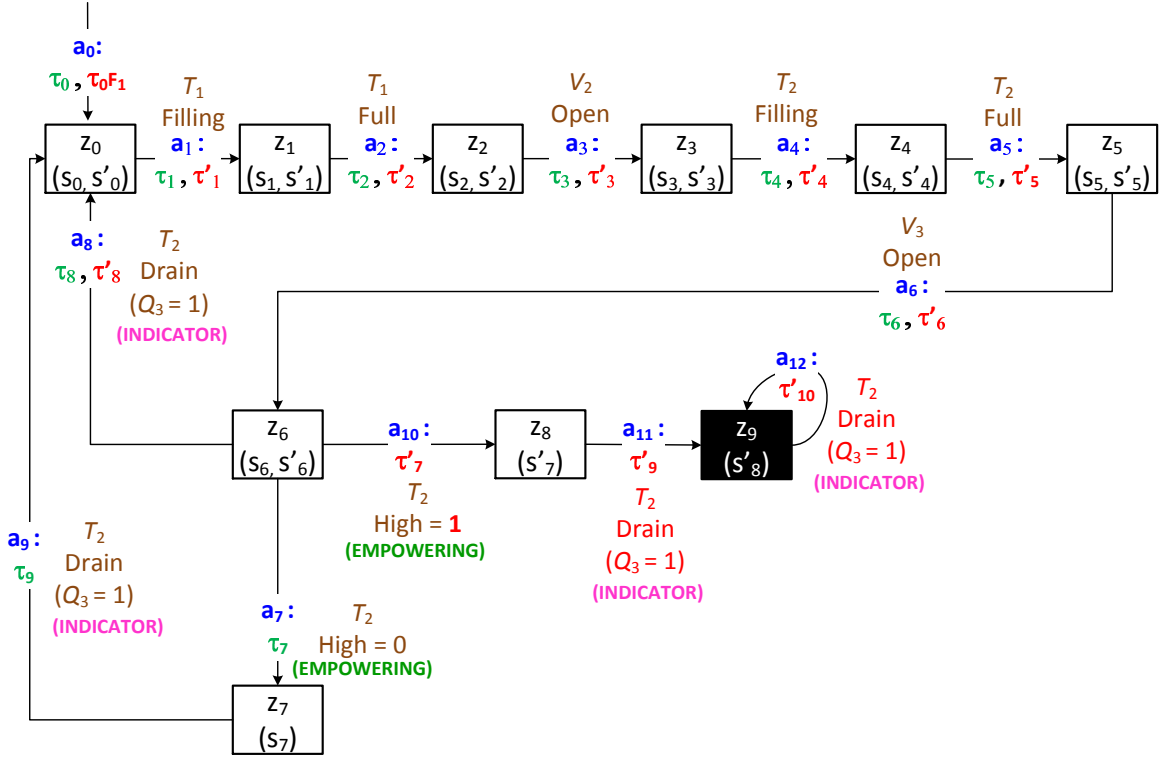


Figure 3.10: I²-DES Diagnoser of the Two Tank System Shown in Fig. 3.8

Now we show that the above fault is non-I-diagnosable but I²-diagnosable. First let us look at the fault diagnosis approach under I-diagnosability framework. The I-diagnosability framework does not require any empowering event. In this example, the flow sensor Q_3 acts as an indicator event. The positive flow indicated by the flow sensor Q_3 ensures that the substance in tank T_2 is drained out. We now show that the diagnoser shown in Fig. 3.10 is non-I-diagnosable but I²-Diagnosable.

In the diagnoser shown in Fig. 3.10, we can see that the trace corresponding to $\langle a_1, a_2, a_3, a_4, a_5, a_6, a_8 \rangle$ forms an F_i -I-indeterminate cycle. As explained earlier, presence of F_i -I-indeterminate cycles leads to non-diagnosability under I-diagnosability framework. An F_i -I-indeterminate cycle requires two conditions to be satisfied: 1) Presence of F_i -I-uncertain cycle. 2) A faulty G -cycle within the F_i -I-uncertain cycle. The F_i -uncertain cycle is composed of the O -nodes $z_0, z_1, z_2, z_3, z_4, z_5, z_6, z_0$ and within the F_i -uncertain cycle, the faulty G -cycle is composed of the G -states $s'_0, s'_1, s'_2, s'_3, s'_4, s'_5, s'_6, s'_0$ making it an F_i -I-indeterminate cycle, leading to non-diagnosability. As a result, no fault diagnosis is possible in such a scenario. As it can be observed from Fig. 3.10, the transition τ'_8 is the indicator transition. Since the flow sensor Q_3 is faulty, and as the diagnoser has no means to check

for the correctness of the flow sensor Q_3 , the faulty state of Q_3 cannot be observed. Thus the I-diagnosability framework fails to detect the presence of fault.

The absence of the empowering event, that ensures that the indicator event sensitizes the sensor, leads to non-diagnosability of the fault. Now we look at how the presence of the empowering event along with the indicator event ascertains the presence of the fault. The empowering event is not present in the I-diagnosability framework but is a part of the I²-diagnosability framework. The I²-diagnosability framework ensures that the flow sensor Q_3 is sensitized such that even if the flow sensor Q_3 reports incorrect system state (i.e., reports positive flow despite no flow).

We look at the trace corresponding to $\langle a_1, a_2, a_3, a_4, a_5, a_6, a_{10}, a_{11} \rangle$ and show how the combination of empowering event and indicator event can help sensitize the failure and eventually help in fault diagnosis. We consider only the failure trace to explain the significance of the proposed I²-diagnosability framework. At O -node z_6 , the controller issued the command to open the valve V_3 . As we have assumed that the flow sensor Q_3 is faulty, it reports positive flow is observed even if no flow is observed. We now show how the empowering event ($T_2\text{High} = 1$, courtesy transition τ_7') sensitizes the faulty sensor Q_3 .

Since the controller has already issued command to open the valve V_3 (CV_3), the level of substance in tank T_2 should start falling gradually. The empowering event checks for the level of substance in tank T_2 after the valve V_3 is opened. In this example, the level of substance in tank T_2 is still at the highest level (indicated by the sensor output $T_2\text{Low} = 0$ and $T_2\text{High} = 1$) even after the valve V_3 is opened. However, the flow sensor Q_3 reports positive flow. Since the level of substance in tank T_2 remains at the highest level even after the valve V_3 is opened, and we have assumed that the level sensors report correct readings, we can conclude that the flow sensor Q_3 is faulty (since if Q_3 reports positive flow, level of substance in tank T_2 should fall). The presence of the empowering event (checking for the level of substance in tank T_2 after valve V_3 is opened) ensures that the flow sensor Q_3 is sensitized.

As seen, the fault in the flow sensor Q_3 which is non-diagnosable under I-diagnosability framework is diagnosable using the I²-DES framework. The only requirement of the I²-DES framework is the presence of the empowering event before the indicator event.

3.5 I²-DES Model for ASMiTM attack

The I²-DES model G under normal and ASMiTM attack scenarios is shown in Fig. 3.11. For readability purposes Fig. 3.11 is annotated with transition number τ_i and the event because

3.5. I²-DES Model for ASMiTM attack

of which the transition τ_i is enabled. States and transitions belonging to normal (attack) model are denoted by non-primed (primed) notations. The various components of G are as follows:

$$X = \{s_0, s_1, s_2, s_3, s_4, s_5, s_6, s'_0, s'_1, s'_2, s'_3, s'_4, s'_5, s'_6, s'_7, s'_8, s'_9\}$$

$$\Sigma = \{\text{ARP-REQUEST, ARP-RESPONSE, ARP-PROBE-REQUEST, APR-PROBE-RESPONSE, UPD}_{PACNUM}, \text{DEAUTHENTICATION}\}$$

$$\mathfrak{S} = \{\tau_0, \tau_1, \tau_2, \tau_3, \tau_4, \tau_5, \tau_6, \tau_7, \tau_8, \tau'_1, \tau'_2, \tau'_3, \tau'_4, \tau'_5, \tau'_6, \tau'_7, \tau'_8, \tau'_9, \tau'_{10}, \tau'_{11}, \tau'_{12}\}$$

$V = \{ip_{src}, ip_{dst}, mac_{src}, mac_{dst}, PACNUM\}$ is the set of model variables. The domain of both mac_{src} and mac_{dst} is $\{xx : xx : xx : xx : xx : xx | x \in [0 - F]\}$ while that of ip_{src} and ip_{dst} is $\{y : y : y : y | y \in [0 - 255]\}$. $mac_{src}(ip_{src})$ and $mac_{dst}(ip_{dst})$ holds source and destination MAC (IP) address contained in the frame respectively. PACNUM contains the packet number of the frame sent and its domain is decimal $\{0, \dots, 2^{48}\}$.

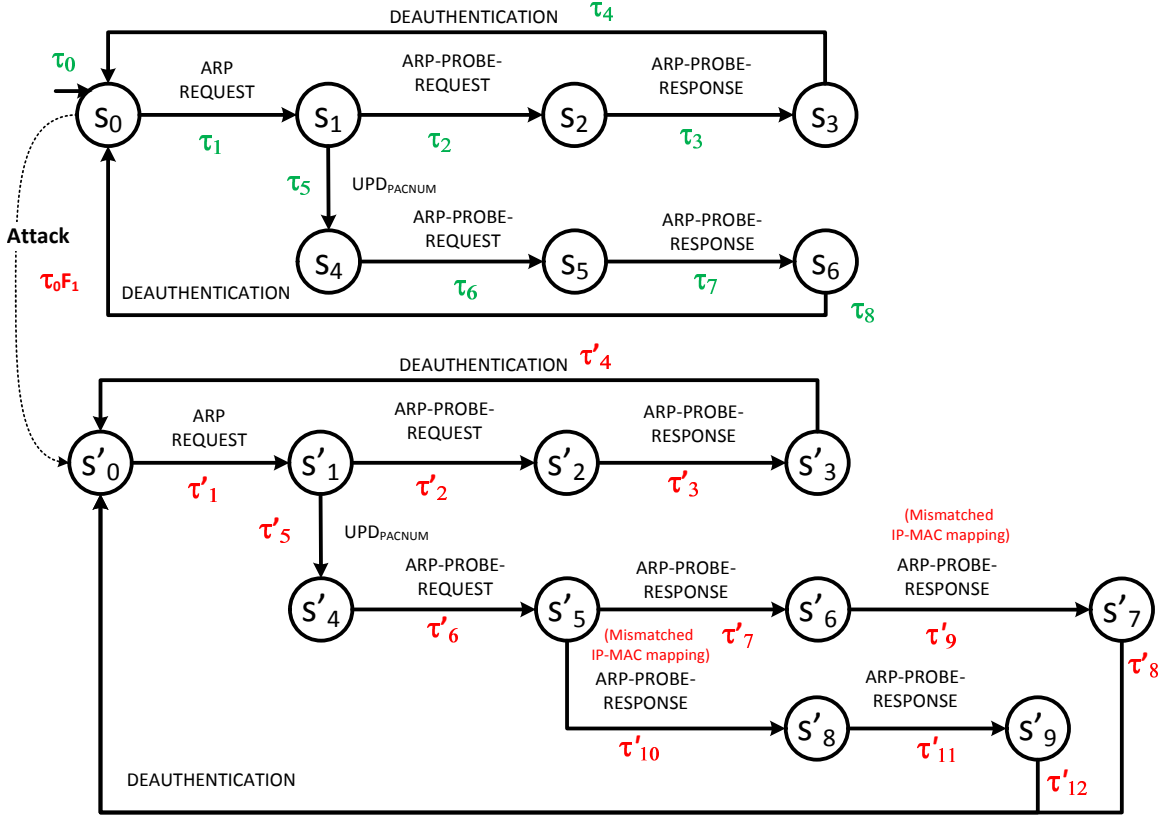


Figure 3.11: Normal and Attack I²-DES Model of ASMiTM Attack

—**Behavior Under Normal Conditions (Attacker absent):** States $\{s_0, s_1, s_2, s_3, s_4, s_5, s_6\}$ and transitions $\{\tau_0, \tau_1, \tau_2, \tau_3, \tau_4, \tau_5, \tau_6, \tau_7, \tau_8\}$ represent the DES model of the system under normal conditions.

- s_0 : The model starts at state s_0 . In state s_0 , the client is about to send an “ARP-REQUEST” frame to the AP.
- $\tau_1(s_0 \rightarrow s_1)$: Here the client sends an ARP request (“ARP-REQUEST”) to the AP. As no checks are made $check(V) = \{--\}$ and $assign(V) = \{ip_{src} \leftarrow ip_{C_1}, mac_{src} \leftarrow mac_{C_1}, ip_{dst} \leftarrow ip_{GTWY}, mac_{dst} \leftarrow mac_{broadcast}\}$. $ip_{src} \leftarrow ip_{C_1}$ and $mac_{src} \leftarrow mac_{C_1}$ is the assignment of SRC IP and MAC address of C_1 to model variable ip_{src} and mac_{src} respectively. On similar lines, the ip_{dst} and mac_{dst} is assigned $GTWY$ IP address and broadcast address respectively. The model variables are used in order to avoid the state explosion problem as explained in the previous chapter.
- $\tau_2(s_1 \rightarrow s_2)$: The IDS sends an ARP probe in order to verify the genuineness of the IP-MAC mapping received during transition τ_1 . Here $check(V) = \{ip_{src} \equiv ip_{IDS}, mac_{src} \equiv mac_{IDS}, ip_{dst} \equiv ip_{C_1}, mac_{dst} \equiv mac_{broadcast}\}$.
- $\tau_3(s_2 \rightarrow s_3)$: Here C_1 replies to the ARP probe sent in previous step. This response has the same mapping as that received in transition τ_1 . Here $check(V) = \{ip_{src} \equiv ip_{C_1}, mac_{src} \equiv mac_{C_1}, ip_{dst} \equiv ip_{IDS}, mac_{dst} \equiv mac_{IDS}\}$. The DES model returns to start state s_0 and the IDS monitors for new ARP request frames sent.
- $\tau_5(s_1 \rightarrow s_4)$: As the IDS monitors the network activities, it updates the PACNUM value for C_1 by using the value of PACNUM obtained in the previous step. Here $check(V)$ ensures that PACNUM of that client is updated whose ARP request is obtained in the previous step. The event UPD_{PACNUM} syncs the PACNUM at AP for C_1 .
- $\tau_6(s_4 \rightarrow s_5)$: The ARP probe sent here is similar to the one sent in transition τ_2 except for the fact that it has the PACNUM updated.
- $\tau_7(s_5 \rightarrow s_6)$: This is the ARP response by the C_1 . This is similar to the transition τ_3 explained above. Here too, the IP-MAC mapping obtained are same as those obtained in transition τ_1 . The DES model returns to start state s_0 and the IDS monitors for new ARP request frames sent.
- $\tau_7(s_6 \rightarrow s_0)$ and $\tau_4(s_3 \rightarrow s_0)$: The client eventually sends a deauthentication frame to end the association with the AP.

—**Behavior Under Attack Conditions (Attacker Present)**: For attack conditions we discuss only those states and transitions that differ from normal conditions. Here M sends a spoofed ARP request frame with IP-MAC mapping as IP-GTWY:MAC- M . States $\{s'_0, s'_1, s'_2, s'_3, s'_4, s'_5, s'_6, s'_7, s'_8, s'_9\}$ and transitions

3.5. I²-DES Model for ASMiTM attack

$\{\tau'_1, \tau'_2, \tau'_3, \tau'_4, \tau'_5, \tau'_6, \tau'_7, \tau'_8, \tau'_9, \tau'_{10}, \tau'_{11}, \tau'_{12}\}$ represent the DES model of the system under **attack** conditions.

- $\tau'_9(s'_6 \rightarrow s'_7)$: This is the second response to the ARP probe sent in transition τ'_9 . However, the IP-MAC mapping obtained here are different than the IP-MAC mapping obtained in transition τ'_1 . Here $check(V) = \{ip_{src} \equiv ip_{GTWY}, mac_{src} \neq mac_M, ip_{dst} \equiv ip_{IDS}, mac_{dst} \equiv mac_{IDS}\}$.
- $\tau'_7(s'_5 \rightarrow s'_6)$: In this case, the first response (τ'_7) to the ARP probe has a different IP-MAC mapping than the one received in transition τ'_1 .

We look into the diagnoser construction in the next section.

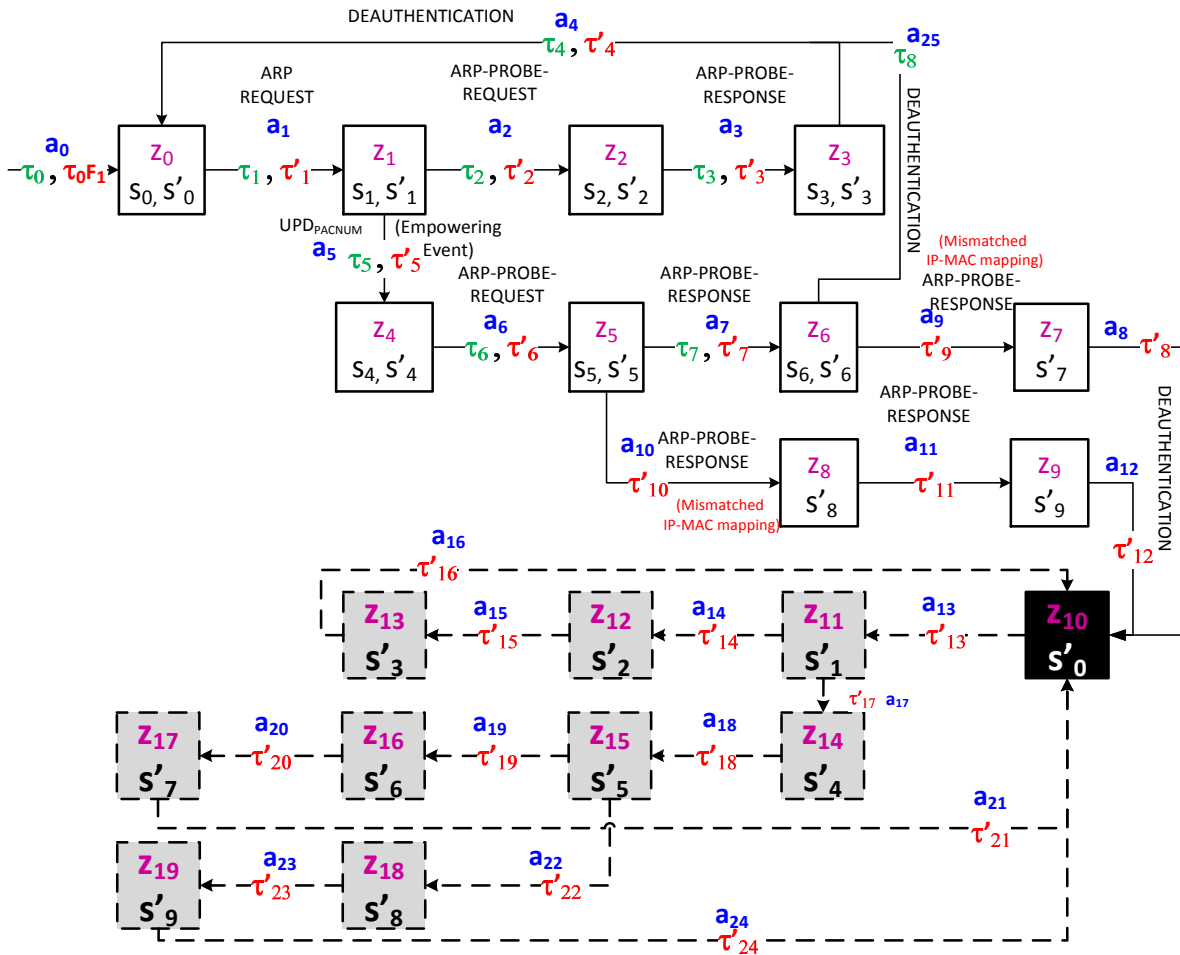


Figure 3.12: Diagnoser for ASMiTM Attack

Diagnoser construction ASMiTM Attack

The diagnoser obtained from the I²-DES model of the ASMiTM attack in Fig. 3.11 is shown in Fig. 3.12. Some of the initial steps for this example are as follows.

1. The initial state of the diagnoser i.e., Z_0 is obtained as follows. X_0 is partitioned into measurement equivalent subsets of G -states which in our case is one i.e., $X_0 = \{X_{01}\}$; there is only a single initial G -state s_0 (as shown in Fig. 3.11) and $X_{01} = \{s_0\}$. Since X_0 can be partitioned into only one subset of measurement equivalent initial G -states, $Z_0 = z_{01}$ and $z_{01} = \mathcal{U}^*(X_{01}) = \mathcal{U}^*(s_0) = \{s_0, s'_0\}$. Thus, there is only one initial O -node z_0 (as shown in Fig. 3.12) and $z_0 = \{s_0, s'_0\}$.
2. The outgoing O -transitions from z_0 are obtained as follows. Here, $\mathfrak{S}_{mz_0} = \{\tau_1, \tau'_1\}$ which are all the outgoing measurable transitions from G -states in z_{01} . Now, $A_{z_{01}} = \{\tau_1, \tau'_1\}$, as $\{\tau_1, \tau'_1\}$ forms a set of measurement equivalent transitions. Corresponding to $\{\tau_1, \tau'_1\}$ there is O -transition a_1 .
3. The destination O -node corresponding to a_1 is obtained as follows. $z_{0a_1}^+ = \{s_1, s'_1\}$ as a_1 comprises G -transitions $\{\tau_1, \tau'_1\}$ and $final(\tau_1) = s_1$ and $final(\tau'_1) = s'_1$. Further, $z_1^+ = \{s_1, s'_1\}$ as $\mathcal{U}^*(s_1) = \{s_1\}$ and $\mathcal{U}^*(s'_1) = \{s'_1\}$ since there is no unmeasurable transition emanating from either of states s_1 or s'_1 . Thus, the destination O -node of the O -transition a_1 is $z_1 : \{s_1, s'_1\}$. Similarly, the construction of the diagnoser continues till no more new O -nodes are created in Step 3.

The diagnoser for ASMiTM attack shown in Fig. 3.12 has one F_i -I-indeterminate cycle $\langle z_0, z_1, z_2, z_3, z_0 \rangle \stackrel{\Delta}{=} Y1$. It can be observed that the diagnoser states $z_0 : \{s_0, s'_0\}$, $z_1 : \{s_1, s'_1\}$, $z_2 : \{s_2, s'_2\}$, $z_3 : \{s_3, s'_3\}$ are F_i -uncertain O -nodes (as per Definition 26). Thus, $Y1$ is an F_i -uncertain cycle. This cycle also contains the indicator event ARP-PROBE-REQUEST. The O -transition a_2 comprises an indicator transition τ_2, τ'_2 . Now, the F_i -states contained in the O -nodes of $Y1$ i.e., s'_0, s'_1, s'_2 and s'_3 which form a failure cycle in G . Hence, $Y1$ is an F_i -I-indeterminate cycle (as per Definition 30). After occurrence of failure F_i (i.e., ASMiTM attack), if the system moves in the cycle s'_0, s'_1, s'_2 and s'_3 infinitely long, then the system is not F_i -I-diagnosable by the DES F_i -I-diagnosability definition. In [72], it is proved that a DES model is F_i -I-diagnosable (for failure F_i and with respect to indicator transition set I_i) if there exists no F_i -I-indeterminate cycle in the diagnoser. As F_i -I-indeterminate cycle is present, I-diagnosability framework fails to detect ASMiTM attack.

3.5.1 An Example of ASMiTM attack Detection Using I²-DES Diagnoser

The empowering event (UPD_{PACNUM}) is instrumental in-order to detect the ASMiTM attack. As a result of updation of PACNUM, both M and C_1 reply to the ARP probe frame

which eventually leads to the detection of ASMiTM attack. Referring the diagnoser shown in Fig. 3.12, it can be seen that there are two attack certain O -nodes: $\langle z_7, z_8 \rangle$. The O -transition a_5 comprises the empowering transition (UPD_{PACNUM}) τ_5, τ'_5 . The O -transition a_6 comprises an indicator transition τ_6, τ'_6 (ARP-PROBE-REQUEST). From the O -node $\langle z_5 \rangle$, two distinct traces can be seen in the diagnoser. The first trace is along $\langle z_5, z_6, z_7, z_{10} \rangle \triangleq Y2$, the second trace corresponds to $\langle z_5, z_8, z_9, z_{10} \rangle \triangleq Y3$. The trace corresponding to $Y2$ consists of an attack certain O -node $\langle z_7 \rangle$. The O -transition a_9 corresponds to the failure (attack) transition τ'_9 . Similarly in $Y3$, the attack certain O -node $\langle z_8 \rangle$ has O -transition a_{10} which corresponds to the failure (attack) transition τ'_{10} . There are no F_i - I^2 -indeterminate cycle in the I^2 diagnoser shown in Fig. 3.12. So the fault (ASMiTM attack) is diagnosable using the I^2 -DES framework. The empowering event, UPD_{PACNUM} ensures that the PACNUM counter at the AP and clients are always in sync. This ensures that multiple responses are obtained to ARP-PROBE-REQUEST which is crucial in detection of ASMiTM attack.

3.6 Results and Discussion

In this section we show statistics of the proposed IDS in terms of detection rate and accuracy followed by the correctness of the proposed scheme.

3.6.1 Network Setup for Evil Twin

The setup for the ASMiTM attack is shown in Fig. 3.5. In an ASMiTM attack the attacker needs to spoof as AP and use the GRPKY for encryption. This is implemented by: (i) using `wpa_supplicant` [137] to obtain the most recent GRPKY used by the clients. (ii) slight modification of the `MadWifi` [139] drivers so that the attacker can use the GRPKY for encryption. (iii) converting a ToDS frame to a FromDS frame. This conversion can be done by a cyclic shift of the address fields of the MAC frame format, setting the ToDS bit to 0 and FromDS bit to 1, as shown in Fig. 3.14. The IDS (wireless sniffer) promiscuously monitors the network communication. The wireless sniffer is written completely in C Language and runs on a Ubuntu 12.04 machine. We used MySQL as the database to maintain information about each client(s) associated with the AP being monitored. The IDS sniffs for the ARP frames traveling to and from the AP and the associated clients and injects ARP probes when it sees an ARP request. For crafting ARP probes we use `scapy` [4] library. The `wpa_supplicant`, `MadWifi` drivers, `scapy`, Ubuntu and MySQL are all open source and available for Linux platform.

Table 3.4 shows the experimentally derived durations of SMiTM and ASMiTM attack on

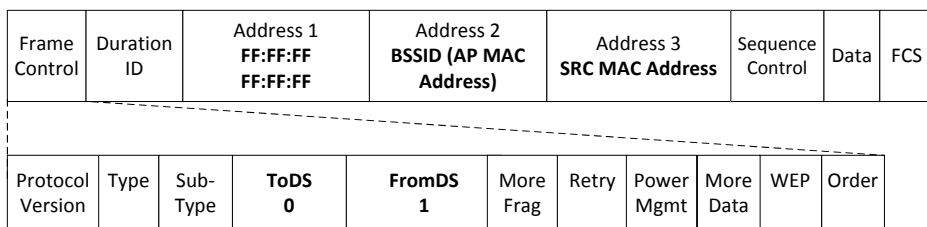


Figure 3.13: FromDS frame

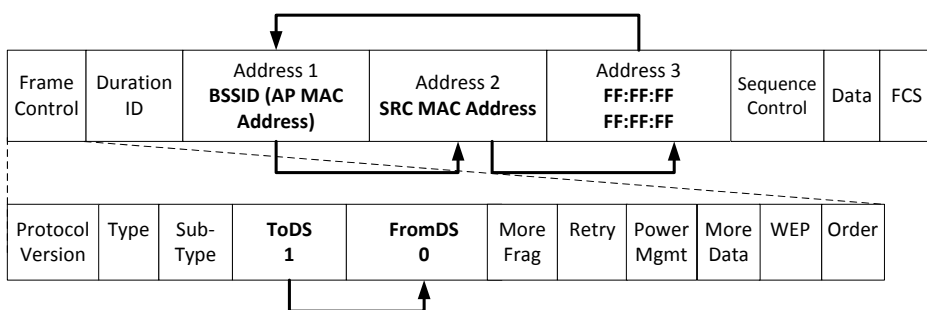


Figure 3.14: A ToDS Frame. Converting a ToDS frame to FromDS requires the cyclic shifts as shown

Table 3.4: Duration (in mins) of SMiTM vs ASMiTM attack.

OS	Default ARP Refresh Rate	SMiTM	ASMiTM
XPSP3	2	2	17.4
BackTrack5R3	6	3.8	23.2
Windows 7	Persistent	1.7	11.9
Ubuntu 14.04	Persistent	7.3	9.2

the basis of ARP refresh policy of different operating systems. As seen in row two of Table 3.4, the effect of SMiTM attack on the XPSP3 machine lasts till the ARP cache is refreshed i.e., 2 minutes. However, on the BackTrack5R3 machine the effect of SMiTM attack is nullified even before the default ARP cache refresh time, because of arrival of a fresh ARP update at the 3.8th minute. Windows 7 and Ubuntu 14.04 have persistent ARP caches. In such cases, SMiTM attack is nullified only by fresh ARP updates. So, SMiTM attack is invalidated only if genuine IP:MAC mapping are present in the ARP cache. This occurs under the following two conditions, whichever is earlier – (i) arrival of a fresh ARP update. (ii) ARP refresh – which erases all the ARP entries (including the spoofed ones). As ARP refresh clears all the ARP entries, the client needs to re-obtain the IP:MAC mapping of the target host with which it wishes to communicate. The client can obtain the (genuine) mapping using the standard ARP request/response sequence. However, ARP refresh cannot nullify the effect of ASMiTM attack. Even if ARP refresh clears the falsified IP:MAC mapping

of a target, the genuine mapping cannot be obtained immediately because the inflated PACNUM update delays the processing of ARP frames coming from the target. So, the duration of ASMiTM attack can be made longer than SMiTM by choosing an appropriate inflated value of the PACNUM. The fourth column of the Table 3.4 shows the influence of ASMiTM attack based on the inflated value of the packet number. A comparison on impact of SMiTM, WDoS and ASMiTM attacks on different network aspects is shown in Table 3.5. Quite clearly, ASMiTM attack is powerful than SMiTM and WDoS attacks.

Table 3.5: Comparison of SMiTM, WDoS and ASMiTM Attacks

Attacks →	SMiTM	WDoS	ASMiTM
Characteristics ↓			
MiTM via ARP Cache Poisoning ?	Y	N	Y
Breaks Replay Counter ?	N	Y	Y
Victim Disconnects ?	N	Y	Y
Broadcast/Multicast Protocol affected ?	N	Y	Y
Detectable by Signature/Anomaly schemes ?	N	N	N

3.6.2 Detection Rate and Accuracy of the Proposed I²-DES Based IDS

The metrics used for measuring the performance of IDS are detection rate and accuracy. Detection Rate is defined as the number of attacks detected by the IDS to the total number of attacks actually present. $Detection\ Rate = TP / (TP + FN)$. Accuracy is the proportion of the total number of attacks that are correctly detected. $Accuracy = TP / (TP + FP)$. Here, TP is True Positive, FP is False Positive, and FN is False Negative. A TP is an instance, which is actually an attack and is classified as attack by the IDS. A $FP(FN)$ is a case when an IDS classifies a normal(attack) activity as attack(normal) activity.

The sending of the ARP probe is instrumental in detecting the ASMiTM attack. Sending of ARP probe for every ARP frame results in higher detection rate and higher accuracy. If every ARP request frame is being probed, an attacker cannot escape detection. However, sending probes for every ARP frame increases the network load. Lowering the number of ARP probe helps to reduce the additional traffic, but the detection rate is lowered since if the ARP probe is not sent in lieu of an ARP request sent by the attacker containing spoofed IP-MAC mapping then the attacker escapes detection. This is clearly seen in Table 3.6 where the detection rate falls when the number of ARP probes are reduced.

From Table 3.6, it can be seen that the detection rate of the IDS is 51% even in those cases when the probe is sent only 10% of the time. This is explained as follows: as the proposed

Table 3.6: ASMiTM Attack Detection and Accuracy Statistics

% Probes Sent	Attack Instances launched	Instances detected using proposed IDS	Detection Rate %	% Probes Sent	Attack Instances launched	Instances detected using proposed IDS	Detection Rate %
100	500	495	99	50	500	395	79
90	500	490	98	40	500	335	67
80	500	465	93	30	500	305	61
70	500	440	88	20	500	280	56
60	500	410	82	10	500	255	51

IDS is a detection system and not a prevention system, it behaves aggressively once the presence of the attack is ascertained. To be specific, once a client is detected to be under ASMiTM attack, the future communication involving the client is not verified by sending the ARP probes. They are directly marked as a possible attack instance. This approach has been adopted since the attacker wants to cause maximum damage to the clients inflicted by the ASMiTM attack. Hence, the detection rate is higher even under the case when the probes sent are low. The accuracy, on the other hand, always stays 100% as long as the IDS receives multiple responses having mis-matched IP-MAC mapping for ARP probe in case a falsified IP-MAC pair is advertised by the attacker.

3.6.3 Correctness of the I²-DES Diagnoser

The I²-DES modeling helps us to formalize a given system and check for correctness and completeness [72]. In this section we show the correctness and completeness of the proposed scheme by considering all the exhaustive cases of the ASMiTM attack. For every case considered, we have shown that the proposed scheme successfully detects the presence of the ASMiTM attack. The proving of correctness and completeness by considering all the exhaustive cases helps to ascertain that the attacker does not escape detection, making the detection scheme robust. In order to prove the correctness of the diagnoser shown in Fig. 3.12, we consider 3 possible cases based on the behavior of the attacker launching ASMiTM attack.

1. Case 1: *Attacker present and its sends spoofed IP-MAC mapping to launch ASMiTM attack* : In this case, after receiving the ARP request the IDS checks the PACNUM value in the frame and sends an ARP probe with an updated PACNUM. The diagnoser reaches *O*-node z_5 . On observing an ARP probe response containing a mis-matched IP-MAC mapping, the I² diagnoser reaches the *O*-node z_8 which is an F_i -certain *O*-node. So, the I² diagnoser correctly identifies the presence of attack. In this case we have assumed that the attacker’s response to the ARP probe comes before the response of the genuine host.

3.7. Conclusion

It is also possible that the order of receipt of the ARP probes is reversed. In that case, the diagnoser eventually reaches the O -node z_7 which is again an F_i -certain O -node. So, irrespective of the order of arrival of the ARP probe response, the presence of ASMiTM attack is detected.

2. Case 2: *Attacker present but is passive*: The attacker is present in the network but only listens to the network traffic passively. No frame injection is done by the attacker. So, when the ARP probe is sent only the genuine client replies. The probe response contains the same IP-MAC mapping as seen during the initial ARP request. The diagnoser traverses the O -nodes $z_0, z_1, z_4, z_5, z_6, z_0$ during this process. As none of the O -nodes traversed by the diagnoser is an F_i -certain (attack) O -node, the I^2 diagnoser reports correctly that the network is under normal conditions.
3. Case 3: *Attacker absent*: Here, the attacker is not present in the network. This case is identical to Case 2.

So, all possible cases of arrival of ARP frames are analyzed and the diagnoser which is implemented as an IDS engine correctly reports the network conditions in each of the case.

3.6.4 Discussion

As ASMiTM attack is proposed by us, to the best of authors's knowledge there are no existing schemes to compare the performance of our scheme with any method that exists in the literature. However, the proposed method depends highly on the ability of the IDS to capture the frames correctly. If the IDS misses critical frames like ARP probe response or misses the initial ARP frame sent by the attacker, the detection rate falls. The environment considered is a WPA2 encrypted Wi-Fi network as the ASMiTM attack can only occur in such networks. ASMiTM attack is not possible in open and WEP based Wi-Fi networks. Also, we have assumed that the attacker does not do a DoS on the AP or any other client while launching the attack.

3.7 Conclusion

In this work, we propose ASMiTM attack that uses ARP spoofing to set up a MiTM environment in WPA2 encrypted Wi-Fi networks. The proposed ASMiTM attack is an insider attack that exploits the Hole 196 vulnerability by combining SMiTM and WDoS attacks. This combination results in amplification of the individual effects of SMiTM and WDoS attacks in terms of duration of attack life, detection complexity and stealthiness. ASMiTM

attack can break the protocols that rely on broadcast/multicast traffic, sniff private data of clients, inject malwares etc. We also propose an I²-DES based IDS in order to detect the ASMiTM attack. The existing I-diagnosability framework cannot be used for detection of ASMiTM attack. The proposed I²-DES framework overcomes the shortcomings of the I-diagnosability framework but requires an additional empowering event, which is instrumental for attack (failure) diagnosis. The empowering event along with the indicator event of I²-Diagnosability framework ascertain that system rendered non-diagnosable by I-diagnosability framework becomes diagnosable.

In the next chapter, we look into Power Save Denial of Service (PS-DoS) attack where an attacker launches DoS attack on the clients. The PS-DoS attack induces frame losses for those clients which are in sleep state in order to conserve their battery life. PS-DoS attack manifests itself in time rather than frame feature characteristics. The PS-DoS attack exploits the timing characteristics involved in the power save operation of 802.11 networks. For such attacks, where timing of occurrence of events is critical, Real Time DES (RTDES) framework are suited because of their capability of representing timing faults leading to failures (attacks) in terms of erroneous delay and deadlines. We propose an RTDES [37, 38] based IDS is proposed in order to detect PS-DoS attack in the next chapter.



“If someone steals your password, you can change it. But if someone steals your thumbprint, you can’t get a new thumb. The failure modes are very different.”

Bruce Schneier
American cryptographer

4

Intrusion Detection System for PS-Poll DoS Attack in Wi-Fi Networks using Real Time Discrete Event System

4.1 Introduction

In the earlier chapters, we saw how an attacker launched a MiTM attack using evil twin or ASMiTM attack in order to compromise client’s security. In this chapter, we look into PS-DoS attack. In PS-DoS attack an attacker can cause frame losses to the client without establishing a MiTM connection. The rapid expansion of Wi-Fi networks coupled with the availability of handheld devices like smart-phones, tablets, phablets etc., having full support for Wi-Fi connectivity has made it possible for the users to stay connected to the Internet all day long. From the point of view of portability and form factor these handheld devices are equipped with limited battery life. Wi-Fi usage leads to higher consumption of battery so if appropriate power saving measures are not employed, the battery of these Wi-Fi device(s) would drain out quickly.

The power save feature of 802.11 standard [93] allows the clients to enter into sleep state to conserve battery life. If any data arrives for the client while it is in sleep state, the AP buffers the data and delivers to the target client when it wakes up. A client informs the AP about its change in power save state from sleep to awake and vice-versa using a PS-Poll or null data frame. A null data frame is so named because it has no data payload field. Its purpose is to indicate a change in the power save mode of the client.

In this chapter we focus on the Power Save Denial of Service (PS-DoS) attack. PS-DoS attack can cause degradation of service by inducing frame losses for sleeping clients and no formal solution is available for its detection. This motivated us to take up PS-DoS attack and propose a solution for it. In PS-DoS attack, an attacker crafts spoofed null data frame in order to fetch buffered frame(s) at the AP causing frame losses for the client whose frames are buffered at the AP. An attacker repeats this process for different clients which leads to severe frame losses for the clients and finally resulting in the PS-DoS attack. We have considered the case in which the attacker causes frame losses to multiple clients. This helps the attacker increase the potency of PS-DoS attack. If the attack is restricted to only one client the PS-DoS attack can be trivially detected using standard anomaly-based technique [140]. The impact of PS-DoS attack on a single client is limited and does not lead to DoS on the network. In order to have a higher attack impact, the attacker targets multiple clients in the network. All the clients whose buffered frames are retrieved by the attacker are termed as victim clients.

Current methods to prevent the PS-DoS attack include encryption [73, 74, 75], Received Signal Strength Indicator (RSSI) based methods [77, 78, 79], up-gradation to newer standards [141, 142] which necessitate firmware upgrades. Encryption requires systematic arrangement of key establishment, key renewal, key revocation leading to increased deployment and maintenance costs. Up-gradation to newer standards require firmware upgrades on the client as well as server, which often incur high cost. Moreover, presence of legacy network(s) makes this task difficult. Received Signal Strength Indicator (RSSI) based approaches can help detect the PS-DoS attack. However, the use of RSSI based techniques require additional specialized hardware equipment which increase costs. So we can see that existing methods escalate deployment and maintenance costs. Signature based IDS uses predefined signatures while anomaly-based IDS makes use of profiling to detect attacks [92]. An attacker crafts the spoofed null data frame using the same parameters as those used by the client while sending a null data frame. Also, injection of just one null data frame is enough to induce frame losses for a client. As a result, generation of signature or statistics for PS-DoS attack is difficult as may not prove to be effective in detecting the PS-DoS attack. Usage of such IDSs may lead to high false positive rate. We therefore propose a Real Time Discrete Event System (RTDES) based IDS that helps to overcome the drawbacks listed above and detect the PS-DoS attack with high detection rate and accuracy.

The core idea of any DES based IDS is to develop the normal and failure model corresponding to normal and failure (attack) scenarios. Subsequently, a diagnoser which is a state estimator is built using the states traversed in the normal and fault (attack) models. The diagnoser which is implemented as the IDS engine observes sequence of events gener-

ated by the system and raises an alarm if the sequence deviates from the normal behavior. The proposed RTDES framework requires certain extensions over classical theory [125] and techniques, which have been used in [143, 144, 41]. The modifications are made as follows:

- The PS-DoS attack manifests itself in time. As a result, timing (delay-deadline) information needs to be incorporated in the model. In order to incorporate timing information we have used the RTDES framework [39] instead of un-timed one.
- The sequence of power save frame exchange under normal and attack conditions is similar. This leads to creation of identical models under normal and attack scenarios thwarting diagnosability. To create differences between normal and attack scenarios, power save probes are injected into the network. It may be noted that power save probes maintain the 802.11 protocol standard.
- We incorporate model variables in the RTDES based IDS in order to overcome the state explosion problem.

The summary of our contributions are:

1. We propose an RTDES based IDS that detects the PS-DoS attack in Wi-Fi networks. The developed IDS adheres to the 802.11 standard.
2. The only hardware requirement is a sensor capable of sniffing the wireless data. So the cost of the proposed scheme is low and can be readily applied to legacy as well as existing networks.
3. As DES is a formal paradigm, the correctness of the scheme is verified by considering all possible attack scenarios based on the arrival timing of the PS-Poll and null data frames.

The rest of the chapter is organized as follows. Section 4.2 describes the power save feature of 802.11 networks and the security vulnerabilities associated with it. We also look into the current approaches to tackle the PS-DoS attack. In Section 4.3, we describe the proposed mechanism for detection of PS-DoS attack. In Section 4.4, we introduce the concept of Failure Detection and Diagnosis (FDD) using Real Time Discrete Event System (RTDES) using a benchmark process of three-tank system. We describe the RTDES based IDS to detect the PS-DoS attack in Section 4.5. The correctness of the RTDES based IDS along with its detection rate, accuracy and network load of the IDS are described in Section 4.6. Section 4.7 concludes the work.

4.2 Background and Motivation

In this section we look at the power save feature and the vulnerabilities associated with it. We look at how these vulnerabilities can be exploited to launch the PS-DoS attack. Next, we look at the existing solutions to detect the PS-DoS attack.

4.2.1 Power Save Feature of 802.11 Standard

Hand-held devices usually have limited battery, so an effective power saving mechanism is must. The 802.11 standard incorporates a power saving feature that enables a client to enter into sleep state, which consumes much less power. When a client is in sleep state, it can neither transmit nor receive frame(s). A client enters into sleep (awake) state by sending null data frame with Power Mgmt bit set to 1 (0). If any data arrives for the client while it is in sleep state, the AP buffers the data on behalf of the client. The AP sets the client's Association IDentifier (AID) bit to 1 in the Traffic Indication Map (TIM) message of the successive beacon frames until the client retrieves all the buffered frames at the AP. Beacon frames are periodically sent by the AP to help the clients detect the presence of the AP. The beacon frame includes TIM information element which consists of a list of AID(s) of those client(s) whose frame(s) are buffered at the AP.

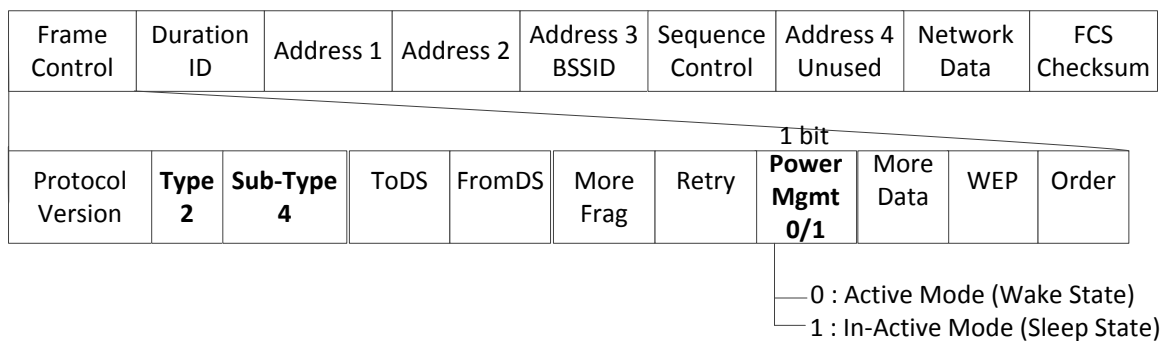


Figure 4.1: Frame format of null data frame

A client in sleep state must periodically wake up and listen to the beacon frame. A client uses the value of Listen Interval (LI) for waking up periodically. If a client is in sleep state, it must wake up after LI number of beacons to check for the presence of buffered frames at the AP. For example, if the client is in sleep state and its LI is 5, the client needs to wake up every 5th beacon to check if any frame(s) are buffered at the AP. The value of LI is decided during the association process. The LI is a 2 byte element in the association request frame sent by the client to the AP. The AP needs to buffer the frame(s) for a sleeping client at-least for the corresponding client's LI. A sleeping client wakes up after the LI duration and reads

the TIM element of the beacon frame. If the AID of the client is set (reset) in TIM it implies that data is buffered (not buffered) at the AP. The client sends a null data frame with Power Mgmt bit set to 0 (indicating that it is awake) to retrieve the buffered frame(s) at the AP. If a client continues to remain in sleep state even after its LI expires, the AP discards the buffered frame(s) for the corresponding client.

4.2.2 Vulnerabilities in Power Save Feature of 802.11 Standard

Encryption schemes like WEP, WPA, WPA2 etc., encrypt only the data payload keeping other fields in clear-text. PS-Poll and null data frame does not contain any data, and are sent in clear-text. Being un-encrypted, spoofing these frames is trivial. The PS-DoS attack is explained using Fig. 4.2.

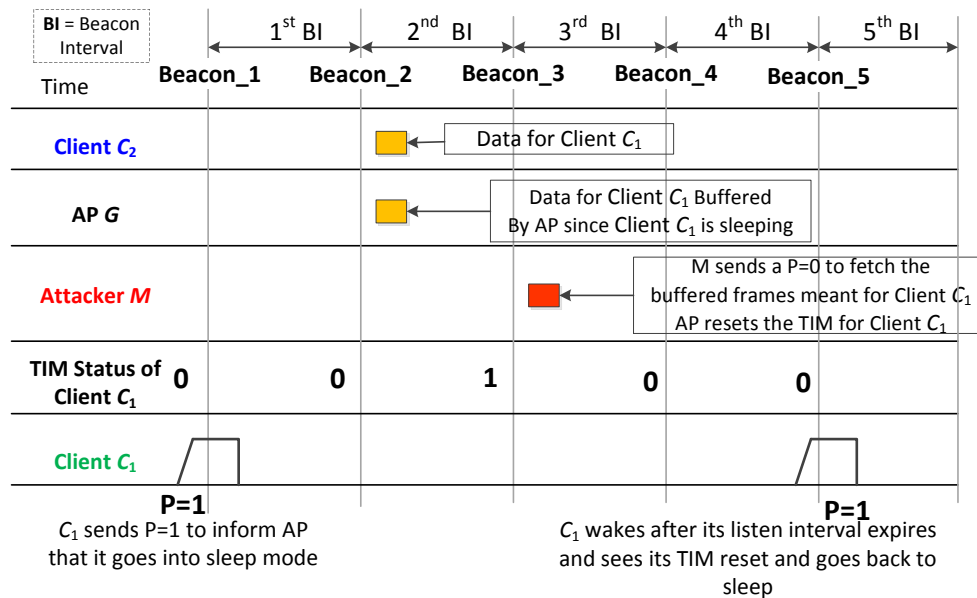


Figure 4.2: Timeline for launching PS-DoS attack

Clients M , C_1 and C_2 are associated with the same AP. M is the attacker while C_1 and C_2 are genuine clients. We assume Beacon Interval (BI) as 100ms and C_1 's LI as 5 for the purpose of explanation. The BI is available in all the beacon frames transmitted by the AP. M gets the LI and AID of the client C_1 by eavesdropping on the association process between the client C_1 and the AP. The timeline shown in Fig. 4.2 is explained below:

- [1st BI] : C_1 sends null data frame with PwrMgmt = 1 to the AP to inform that it is entering sleep state. TIM for C_1 is set to 0 as there are no outstanding frame(s) for C_1 at the AP.
- [2nd BI] : C_2 sends one data frame to C_1 which is buffered by the AP as C_1 is in sleep

state. AID in the TIM for C_1 is set to 1 in all successive beacon frames till all the buffered frame(s) are retrieved by C_1 .

- [3rd BI] : M captures a beacon and finds the AID of C_1 is set in TIM. The attacker sends a spoofed null data frame with source (SRC) MAC address set to MAC address of C_1 and PwrMgmt bit set to 0. On receiving the null data frame the AP sends all the buffered frames which are acknowledged by M on behalf of C_1 . After all buffered frames of C_1 are delivered, the AP resets the AID of C_1 in TIM of the successive beacons.
- [4th BI] : No frame exchange for C_1 . TIM = 0 for C_1 .
- [5th BI] : C_1 's LI expires. It wakes up to read the TIM bit of the beacon frame. C_1 finds that its AID in TIM is reset indicating absence of any buffered data at the AP. C_1 goes back to sleep state by sending null data frame with PwrMgmt = 1 to the AP.

As seen above, the attacker M silently steals the buffered frame(s) targeted at C_1 . C_1 as a result becomes a victim of PS-DoS attack as it does not receive the intended frame(s). C_2 also indirectly becomes a victim as it assumes that frame(s) are successfully delivered to C_1 , but instead they are delivered to M . So in the PS-DoS attack both the sender and the receiver are victimized. M should repeat this process for different clients at arbitrary intervals in the network to cause frame losses to clients resulting in the PS-DoS attack. The attacker should choose arbitrary intervals to launch PS-DoS attack. If attacks are launched at regular intervals may lead to detection by an anomaly-based IDS. The PS-DoS attack can be easily launched using minimal resources and possesses the potential to cause high frame losses. In the following sub-section, we look into various approaches to detect and prevent the PS-DoS attack.

4.2.3 Existing Approaches to Detect or Prevent PS-DoS Attack

Encryption based methods

An intuitive solution is to encrypt all the management and control frames along with the data frames as suggested by Bellardo et al. in [73]. Encryption requires an establishment of systematic secure key distribution, management, renewal and revocation system, which involves a huge overhead. As the PS-DoS attack involves spoofing of PS-Poll and null data frame, encrypting all management and control frames can prevent the PS-DoS attack. However, encrypting and decryption all management and control frames puts additional load on

the clients and the AP. This in turn leads to increased CPU cycles leading to faster draining off the batteries of the clients. It also necessitates up-gradation of the client and the AP firmware which is costly. Qureshi et al. [74] propose an encryption based scheme to prevent the PS-DoS attack by encrypting the AID portion of the PS-Poll frame using pre-established PVTKY. As PVTKY is used, this method is not applicable to open and WEP based networks. Null data frame does not contain the AID field, which limits this method to those clients using PS-Poll frames for power save operations.

Leandro Meiners [75] proposes that the clients must use non-empty data frame like ICMP/ARP for reporting the change in power save mode. The motive behind this solution is to eliminate all possible frame candidates that are vulnerable to the PS-DoS attack. As ICMP/ARP frame contain data, the data portion is encrypted which prevents possible spoofing by an adversary. However, this solution has fundamental drawbacks. First, it breaks the AP compatibility with those clients that use traditional frames like null data frames to inform about the change in power save mode. The null data frames are used by Network Interface Card (NICs) for managing power, scanning channel and keeping the association awake [76]. Eliminating the processing of such frames prevents the client from performing these functions.

Received Signal Strength Indicator (RSSI) based Methods

Faria et al. [77] use the AP(s) as sensors and obtain the RSSI values for each client within its range. They have shown that the signalprints of a client and its physical location are closely correlated. Azimi et al. [78] and Chen et al. [79] also make use of physical layer countermeasures like RSSI values and RF signal print to detect and localize the attacker. In RSSI based techniques the approximate location of the sender is determined. Following this, the location of the source MAC address in the received frame is determined. If the difference in the location exceeds a certain threshold, the frame is not processed and tagged as spoofed. Though physical layer countermeasures are effective, they require specialized hardware and firmware changes in 802.11. If the clients are located close to each other, their physical characteristics are similar, which may result in false positives.

Up-gradation to Newer IEEE Standards

IEEE 802.11w standard provides protection for the management frames. However, the proposed standard does not include protection for control frames [142]. PS-Poll frame being a control frame, 802.11w leaves the PS-Poll frame unprotected. So, upgrading to 802.11w protocol does not help to prevent PS-DoS attack. It also involves additional deployment

costs, firmware upgrades for both the client and the AP. A large number of legacy devices exist today, which do not support 802.11w standard [141].

In brief, the drawbacks of the existing schemes to detect or prevent the PS-DoS attack are:

- Requirement of Encryption.
- Firmware up-gradation
- Up-gradation to newer standards.
- Installation of specialized hardware.

From the above summary it is clear that a strategy to detect the PS-DoS attack is required having the following features.

- No alteration in 802.11 protocol is required.
- Hardware costs should not be exorbitant.
- It must be easily deployable to the existing as well as new networks.
- It must not require patching of underlying operating system or installation of new software.
- If the IDS generates extra traffic, it should be as low as possible.

Signature and anomaly-based IDS usually generate a lot of false positives when used for detecting the PS-DoS attack and related attacks, which do not alter frame semantics under normal and attack conditions. In such cases, DES based IDS have proven to be an effective mechanism for detecting network attacks without any need for protocol modification, encryption or installation of proprietary hardware. A DES based IDS can be formally proved to be correct. In this chapter we propose RTDES based IDS for the PS-DoS attack that incorporates the features listed above and overcomes the drawbacks of the existing approaches.

4.3 Proposed Scheme for the Detection of PS-DoS Attack

In this section we present the working principle of the IDS to detect the PS-DoS attack followed by attacker and IDS components.

4.3.1 Working Principle of the IDS for Detecting PS-DoS Attack

Principle: If the buffered frames for a client are fetched before the expiry of its LI, IDS marks this activity as suspicious. Such activity cannot be directly marked as attack since the 802.11 standard permits the Wi-Fi clients to wake up earlier than their scheduled wake up. This is plausible as it may happen that the client may have to transmit some critical data for which it may have to break its sleep cycle. So, every client that wakes up earlier than its scheduled wake up cannot be assumed to be an occurrence of the PS-DoS attack. In the proposed scheme we have the dummy clients as part of detection methodology. The dummy clients are software controlled and their communication is handled by the IDS. The IDS ensures that the dummy clients never wake up before the expiry of their LI. Only the IDS possesses the dummy client's MAC address which is regularly updated. The need for updating the dummy MAC address and other characteristics of the dummy clients are explained later. Upon observing an early wake up frame¹ for any client(s) associated with the monitored AP, the IDS sends a power save probe to the dummy client. As the dummy client is in sleep state at the time IDS sends a power save probe, the frame is buffered at the AP. The power save probe is a simple 802.11 data frame sent from IDS destined to the dummy client. If the buffered frame(s) meant for the dummy client are fetched before the expiry of the LI of the dummy client to whom the probe is sent, the presence of the PS-DoS attack is confirmed.

Reason: The dummy clients never wake up before the expiry of their LI. So, if the buffered frames meant for the dummy clients are fetched before the expiry of their LI, it must have been fetched by the attacker on behalf of the dummy client in its quest to fetch the buffered frame(s) of the sleeping clients.

Using the above principle we show an example of the PS-DoS attack detection technique with the help of the timeline shown in Fig. 4.3. M , C_1 and C_2 are associated with the same AP. M is the attacker, C_1 and C_2 are the genuine clients while D_1 is the dummy client. The timeline has 7 distinct time slots. Each time slot corresponds to a Beacon Interval (BI).

- [1st BI] : C_1 goes to sleep. C_1 's scheduled wake up is at BI₆. The dummy client D_1 is in sleep state. D_1 's scheduled wake up is at BI₇.
- [2nd BI] : C_2 sends data to C_1 . As C_1 is in sleep state, the data is buffered by the AP. The AP sets the AID for C_1 in TIM bit for successive beacons till all buffered frame(s) are retrieved by C_1 .

¹For simplicity of explanation of the formal (RTDES) modeling we refer null data frame with $PwrMgmt = 1$ as **sleep** frame and null data frame with $PwrMgmt = 0$ as **wake** frame.

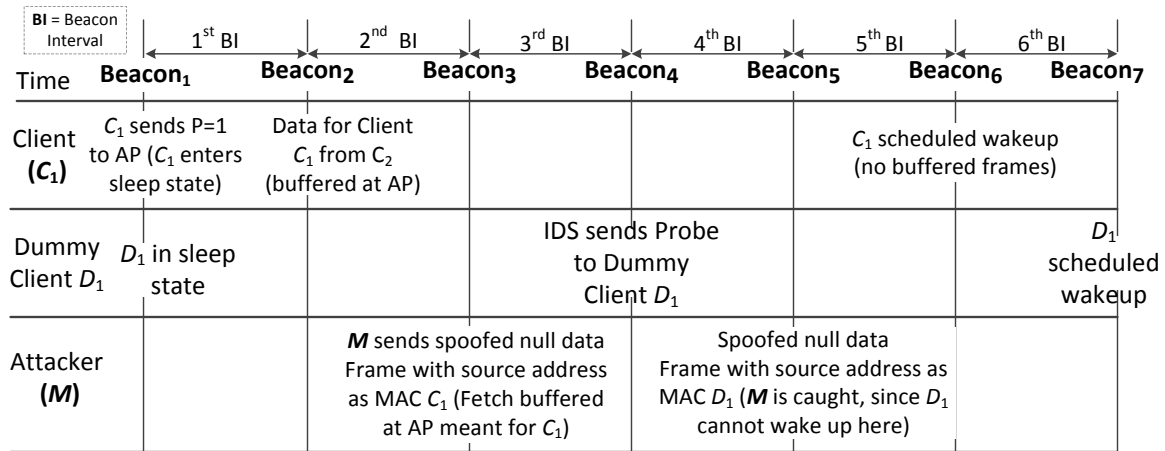


Figure 4.3: Timeline for detecting the PS-DoS attack

- [3rd BI] : M sends a wake frame spoofing as C₁ to the AP. All buffered frame(s) meant for C₁ are retrieved by M. M acknowledges the AP on behalf of C₁.
- [4th BI] : IDS observes early wake from the client C₁. IDS sends a power save probe to the dummy client D₁ to verify the early wake of C₁. The dummy client’s scheduled wake up is at BI₇. The AP resets the AID for C₁ in the TIM bit for successive beacons as no buffered data is left at the AP.
- [5th BI] : IDS sniffs a wake frame to retrieve buffered frame targeted at D₁. As D₁ never fetches frame before scheduled wake up, the request for fetching frame(s) must have been made by the attacker on behalf of the dummy client. Thus, presence of the PS-DoS attack is detected.
- [6th BI] : C₁’s scheduled wake up time. C₁ finds its TIM is reset and goes back to sleep.
- [7th BI] : D₁’s scheduled wake up time. D₁ goes back to sleep as no buffered frame(s) are present for it.

As seen, C₁ is the victim client that lost its buffered frame(s) because of the PS-DoS attack by M. The sending of power save probes to D₁ helps to detect the presence of M in the network. The timing of the response of the power save probes is vital in ascertaining the presence of attacker.

4.3.2 IDS Components

The block diagram for detecting the PS-DoS attack is shown in Fig. 4.4. The components are described as follows:

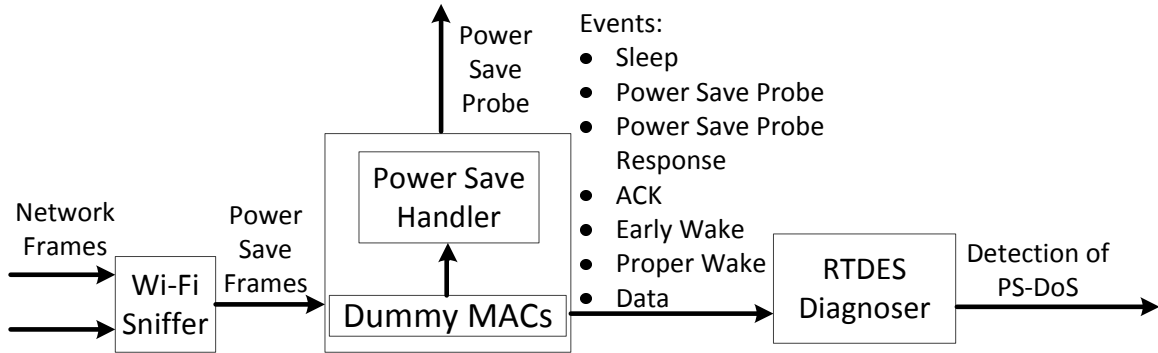


Figure 4.4: Components of the proposed IDS for detection of PS-DoS attack

- **Wi-Fi Sniffer:** The Wi-Fi sniffer works in promiscuous mode and captures all Wi-Fi frame(s) traveling in the network. Only those frame(s) destined to and from the monitored AP are sniffed. Frame(s) to other APs are dropped. The Wi-Fi sniffer forwards the captured frame(s) to “Power Save Handler”.
- **Power Save Handler:** The Power Save Handler is responsible for extracting vital information like LI, BI, AID, MAC address of the source (SRC) client from frame headers. The Power Save Handler component is also responsible for the generation of events like *Sleep*, *ACK*, *Early Wake*, *Proper Wake*, *Power Save Probe*, *Power Save Probe Response*, *Data*. The Power Save Handler forwards the generated event(s) to RTDES diagnoser. The RTDES diagnoser determines if the PS-DoS attack has occurred or not based on the events captured.
- **Dummy clients:** IDS maintains a list of dummy clients with it. The dummy clients are software controlled and their communication is handled by the IDS. As already explained in the principle of attack detection, the 802.11 standard allows a client to wake up before the expiry of its LI. In order to check the genuineness of the early wake frame sent by the client, the IDS sends a power save probe destined to a dummy client while it is in sleep state. As the communication of the dummy clients is handled by the IDS, the dummy clients never wake up before the expiry of their LI. So, in-case a wake frame is seen to fetch the buffered frame(s) meant for the dummy client in the network before the expiry of its LI (i.e., LI of dummy client), the IDS raises an alarm indicating the occurrence of the PS-DoS attack. In case the buffered frame(s) are fetched after the expiry of the LI of a dummy client the network is assumed to be operating under normal conditions.
- **RTDES Diagnoser:** The RTDES diagnoser is actually implemented as a software module and used as attack detector. The RTDES diagnoser forms the crux of the detection

methodology and is constructed from the DES model under normal and attack conditions. The construction and uses of the diagnoser are described in Subsection 4.4.4.

4.3.3 Attacker and IDS Assumptions

Attacker Assumptions

- **Attacker fetches buffered frame(s) at the AP immediately for the clients that are in sleep mode.**

An attacker fetches frame(s) buffered at the AP for the targeted sleeping clients immediately. If the attacker delays in fetching the frame(s) buffered at the AP it is possible that the real client may wake up and fetch the frame(s). This may reduce the impact of PS-DoS attack. Clients staying awake persistently never have buffered frame(s) at the AP. So the PS-DoS attack is not possible on such clients.

- **Attacker launches the PS-DoS attack on multiple clients simultaneously at arbitrary intervals.**

The attacker targets multiple clients simultaneously. The attacker first does a passive scanning of the network to determine the list of associated clients with the target AP. The attacker eavesdrops on the communication between the clients and the AP to obtain useful parameters like the network's BI, client's LI and AID. Using these parameters the attacker crafts spoofed null data frame in order to fetch the buffered frame(s) at the AP for the targeted sleeping clients. For the success of the PS-DoS attack on a client, two conditions must be satisfied – (i) the client is in sleep mode and (ii) the AP has buffered frame(s) for the client. Experimentally it has been observed that occurrence of these two scenarios is infrequent. So, in order to increase the impact of the PS-DoS attack to a reasonable level, multiple clients are targeted by the attacker.

IDS Assumptions

- **Monitoring of the authorized AP(s) only.**

The IDS maintains a white-list of the MAC address of the AP that need to be protected. Only the frame(s) destined to and from these AP(s) are monitored. Frame(s) destined to other AP(s) are discarded as the primary goal of installing the IDS is to detect the attacks on the APs deployed by the administrator and not other AP(s).

- **IDS keeps track of sleep and wake up schedules of the associated clients.**

Wi-Fi clients follow their sleep and wake schedule(s) so that they can conserve power

by being in sleep state when they have no data to transmit. In case of the PS-DoS attack the frequency of early wake by the clients get increased as the attacker fetches the buffered frame(s) available at the AP on behalf of the clients while they are in sleep state. By keeping a track of the sleep and wake schedules, the IDS can identify those clients that wake up earlier than their scheduled wakeup timing. Clients which are frequently seen to wake up before completion of their sleep schedule(s) may be the potential victims of the PS-DoS attack. This also helps the IDS to determine the number of dummy clients to be kept in the network by following the philosophy – more the potential victims, more dummy clients are needed.

- **Proposed IDS has sniffing and injection capabilities.**

The IDS sniffs the wireless frames traveling in the air. If the IDS observes an early wake frame it sends a power save probe destined to the dummy client. The IDS maintains a list of AIDs, LI, sleep-wake timing of all the associated clients for the AP begin monitored. If the IDS does not have sniffing capabilities then early wake by the clients cannot be detected. If the IDS does not possess the frame injection capability, it cannot inject power save probes into the network to ascertain the presence of the attacker.

- **IDS regularly updates the dummy client's MAC address list.**

IDS regularly updates the dummy client's MAC address list to prevent possible learning of the dummy client's MAC address by the attacker. To elaborate, most of the Wi-Fi clients are mobile in nature. As a result, large number of clients join and leave the network over a period of time. Even though the genuine clients have fixed MAC addresses, their joining and leaving pattern with respect to the network is highly dynamic. A genuine client may join the network and leave the network in a few minutes or hours and may never return to the same network. Few of the clients may join the network and leave after some time and may associate to some other AP in the same network. However, some of the clients (like employees working for a firm) may show a static behavior in terms of joining and leaving, but they are few. To mimic a similar dynamic trend with that of the genuine clients, the IDS regularly updates the dummy client's MAC address list. So, even if the genuine clients have fixed MAC addresses the attacker cannot learn whether the clients are normal or dummy by looking at whether the MAC address appeared in the historical data. In other words, if the list of dummy client's MAC address is not dynamic in nature, an attacker may eventually learn the list of dummy MAC address in the network by observing the historical data of the MAC addresses seen in the network. Once the attacker gets the MAC addresses of these dummy clients, it does not respond to any of the power save probes having

these MAC addresses assuming them to be dummy clients. So, the list of dummy client's MAC address needs to be updated regularly to prevent such possible learning by the attacker.

So, from the above discussion it is clear that timing of the various network activities (sending probe, fetching probe frames etc.) is important in order to detect the PS-DoS attack. As RTDES modeling is capable of capturing timing information into the model, we have chosen the RTDES framework for modeling the PS-DoS attack.

4.4 Fault Detection and Diagnosis Theory of Real Time Discrete Event System (RTDES): Three Tank System

In this section we present the RTDES framework augmented with *model variables*. The *RTDES model* G is defined as:

$$G = \langle X, X_0, \Sigma, \mathfrak{S}, V, t \rangle \quad (4.1)$$

where

- X is the finite set of states.
- X_0 is the initial state.
- Σ is the set of events. Note that an event can be measurable or unmeasurable.
- \mathfrak{S} is the set of transitions.
- V is the set of model variables. Each element v_i of V can take values from a domain Dom_i .
- t is a clock variable with $type(t) = \mathbb{N}$, the set of all natural numbers. The clock variable represents time on a global clock.

A transition $\tau \in \mathfrak{S}$ from a state x to another state x^+ is an ordered seven-tuple

$\tau = \langle x, x^+, \sigma, l_\tau, u_\tau, check(V), assign(V) \rangle$, where,

- x is the initial state of the transition, denoted as $initial(\tau)$.

- x^+ is the final state of the transition, denoted as $final(\tau)$.
- σ is the event on which the transition is fired.
- l_τ, u_τ are the delay and deadline time bounds, denoted as $delay(\tau)$ and $deadline(\tau)$, respectively. Let $t_{c\tau}$ be the time instant when τ is enabled. A transition can take place at any time instant t when $t_{c\tau} + l_\tau \leq t \leq t_{c\tau} + u_\tau$, provided that the transition remains enabled throughout the interval $[t_{c\tau}, t]$. Therefore, a transition does not take place before the *delay* and must take place before the *deadline*.
- $check(V)$ represents conditions on a subset of model variables. For firing τ , along with the enabling event σ , $check(V)$ should hold true.
- $assign(V)$ represents a subset of model variables and assignment of values from their corresponding domain, when τ fires.

A transition τ from x to x^+ is denoted as $\tau : \langle x, x^+ \rangle$ for brevity when its other components are clear from the context. The *tick transition*, or simply *tick*, denoted as η , is defined as $\eta = \langle x, x, true, -, -, -, - \rangle$. Each occurrence of tick results in an increment of the clock t by 1 and leaves the other variables unchanged. In fact, tick is the only transition that changes the value of t . *Tick occurs infinitely often and is not explicitly included in \mathfrak{S}* . No model variables are defined for the *tick transition*.

A *trace* of model G is a sequence of transitions *generated* by G denoted as $s = \langle \tau_1, \tau_2, \dots \rangle$, where $initial(\tau_1)$ is an initial state, and the juxtaposition property holds, that is, $initial(\tau_{i+1}) = final(\tau_i)$, for $i \geq 1$. Henceforth, we assume the juxtaposition property for “sequence of transitions”. A state x is said to be in a trace s , if $x = initial(\tau_i)$, for some $i \geq 1$. The set of all traces *generated* by G along with all their finite prefixes is the language of G , denoted as $L(G)$. $L_f(G)$ denotes the subset of $L(G)$ comprising the finite prefixes. For any trace $s = \langle \tau_1, \tau_2, \dots \rangle$, $initial(s) = initial(\tau_1)$ and for a finite trace $s = \langle \tau_1, \tau_2, \dots, \tau_f \rangle$, $final(\tau_f) = final(s)$. Naturally, $L(G)$ is a subset of \mathfrak{S}^w , where \mathfrak{S}^w is the set of all infinite sequences of \mathfrak{S} ; $L_f(G)$ is a subset of \mathfrak{S}^* , the Kleene closure of \mathfrak{S} . The post language of G after a trace s is denoted as $L(G)/s = \{t \in \mathfrak{S}^* \mid st \in L(G)\}$. $L_f(G)/s \subset L(G)/s$ comprises finite prefixes of the infinite traces of $L(G)/s$.

4.4.1 RTDES Modeling: Measurement Limitations and Failure Diagnosis

Limitations of measurement give rise to uncertainty in transitions in the observed dynamics of the model. In this sub-section the notion of measurement limitation in the RTDES framework is formally introduced and the consequent uncertainty in transitions in G is

characterized. In order to explain the definitions in a more clear and concise way we take help of the three tank system explained in Subsection 4.4.2. Very briefly, the three tank system involves filling of tank T_1 followed by filling of tank T_2 . Both the tanks are drained into tank T_3 . After tank T_3 gets full, the mixture in tank T_3 is drained off. We have reproduced few standard definitions available in the RTDES literature [72, 124, 125] for the sake of completeness and simplicity of explanation.

Definition 32. Measurable and unmeasurable events/transitions: Any event that can (cannot) be measured using sensors are measurable (unmeasurable) events. A **transition** $\tau_i = \langle x, x^+, \sigma, check(V), assign(V) \rangle$ is said to be a measurable (unmeasurable) transition if σ is a measurable (unmeasurable) event. \mathfrak{S}_m and \mathfrak{S}_u denote the set of measurable and unmeasurable transitions. In Fig. 4.6 the event “ T_1 Filling” is a measurable event so the transition τ_1 associated with the event “ T_1 Filling” is also measurable.

Definition 33. Measurement equivalent transitions and states: Two transitions $\langle x_1, x_1^+, \sigma_1, l_{\tau_1}, u_{\tau_1}, check_1(V), assign_1(V) \rangle$ and $\langle x_2, x_2^+, \sigma_2, l_{\tau_2}, u_{\tau_2}, check_2(V), assign_2(V) \rangle$ are equivalent if $\sigma_1 = \sigma_2$ (the same event), $l_{\tau_1} = l_{\tau_2}$ & $u_{\tau_1} = u_{\tau_2}$ (the same delay and deadline), $check_1(V) \equiv check_2(V)$ (the same equalities over the same subset of variables in V), and $assign_1(V) \equiv assign_2(V)$ (the same subset of model variables with the same assignment). If $\tau_1 \equiv \tau_2$ then the source states of the transitions are equivalent and so are the destination states, i.e., $x_1 \equiv x_2$ and $x_1^+ \equiv x_2^+$. In Fig. 4.6, upon comparing the transitions τ_1 and τ'_1 we observe that the same event (T_1 Filling) is associated with both the transitions. Their delay-deadlines are also same. So, $\tau_1 \equiv \tau'_1$ which implies $s_0 \equiv s'_0$ and $s_1 \equiv s'_1$. As a result when the event “ T_1 Filling” occurs, it cannot be said with certainty whether the system has taken the transition τ_1 or τ'_1 . So, the transitions τ_1 and τ'_1 are said to be measurement equivalent transitions.

Definition 34. Projection and Inverse Projection Operator: A **projection operator** $P : \mathfrak{S}^* \rightarrow \mathfrak{S}_m^*$ is defined as: $P(\epsilon) = \epsilon$ (null string); $P(\tau) = \tau$ if $\tau \in \mathfrak{S}_m$; $P(\tau) = \epsilon$ if $\tau \in \mathfrak{S}_u$; $P(s\tau) = P(s)P(\tau)$, where $s \in L_f(G)$, $\tau \in \mathfrak{S}$. The function P erases the unmeasurable transitions from the argument finite trace. $P(s)$ is termed as the *measurable finite trace* corresponding to the finite trace s . An **inverse projection operator** $P^{-1} : \mathfrak{S}_m^* \rightarrow 2^{\mathfrak{S}^*}$ is defined as: $P^{-1}(s) = \{s' \in L_f(G) \mid sEs'\}$. Thus, $P^{-1}(s)$ encompasses all possible sequences of transitions that are equivalent to the finite trace s . The projection function P , the inverse function P^{-1} and the measurement equivalence E of finite traces can be extended to traces $\in \mathfrak{S}^w$, in a natural way.

Definition 35. Measurable Equivalent Traces: Two finite traces s and s' are said to be measurement equivalent if the following relation holds: $P(s) = \langle \tau_1, \tau_2, \dots, \tau_n \rangle$, $P(s') = \langle \tau'_1, \tau'_2, \dots, \tau'_n \rangle$ and $\tau_i E \tau'_i$, $1 \leq i \leq n$.

We use the symbol E to denote measurement equivalence of finite traces as well as that of transitions, with slight abuse of notation. The equivalence of finite traces s and s' implies that if measurable transitions are extracted from s and s' by use of the operator P , then all the transitions are measurement equivalent. Following Definition 33, it can be seen that the trace $\langle \tau_1, \tau_2, \tau_3 \rangle$ in Fig. 4.6, is measurement equivalent to the trace $\langle \tau'_1, \tau'_2, \tau'_3 \rangle$.

Definition 36. Normal G -state/ G -transition and Failure G -state/ G -transition: States that are traversed by the system when operating without any faults (attack) are known as **normal G -state**. X_N denotes the set of all normal states. A G -transition $\langle x, x^+ \rangle$ is called a *normal G -transition* if $x, x^+ \in X_N$. States that are traversed by the system when operating under **failure** circumstances are known as **Failure G -state**. X_{F_i} denotes the set of all failure states. A G -transition $\langle x, x^+ \rangle$ is called a *failure G -transition* if $x, x^+ \in X_{F_i}$. In Fig. 4.6, the states s_0, s_1, s_2 are normal G -states. The transitions associated with these states viz. τ_1, τ_2 are normal G -transitions. The states s'_0, s'_1, s'_2 are failure G -states. The transitions associated with these states viz. τ'_1, τ'_2 are failure G -transitions.

Definition 37. Failure causing G -transition: A transition $\langle x, x^+ \rangle$, where $x \in X_N$ and $x^+ \in X_{F_i}$, is called a *failure causing G -transition* indicating the occurrence of some failure. Since failures are assumed to be *permanent*, there is no transition from any $x \in X_{F_i}$ to $x^+ \in X_N$. In Fig. 4.6, the transition τ_{0F_1} is the failure causing G -transition as it moves the model from normal to the failure state. All failure causing G -transition are inherently unmeasurable.

The objective of the failure diagnosis problem is to determine the occurrence of a failure F_i . If the event (σ) corresponding to τ_{F_i} is measurable, failure diagnosis is trivial. So the failure causing transitions are assumed to be unmeasurable. For such failure causing transitions, σ is unmeasurable. As σ is unmeasurable, there are no checks or assignment for model variables. As failures are assumed to be *permanent*, there is no transition from any state in x_{F_i} to any state in X_N . The event related to causing F_i is denoted as σ_{F_i} .

4.4.2 Application of Failure Detection and Diagnosis Theory of RTDES on Three Tank System

We demonstrate the Failure Detection and Diagnosis (FDD) theory of the RTDES using an example of three connected tanks [126] viz. T_1, T_2 and T_3 as shown in Fig. 4.5. Tanks T_1 and T_2 are supplied substances from reservoir tanks MT_1 and MT_2 using pumps P_1 and P_2 , respectively. The flow through pumps P_1 and P_2 are controlled using valves V_1 and V_2 , respectively. Tanks T_3 and T_1 are connected by means of valve V_3 . Tanks T_3 and T_2 are

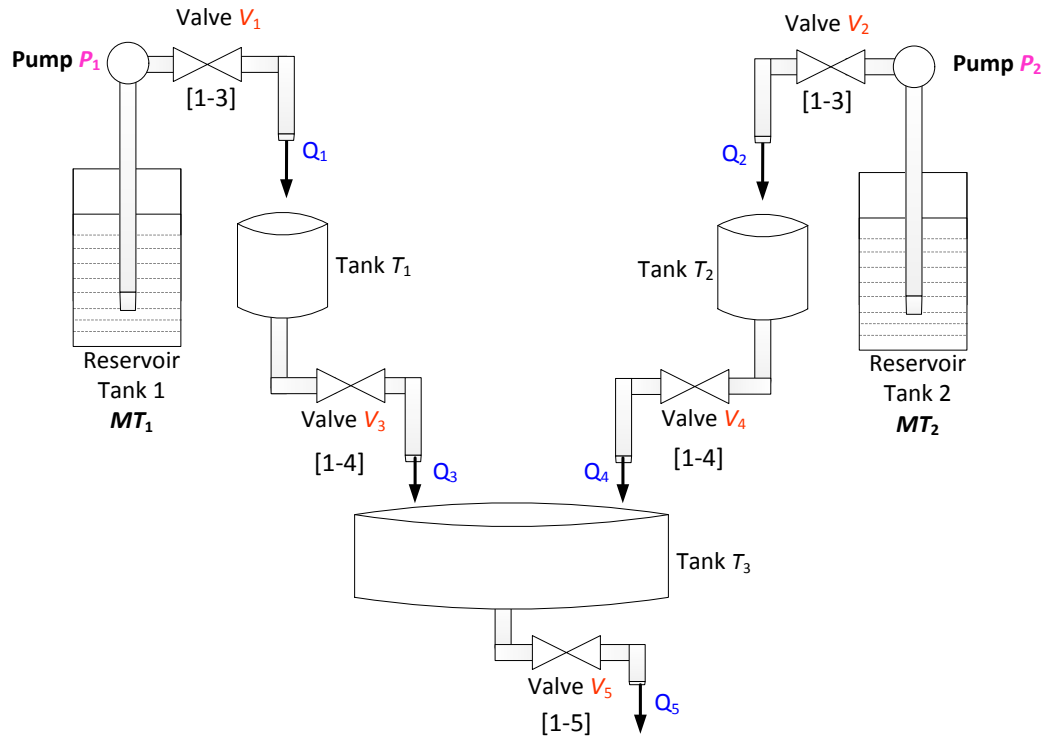


Figure 4.5: The three tank system

connected by means of valve V_4 . This broad arrangement of three tanks is used in many industrial process [145] e.g., which require mixing of two substances in a predetermined ratio (β , say). To elaborate, MT_1 and MT_2 contain the substances that are to be mixed and the ratio of the volume of tank T_1 to T_2 is $\beta : 1$. For this example, we assume $\beta = 1$ (so 1 unit of substance is added from each tank). First the substance from MT_1 is filled in the tank T_1 followed by filling of T_2 from MT_2 . Then the substances from T_1 and T_2 are drained into the tank T_3 . The substance in T_3 is stirred to ensure that the mixture is homogeneous. Once T_1 and T_2 are emptied, they are refilled again and the process repeats. When T_3 is full the homogenous mixture is drained out for usage.

The control of flows in the system is done by opening and closing of the valves by a controller which in turn depends on the two types of sensor outputs viz. (i) level sensors of the tanks and (ii) flow sensors of the valves. The tanks are equipped with two level sensors each in order to determine whether the level of the substance in the tank is low or high. For example, in the tank T_1 if the level of substance is at the lowest (highest) point, the low (high) level sensor indicated by $T_1\text{Low}$ ($T_1\text{High}$) gives output 1. There is a flow sensor (indicated as Q_1, \dots, Q_5) beside every valve that indicates whether substance is flowing through the adjoining pipe or not. For example, $Q_3 = 1$ (0) if substance is flowing (not flowing) through the pipe corresponding to Q_3 which connects T_1 to T_3 . Table 4.1 shows

the details of the sensors, their possible outputs and their interpretations.

Table 4.1: Sensor map for three tank system

Sensor	Possible Outputs	Interpretation
$T_i\text{Low}$ ($i = 1, 2, 3$)	0	$T_i\text{Low} = 0$ implies substance in the tank T_i is NOT at the lowest level.
	1	$T_i\text{Low} = 1$ implies substance in the tank T_i IS at the lowest level.
$T_i\text{High}$ ($i = 1, 2, 3$)	0	$T_i\text{High} = 0$ implies substance in the tank T_i is NOT at the highest level.
	1	$T_i\text{High} = 1$ implies substance in the tank T_i IS at the highest level.
Q_i ($i = 1, 2, 3, 4, 5$)	0	NO Flow measured by Flow sensor Q_i
	1	POSITIVE Flow measured by Flow sensor Q_i

Now we elaborate the working of the three tank system in terms of sensor outputs and controller commands to open/close the valves. Initially, all the tanks have their substances at the lowest levels, indicated by $T_1\text{Low} = T_2\text{Low} = T_3\text{Low} = 1$ (and obviously $T_1\text{High} = T_2\text{High} = T_3\text{High} = 0$). As all the valves are closed there is no flow in any of the pipes, so flow sensor outputs: $Q_1 = 0, \dots, Q_5 = 0$. First T_1 is to be filled which is initiated by the controller issuing the command $CV_1 = 1$. This results in opening of the valve V_1 to allow the flow of substance into T_1 . One important point to be noted here is that all the controller commands are bound by strict time constrains i.e., the controller defines the delay-deadline between which the commands needs to be executed. For example, in Fig. 4.6, when the controller issues the command $CV_1 = 1$ it has to be issued within $[1-3]$ time units. Similarly, for other commands also the time constrains shown in terms of delay-deadline in Fig. 4.6 needs to be followed. Once the substance starts flowing into T_1 from MT_1 , Q_1 becomes 1 and $T_1\text{Low}$ becomes 0. After the tank T_1 is full $T_1\text{High}$ becomes 1 and the controller issues the command $CV_1 = 0$ to close the valve V_1 . Flow to T_1 stops and Q_1 becomes 0.

Next, in a similar manner, valve V_2 is opened within the delay-deadline of $[1-3]$ time units in order to fill the tank T_2 ($Q_2 = 1$ and $T_1\text{Low} = 0$). After T_2 gets full, $T_2\text{High} = 1$ and controller makes $CV_2 = 0$ which stops the flow to T_2 making $Q_2 = 0$. After both T_1 and T_2 are full the controller issues the command $CV_3 = 1$ and $CV_4 = 1$ which open the valves V_3, V_4 simultaneously (within the delay-deadline of $[1-4]$ time units) and substances from T_1 and T_2 are allowed to fall into the tank T_3 ; $Q_3 = 1, Q_4 = 1$ and $T_3\text{Low} = 0$. We have assumed that $\beta = 1$ and the flow rate from T_1 and T_2 to T_3 are same. So T_1 and T_2 get emptied at the same time (sensor outputs $T_2\text{Low} = 1$ and $T_2\text{Low} = 1$). Tanks T_1 and T_2 are refilled again and the process continues till T_3 becomes full. In the current system it is assumed that the volume of the tank T_3 is ' h ' times the volume of the tanks T_1 and T_2 taken together. So after ' h ' iterations of dropping of the substances from T_1 and T_2 , T_3 gets full (indicated by $T_3\text{High} = 1$). Controller opens the valve V_5 by the command $CV_5 = 1$ (within the delay-deadline of $[1-5]$ time units) and the mixture is drained out of tank T_3 for usage. When T_3 becomes empty (indicated by $T_3\text{Low} = 1$) the whole process is repeated.

Here, we consider those failures that are manifested in terms of time i.e., in terms of delay-deadline. As seen earlier, once the tank T_3 gets full, it needs to be emptied with the delay-deadline of $[1 - 5]$ time units in order to ensure smooth operations. However, because of some fault, the tank T_3 get emptied during $[6 - 10]$ time units instead of the scheduled $[1 - 5]$ time units. Although, the tank gets emptied eventually, the late emptying of the tank leads to degraded system performance. Such faults can be detected by RTDES models without needing to resort to any complex frameworks like hybrid systems that employ continuous dynamics [72]. Now we discuss the modeling of the three tank system using the RTDES framework. The RTDES model G used to represent three tank system under normal and fault scenarios is shown in Fig. 4.6. The various components of G are as follows:

$$X = \{s_0, s_1, s_2, s_3, s_4, s_5, s_6, s_7, s_8, s'_0, s'_1, s'_2, s'_3, s'_4, s'_5, s'_6, s'_7, s'_8\}$$

$$X_0 = \{s_0\}$$

$$\Sigma = \{T_1 \text{ Empty}, T_1 \text{ Filling}, T_1 \text{ Full}, T_2 \text{ Empty}, T_2 \text{ Filling}, T_2 \text{ Full}, T_3 \text{ Empty}, T_3 \text{ Filling}, T_3 \text{ Full_Drain}, T_1 \ \& \ T_2 \text{ Refill}, T_3 \text{ Full}\}$$

$$\mathfrak{S} = \{\tau_0, \tau_1, \tau_2, \tau_3, \tau_4, \tau_5, \tau_6, \tau_7, \tau_8, \tau_9, \tau_{11}, \tau_{0F1}, \tau'_1, \tau'_2, \tau'_3, \tau'_4, \tau'_5, \tau'_6, \tau'_7, \tau'_8, \tau'_{10}, \tau'_{11}\}$$

$$V = \{\epsilon\}^2$$

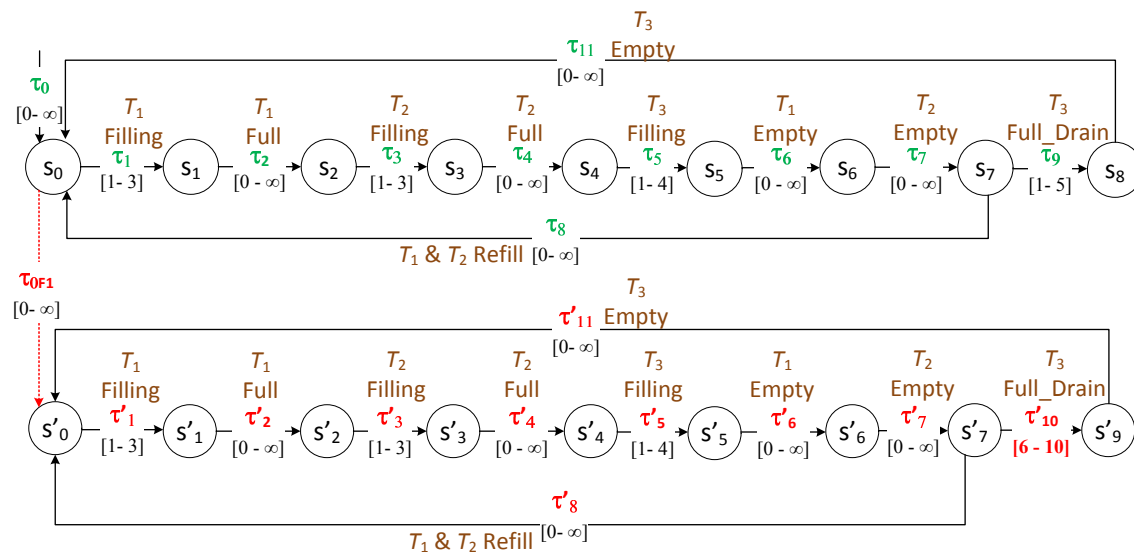


Figure 4.6: RTDES of the three tank system shown in Fig. 4.5

States and transitions belonging to normal (fault) model are denoted by the non-primed (primed) notations. The occurrence of fault is modeled by the failure causing transition τ_{0F1} . For simplicity of illustration, we assume that fault can occur only from state s_0 . In Fig. 4.6, the transitions are not explicitly detailed as their six tuples, however, the corresponding

²As the number of states in the three tank system is not large, model variables are not used as explained in earlier chapters.

4.4. FDD Theory of RTDES: Three Tank System

Table 4.2: Transitions along with their representation. Events, sensor conditions, controller commands of the RTDES model of the three tank system shown in Fig. 4.6

Transition	What it Represents	Event	Delay	Deadline	Sensor Conditions	Controller Commands
τ_0	All Tanks are Empty	Start	0	∞	$T_1\text{Low} = 1, T_2\text{Low} = 1, T_3\text{Low} = 1,$ $T_1\text{High} = 0, T_2\text{High} = 0, T_3\text{High} = 0,$ $Q_1 = 0, Q_2 = 0, Q_3 = 0, Q_4 = 0, Q_5 = 0.$	$CV_1 = 0, CV_2 = 0, CV_3 = 0,$ $CV_4 = 0, CV_5 = 0,$
τ_1 & τ'_1	Tank T_1 Filling	$T_1\text{Filling}$	1	3	$T_1\text{Low} = 0, T_2\text{Low} = 1, T_3\text{Low} = 1,$ $T_1\text{High} = 0, T_2\text{High} = 0, T_3\text{High} = 0,$ $Q_1 = 1, Q_2 = 0, Q_3 = 0, Q_4 = 0, Q_5 = 0.$	$CV_1 = 1, CV_2 = 0, CV_3 = 0,$ $CV_4 = 0, CV_5 = 0,$
τ_2 & τ'_2	Tank T_1 Full	$T_1\text{Full}$	0	∞	$T_1\text{Low} = 0, T_2\text{Low} = 1, T_3\text{Low} = 1,$ $T_1\text{High} = 1, T_2\text{High} = 0, T_3\text{High} = 0,$ $Q_1 = 0, Q_2 = 0, Q_3 = 0, Q_4 = 0, Q_5 = 0.$	$CV_1 = 0, CV_2 = 0, CV_3 = 0,$ $CV_4 = 0, CV_5 = 0,$
τ_3 & τ'_3	Tank T_2 Filling	$T_2\text{Filling}$	1	3	$T_1\text{Low} = 0, T_2\text{Low} = 0, T_3\text{Low} = 1,$ $T_1\text{High} = 1, T_2\text{High} = 0, T_3\text{High} = 0,$ $Q_1 = 0, Q_2 = 1, Q_3 = 0, Q_4 = 0, Q_5 = 0.$	$CV_1 = 0, CV_2 = 1, CV_3 = 0,$ $CV_4 = 0, CV_5 = 0,$
τ_4 & τ'_4	Tank T_2 Full	$T_2\text{Full}$	0	∞	$T_1\text{Low} = 0, T_2\text{Low} = 0, T_3\text{Low} = 1,$ $T_1\text{High} = 1, T_2\text{High} = 1, T_3\text{High} = 0,$ $Q_1 = 0, Q_2 = 0, Q_3 = 0, Q_4 = 0, Q_5 = 0.$	$CV_1 = 0, CV_2 = 0, CV_3 = 0,$ $CV_4 = 0, CV_5 = 0,$
τ_5 & τ'_5	Tank T_3 Filling, T_1 and T_2 Draining	$T_3\text{Filling}$	1	4	$T_1\text{Low} = 0, T_2\text{Low} = 0, T_3\text{Low} = 1,$ $T_1\text{High} = 0, T_2\text{High} = 0, T_3\text{High} = 0,$ $Q_1 = 0, Q_2 = 0, Q_3 = 1, Q_4 = 1, Q_5 = 0.$	$CV_1 = 0, CV_2 = 0, CV_3 = 1,$ $CV_4 = 1, CV_5 = 0,$
τ_6 & τ'_6	Tank T_1 Empty	$T_1\text{Empty}$	0	∞	$T_1\text{Low} = 1, T_2\text{Low} = 0, T_3\text{Low} = 0,$ $T_1\text{High} = 0, T_2\text{High} = 0, T_3\text{High} = 0,$ $Q_1 = 0, Q_2 = 0, Q_3 = 0, Q_4 = 0, Q_5 = 0.$	$CV_1 = 0, CV_2 = 0, CV_3 = 0,$ $CV_4 = 0, CV_5 = 0,$
τ_7 & τ'_7	Tank T_2 Empty	$T_2\text{Empty}$	0	∞	$T_1\text{Low} = 1, T_2\text{Low} = 1, T_3\text{Low} = 0,$ $T_1\text{High} = 0, T_2\text{High} = 0, T_3\text{High} = 0,$ $Q_1 = 0, Q_2 = 0, Q_3 = 0, Q_4 = 0, Q_5 = 0.$	$CV_1 = 0, CV_2 = 0, CV_3 = 0,$ $CV_4 = 0, CV_5 = 0,$
τ_8 & τ'_8	Tank T_1 & T_2 Re-Filling	T_1 & T_2 Refill	0	∞	$T_1\text{Low} = 1, T_2\text{Low} = 1, T_3\text{Low} = 0,$ $T_1\text{High} = 0, T_2\text{High} = 0, T_3\text{High} = 0,$ $Q_1 = 0, Q_2 = 0, Q_3 = 0, Q_4 = 0, Q_5 = 0.$	$CV_1 = 0, CV_2 = 0, CV_3 = 0,$ $CV_4 = 0, CV_5 = 0,$
τ_9	Tank T_3 Full and Draining	$T_3\text{Full_Drain}$	1	5	$T_1\text{Low} = 1, T_2\text{Low} = 1, T_3\text{Low} = 0,$ $T_1\text{High} = 0, T_2\text{High} = 0, T_3\text{High} = 1,$ $Q_1 = 0, Q_2 = 0, Q_3 = 0, Q_4 = 0, Q_5 = 1.$	$CV_1 = 0, CV_2 = 0, CV_3 = 0,$ $CV_4 = 0, CV_5 = 1,$
τ_{1F_i}	Failure Causing	Fault	0	∞	$T_1\text{Low} = 1, T_2\text{Low} = 1, T_3\text{Low} = 1,$ $T_1\text{High} = 0, T_2\text{High} = 0, T_3\text{High} = 0,$ $Q_1 = 0, Q_2 = 0, Q_3 = 0, Q_4 = 0, Q_5 = 0.$	$CV_1 = 0, CV_2 = 0, CV_3 = 0,$ $CV_4 = 0, CV_5 = 0,$
τ_{11} & τ'_{11}	Tank T_3 Empty	$T_3\text{Empty}$	0	∞	$T_1\text{Low} = 1, T_2\text{Low} = 1, T_3\text{Low} = 1,$ $T_1\text{High} = 0, T_2\text{High} = 0, T_3\text{High} = 0,$ $Q_1 = 1, Q_2 = 0, Q_3 = 0, Q_4 = 0, Q_5 = 0.$	$CV_1 = 1, CV_2 = 0, CV_3 = 0,$ $CV_4 = 0, CV_5 = 0,$
τ'_{10}	Tank T_3 Full and Draining	$T_3\text{Full_Drain}$	6	10	$T_1\text{Low} = 1, T_2\text{Low} = 1, T_3\text{Low} = 0,$ $T_1\text{High} = 0, T_2\text{High} = 0, T_3\text{High} = 1,$ $Q_1 = 0, Q_2 = 0, Q_3 = 0, Q_4 = 0, Q_5 = 1.$	$CV_1 = 0, CV_2 = 0, CV_3 = 0,$ $CV_4 = 0, CV_5 = 1,$

event is shown with their respective delay-deadline. Table 4.2 illustrates the events corresponding to the sensor outputs and control commands. The transitions which are enabled by these events are shown in the Table 4.2. For explanation of the modeling we discuss the details of a normal G -transition (τ_1) and an F_i - G -transition (τ'_{10}).

τ_1 has the event $T_1\text{Filling}$. When the sensor outputs for the tank T_1 are $T_1\text{Low} = 1$ and $T_1\text{High} = 0$, the controller issues the command $CV_1 = 1$ which opens the valve V_1 (within the delay-deadline of $[1 - 3]$ time units). This allows flowing of the substance to T_1 and the flow sensor output $Q_1 = 1$. These sensor outputs and the controller command are represented by the event $T_1\text{Filling}$ that corresponds to the transition τ_1 .

From s_0 there is another transition τ_{0F_1} which indicates the occurrence of a failure. Let us consider the F_i - G -transition τ'_{10} which has the event $T_3\text{Full}$ associated with it and is issued within the delay-deadline of $[6 - 10]$ time units. When the system is in state s'_7 (if F_i has

occurred), the sensor outputs for the T_3 are $-T_3\text{Low} = 0$ and $T_3\text{High} = 1$, indicating that T_3 is full and the mixture must be drained out. Upon reading the sensor outputs, the controller issues the command $CV_5 = 1$ (within the delay-deadline of $[1 - 5]$ time units) which should open the valve V_5 leading to draining out of the mixture. However, because of failure F_i , the command is executed between the delay-deadline of $[6 - 10]$ time units affecting the performance of the system. Although, even after late execution of the controller command, the tank T_3 eventually gets empty, however, this delay leads to serious performance issues. The system moves from state s'_7 to s'_9 .

On the other hand, if the system is normal, when T_3 becomes full, the controller issues the command to empty the tank T_3 within the delay-deadline of $[1 - 5]$ time units. This is indicated by the transition τ_{10} . Following that the tank T_3 becomes empty and it is modeled by the transition τ_{11} . In a similar manner, referring to Table 4.2 and the discussion on the working of the three tank system, the whole modeling given in Fig. 4.6 can be explained.

In the three tank system under consideration, we have assumed that the volume of the tank T_3 is $h = 4$ times the volume of tank T_1 and T_2 taken together. This implies that after four iterations of draining of the substance from both T_1 and T_2 the tank T_3 gets full. So, from the RTDES model in Fig. 4.6 it can be observed that in order for T_3 to get full, the system moves in the trace containing transitions $\langle \tau_1, \tau_2, \tau_3, \tau_4, \tau_5, \tau_6, \tau_7, \tau_8 \rangle$ for three times and during the fourth iteration the system takes the trace $\langle \tau_1, \tau_2, \tau_3, \tau_4, \tau_5, \tau_6, \tau_7, \tau_9 \rangle$ which breaks out of the loop and the tank T_3 gets filled. Thus, the trace containing the transition τ_8 is traversed three times while the transition τ_9 is traversed only once out of four times.

Now we discuss measurable/unmeasurable transitions of the model and consequently the equivalent states and transitions are identified. In this system all the sensor outputs are measurable and so are the controller commands. So any transition whose enabling event is based on the change in some sensor output or controller command, is measurable. For example, in case of τ_2 the event is $T_1\text{Full}$, whose corresponding change in sensor outputs are $T_1\text{Low} = 0$ (from 1), $T_1\text{High} = 1$ (from 0), $Q_1 = 0$ (from 1) and controller command is $CV_1 = 0$ (from 1). So τ_2 is a measurable transition. In a similar way it can be shown that all transitions except τ_{0F1} are measurable. τ_{0F1} is the failure causing transition and is unmeasurable because it is not caused by a change of any sensor output or controller command.

Two transitions are measurement equivalent if the corresponding changes in the sensor outputs and the controller commands are same. Events associated with equivalent transitions are also same. For example, transitions τ_2 and τ'_2 are measurement equivalent because they are caused by same changes in sensor outputs, delay-deadline and controller commands i.e., $T_1\text{Low} = 0$, $T_1\text{High} = 1$, $Q_1 = 0$, delay-deadline of $[0 - \infty]$ and controller command

is $CV_1 = 0$. Also the event associated with both these transitions is $T_1\text{Full}$. As per the Definition 33, $s_0Es'_0$ and $s_1Es'_1$, because the source states and also the destination states of equivalent transitions are equivalent. In a similar way it can be verified that $\tau_iE\tau'_i$, $1 \leq i \leq 8$. It may be noted that in case of F_i -transitions τ'_i , $1 \leq i \leq 8$ there is an equivalent normal transition e.g., $\tau_1E\tau'_1$. So, after the failure as long as the system moves through F_i -transitions τ'_i , $1 \leq i \leq 8$, the fault cannot be diagnosed because there is no transition that distinguishes the faulty behavior from the normal condition. To elaborate, F_i -transitions τ'_i , $1 \leq i \leq 8$ do not capture failure manifestation (in terms of distinguishing sensor outputs and controller commands) and hence cannot detect the fault.

Now let us consider the transitions τ_9 and τ'_{10} . The sensor outputs and the controller command for the transition τ_9 are $T_3\text{Low} = 0$, $T_3\text{High} = 1$, $CV_5 = 1$ and $Q_5 = 1$ with the delay-deadline of $[1 - 5]$ time units. In case of the transition τ'_{10} the sensor outputs are same expect for the fact that the command is executed within the delay-deadline of $[6 - 10]$ time units. It may be noted that for both the transitions, the controller issues the command $CV_5 = 1$ after detecting that T_3 is full (by sensor outputs $T_3\text{Low} = 0$, $T_3\text{High} = 1$). In case of τ_9 , as the system is normal as it is executed within the delay-deadline of $[1 - 5]$ time units and is captured by the sensor output $Q_5 = 1$. However, in case of τ'_{10} , the controller issues the command $CV_5 = 1$ within the delay-deadline of $[6 - 10]$ time units which deviates in terms of the scheduled time of $[1 - 5]$ units. So transition τ'_{10} captures the fault manifestation. As F_i -transition τ'_{10} captures failure manifestation its occurrence is required for detection of F_i . Next we look at the diagnosability condition and the diagnoser construction for the three tank system.

4.4.3 Diagnosability

The objective of the failure diagnosis problem is to determine the occurrence of a failure F_i . If the event (σ) corresponding to τ_{F_i} is measurable, failure diagnosis is trivial. So the failure causing transitions are assumed to be unmeasurable. For such failure causing transitions, σ is unmeasurable. As σ is unmeasurable, there are no checks or assignment for model variables. As failures are assumed to be *permanent*, there is no transition from any state in x_{F_i} to any state in X_N . The event related to causing F_i is denoted as σ_{F_i} .

Informally, an DES G is diagnosable if it is always possible to determine the failure status of the states beyond a certain point along all the possible traces of G after the occurrence of a failure, using the sequence of measurements. A few terms are introduced before formally defining diagnosability.

Let $\psi(X_{F_i}) = \{s | s \in L_f(G) \text{ and } final(s) \in X_{F_i} \text{ and } s \text{ ends in a measurable transition} \}$.

Definition 38. F_i -Diagnosability: An DES model G (under a given measurement limitation) is said to be diagnosable for failure F_i iff the following holds.

$$(\exists n_j \in \mathbb{N})[\forall s \in \Psi(X_{F_i})](\forall t \in L_f(G)/s)[|t| \geq n_j \Rightarrow D] \quad (4.2)$$

where the condition D is $\forall y \in \{P^{-1}[P(st)]\}$, $final(y) \in X_{F_i}$

The above definition means the following. Let s be any finite prefix of a trace of G that ends in an F_i -state and let t be any sufficiently long continuation of s . Condition D then requires that every sequence of transitions, measurement indistinguishable with st , should end into an F_i -state. This implies that, along every continuation t of s , one can detect the occurrence of failure F_i with a finite delay, specifically in at most n_j transitions of the system after s .

The fault diagnosis problem is to determine if the fault F_i has occurred within finite number n_{F_i} (where $n_{F_i} \in \mathbb{N}$) say, of transitions after the occurrence of the failure causing transition τ_{F_i} . Let us consider a trace of the RTDES model of the three tank system; $s = \langle \tau_0, \tau_{0F1}, \tau'_1 \rangle$; obviously $s \in \Psi(X_{F_i})$. For diagnosing F_i , any sufficiently long but finite extension t of s of length n_{F_i} must ascertain that fault has occurred. In this case, if we extend $s = \langle \tau_0, \tau_{1F_i}, \tau'_1 \rangle$ as $t = \langle (\tau'_2, \tau'_3, \tau'_4, \tau'_5, \tau'_6, \tau'_7, \tau'_8, \tau'_1)^k \rangle$, where k is arbitrarily large, we get $\exists y = \langle \tau_0, \tau_1, (\tau_2, \tau_3, \tau_4, \tau_5, \tau_6, \tau_7, \tau_8, \tau_1)^k \rangle \in P^{-1}(P(st)) \wedge final(y) = x_1 \notin X_{F_i}$. In other words, as the F_i - G -trace $\langle \tau'_1, (\tau'_2, \tau'_3, \tau'_4, \tau'_5, \tau'_6, \tau'_7, \tau'_8, \tau'_1)^k \rangle$ is equivalent to $\langle \tau_1, (\tau_2, \tau_3, \tau_4, \tau_5, \tau_6, \tau_7, \tau_8, \tau_1)^k \rangle$ (normal condition), so this F_i - G -trace cannot detect the fault. As already discussed, as none of the transitions involved in the F_i - G -trace under question captures failure manifestation, it is not helpful in fault detection.

In this example there is only one more way of extending s , namely, $t1$ is $\langle \tau'_1, \dots, \tau'_7, \tau'_{10} \rangle$. It may be noted that $\nexists y \in P^{-1}(P(st1))$ such that $final(y) \notin X_{F_i}$ (Since the delay-deadline of τ'_{10} is $[6, 10]$ as against the delay deadline for τ_9 which is $[1, 5]$). So the fault is diagnosable. In other words, the transition τ'_{10} captures failure manifestation. So the trace $st1$ detects the fault making the fault diagnosable.

4.4.4 RTDES Diagnoser Construction Fault Detection in Three Tank System

The diagnoser is a directed graph represented by $O = \langle Z, A \rangle$; where Z is the set of diagnoser nodes, called O -nodes, and $A \subseteq Z \times Z$ is the set of diagnoser transitions, called O -transitions. Each O -node $z \in Z$ corresponds to a set of G -states representing the uncertainty about the actual state. Similarly, each O -transition $a \in A$ of the form $\langle z_i, z_f \rangle$ is a set of measurement equivalent transitions representing the uncertainty about the actual measurable transition

that occurs. The *unmeasurable successor* (set) of a set Y of states is defined as $\mathcal{U}(Y) = \bigcup_{x \in Y} \{x^+ | \tau = \langle x, x^+ \rangle \in \mathfrak{S}_u\}$. The *unmeasurable reach* of a set Y of states, denoted as $\mathcal{U}^*(Y)$, is the reflexive-transitive closure of unmeasurable successors of Y .

Diagnoser Construction: The states in X_0 are partitioned into equivalent subsets denoted as $X_{01}, X_{02}, \dots, X_{0m}$. For all i , $1 \leq i \leq m$, an initial O -node z_{0i} is obtained as the unmeasurable reach of X_{0i} , i.e., $z_{0i} = \mathcal{U}^*(X_{0i})$. The set of all initial O -nodes is denoted as $Z_0 = z_{01} \cup \dots \cup z_{0m}$. The initial O -nodes capture the fact that the diagnoser can infer a set z_{0i} of possible initial system states (or their unmeasurable reach) by measuring the variables without waiting for the first measurable transition. Given any O -node z , the O -transitions emanating from z are obtained as follows. Let \mathfrak{S}_{mz} denote the set of measurable G -transitions from the states $x \in z$. Let A_z be the set of all equivalence classes of \mathfrak{S}_{mz} under E . For each $a \in A_z$, a successor O -node z^+ of z such that $z^+ = final(a)$ can be created as follows. Let $z_a^+ = \{final(\tau) | \tau \in a\}$; then $z^+ = \mathcal{U}^*(z_a^+)$ and a is designated as: $\langle z, z^+ \rangle$. The set of the diagnoser transitions is augmented as: $A \leftarrow A \cup \{a\}$, and the set of O -nodes is augmented as: $Z \leftarrow Z \cup \{z^+\}$. Each $a \in A$ is an ordered pair $\langle z, z^+ \rangle$, where $z = initial(a)$ and $z^+ = final(a)$. Thus, each O -node contains equivalent states. The detailed algorithm for diagnoser construction is shown in Algorithm 3

Algorithm 3: Algorithm for construction of diagnoser O for an RTDES model G

Input: RTDES model G
Output: RTDES Diagnoser

- 1 Partition X_0 into equivalent subsets $X_{01}, X_{02}, \dots, X_{0m}$
- 2 **for all** i , $1 \leq i \leq m$ **do**
- 3 $z_{0i} = \mathcal{U}^*(X_{0i})$
- 4 **end**
- 5 $Z_0 \leftarrow z_{01} \cup \dots \cup z_{0m}$
- 6 $Z \leftarrow Z_0$
- 7 $A \leftarrow \phi$
- 8 **for all** $z \in Z$ **do**
- 9 /* Find the set of measurable G -transitions (\mathfrak{S}_{mz}) outgoing from z */
 $\mathfrak{S}_{mz} \leftarrow \{\tau | \tau \in \mathfrak{S}_m \wedge initial(\tau) \in z\}$
 /* Find the set of all measurement equivalent classes A_z , of \mathfrak{S}_{mz} */
- 10 **for all** $a \in A_z$ **do**
- 11 $z_a^+ = \{final(\tau) | \tau \in a\}$
- 12 $z^+ = \mathcal{U}^*(z_a^+)$
- 13 $Z = Z \cup \{z^+\}$
- 14 $A = A \cup \{a\}$
- 15 **end**
- 16 **end**

Henceforth, we refer to states, transitions, and traces of G as G -states, G -transitions and

G -traces, respectively. Similarly, for the diagnoser nodes and transitions, we use O -nodes, O -transitions and O -traces respectively. Now, we look into few definitions and properties related to diagnoser.

Definition 39. (Embedding of G -traces in O -traces): Given a O -trace $\gamma = \langle a_1, a_2, \dots, a_k \rangle$, a G -trace s , where $P(s) = \langle \tau_1, \tau_2, \dots, \tau_k \rangle$, is said to be embedded in γ , if $\tau_i \in a_i, 1 \leq i \leq k$. The set of all G -traces embedded in a O -trace γ is represented as $A_D(\gamma)$.

Property 3. If two traces $t, y \in A_D(\gamma)$, where t is F_i - G -trace and y is non- F_i - G -trace, then the O -nodes traversed by γ are F_i -uncertain.

Proof. The property also follows from the diagnoser construction. As any O -transition $a \in \gamma$ has an non- F_i - G -transition and a F_i - G -transition (which are equivalent), so source and destination O -nodes of a are F_i -uncertain. \square

Definition 40. F_i - O -node: An O -node, which contains an F_i - G state, is called an F_i - O -node, denoted as z_{F_i} . The set of all F_i - O -nodes is denoted as Z_{F_i} . In Fig. 4.7 the O -nodes $z_0, \dots, z_7, z_9, \dots, z_{18}$ are F_i - O -nodes as each O -node contains an F_i - G -state.

Definition 41. F_i -certain O -node and F_i -uncertain O -node: An F_i - O -node z is called an F_i -certain O -node if $z \subseteq X_{F_i}$. In Fig. 4.7 the O -node z_9 are F_i -certain O -node as it contains only failure G -states. An F_i - O -node which is not F_i -certain is called F_i -uncertain- O -node. In Fig. 4.7 the O -nodes z_0, \dots, z_7 are F_i -uncertain O -nodes as they contain both normal G -states as well as failure G -states.

In words, F_i -certain O -node comprises only F_i - G states, while F_i -uncertain O -node comprises some F_i - G states and some non F_i - G -states. So, if the diagnoser reaches any F_i -certain O -node failure is diagnosed. By Property 3 and Definition 39, if there is a O -trace γ which moves in F_i -uncertain O -nodes, there is a F_i - G -trace t which is embedded in γ . After failure, diagnoser moves in γ by virtue of t . However, as there is another non- F_i - G -trace y say, equivalent to t , fault cannot be diagnosed till γ is exited.

Definition 42. F_i - O -path (γ_{F_i}): A path of the diagnoser O is a sequence of O -transitions $\gamma = \langle a_1, a_2, \dots \rangle$, with the consecution property $initial(a_{i+1}) = final(a_i), i \geq 1$. An F_i - O -path γ is an O -path in which every O -node is an F_i - O -node.

Definition 43. F_i -uncertain cycle: An F_i -uncertain cycle is an F_i - O -cycle in which there is no F_i -certain O -node. In Fig. 4.7, the O -transitions sequence $\langle a_1, a_2, a_3, a_4, a_5, a_6, a_7, a_8 \rangle$ associated with the diagnoser state sequence is $\langle z_0, z_1, z_2, z_3, z_4, z_5, z_6, z_7, z_0 \rangle$ represents an F_i -uncertain cycle. This is because, none of the O -nodes ($z_0, z_1, z_2, z_3, z_4, z_5, z_6, z_7, z_0$) is an F_i -certain O -node.

Definition 44. *F_i -indeterminate cycle:* An F_i -uncertain cycle γ in which the F_i -states contained in the O -nodes of γ form a cycle in G comprising transitions from γ , is called an *F_i -indeterminate cycle*. Consider a sequence $\langle x_1, x_2, x_3, \dots, x_k \rangle$ that corresponds to a normal cycle and measurement equivalent failure cycle $\langle x'_1, x'_2, x'_3, \dots, x'_k \rangle$. If the system is under normal conditions, the diagnoser moves into normal cycle and once a failure occurs it moves in the failure cycle. As both the normal and attack cycles are measurement equivalent, the normal and failure cycles are indistinguishable from one another. As a result of the presence of the indeterminate cycle it is not possible to predict whether the diagnoser is moving under normal or failure cycle leading to non-diagnosability. Thus, an F_i -indeterminate cycle is an F_i -uncertain cycle with the special property as stated below:

“There is also a cycle involving F_i -states of the composite model that corresponds to the F_i -uncertain diagnoser cycle.” In simple words, the existence of an F_i -indeterminate cycle in the diagnoser implies that there are at least two measurement indistinguishable *syntactic* cycles in G , one comprising only non- F_i -states and the other comprising F_i -states. This implies that if the system moves in an F_i -indeterminate cycle, then the measurable variables are observed to be similar in both non- F_i and F_i conditions. Thus, if the diagnostic estimate moves along such an F_i -indeterminate cycle, then the fault F_i cannot be diagnosed, because, at each point in the cycle there exists uncertainty regarding the occurrence of F_i and as faults are assumed to be permanent, the system may not exit from such a cycle. The existence of an F_i -indeterminate cycle thwarts diagnosability. The equivalence between F_i -diagnosability and the absence of F_i -indeterminate cycles has been formally established for DES models [72].

The diagnoser for the RTDES model of Fig. 4.6 is shown in Fig. 4.7. Some of the initial steps for this example are as follows:

- The initial state of the diagnoser i.e., z_0 is obtained as follows. First, $s_0 \in X_0$ is inserted in z_0 . Now, all states in $U^*(s_0)$ are inserted in z_0 ; s'_0 is within unmeasurable reach of s_0 and is inserted in z_0 . So, $z_0 = \langle s_0, s'_0 \rangle$.
- The outgoing O -transitions from z_0 are obtained as follows. Here, $\mathfrak{S}_{mz_0} = \{\tau_1, \tau'_1\}$ which are all the outgoing measurable transitions from G -states in z_0 . Now, $A_{z_1} = \{\{\tau_1, \tau'_1\}\}$ as $\tau_1 E \tau'_1$. Corresponding to $\{\tau_1, \tau'_1\}$ there is a O -transition a_1 .
- The destination O -node corresponding to a_1 is obtained as follows. $z_1 a_1^+ = \{\langle s_1, s'_1 \rangle\}$ as a_1 comprises O -transitions τ_1, τ'_1 and $final(\tau_1) = s_1$ and $final(\tau'_1) = s'_1$. Further, $z_1^+ = \{s_1, s'_1\}$ as $U^*(\{s_1\}) = \{s_1, s'_1\}$ and $U^*(\{s'_1\}) = \{s'_1\}$. Thus, the destination O -node of the O -transition a_1 is $z_1 : \{\langle s_1, s'_1 \rangle\}$.

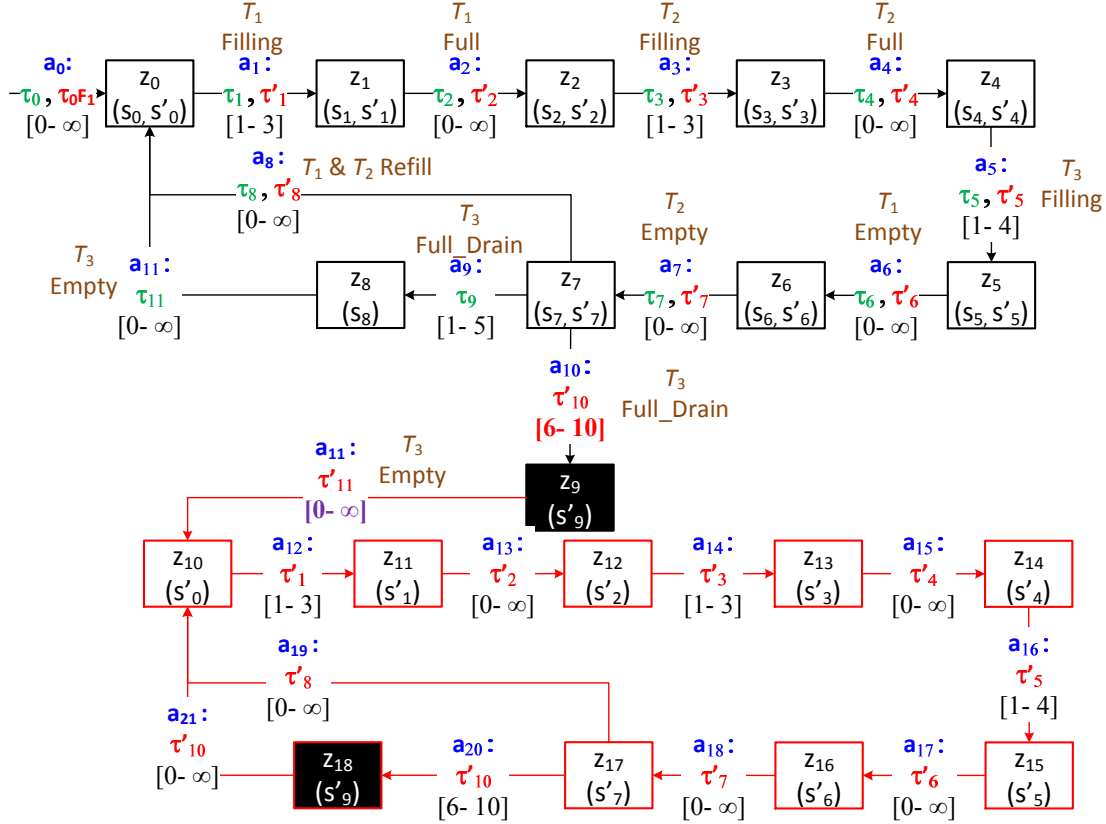


Figure 4.7: Diagnoser obtained from Fig. 4.6

There is no F_i -indeterminate cycle present in the diagnoser for the pump valve system shown in Fig. 4.7. Hence the fault is diagnosable. Referring to the diagnoser the F_i -certain O -node z_9 comprises the F_i - G -state s'_9 . The state s'_9 corresponds to controller command 'Valve_{OPEN}' after the tank T_3 is full, but the command is executed between the delay-deadline of $[6, 10]$ units. As discussed earlier, the command must execute within the delay-deadline of $[1, 5]$ units. So, the fault which manifested in terms of time, has been successfully diagnosed using the RTDES framework.

4.5 RTDES Model for PS-DoS Attack

The RTDES model G used to represent PS-DoS attack under normal and attack scenarios is shown in Fig. 4.8. For readability purposes Fig. 4.8 is annotated with transition number τ_i , delay-deadline of the transition $[delay, deadline]$ and the event because of which the transition τ_i is fired. The transitions of the RTDES model G shown in Fig. 4.8 are explained in Table 4.3. States and transitions belonging to normal (attack) model are denoted by the non-primed (primed) notations. The various components of G are as follows:

4.5. RTDES Model for PS-DoS Attack

$$X = \{s_0, s_1, s_2, s_3, s_4, s_5, s_6, s_7, s'_0, s'_1, s'_2, s'_3, s'_4, s'_5\}$$

$\Sigma = \{\text{Sleep, ACK, Early Wake, Proper Wake, Data, Power Save Probe, Power Save Probe Response}\}$

$V = \{mac_{src}, mac_{dst}\}$ is the set of model variables. The domain of both mac_{src} and mac_{dst} is

$\{xx : xx : xx : xx : xx | x \in [0 - F]\}$. mac_{src} and mac_{dst} holds source and destination MAC address contained in the frame respectively.

$$\mathfrak{S} = \{\tau_1, \tau_2, \tau_3, \tau_4, \tau_5, \tau_6, \tau_7, \tau_8, \tau_9, \tau_{10}, \tau_{11}, \tau_{12}, \tau_{13}, \tau_{14}, \tau'_{1}, \tau'_{2}, \tau'_{3}, \tau'_{4}, \tau'_{5}, \tau'_{6}, \tau'_{8}, \tau'_{15}\}$$

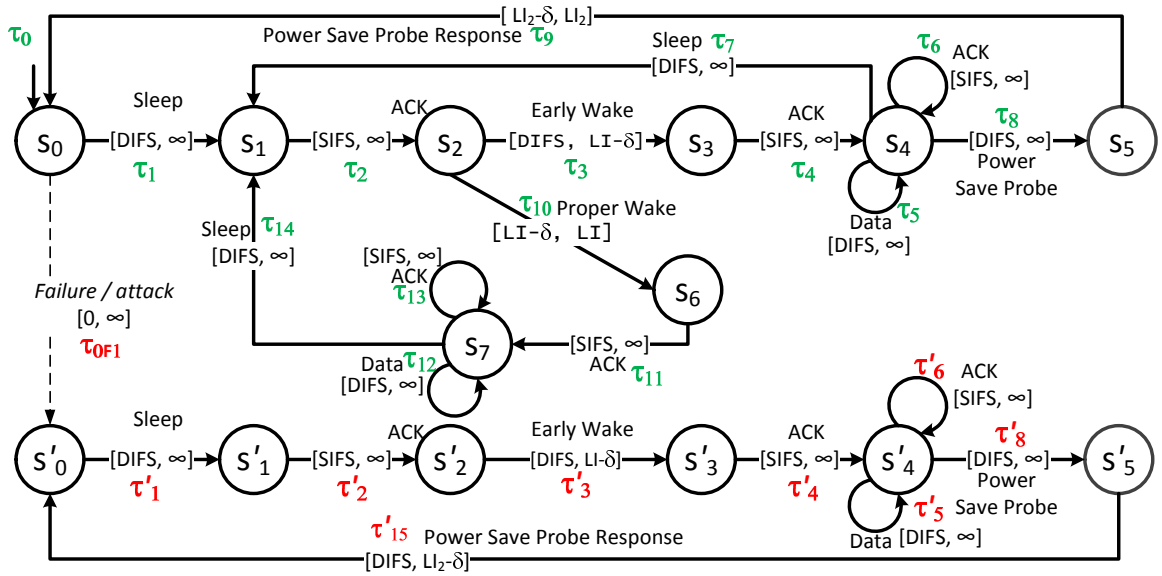


Figure 4.8: DES model for PS-DoS attack

—**Behavior Under Normal Conditions:** States $\{s_0, s_1, s_2, s_3, s_4, s_5, s_6, s_7\}$ and transitions $\{\tau_1, \tau_2, \tau_3, \tau_4, \tau_5, \tau_6, \tau_7, \tau_8, \tau_9, \tau_{10}, \tau_{11}, \tau_{12}, \tau_{13}, \tau_{14}\}$ represent the DES model of the system under **normal** conditions.

- s_0 : The model starts at state s_0 . In state s_0 , the client is about to send a sleep frame to the AP.
- $\tau_1(s_0 \rightarrow s_1)$: At state s_0 , the client sends a sleep frame to the AP and the model reaches state s_1 by traversing transition τ_1 . The initial $(\tau_1) \equiv s_0$, final $(\tau_1) \equiv s_1$, $\sigma \equiv \text{Sleep}$. Here $check(V) = \{--\}$ and $assign(V) = \{mac_{src} \leftarrow mac_{client}, mac_{dst} \leftarrow mac_{AP}\}$. $mac_{src} \leftarrow mac_{client}$ is the assignment of SRC MAC address to model variable. If model variables (V) are not used it leads to state explosion problem as explained in earlier chapters. mac_{src} and $mac_{dst} \leftarrow mac_{AP}$ is the assignment of DST MAC address

to model variable mac_{dst} . The sleep frame must be sent after the medium is free for at-least the Distributed Inter Frame Spacing (DIFS) duration. Hence the delay duration is DIFS time units. The client may send the sleep frame anytime after the DIFS duration. So, the deadline is assumed to be infinite. The “Power Save Handler” generates the “Sleep” event.

- $\tau_2(s_1 \rightarrow s_2)$: After receiving the sleep frame from the client, the AP sends an acknowledgment (ACK) to the client. This is indicated by the transition τ_2 . The ACK must be received after Short Inter Frame Spacing (SIFS) duration has elapsed. The receipt of ACK frame allows the client to enter sleep state. While a client is in sleep state, any frame(s) destined for the client are buffered at the AP. Here $check(V) = \{mac_{src} \equiv mac_{AP}, mac_{dst} \equiv mac_{client}\}$. These conditions are checked to verify that the ACK belongs the sleep frame received in the previous step and does not belong to any other client. As no assignment is done during this transition $assign(V) = \{--\}$. All ACK events have delay-deadline as $[SIFS, \infty]$ in model G shown in Fig. 4.8.
- $\tau_3(s_2 \rightarrow s_3)$ and $\tau_{10}(s_2 \rightarrow s_6)$: At state s_2 the sender sends a wake frame. Now there arises two possibilities. The client wakes up before or after the expiry of LI. If the client wakes up before the expiry of LI (denoted by event “Early Wake”), the RTDES model takes transition τ_3 . The delay-deadline for transition τ_3 is $[DIFS, LI - \delta]$. δ is subtracted from LI as the clients tend to wake up just before the expiry of LI [76]. If the client wakes up after the expiry of LI (denoted by event “Proper Wake”), the RTDES model takes transition τ_{10} . In both the transitions, $check(V) = \{mac_{src} \equiv mac_{client}, mac_{dst} \equiv mac_{AP}\}$ and $assign(V) = \{--\}$.
- $\tau_4(s_3 \rightarrow s_4)$ and $\tau_{11}(s_6 \rightarrow s_7)$: The transition τ_4, τ_{11} are the ACK frames sent by the AP to the client. Their explanation is similar to transition τ_2 above. Here $check(V) = \{mac_{src} \equiv mac_{AP}, mac_{dst} \equiv mac_{client}\}$ and $assign(V) = \{--\}$.
- $\tau_5, \tau_6(s_4 \rightleftharpoons s_4)$ and $\tau_7(s_4 \rightarrow s_1)$: At state s_4 the client fetches the buffered frame(s) at the AP. The client also responds with ACK frame for the data successfully received. At state s_4 the transition τ_5 represents the data received by the client and transition τ_6 represents the ACK sent to the AP by the client. After the communication between the client and the AP ends, the client sends a sleep frame to the AP. Transition τ_7 denotes the sending of sleep frame by the client to the AP. The delay-deadline of transition τ_7 is $[DIFS, \infty]$. For transition τ_5 , $check(V) = \{mac_{SRC} \equiv mac_{AP}, mac_{DST} \equiv mac_{client}\}$ to check whether the data frame(s) are being sent to the the same client from which the wake frame is obtained in transition τ_3 . For transitions τ_6, τ_7 $check(V) = \{mac_{SRC} \equiv mac_{client}, mac_{DST} \equiv mac_{AP}\}$ checks whether the ACK

frame received for the data frame(s) sent in transition τ_5 belong to the same client. The checks for transition τ_7 is the same as τ_6 . $assign(V) = \{--\}$ for both τ_6, τ_7 .

- $\tau_8(s_4 \rightarrow s_5)$: The transition sequence $\langle \tau_3, \tau_4, \tau_5, \tau_6, \tau_7 \rangle$ represents waking of the client before the expiry of LI (Early Wake). The IDS sends power save probe frame to determine if the early wake is initiated by the client or the attacker. The power save probe consists of a data frame having SRC MAC address of IDS and DST MAC of a dummy client in it. The delay-deadline of transition τ_8 representing the sending of power save probe is $[DIFS, \infty]$. Here $check(V) = \{--\}$ and $assign(V) = \{mac_{SRC} \leftarrow mac_{IDS}, mac_{DST} \leftarrow mac_{D_1}\}$.
- $\tau_9(s_5 \rightarrow s_0)$: The transition τ_9 represents the “power save probe response” to the power save probe sent by the IDS. The delay-deadline of transition τ_9 is $[LI_2 - \delta, LI_2]$. LI_2 is the LI of the dummy client D_1 . The delay-deadline $[LI_2 - \delta, LI_2]$ represents the time after the expiry of LI_2 . Here $check(V) = \{mac_{SRC} \equiv mac_{D_1}, mac_{DST} \equiv mac_{IDS}\}$ to check that the power save probe response received is for the power save probe sent in transition τ_8 . Here $assign(V) = \{--\}$.
- $\langle \tau_{10}, \tau_{11}, \tau_{12}, \tau_{13}, \tau_{14} \rangle (s_2 \rightarrow s_6 \rightarrow s_7 \rightarrow s_1)$: The transition sequence $\langle \tau_{10}, \tau_{11}, \tau_{12}, \tau_{13}, \tau_{14} \rangle$ represents waking of the client after the expiry of LI (Proper Wake). As the client wakes up after the expiry of its LI, no power save probe is sent. $check(V)$ and $assign(V)$ are the same as for the Early Wake scenario explained earlier.

—**Behavior Under Attack Conditions:** For attack conditions we discuss only those states and transitions that differ from normal conditions. States $\{s'_0, s'_1, s'_2, s'_3, s'_4, s'_5\}$ and transitions $\{\tau'_1, \tau'_2, \tau'_3, \tau'_4, \tau'_5, \tau'_6, \tau'_8, \tau'_{15}\}$ represent the DES model of the system under **attack** conditions.

- $\tau'_{15}(s'_5 \rightarrow s'_0)$: The transition τ'_{15} represents the “power save probe response” to the power save probe sent by the IDS during transition τ'_8 . The delay-deadline of the transition τ'_{15} representing the power save probe response is $[DIFS, LI_2 - \delta]$. The delay-deadline $[DIFS, LI_2 - \delta]$ represents the time before the expiry of LI_2 . Here $check(V) = \{mac_{SRC} \equiv mac_{D_1}, mac_{DST} \equiv mac_{AP}\}$. The check is done to ensure that the response received for the power save probe is the one which is sent during the transition τ'_8 . As no assignment is done, $assign(V) = \{--\}$.

An important thing to note here is that the transitions τ_9, τ'_9 both represent the same event, “Power Save Probe Response”. However, the delay-deadline are different for both. τ_9 has delay-deadline of $[LI_2 - \delta, LI_2]$ representing fetching of the frame(s) *after*

Table 4.3: Transition table for Fig. 4.8

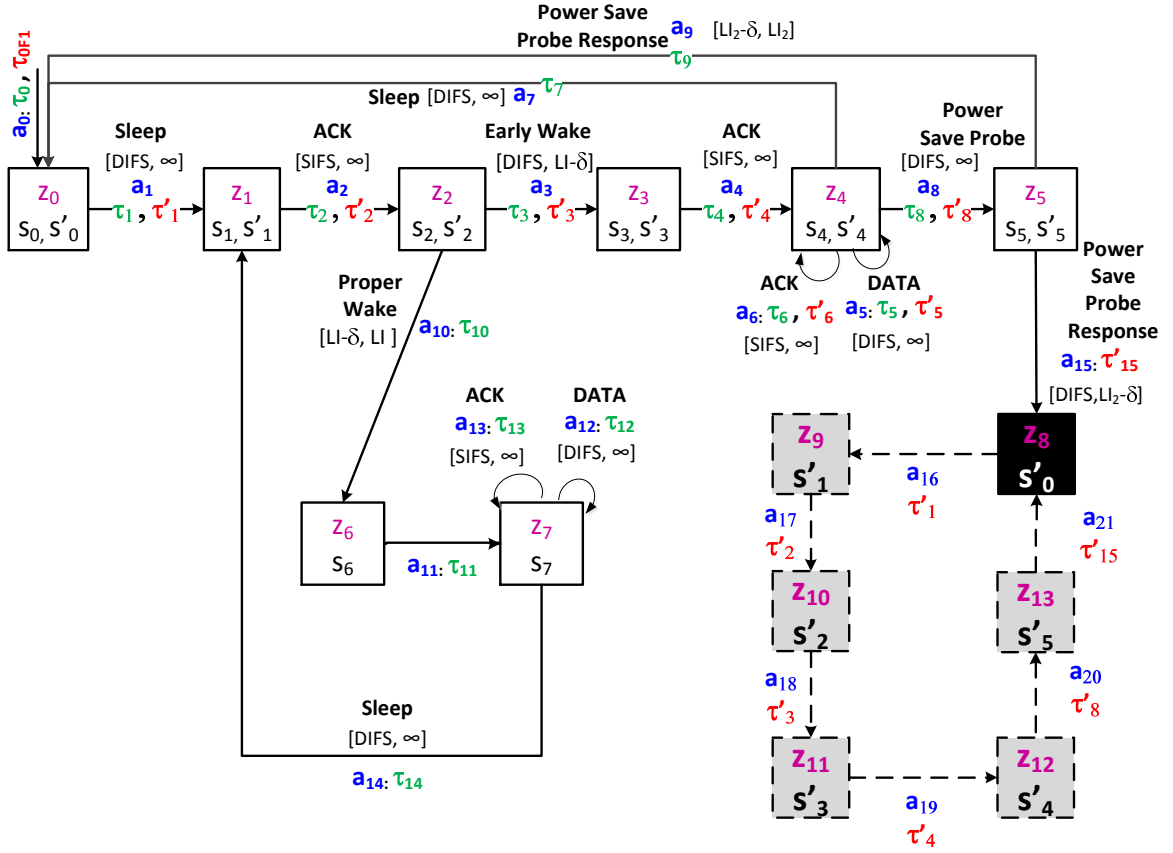
Transition (τ)	Initial State (x)	Final State (x^+)	Event (σ)	Delay (l_τ)	Deadline (u_τ)	$check(V)$	$assign(V)$
τ_1 (τ'_1)	s_0 (s'_0)	s_1 (s'_1)	Sleep	DIFS	∞	-	$mac_{SRC} \leftarrow mac_{client}$ $mac_{DST} \leftarrow mac_{AP}$
τ_2 (τ'_2)	s_1 (s'_1)	s_2 (s'_2)	ACK	SIFS	∞	$mac_{SRC} \equiv mac_{AP}$ $mac_{DST} \equiv mac_{client}$	-
τ_3 (τ'_3)	s_2 (s'_2)	s_3 (s'_3)	Early Wake	DIFS	$LI - \delta$	$mac_{SRC} \equiv mac_{client}$ $mac_{DST} \equiv mac_{AP}$	-
τ_4 (τ'_4)	s_3 (s'_3)	s_4 (s'_4)	ACK	SIFS	∞	$mac_{SRC} \equiv mac_{AP}$ $mac_{DST} \equiv mac_{client}$	-
τ_5 (τ'_5)	s_4 (s'_4)	s_4 (s'_4)	Data	DIFS	∞	$mac_{SRC} \equiv mac_{AP}$ $mac_{DST} \equiv mac_{client}$	-
τ_6 (τ'_6)	s_4 (s'_4)	s_4 (s'_4)	ACK	SIFS	∞	$mac_{SRC} \equiv mac_{client}$ $mac_{DST} \equiv mac_{AP}$	-
τ_7	s_4	s_1	Sleep	DIFS	∞	$mac_{SRC} \equiv mac_{client}$ $mac_{DST} \equiv mac_{AP}$	-
τ_8 (τ'_8)	s_4 (s'_4)	s_5 (s'_5)	Power Save Probe	DIFS	∞	-	$mac_{SRC} \leftarrow mac_{IDS}$ $mac_{DST} \leftarrow mac_{D_1}$
τ_9	s_5	s_0	Power Save Probe Response	$LI_2 - \delta$	LI_2	$mac_{SRC} \equiv mac_{D_1}$ $mac_{DST} \equiv mac_{IDS}$	-
τ_{10}	s_2	s_6	Proper Wake	$LI - \delta$	LI	$mac_{SRC} \equiv mac_{client}$ $mac_{DST} \equiv mac_{AP}$	-
τ_{11}	s_6	s_7	ACK	SIFS	∞	$mac_{SRC} \equiv mac_{AP}$ $mac_{DST} \equiv mac_{client}$	-
τ_{12}	s_7	s_7	Data	DIFS	∞	$mac_{SRC} \equiv mac_{AP}$ $mac_{DST} \equiv mac_{client}$	-
τ_{13}	s_7	s_7	ACK	SIFS	∞	$mac_{SRC} \equiv mac_{client}$ $mac_{DST} \equiv mac_{AP}$	-
τ_{14}	s_7	s_1	Sleep	DIFS	∞	$mac_{SRC} \equiv mac_{client}$ $mac_{DST} \equiv mac_{AP}$	-
τ'_{15}	s'_5	s'_0	Power Save Probe Response	DIFS	$LI_2 - \delta$	$mac_{SRC} \equiv mac_{D_1}$ $mac_{DST} \equiv mac_{AP}$	-

the expiry of the LI of the dummy client. On the other hand, τ_9' has delay-deadline of $[DIFS, LI_2 - \delta]$ representing fetching of the frames *before* the expiry of the LI of the dummy client. This timing difference is successfully captured by the RTDES framework and proves vital in detecting PS-DoS attack as explained later.

Diagnoser construction for PS-DoS attack

Fig. 4.9 is the diagnoser for the RTDES model G shown in Fig. 4.8. The diagnoser is built following the steps listed in Algorithm 3. In order for the diagnoser to detect PS-DoS attack, the diagnoser should reach the O -node z_8 which is an F_i -certain O -node (attack certain O -node). However, if the diagnoser gets stuck in an F_i -indeterminate cycle before reaching z_8 it leads to non-diagnosability. The RTDES diagnoser for PS-DoS attack shown in Fig. 4.9 does not have any F_i -indeterminate cycles. As the diagnoser does not have

any F_i -indeterminate cycles, the fault (attack) is diagnosable. Thus the RTDES framework successfully detects the PS-DoS attack in 802.11 networks.



To ascertain the presence of an attacker, the IDS sends a power save probe frame which has SRC MAC as IDS MAC address DST MAC address as the dummy client’s MAC address. “Power Save Handler” generates the event “Power Save Probe” and the diagnoser moves to O -node z_5 . Now, assume that the IDS sniffs a wake frame meant to fetch the buffered frame(s) for the dummy client at 3600 ms instead of the dummy client’s LI expiry interval of 4950 ms. “Power Save Handler” generates the event “Power Save Probe Response” for the event. Dummy client never wake up early for data fetch which means that the query to fetch the frame(s) is sent by the attacker. The early fetching is denoted by O -transition a_{15} and the diagnoser reaches O -node z_8 which is an F_i -certain O -node. Thus the diagnoser successfully determines the presence of the attacker. Once the attack is detected, the diagnoser traverses only F_i -certain O -nodes sequence $\langle z_8, z_9, z_{10}, z_{11}, \dots, z_8 \rangle$ as failures (attack) are assumed to be permanent.

Table 4.4: Parameters values for beacon interval and listen intervals

Parameter	Real Client	Dummy Client
Beacon Interval (BI)	100 ms	100 ms
Listen Interval (LI)	20	50
Delta (δ)	50 ms	50 ms
BI * LI	2000 ms	5000 ms
BI * LI - δ	1950 ms	4950 ms
Early Wake (For this example)	1600 ms	3600 ms

Now we look into an example corresponding to normal network conditions. Under normal network condition the diagnoser must not reach any F_i -certain O -node. The states and transitions till O -node z_2 are similar to those explained above for the attack scenario. We assume the case of proper wake for normal network scenarios. The IDS sniffs a wake frame from the client. The “Power Save Handler” generates the event “Proper Wake”. As the wake frame is received after the expiry of the LI of the client, the IDS does not send any power save probes. The client receives an ACK from the AP. The “Power Save Handler” generates the event “ACK”. The diagnoser traverses O -transition sequence $\langle a_{10}, a_{11} \rangle$ during this process. At O -node z_7 the client receives buffered frame(s) from the AP and sends ACK back to the AP. The “Power Save Handler” generates the events “Data” and “ACK” respectively. The O -transitions for “Data” and “ACK” events are a_{12}, a_{13} respectively. After the buffered frame(s) are retrieved, the client sends a sleep frame to the AP to inform the AP that it is entering the sleep state. The “Power Save Handler” generates the event “Sleep”. The O -transition for “Sleep” event is a_{14} . So, the O -nodes sequence traversed during normal conditions by the diagnoser is given as $\langle z_0, z_1, z_2, z_6, z_7 \rangle$, none of which are F_i -certain

O-node. So, the diagnoser reports it correctly as normal activity.

4.6 Results and Discussions

In this section we discuss the accuracy, detection rate and network load of the proposed IDS followed by proving the correctness of the RTDES diagnoser.

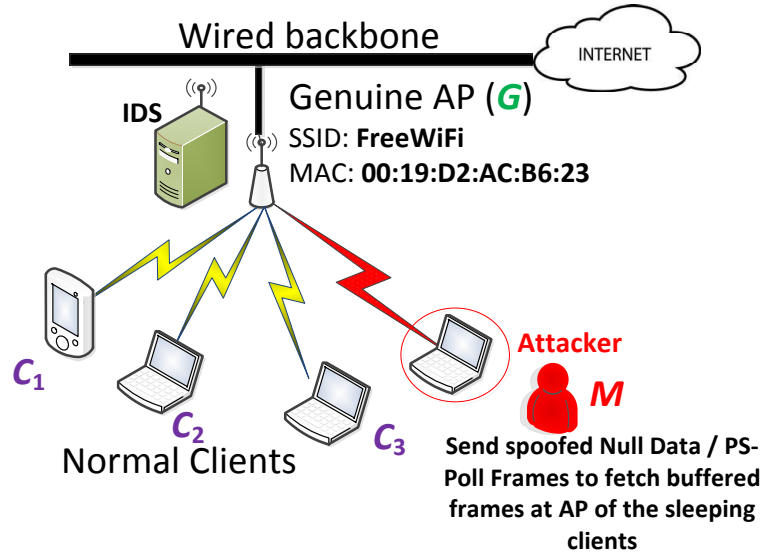


Figure 4.10: Experimental setup

4.6.1 Network Setup for PS-DoS

The network setup for the PS-DoS attack is shown in Fig. 4.10. We have an open AP with SSID “FreeWiFi”, IDS, three client machines and one attacker machine. The IDS has two network interfaces. The attacker machine (*M*) is equipped with BackTrack 5R3 [146]. The IDS is implemented in C language on Ubuntu 12.04 machine. Scapy is used for injecting power save probes in the network. The three clients (*C*₁, *C*₂ and *C*₃) have Ubuntu 12.04, Windows XP and Windows 7. The experiment is performed for a duration of 3 hours and the attack is launched randomly on different systems.

4.6.2 Detection Rate and Accuracy of the Proposed RTDES Based IDS

The metrics used for measuring the performance of IDS are detection rate and accuracy. Detection Rate is defined as the number of attacks detected by the IDS to the total number of attacks actually present. $Detection\ Rate = TP / (TP + FN)$. Accuracy is the proportion

Table 4.5: PS-DoS attack detection and accuracy statistics

% Probes Sent	Attack Instances launched	Instances detected using proposed IDS	Detection Rate %	% Probes Sent	Attack Instances launched	Instances detected using proposed IDS	Detection Rate %
100	400	396	99	50	400	320	80
90	400	388	97	40	400	288	72
80	400	368	92	30	400	264	66
70	400	356	89	20	400	248	62
60	400	336	84	10	400	236	59

of the total number of attacks that are correctly detected. $Accuracy = TP/(TP + FP)$. Here, TP is True Positive, FP is False Positive, and FN is False Negative. A TP is an instance, which is actually an attack and is classified as attack by the IDS. A $FP(FN)$ is a case when an IDS classifies a normal(attack) activity as attack(normal) activity.

Table 4.5 shows the detection rate of the proposed IDS under various probing circumstances. The number of power save probes sent is varied between 10% to 100%. An interesting observation can be made from Table 4.5 that the detection rate is 99% even when 100% power save probes are sent. Wi-Fi being a lossy medium it is quite possible that the IDS may fail to capture the spoofed null data frame sent by the attacker to the AP. As the spoofed null data frame is not captured, no probes are sent by the IDS. In such cases, even if the IDS captures all other null data frames successfully and sends probes for the captured null data frames (so 100% percent probing from IDS perspective), the detection rate remains less than 100% (99% in this case) because of the failure in capturing the (spoofed) null data frame. In general, various kinds of frame losses may lead to a reduced detection rate. On the other hand, the accuracy touches 100% in all the runs. The IDS raises an alarm only when frames for dummy clients are fetched. Once frames for dummy stations are fetched, the IDS is 100% sure about the presence of PS-DoS attacker. So, no false positives are encountered which ensures that the accuracy stays at 100%.

From Table 4.5, it can be seen that the detection rate of the IDS is 59% even in those cases when the probe is sent only 10% of the time. This is explained as follows: as the proposed IDS is a detection system and not a prevention system, it behaves aggressively once the presence of the attack is ascertained. For example, consider the network setup shown in Fig 4.10. Assume that the attacker is under the process of fetching buffered frame(s) for the client C_2 of the network. Once the IDS ascertains that frames for C_2 are being fetched by the attacker, all the subsequent early frame fetches using the MAC address of the client C_2 are marked as frame(s) captured by the attacker without sending any additional power save probes. This approach taken by the IDS seems plausible as the attacker is assumed to fetch all the buffered frame(s) for a client at the AP while the client C_2 is in sleep state.

Hence, the detection rate is higher even under the case when the probes sent are low.

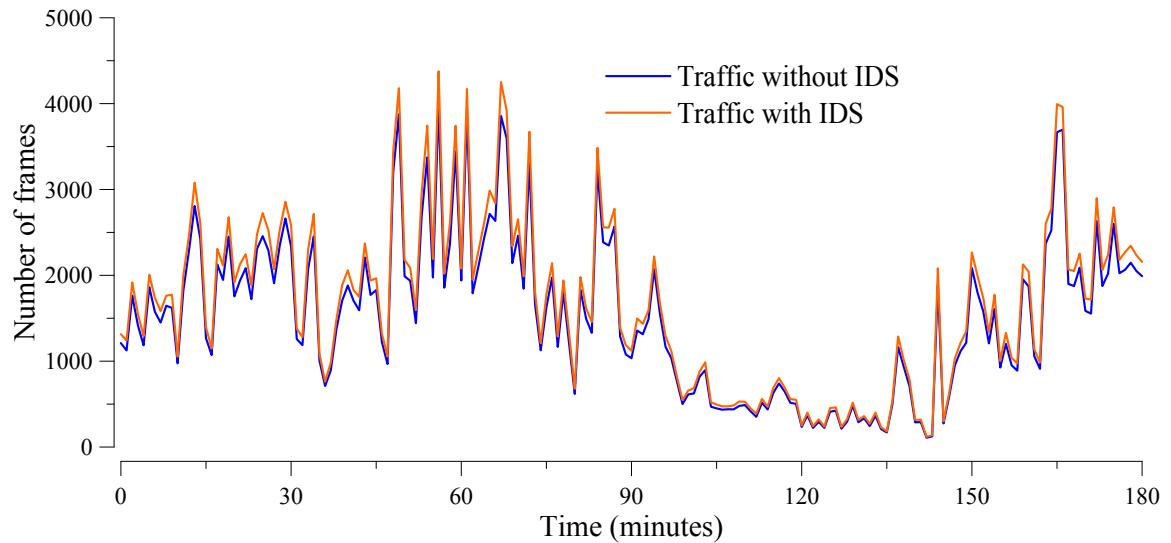


Figure 4.11: Network traffic with and without use of IDS

4.6.3 Network Load because of Power Save Probes

Power save probes and the dummy clients are required for detecting the PS-DoS attack, which lead to an increase in the network traffic. However, there is a trade-off between the sending of probes and detection rate. As seen in Table 4.5, the detection rate falls with the reduction in the probes sent. This is because as the number of probes sent are reduced, the chances of the attacker escaping detection increases. For example, consider an early wake frame sent by the attacker for which no power save probe is sent. The attacker fetches the buffered frame(s) using the spoofed wake frame but is not caught as no power save probe frame is sent. Although, sending of lesser probes conserves network bandwidth, it affects the detection rate. However, no proportional drop is observed when the percentage of probes is reduced.

Power save probes are sent only in those cases when a sleeping client has buffered frame(s) and are fetched before the expiry of the client's LI. The graph in Fig. 4.11 shows the network traffic with and without the use of IDS during a three hour test run. In the test run, the IDS varies the dummy clients from one to five depending upon the frequency of improper wakes by the clients in the three hour test run. As explained earlier, the number of dummy clients are decided by the IDS. Different runs may have different number of dummy clients depending on the characteristics of the network and the number of observed early wakes. So, it can be observed that at few points the overhead is slightly above the normal traffic. At places where the frequency of improper wakes is low, the traffic with and with-

out IDS almost overlaps. The reason for such an observation is that when the frequency of improper wakes by the clients is low, fewer power save probes are injected into the network and the number of dummy clients is also low. In the test run, an average of 1.14% to 6.23% increase in the network traffic is observed as a result of injecting power save probes in the network which is reasonable considering the detection rate and accuracy obtained.

Now, we discuss intuitively why the traffic overheard because of the power save probes and presence of the dummy clients is not high. Under normal circumstances when the clients do not wake up early, the IDS does not send any power save probes to the dummy clients. So, the proposed scheme does not add any kind of overhead under normal network conditions. Under attack conditions, a power save probe is sent only when buffered frame(s) are present at the AP and the client wakes up early. Even under those circumstances, only one power save probe frame is sent per client irrespective of the number of buffered frame(s) present at the AP for that client. So, the overhead caused by sending probes is low.

In the proposed scheme, a minimum number of dummy clients are present in the network at a given instant. Though, this feature is implementation specific, a bare minimum of one dummy client is required for the detection scheme to work correctly. By observing the frequency of improper sleep and wake cycles, the IDS can increase or decrease the number of dummy clients in the network. This dynamic behavior for the presence of the dummy clients adopted by the IDS coupled with the sending of only one power save probe for every early wake per client leads to sparse overhead of the traffic generated by the dummy clients. So, the overhead induced by the dummy clients in the network is low.

4.6.4 Correctness of the RTDES Diagnoser

The RTDES modeling helps us to formalize a given system and check for correctness and completeness [72]. In this section we show the correctness and completeness of the proposed scheme by considering all the exhaustive cases of the PS-DoS attack. For each and every case considered, we have shown that the proposed scheme successfully detects the presence of the PS-DoS attack. The proving of correctness and completeness by considering all the exhaustive cases helps to ascertain that the attacker does not escape from detection thus making the detection scheme robust. If formal modeling is not taken into consideration, the system might contain certain loopholes unobserved, which can be exploited by an attacker in order to evade detection. Formalism helps us to verify all the possible states a system may traverse during its lifetime thereby ensuring no such loopholes are left.

There are a number of ways in which the PS-DoS attack can be launched. In order to

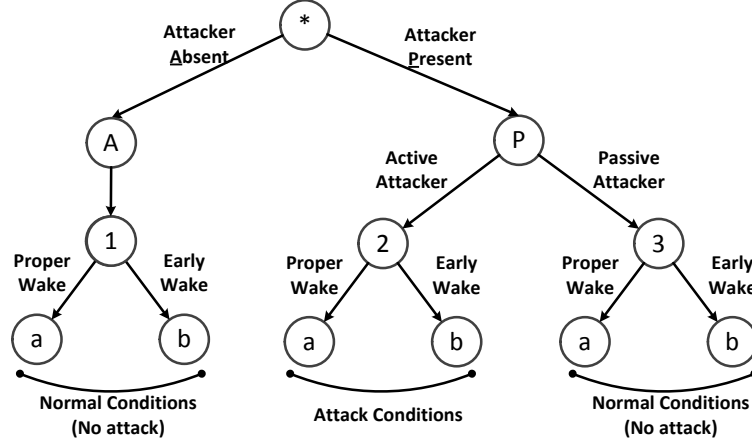


Figure 4.12: Six possible cases of arrival of null data frames

prove the correctness of the diagnoser shown in Fig. 4.9, we consider 6 possible cases of the arrival of null data frame which are depicted in the tree shown in Fig. 4.12. We denote C_1 as the victim client, M as the attacker, C_2 as the genuine client and D_1 as the dummy client.

1. *Attacker Absent (Normal Network Conditions):*

a) Proper Wake: In this case C_1 wakes after the expiry of its LI. Initially C_1 sends a sleep frame to the AP and receives an ACK from the AP. The diagnoser takes O -transition sequence $\langle a_1, a_2 \rangle$. C_1 sends a wake frame after expiry of LI and receives an ACK from the AP. The diagnoser takes O -transition sequence $\langle a_{10}, a_{11} \rangle$. At state z_7 , C_1 fetches the buffered frame(s) from the AP and sends ACK back to the AP. This is indicated by O -transition sequence $\langle a_{12}, a_{13} \rangle$. After exchanging the frame(s), C_1 sends a sleep frame to the AP and the diagnoser reaches state z_1 . None of the states traversed by the diagnoser is an F_i -certain (attack) state. Hence the diagnoser treats the scenario as normal network activity.

b) Early Wake: Here C_1 sends a wake frame before the expiry of its LI. To verify the genuineness of the wake frame power save probe is sent to D_1 . The initial sleep and ACK frames are represented by the O -transition sequence $\langle a_1, a_2 \rangle$. The early wake is denoted by the O -transition a_3 . The O -transition a_4 is the ACK sent by the AP in response to early wake. At state z_4 C_1 fetches the buffered frame(s) from the AP and sends back the ACK to the AP. The O -transition sequence $\langle a_5, a_6 \rangle$ denotes the fetching and ACK events. The sending of power save probe frame is denoted by O -transition a_8 . The power save probe response is obtained *after* the expiry of the LI of D_1 . M is assumed to fetch every buffered frame(s) available instantly. As M did not fetch the frame(s) available for D_1 the early wake frame sent by C_1 must be genuine. The

diagnoser takes the O -transition a_9 . This completes the detection cycle of IDS and it returns to start state and monitors again for the PS-DoS attack. Even though an early wake frame is received, no states traversed by the diagnoser is an F_i -certain (attack) state, which exemplifies that the network is under normal conditions.

2. *Attacker Present (Active Attacker):*

M needs to send a wake frame before the expiry of LI of C_1 in order to successfully launch the PS-DoS attack. The diagnoser must reach an F_i -certain O -node to ascertain that the attacker is caught.

a) Proper Wake: In this case, M sends a spoofed wake frame after the expiry of the LI of C_1 . C_1 also wakes up after expiry of its LI to check for buffered frame(s) at the AP. Both C_1 and M are awake simultaneously and both receive the buffered frame(s) from the AP. The diagnoser follows the O -transition sequence $\langle a_1, a_2, a_{10}, a_{11}, a_{12}, a_{13} \rangle$. As none of the O -nodes are F_i -certain (attack) the diagnoser treats this as normal activity. As both C_1 and M are awake simultaneously M does not cause any frame losses to C_1 defeating the purpose of the PS-DoS attack. Technically, the PS-DoS attack is launched by M but has not caused any frame losses to C_1 . Due to this, the diagnoser treats this as normal activity as it causes no frame losses.

b) Early Wake: The O -nodes and O -transitions till z_5 are as explained in **Early Wake** scenario of Case 1. M is assumed to fetch every buffered frame(s) and does not possess the knowledge of the MAC address of D_1 . Due to this M fetches the buffered frame(s) targeted at D_1 before the expiry of LI of D_1 . This is indicated by the O -transition a_{15} which takes the diagnoser to state z_8 which is an F_i -certain (attack) state. As F_i -certain (attack) state is reached the diagnoser detects the PS-DoS attack in the network. As failures are assumed to be permanent, the diagnoser moves into an attack certain cycle $\langle z_8, z_9, z_{10}, z_{11}, z_{12}, z_{13}, z_8 \rangle$.

3. *Attacker Present but Passive (Passive Attacker):*

In this case M only eavesdrops on the network. It does not send a wake frame in spite of buffered frame(s) being available at the AP. As attacker does not send spoofed wake frames at all, no PS-DoS attack is possible.

a) Proper Wake: Same as Proper Wake of Case 1.

b) Early Wake: Same as Early Wake of Case 1.

The network remains under normal circumstances in spite of the presence of M . The diagnoser correctly labels this condition as normal activity of the network.

4.6.5 Discussion

Table 4.6 compares the various existing mitigation techniques for the PS-DoS attack. We have categorized the PS-DoS attack based on the frame type used for launching it, viz., PS-Poll or Null data frame. The other features that we compare are the requirements of authentication, encryption, specialized hardware and resource overhead. The remarks column of Table 4.6 describes the pros and cons of the techniques discussed.

Table 4.6: Comparison of existing mitigation solutions for PS-DoS attack

Method	Detects PS-DoS attack using PS-Poll	Detects PS-DoS attack using Null Data	Requires encryption	Requires Non Null Data/ PS-Poll Frame	Requires Specialized hardware	Overhead	Remarks
Encryption [73, 74]	Y	Y	Y	N	N	High	Difficult to deploy. Requires upgradation on client and AP.
Non-null data frame [75]	Y	Y	N	Y	Y	High	Requires upgradation on client and AP.
BSSI based Methods [77, 78, 79]	Y	Y	N	N	Y	High	Increase in cost due to specialized hardware
Proposed Scheme	Y	Y	N	N	N	Low	Easy to deploy. Encryption Free. Low resource overhead. Formally verifiable. No protocol modification required.

The proposed method depends highly on the ability of the IDS to capture the power save frames correctly. If the IDS misses critical frames like power save probe probe response or misses the initial null data frame or PS-Poll frame sent by the attacker, the detection rate falls. The environment considered is an open Wi-Fi network, but the methods can be extended to encrypted Wi-Fi networks also.

4.7 Conclusion

In this chapter, RTDES framework has been adapted and used for detecting the PS-DoS attack in 802.11 Wi-Fi networks. In the PS-DoS attack an attacker fetches the buffered frame(s) of the genuine clients while they are in sleep state by injecting spoofed null data or a PS-Poll frame causing frame losses. Existing schemes for the PS-DoS attack detection or prevention suffer from expensive setup, maintenance, scalability, deployment issues and lack of formal frameworks for design of the attack detector etc. The proposed RTDES based IDS helps to detect the PS-DoS attack with high detection rate and accuracy and overcomes the shortcomings of existing approaches. It is also shown that the delay-deadline DES framework needs to be augmented with model variables to make it capable of modeling and detecting the PS-DoS attack. The proposed IDS makes use of active probing in order to create differences between normal and attack scenario. Though injecting power save probes increases network traffic, but with slight increase in overall traffic presence of the PS-DoS attack is determined accurately. Another major advantage of RTDES based IDS is that it does not require protocol modifications, use of any encryption algorithms or firmware

upgrades either on the AP or on the client side. Besides this, the proposed methodology can be applied on legacy as well as modern day systems.

The attacks discussed till now have been detected successfully using different DES frameworks namely: untimed DES, I²-DES and RTDES. However, in all these DES frameworks we have assumed that the IDS reliably receives the frame(s) from the genuine client, the attacker and during probing. However, Wi-Fi being a lossy medium, frame losses are common. So, it is possible that few frames might not be captured or missed by the IDS because of capturing errors. Such frame losses lead to inconsistent measurement which may hamper the attack detection rate in case critical frames are lost. The traditional DES frameworks treat such inconsistent measurements as permanently unmeasurable and never uses them for fault diagnosis (attack detection) which may lead to weak diagnosis. In the next chapter, we develop an IDS for rogue DHCP server attack using the proposed Measurement Inconsistent Discrete Event System (MIDES) framework which is capable of handling inconsistent measurements in an efficient manner as compared to traditional DES frameworks.



“Uncertainty is the only certainty there is, and knowing how to live with insecurity is the only security.”

John Allen Paulos
American professor

5

Intrusion Detection System for Rogue DHCP Server Attack in Wi-Fi Networks using Measurement Inconsistency Discrete Event System

5.1 Introduction

As seen in Chapter 2, in order to authenticate and associate itself with the AP a client needs to perform a four-way handshake with the AP. After the client is successfully authenticated and associated with the AP it requests for its IP configuration. The IP configuration can be done statically or dynamically. Static IP configuration is tedious in dynamic environments as the network administrator has to go to every client’s terminal and set its IP configuration manually. Wi-Fi networks are usually deployed in dynamic environments like airports, malls, libraries etc., which makes static IP configuration cumbersome. To solve this problem and to automate the task of IP configuration, Dynamic Host Configuration Protocol (DHCP) is used. The DHCP server contains a pool of IP address that can be allocated when a client requests for an IP address. The primary function of a DHCP server is to allocate IP address and other vital information like subnet mask, default gateway, DNS address to the clients requesting it.

A client needs to perform a four-way handshake with the DHCP server in order to obtain its IP configuration. In Wi-Fi networks, the initial four-way handshake is usually followed by the four way DHCP handshake. It is also possible for an administrator to have multiple DHCP server(s). Multiple DHCP server(s) are usually deployed for providing fault toler-

ance, in case one of the DHCP server fails. When multiple DHCP server(s) are present, the client may obtain multiple DHCP offers i.e., multiple IP configurations. The client is free to choose any one of these multiple offers. The four way DHCP handshake that occurs between the client and the DHCP server is vulnerable to various security attacks as the frame exchange during the four-way handshake occurs in plain text. An attacker can set up a rogue DHCP server (software based DHCP server) [147] by spoofing the IP and MAC address of the genuine DHCP server and sending fictitious IP address, DNS and gateway address (or a combination of these) to the client requesting DHCP services. By supplying wrong default gateway and DNS server address an attacker can re-direct client's traffic via its terminal thereby sniffing client's information, re-directing clients to phishing websites, install malware into the client's machine etc. Thus, a rogue DHCP server is a serious threat to a Wi-Fi network.

Current methods to prevent the rogue DHCP server include use of network wide scanning and monitoring [81], protocol modifications [148], use of white-list of genuine DHCP servers [82], digital certificates [86, 87, 88] and various authentication methods [83, 84], use of specialized servers [90, 89]. The use of digital certificate offer robust protection but adds to certificate management issues and increases communication overhead. Use of asymmetric key requires higher computation and may lead to faster battery draining of handheld Wi-Fi devices. The sequence of frame exchange in the four-way handshake remains the same nor the traffic statistics shows significant deviations under normal and rogue DHCP server conditions. As a result, generation of signature or statistics from this four way frame exchange is difficult and may result in high amounts of false positives. So we see that existing methods to detect rogue DHCP server escalate deployment and maintenance costs.

In this chapter we propose the Measurement Inconsistent Discrete Event System (MIDES) based DES framework to design an IDS to combat against rogue DHCP server attacks. Similar to the DES framework discussed till now (simple (untimed) DES, I^2 -DES and RTDES) MIDES based DES framework for IDS, requires modeling of the network under normal and rogue DHCP server attack(s) conditions. Following that, an estimator diagnoser is built that determines the network conditions based on the sequence of DHCP frame exchange and detects the rogue DHCP server attack if the sequence violates the normal behavior.

Rogue DHCP server attack is similar to evil twin based attack. So the DES framework [124] used for evil twin based attacks (in Chapter 2) should have been applicable for rogue DHCP server attack also. However, it may be noted that in all the DES frameworks (simple (untimed) DES, I^2 -DES and RTDES) discussed in the last three chapters, we have assumed that the IDS reliably receives the frame(s) from the genuine client, the attacker and during

probing. However, frame losses are common in Wi-Fi networks. So, it not uncommon that few frames might be lost or missed because of capturing related issues. Such lost or missed frames lead to inconsistent measurement which may hamper the attack detection rate in case critical frames are lost. For example, if the probe response is not captured by the IDS, it may conclude the network to be under normal circumstances even when it may be under attack circumstances.

As in the previous three chapters, in this chapter also we show that the DES framework basically developed for industrial processes for fault diagnosis can also be used for detection of network attacks. One of the major infrastructure involved in any fault diagnosis scheme is the sensors that measure the system parameters continuously [149]. The success of any fault diagnosis scheme depends on the ability of the sensors to reliably report about the state of the system they are monitoring. Most of the fault diagnosis schemes implicitly assume that the sensors always report reliable readings [150]. However, there are instances when the sensors provide inconsistent measurements because of intermittent faults, degradation and aging, error on communication paths etc. [150], which may hamper fault diagnosis.

Many fault diagnosis schemes like Analytical Redundancy (ARR), Principal Component Analysis (PCA) etc., can handle inconsistent measurements by the sensors. ARR based methods consist of two steps. 1) Residuals are generated by comparing the measured signals from the system with estimated values. 2) Perform fault diagnosis based on the difference of the measured and estimated values. The residual signal and estimation filters are designed such that they are sensitive to faults, while at the same time robust to known or unknown disturbances in order to avoid false alarms. Depending on the nature of inconsistent measurements, specially designed estimation filters (e.g., Kalman filter, Unscented Kalman filters [151] etc.) have been suggested in the literature. In PCA model, the measurement space is partitioned as principal component subspace and a residual component subspace. The principal (residual) component subspace represents the normal (fault) condition. The final diagnosis is performed using statistical hypothesis testing of the two subspaces. In order to cater the inconsistent measurements, various methods like Iterative Principal Components Analysis (IPCA) Imputation Algorithm, IPCA Data Reconciliation [152, 153] etc., are employed that improve fault diagnosis. Though these schemes have mechanisms to handle measurement inconsistency, however, these schemes are computationally expensive and require extensive training depending on the system under consideration.

DES model based methods are used in fault diagnosis for a wide range of applications because of simplicity of both the model and the associated algorithms [124, 128]. A measurement inconsistent transition is sometimes measurable and sometimes unmeasurable. However, the DES philosophy suggested in [124, 128] which is based on Measurement

Limitation, handles measurement inconsistency rather strictly. The framework called Measurement Limitation DES (MLDES) treats such inconsistent measurements as permanently unmeasurable and never uses them for fault diagnosis even if they may be measurable in future and could aid in fault diagnosis. These inconsistent transitions are inherently measurable, so considering them as permanently unmeasurable may lead to weak diagnosis. For example, if the IDS is unable to capture the probe response during a particular instance, it does not imply that all future probe responses are unmeasurable.

This motivated us to come up with a new DES framework that can handle measurement inconsistent transitions in a much more efficient manner. So we propose a Measurement Inconsistent Discrete Event System (MIDES) framework which does not assume measurement inconsistent transitions as permanently unmeasurable. If a transition is measured it is used for fault (attack) diagnosis and if the same transition leads to measurement inconsistency the possible system state is predicted using an estimator diagnoser. So, if the DES framework used for evil twin detection is used for rogue DHCP server attack detection it may hamper the detection rate because of measurement inconsistency arising out of frame losses or capturing errors. Hence, we propose a MIDES based IDS for the detection of rogue DHCP server attack in Wi-Fi networks. The summary of our contributions are:

1. Unlike the traditional DES based fault diagnosis, which assumes measurement inconsistencies as permanently unmeasurable, our proposed Measurement Inconsistent Discrete Event System (MIDES) framework handles measurement inconsistent transitions in a flexible manner. If the measurement inconsistent transitions are observable, the proposed MIDES framework uses them for fault diagnosis, else if they are unobservable it tries to perform fault diagnosis by predicting the possible state(s) the system could be in using the subsequent measured transitions. In order to show the effectiveness of the proposed MIDES framework in handling inconsistency, a benchmark process of two-tank system is considered. Here, the traditional DES based fault diagnosis proposed in Sampath et al. [124] and Zad et al. [128] fails to diagnose the fault because of measurement inconsistency, while the proposed framework successfully diagnoses it.
2. We have also developed a MIDES based Intrusion Detection System (IDS) that detects the rogue DHCP server attack in Wi-Fi networks. Wi-Fi networks usually involve a lot of measurement inconsistencies because of frame losses. The traditional Measurement Limitation DES (MLDES) based IDS assumes that all the network frames are always measurable and marks missed frames as permanently unmeasurable, thereby having lower detection rate and accuracy as compared to the proposed MIDES based IDS.

The rest of the chapter is organized as follows. In Section 5.2, we discuss the security

vulnerabilities associated with Wi-Fi networks, rogue DHCP server attack and the current approaches to tackle the rogue DHCP server attack. In Section 5.3, we describe the proposed scheme to detect the rogue DHCP server attack. In Section 5.4, we introduce the concept of Failure Detection and Diagnosis (FDD) using Measurement Inconsistent Discrete Event System (MIDES). Section 5.5 describes the MIDES based IDS to detect the rogue DHCP server. The correctness of the IDS along with its detection rate and accuracy are described in Section 5.6. Section 5.7 concludes the work.

5.2 Background and Motivation

5.2.1 Basic Operation of DHCP

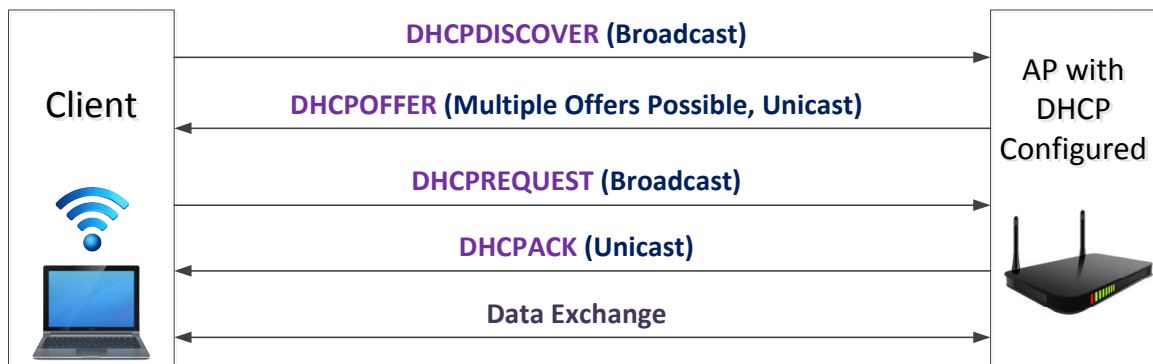


Figure 5.1: Four way DHCP handshake

The DHCP server contains a pool of IP address that can be allocated when a client requests for an IP address. The basic DHCP operation is shown in Fig. 5.1 and is explained as follows:

1. A client broadcasts a DHCPDISCOVER message to the DHCP server. All the DHCP server(s) present in the network receive the DHCPDISCOVER message. The client chooses a random number known as Transaction ID which is used by the client and DHCP server to associate DHCP messages and their responses between the client and the server. The Transaction ID is unique for every DHCP handshake.
2. Each DHCP server that receives the DHCPDISCOVER replies with a DHCPOFFER message consisting of an IP address from its pool. This is a unicast message.
3. Upon receiving multiple DHCP offer(s) from the DHCP server(s), the client chooses one of the offer(s) based on the parameters in the DHCPOFFER message and replies with a broadcast DHCPREQUEST message. The broadcast DHCPREQUEST message which contains the DHCP server identifier ensures two things: it informs the selected DHCP

server about the acceptance of its DHCP offer while at the same time informing other DHCP server(s) about the rejection of their offers.

- The selected DHCP server replies with a unicast DHCPACK message to the client. The DHCPACK message binds the IP address allocated by the DHCP server to the MAC address of the client. The DHCP server also includes a lease period with the DHCPACK message. The client needs to renew the lease before the lease period expires.

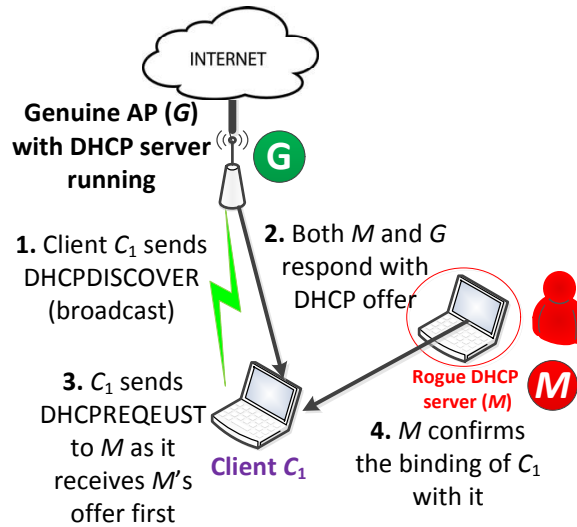


Figure 5.2: Rogue DHCP setup

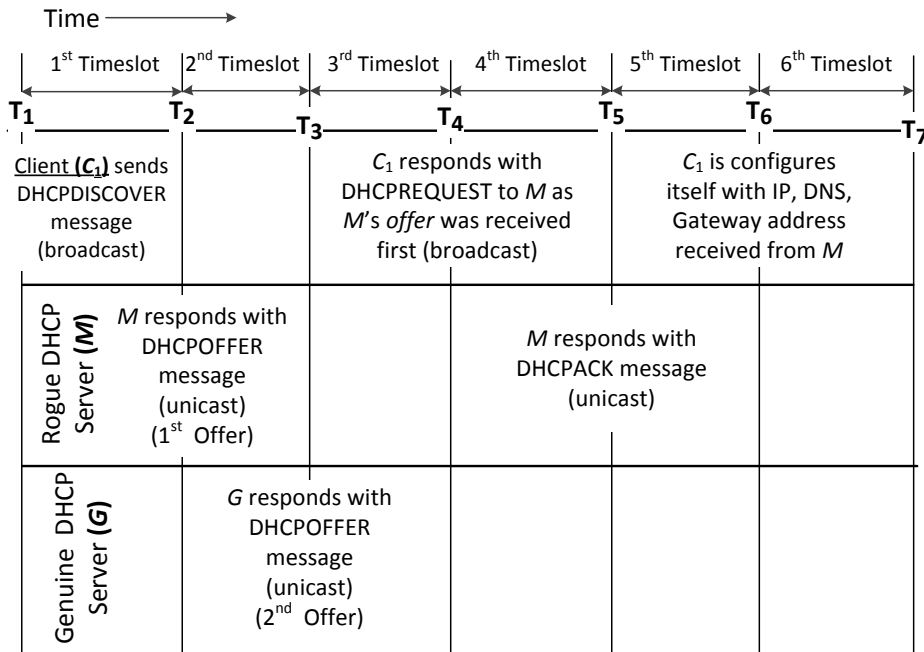


Figure 5.3: Timeline of the rogue DHCP server attack

5.2.2 Vulnerabilities in DHCP Message Exchange

The DHCP is inherently insecure, as an attacker can easily spoof the DHCP messages exchanged between the client and the DHCP server. The rogue DHCP server is explained using Fig. 5.2 and Fig. 5.3. Client C_1 and attacker M who sets up the rogue DHCP server are associated with the genuine AP G which is configured as the DHCP server. The timeline shown in Fig. 5.3 explains the operation of the rogue DHCP server attack.

- [1st Timeslot] : C_1 broadcasts DHCPDISCOVER message requesting for an IP address.
- [2nd Timeslot] : (1st offer.) As the DHCPDISCOVER message is a broadcast message both M and G receive the DHCPDISCOVER message. In this scenario, we assume that M responds first to the DHCPDISCOVER message. M spoofs the IP and MAC address of G and sends a *unicast* DHCPOFFER message to C_1 .
- [3rd Timeslot] : (2nd offer.) Here G responds with a DHCPOFFER message to the client. If the first DHCPOFFER contains all the necessary information requested by the client C_1 , it accepts those parameters and ignores all the subsequent DHCP offer(s) sent to it. So, if the DHCP offer from the rogue DHCP server M reaches the client C_1 first, . Subsequently, accepts the offer from the rogue DHCP server M and ignores the offer from G .
- [4th Timeslot] : As C_1 receives the DHCPOFFER from M first, it sends a *broadcast* DHCPREQUEST to M requesting for the assigned IP along with other parameters like DNS, gateway address.
- [5th Timeslot] : M sends back a *unicast* DHCPACK message confirming the mapping of C_1 along with a lease time. M also sends the DNS, gateway address in the DHCPACK message.
- [6th Timeslot] : C_1 configures itself with the IP, DNS, gateway address offered by M .

As seen above, the rogue DHCP server M is successful in assigning the IP, DNS, gateway address to C_1 . M may give its own IP address as gateway address so that C_1 's traffic is routed via M in order to sniff C_1 's data. Worse, M can assign a fake DNS server and direct the client C_1 to a genuine looking phishing website to steal C_1 's credentials. As can be observed, the rogue DHCP server can be easily launched using minimal resources and can cause serious damage to a client. In the following sub-section, we look in to the various approaches to detect and prevent the rogue DHCP server.

5.2.3 Existing Approaches to Detect or Prevent Rogue DHCP Server Attack

1. **DHCP Snooping, network wide scanning and monitoring:** With the DHCP snooping feature [81], an administrator can configure individual switch ports to be trusted or not trusted. Only trusted ports are allowed to serve DHCP OFFER and DHCP ACK frames. If a non trusted port is generating DHCP OFFER or DHCP ACK frame, it is blocked at the switch level itself. This feature works well for wired networks however, for Wi-Fi networks the AP itself has the DHCP component inside it. In Wi-Fi networks the clients are connected over the air to the AP and are not connected via switches. Hence, DHCP snooping technique may not work in the case of Wi-Fi networks. Some security experts postulate for *network wide scanning* for studying the IP-MAC mappings of all the clients in the network. As the IP address of the genuine DHCP server(s) is known beforehand, those IP addresses providing DHCP service but not in the white-list of genuine DHCP server(s) list can be marked as rogue [82]. However network wide scanning leads to generation of too much traffic and white-list based methods can be defeated by spoofing the IP and MAC address of the genuine DHCP server.
2. **Authenticating DHCP messages and use of digital certificates:** As DHCP lacks authentication, the RFC 3118 [83] provided the authentication option with an aim to resolve the security related issues associated with DHCP. The authors in [84] suggest the use of RSA signatures for authentication purposes. Although RSA provides a significant level of security, it is computationally expensive which may further lead to faster draining of the batteries of hand-held Wi-Fi devices. The major issue in the adoption of the authentication option in Wi-Fi network is the handling and management of key management for the large number of clients [85, 154]. Xu et al. [86], Glazer et al. [87], Demerjian et al. [88] proposed various methods that make use of digital certificates for both entity authentication as well as message authentication and is based on RFC 3118. Younes et al. [148] introduces a modified scheme called Secure DHCP (S-DHCP) to secure DHCP protocol. For authentication it uses two methods: a) Using Diffie-Hellman key exchange algorithm and a strong cryptographic one-way hash function b) Use of digital signature to authenticate the DHCP messages exchanged between the clients and server. The usage of digital certificate provides sufficient authentication and protects against the rogue DHCP server attacks. However, the usage of digital signature brings in issues like certificate management, revocation, overhead between client and DHCP server, trust issues etc.
3. **Using specialized servers for DHCP frame authentication:** Graaf et al. [89] in their patent describe a method that makes use of special Authentication, Authoriza-

tion and Accounting (AAA) server that achieves authentication using shared secret between client and AAA server. Similar to this method, the authors in [90] make use of Kerberos V for mutual authentication of the DHCP server and the client, and for the DHCP message authentication. The main disadvantage of this methodology is the additional communication overhead between the Kerberos, AAA server and the DHCP server.

4. **Signature and Anomaly-based IDS:** Signature-based IDS makes use of predefined signature patterns while anomaly-based IDS makes use of statistical methods to detect attacks [92]. The sequence of frame exchange in the four-way handshake remains the same under normal and rogue DHCP server conditions. So, just by observing the frame exchange the presence of rogue DHCP server cannot be detected. A rogue DHCP server does not bring about a significant change in the network traffic also. As a result, generation of signature or statistics from this four way frame exchange is difficult and may result in high amounts of false positives [92].

In brief, the drawbacks of the existing schemes to detect or prevent the rogue DHCP server attack are: 1) Require Digital Certificates. 2) Use of specialized servers like Kerberos. 3) Requires extensive key management strategies. From the above summary it is clear that a strategy to detect the rogue DHCP server attack should have the following features:

- Should not require use of digital certificate or extensive key management.
- Should not require additional client communication.
- Hardware costs should not be high.
- It must be easily deployable to existing and new networks
- Should not require patching of underlying operating system or installation of new software.

5.3 Proposed Scheme for the Detection of Rogue DHCP Server Attack

In this section we look into the principle to detect the rogue DHCP server attack, the architecture of the proposed IDS followed by attacker and IDS assumptions.

5.3.1 Working Principle of the IDS for Detecting Rogue DHCP Server Attack

Principle: If a client receives multiple offers from the DHCP server(s), IDS marks that activity as suspicious. Such activity cannot be marked as rogue DHCP server as multiple genuine DHCP servers can be present in the network which reply to the DHCPDISCOVER message. We have the dummy clients as a part of the detection methodology. The dummy clients are software controlled and their communication is handled by the IDS. The dummy clients have fixed IP-MAC mapping pre-configured at the genuine DHCP server. Only the IDS possesses the dummy client's IP-MAC mapping. Upon observing more than one DHCPOFFER frame(s) for any client(s) associated with the monitored AP, the IDS sends a DHCP probe on behalf of the dummy client. The DHCP probe is a DHCPDISCOVER frame with source MAC address of the dummy client. If the IP address offered to the dummy client in the DHCPOFFER message is different than the one pre-configured on the DHCP server, the presence of the rogue DHCP server is confirmed.

Reason: DHCP server provides an option to bind MAC address to fixed IP address. If DHCPDISCOVER is received from such clients whose IP-MAC mapping is pre-configured at the DHCP server, the server offers the pre-configured IP address to the client and not a randomly available IP address from the pool. The dummy clients have their IP-MAC mapping already pre-configured. If an IP-MAC mapping is pre-configured at the DHCP server, the DHCP server provides that IP address to the respective client only. Even if the client having a pre-configured IP-MAC mapping is not present in the network and the address pool of the DHCP server is exhausted, the DHCP server does *not* allocate the pre-configured IP address to any other client requesting for an IP address. Hence, if the DHCPOFFER message destined to dummy clients contain an IP address different than the one that is pre-configured for it at the genuine DHCP server, the presence of rogue DHCP server is confirmed.

Using the above principle we show an example of the rogue DHCP server detection by taking help of the timeline shown in Fig. 5.4. D_1 is the dummy client whose IP-MAC mapping is already pre-configured at G . The timeline has 8 distinct time slots.

- [7th Timeslot] : IDS observes two DHCP offer frames. In order to verify that the offers sent are genuine, the IDS sends a broadcast DHCP PROBE.
- [8th Timeslot] : G and M offer an IP address to the dummy client D_1 in response to the DHCP probe sent in previous step. The IP address for the dummy client D_1 is already pre-configured at G . So G offers the same pre-configured IP address to D_1 . However, M offers a different IP address to D_1 as it is unaware of the address pre-configured at G for D_1 . This discrepancy in the offered address to D_1 confirms the presence of the rogue

5.3. Proposed Scheme for the Detection of Rogue DHCP Server Attack

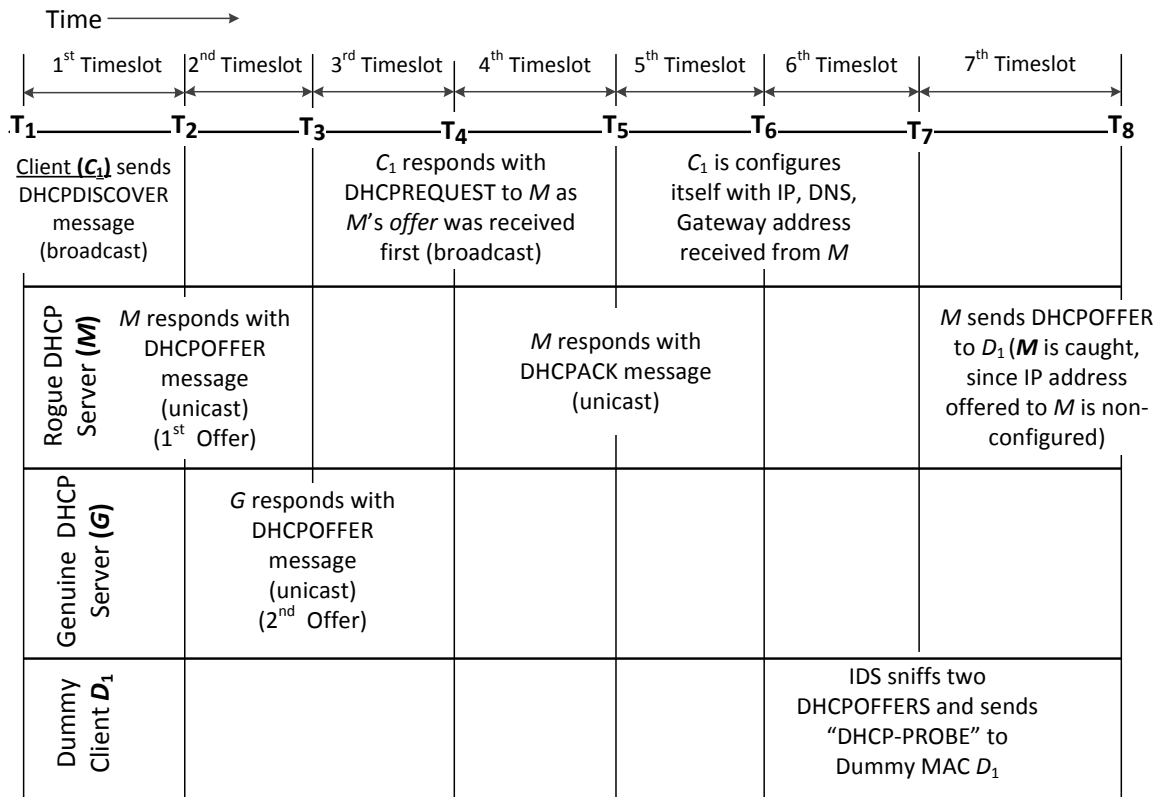


Figure 5.4: Timeline of the rogue DHCP server attack detection methodology.

DHCP server M .

The feature of the IDS wherein it actively injects DHCP probe into the network in order to detect the presence of rogue DHCP server is called as active probing mechanism.

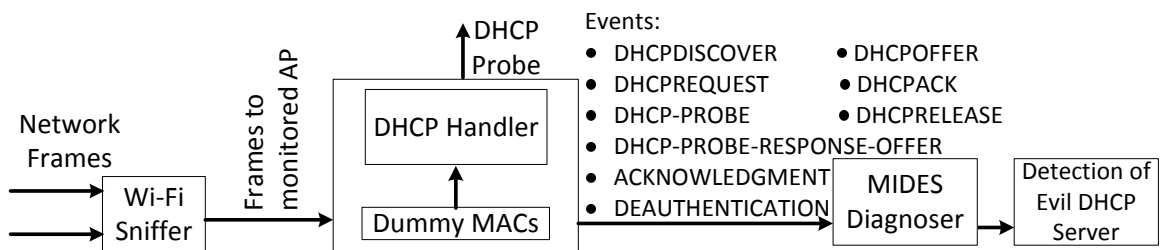


Figure 5.5: Components of the proposed IDS for detection of rogue DHCP server attack

5.3.2 IDS Components

The block diagram for the IDS used for detection of the rogue DHCP server is shown in Fig. 5.5. The different components are described as follows:

- **Wi-Fi Sniffer:** A Wi-Fi sniffer is capable of capturing all the Wi-Fi frame(s) traveling in

the network. However, in our proposed scheme, only the frames destined to and from the monitored APs are captured. Frame(s) to other APs are ignored. The Wi-Fi sniffer forwards the captured frame(s) to 'DHCP Handler'.

- **DHCP Handler:** The DHCP Handler is responsible for extracting vital information like IP and MAC addresses of the source (SRC) client from the frame headers. The DHCP Handler component is responsible for the generation of events like DHCPDISCOVER, DHCPOFFER, DHCPREQUEST, DHCPACK, DHCPRELEASE, DHCP-PROBE, DHCP-PROBE-RESPONSE-OFFER, ACKNOWLEDGMENT, DEAUTHENTICATION. The DHCP Handler also makes use of the value of the attributes like source MAC address (MACS), source IP address (IPS), destination MAC address (MACD), destination IP address (IPD), Transaction Identifier (TID) contained in these network frames (events). The DHCP handler forwards these event(s) and attribute(s) to the MIDES diagnoser which determines if the rogue DHCP server is present or not.
- **Dummy clients:** The IDS maintains a list of dummy clients whose IP-MAC mappings are pre-configured at the genuine DHCP server and its behavior is handled by the IDS. In order to check the authenticity of the multiple DHCPOFFER(s) received, the IDS sends a DHCP probe on behalf of the dummy client. The DHCP probe is a DHCPDISCOVER message with source MAC address of the dummy client. If the IP address offered to the dummy client matches with the IP address pre-configured for it, the network is under normal conditions else the IDS raises an alarm signaling the presence of a rogue DHCP server for the reasons explained earlier.
- **MIDES Diagnoser:** The MIDES diagnoser is implemented as a software module and used for attack detection purposes. The MIDES diagnoser is constructed from the DES model under normal and attack conditions and is the principle component of the detection methodology. The construction and uses of the MIDES diagnoser are described in Subsection 5.4.6.

5.3.3 Attacker and IDS Assumptions

- **Attacker sends DHCPOFFER for every DHCPDISCOVER message:** This is done by the attacker to inject forged IP, gateway, and DNS address to the clients.
- **Attacker spoofs the IP and MAC address of the genuine DHCP server:** By doing this the attacker makes the rogue DHCP server more stealthier in nature.

- **IDS has sniffing and injection capabilities:** The IDS needs to sniff the frames traveling to and from the monitored AP while it needs injection capabilities to send DHCP probe frames.
- **Dummy clients can never get an IP address other than the one pre-configured for them at the DHCP server:** as their IP-MAC mapping is pre-configured at the DHCP server.
- **IDS regularly updates the dummy client's MAC address list:** This is done to prevent possible learning of the IP-MAC mappings of the dummy clients by the attacker.

So, from the above discussion it is clear that capturing of various frames (events) is necessary for the detection of rogue DHCP server. However, as Wi-Fi is a lossy medium it is possible that some frames may get lost or the IDS fails to capture few of the frames at a particular instance. Such frames cannot be modeled as permanently unmeasurable as they may be measurable in future. This leads to measurement inconsistency. We now look how the MIDES framework that is capable of incorporating the measurement inconsistency and can help to detect the presence of rogue DHCP server in the network even if certain frames are lost.

5.4 Fault Detection and Diagnosis Theory of Measurement Inconsistent Discrete Event System (MIDES): Two Tank System

In this section we present the proposed the MIDES framework augmented with *model variables*. The *MIDES model* G is defined as:

$$G = \langle X, X_0, \Sigma, \mathfrak{S}, V \rangle \quad (5.1)$$

- X is the finite set of states.
- X_0 is the initial state.
- Σ is the set of events. Note that an event can be measurable or unmeasurable.
- \mathfrak{S} is the set of transitions.
- V is the set of model variables. Each element v_i of V can take values from a domain Dom_i .

A transition $\tau \in \mathfrak{S}$ is defined as a five-valued tuple $\langle x, x^+, \sigma, check(v), assign(v) \rangle$, where

- x is the initial state of the transition denoted as $initial(\tau)$.
- x^+ is the final state of the transition denoted as $final(\tau)$.
- $\sigma \in \{\Sigma \cup \epsilon\}$ is an event on which the transition τ is enabled.
- $check(V)$ represents the conditions on a subset of the model variables. For firing τ , along with the enabling event σ , $check(V)$ should hold true.
- $assign(V)$ represents a subset of the model variables and assignment of the values from their corresponding domain, when τ fires.

A *trace* of the model G is a sequence of transitions generated by G denoted as $s = \langle \tau_1, \tau_2, \dots, \tau_f \rangle$, where $initial(\tau_{i+1}) = final(\tau_i)$, for $i = 1$ to $(f - 1)$. We denote $initial(\tau_1)$ as $initial(s)$ and $final(\tau_f)$ as $final(s)$. The set of all traces generated by G is the language of G , denoted as $L(G)$. Naturally, $L(G)$ is a subset of \mathfrak{S}^w , where \mathfrak{S}^w is the set of all infinite sequences of \mathfrak{S} . Any finite member of $L(G)$ is in \mathfrak{S}^* , the Kleene closure of \mathfrak{S} . The post language of G after a trace s is denoted as $L(G)/s = \{t \in \mathfrak{S}^* \mid st \in L(G)\}$. $L_f(G)/s \subset L(G)/s$ comprises finite prefixes of the infinite traces of $L(G)/s$.

5.4.1 Need for MIDES Framework

As seen earlier, the assumption of the MLDES based framework wherein the inherently measurable inconsistent transition(s) are modeled as permanently unmeasurable ones leading to weaker fault diagnosis. Consequently if MLDES framework based IDS is developed for Wi-Fi networks, it treats frame losses as permanently unmeasurable which results in lower attack detection rate. We now show how the MLDES may prove to be ineffective while at the same time the MIDES framework can still perform fault diagnosis in case an inconsistent behavior occurs.

As seen in Section 5.2, a four-way handshake occurs between the client and the DHCP server when the client requests for an IP address from the DHCP server. All the 4 frames which are a part of the four-way handshake are measurable frames. Let us assume that in a particular instance, the Wi-Fi sniffer captures the DHCP handshake in the following sequence: DHCPDISCOVER, DHCPOFFER, DHCPACK. As it can be seen that the third frame (DHCPREQUEST) of the four-way handshake is missed by the Wi-Fi sniffer in this instance. The missing of the DHCPREQUEST during this instance is termed a measurement inconsistency. We use the term measurement inconsistent since DHCPREQUEST by itself is *not*

unmeasurable. It is not be measured by the sniffer during a particular instance (hence “inconsistency”).

The existing MLDES philosophy terms DHCPREQUEST as permanently unmeasurable transition. It further implies that even if there exists a trace that can lead to fault diagnosis using the DHCPREQUEST frame in future, it should not be used for fault diagnosis. So, the MLDES philosophy may result in lower attack detection (fault diagnosis) as occasionally lost frames (which are inherently measurable) are modeled as permanently unmeasurable. On the other hand, the proposed MIDES framework takes into account the measurement inconsistency and tries to predict the system state on observing the DHCPACK event. On observing the DHCPACK frame directly after the DHCPOFFER frame, the MIDES assumes that the four-way handshake of the client is completed and waits for the future frames. Hence, we have suggested the MIDES framework that takes into account the measurement inconsistency and tries to predict the state of the system by observing the future transitions.

An added advantage of any DES based IDS is that they do not require protocol modification, encryption or installation of proprietary hardware. A DES based IDS can be formally proved to be correct. In this chapter we propose a MIDES based IDS for the rogue DHCP server attack that incorporates the features listed above and overcomes the drawbacks of the existing approaches like cryptographic requirements, certificate management, protocol modifications etc.

The MIDES framework basically combines the philosophies of measurement limitation and measurement inconsistency. Just like MLDES the MIDES framework assumes permanently measurable transitions as measurable transitions while permanently unmeasurable transitions are modeled as unmeasurable transitions and are never used for fault diagnosis. The principle difference lies in the treatment of those transitions that are sometimes measurable and sometimes unmeasurable leading to inconsistency. The MLDES framework treats all such transitions as permanently unmeasurable. As against this, the MIDES framework assumes measurement inconsistent transition(s) as measurable at the instances when it is measured and tries to predict the behavior of a system should an inconsistency arise. Thus the proposed framework not only encompasses the salient features of MLDES but also extends the MLDES in order to incorporate the inconsistent behavior which is ignored by the MLDES framework. In the following sub-sections, we have separately discussed the terminologies associated with the measurement limitations and measurement inconsistency.

5.4.2 MIDES Model: Measurement Limitations and Failure Diagnosis

Limitations of measurement give rise to uncertainty in transitions in the observed dynamics of the model. In this sub-section the notion of measurement limitation in the MIDES framework is formally introduced and the consequent uncertainty in transitions in G is characterized. In order to explain the definitions in a more clear and concise way we take help of the three tank system explained in Subsection 5.4.4. Very briefly, the two tank system involves filling of tank T_1 , followed by filling of tank T_2 . After tank T_2 gets full, the mixture in tank T_2 is drained off. We have reproduced few standard definitions available in the DES literature [72, 124, 125] for the sake of completeness and simplicity of explanation.

Definition 45. Measurable and unmeasurable events/transitions: Any event that can (cannot) be measured using sensors are measurable (unmeasurable) events. A **transition** $\tau_i = \langle x, x^+, \sigma, check(V), assign(V) \rangle$ is said to be a measurable (unmeasurable) transition if σ is a measurable (unmeasurable) event. \mathfrak{S}_m and \mathfrak{S}_u denote the set of measurable and unmeasurable transitions. In Fig. 5.7 the event “ T_1 Filling” is a measurable event so the transition τ_1 associated with the event “ T_1 Filling” is also measurable.

Definition 46. Measurement equivalent transitions and states: Two transitions $\langle x_1, x_1^+, \sigma_1, check_1(V), assign_1(V) \rangle$ and $\langle x_2, x_2^+, \sigma_2, check_2(V), assign_2(V) \rangle$ are equivalent if $\sigma_1 = \sigma_2$ (same event), $check_1(V) \equiv check_2(V)$ (same equalities over the same subset of variables in V), and $assign_1(V) \equiv assign_2(V)$ (same subset of model variables with same assignment). If $\tau_1 \equiv \tau_2$ then the source states of the transitions are equivalent and so are the destination states, i.e., $x_1 \equiv x_2$ and $x_1^+ \equiv x_2^+$. In Fig. 5.7, upon comparing the transitions τ_1 and τ'_1 we observe that the same event (T_1 Filling) is associated with both the transitions. So, $\tau_1 \equiv \tau'_1$ which implies $s_0 \equiv s'_0$ and $s_1 \equiv s'_1$. As a result when the event “ T_1 Filling” occurs, it cannot be said with certainty whether the system has taken the transition τ_1 or τ'_1 . So, the transitions τ_1 and τ'_1 are said to be measurement equivalent transitions.

Definition 47. Projection and Inverse Projection Operator: A **projection** operator $P : \mathfrak{S}^* \rightarrow \mathfrak{S}_m^*$ is defined as: $P(\epsilon) = \epsilon(\text{null string})$; $P(\tau) = \tau$ if $\tau \in \mathfrak{S}_m$; $P(\tau) = \epsilon$ if $\tau \in \mathfrak{S}_u$; $P(s\tau) = P(s)P(\tau)$, where $s \in L_f(G)$, $\tau \in \mathfrak{S}$. The function P erases the unmeasurable transitions from the argument finite trace. $P(s)$ is termed as the *measurable finite trace* corresponding to the finite trace s . An **inverse projection** operator $P^{-1} : \mathfrak{S}_m^* \rightarrow 2^{\mathfrak{S}^*}$ is defined as: $P^{-1}(s) = \{s' \in L_f(G) \mid sEs'\}$. Thus, $P^{-1}(s)$ encompasses all possible sequences of transitions that are equivalent to the finite trace s . The projection function P , the inverse function P^{-1} and the measurement equivalence E of finite traces can be extended to traces $\in \mathfrak{S}^w$, in a natural way.

Definition 48. Measurable Equivalent Traces: Two finite traces s and s' are said to

be measurement equivalent if the following relation holds: $P(s) = \langle \tau_1, \tau_2, \dots, \tau_n \rangle$, $P(s') = \langle \tau'_1, \tau'_2, \dots, \tau'_n \rangle$ and $\tau_i E \tau'_i$, $1 \leq i \leq n$.

We use the symbol E to denote measurement equivalence of finite traces as well as that of transitions, with slight abuse of notation. The equivalence of finite traces s and s' implies that if measurable transitions are extracted from s and s' by use of the operator P , then all the transitions are measurement equivalent. Following Definition 46, it can be seen that the trace $\langle \tau_1, \tau_2, \tau_3 \rangle$ in Fig. 5.7, is measurement equivalent to the trace $\langle \tau'_1, \tau'_2, \tau'_3 \rangle$.

Definition 49. Normal G -state/ G -transition and Failure G -state/ G -transition: States that are traversed by the system when operating without any faults (attack) are known as **normal G -state**. X_N denotes the set of all normal states. A G -transition $\langle x, x^+ \rangle$ is called a *normal G -transition* if $x, x^+ \in X_N$. States that are traversed by the system when operating under **failure** circumstances are known as Failure G -state. X_{F_i} denotes the set of all failure states. A G -transition $\langle x, x^+ \rangle$ is called a *failure G -transition* if $x, x^+ \in X_{F_i}$. In Fig. 5.7, the states s_0, s_1, s_2 are normal G -states. The transitions associated with these states viz. τ_1, τ_2 are normal G -transitions. The states s'_0, s'_1, s'_2 are failure G -states. The transitions associated with these states viz. τ'_1, τ'_2 are failure G -transitions.

Definition 50. Failure causing G -transition: A transition $\langle x, x^+ \rangle$, where $x \in X_N$ and $x^+ \in X_{F_i}$, is called a *failure causing G -transition* indicating the occurrence of some failure. Since failures are assumed to be *permanent*, there is no transition from any $x \in X_{F_i}$ to $x^+ \in X_N$. In Fig. 5.7, the transition τ_{0F1} is the failure causing G -transition as it moves the model from normal to the failure state. All failure causing G -transition are inherently unmeasurable.

5.4.3 MIDES Model: Measurement Inconsistency

A DES consists of a set of states and transitions emanating from those states. Consider a DES G whose measurable transitions include: $\tau_1, \tau_2, \tau_3, \dots, \tau_i, \tau_j, \tau_k$. Consider a state x of the same DES which has the transitions $\tau_1, \tau_2, \tau_3, \dots, \tau_i (i < k)$ emanating from state x . Let us assume that a transition τ_k is observed at state x . As transition τ_k cannot be executed from state x , transition τ_k is said to be *measurement inconsistent* with respect to state x . A point to be noted here is that only measurable transitions can be measurement inconsistent. However, if the transition τ_k emanates from some future DES state y , then it is possible that the transition sequence between state x upto y is missed. This does not imply that the transition sequence between the states x and y is unmeasurable. It simply means that during a particular instance the transition sequence between the states x and

y is missed. Measurement inconsistent transitions are measurable transitions but become unmeasurable temporarily.

Definition 51. Measurement Inconsistency Causing G -transition (τ_{ub}): Given a G -state x_{ub} and a G -transition τ_{ub} , such that $initial(\tau_{ub}) \neq x_{ub}$ and $\tau_{ub} \in \mathfrak{S}_m$, then the G -transition τ_{ub} is termed as measurement inconsistency causing G -transition if τ_{ub} is observed at state x_{ub} . As shown in Fig. 5.7, if a G -transition sequence τ_1, τ_3 is observed, then the measurement inconsistency causing G -transition (τ_{ub}) is τ_3 whereas the measurement inconsistency causing G -state (x_{ub}) is s_1 . This is because on observing G -transition τ_1 the DES model moves to G -state s_1 . At s_1 the observed G -transition is τ_3 which is a measurement inconsistent G -transition as none of the outgoing G -transitions from G -state s_1 is τ_3 .

Under MLDES philosophy the measurement inconsistent G -transition $\tau_{ub}(\tau_3)$ is modeled permanently unmeasurable and is not be used for fault diagnosis at all. In contrast, under MIDES framework upon observation of $\tau_{ub}(\tau_3)$ the framework tries to predict the possible G -states the model could be in. The MIDES framework also considers all future measurements of $\tau_{ub}(\tau_3)$ for fault diagnosis instead of assuming it to be permanently unmeasurable. Unlike ML based DES where the transitions are classified offline as measurable or unmeasurable in the proposed MIDES framework the measurement inconsistent transitions are determined online. So at a given instance, if no inconsistency arises, the MIDES framework behaves identical to the MLDES framework. In case an inconsistency arises, the proposed MIDES framework calls an estimator to predict the system state based on future transitions observed. This concept is elaborated later.

5.4.4 Application of Failure Detection and Diagnosis Theory of MIDES on Two Tank System

We demonstrate the Failure Detection and Diagnosis (FDD) theory of the MIDES using an example of two connected tanks [126] viz. T_1 and T_2 as shown in Fig. 5.6. Tank T_1 is supplied substance from reservoir tank MT_1 using pump P_1 . The flow through pump P_1 is controlled using valve V_1 . Tanks T_1 and T_2 are connected by means of valve V_2 . Tank T_2 has an outlet pipe whose flow is controlled by means of valve V_3 . This broad arrangement of two tanks is used in many industrial process. First the substance from MT_1 is filled in the tank T_1 followed by filling of T_2 . The volume of T_2 is 'n' times the volume of tank T_1 . So the tank T_1 needs to be filled and emptied 'n' times before T_2 gets full. The substances in tank T_1 and T_2 are stirred to ensure that the mixture is homogeneous. Once T_1 and T_2 are emptied, they are refilled again and the process repeats. When T_2 is full the homogenous mixture is drained out for usage.

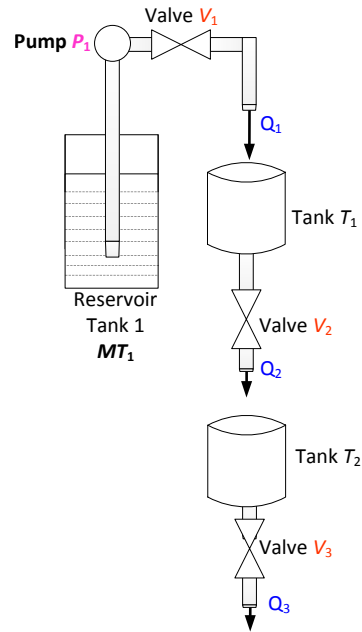


Figure 5.6: The two tank system

The control of flows in the system is done by opening and closing of the valves by a controller which in turn depends on the two types of sensor outputs viz. (i) level sensors of the tanks and (ii) flow sensors of the valves. The tanks are equipped with two level sensors each in order to determine whether the level of the substance in the tank is low or high. For example, in the tank T_1 if the level of substance is at the lowest (highest) point, the low (high) level sensor indicated by $T_1\text{Low}$ ($T_1\text{High}$) gives output 1. There is a flow sensor (indicated as Q_1 , Q_2 , Q_3) beside every valve that indicates whether substance is flowing through the adjoining pipe or not. For example, $Q_1 = 1$ (0) if substance is flowing (not flowing) through the pipe corresponding to Q_1 which connects MT_1 to T_1 . Table 5.1 shows the details of the sensors, their possible outputs and their interpretations.

With the advent of sophisticated instruments and advancement of electronics, these benchmark process of two-tank system can be controlled electronically by remotely sending signals over the communication medium [155]. However, inconsistencies may arise in the system because of signal losses/degradation [150].

Now we elaborate the working of the two tank system in terms of sensor outputs and controller commands to open/close the valves. Initially, all the tanks have their substances at the lowest levels, indicated by $T_1\text{Low} = T_2\text{Low} = 1$ (and obviously $T_1\text{High} = T_2\text{High} = 0$). As all the valves are closed there is no flow in any of the pipes, so flow sensor outputs: $Q_1 = 0$, $Q_2 = 0$, $Q_3 = 0$. First T_1 is to be filled which is initiated by the controller issuing the command $CV_1 = 1$. This results in opening of the valve V_1 to allow the flow of substance

Table 5.1: Sensor map for two tank system

Sensor	Possible Outputs	Interpretation
$T_i\text{Low}$ ($i = 1, 2$)	0	$T_i\text{Low} = 0$ implies substance in the tank T_i is NOT at the lowest level.
	1	$T_i\text{Low} = 1$ implies substance in the tank T_i IS at the lowest level.
$T_i\text{High}$ ($i = 1, 2$)	0	$T_i\text{High} = 0$ implies substance in the tank T_i is NOT at the highest level.
	1	$T_i\text{High} = 1$ implies substance in the tank T_i IS at the highest level.
Q_i ($i = 1, 2, 3$)	0	NO Flow measured by Flow sensor Q_i
	1	POSITIVE Flow measured by Flow sensor Q_i

into T_1 . While the tank T_1 is getting filled, care must be taken to ensure that the valve V_2 is always in a closed state. Once the substance starts flowing into T_1 from MT_1 , Q_1 becomes 1 and $T_1\text{Low}$ becomes 0. After the tank T_1 is full $T_1\text{High}$ becomes 1 and the controller issues the command $CV_1 = 0$ to close the valve V_1 . Flow to T_1 stops and Q_1 becomes 0.

After T_1 becomes full the controller issues the command $CV_2 = 1$ which opens the valves V_2 and substance from T_1 is allowed to fall into the tank T_2 ; $Q_2 = 1$ and $T_2\text{Low} = 0$. As the volume of T_2 is ‘n’ times the volume of T_1 , this process of filling and emptying of tank T_1 repeats ‘n’ times till T_2 gets full (i.e., $T_2\text{High} = 1$). While the tank T_2 is getting filled, care must be taken to ensure that the valve V_3 is always in a closed state.

We consider the ‘stuck-open’ fault of valve V_3 for the current system. As a result of ‘stuck-open’ fault, the flow sensor always reports a positive flow ($Q_3 = 1$) despite the close valve command is issued by the controller. Due to the ‘stuck-open’ fault, the mixture from tank T_2 is drained out before it gets full thereby degrading the overall system process.

Now we discuss the modeling of the two tank system using the MIDES framework. The MIDES model G used to represent two tank system under normal and fault scenarios is shown in Fig. 5.7. The various components of G are as follows:

$$X = \{s_0, s_1, s_2, s_3, s_4, s_5, s_6, s_7, s_8, s'_0, s'_1, s'_2, s'_3, s'_4, s'_5\}$$

$$X_0 = \{s_0\}$$

$$\Sigma = \{T_1\text{Empty}, T_1\text{Filling}, T_1\text{Full}, T_2\text{Empty}, T_2\text{Filling}, T_2\text{Full}, T_2\text{Drain}, V_2\text{Close}, V_3\text{Close}, V_3\text{Open}\}$$

$$\mathfrak{S} = \{\tau_0, \tau_1, \tau_2, \tau_3, \tau_4, \tau_5, \tau_6, \tau_7, \tau_8, \tau_9, \tau_{10}, \tau_{0F1}, \tau'_1, \tau'_2, \tau'_3, \tau'_4, \tau'_5\}$$

$$V = \{\epsilon\}^1$$

States and transitions belonging to normal (fault/attack) model are denoted by the non-primed (primed) notations. The occurrence of fault is modeled by the failure causing transition τ_{0F1} . For simplicity of illustration, we assume that fault can occur only from state

¹As the number of states in the two tank system are not large, model variables are not used as explained in earlier chapters.

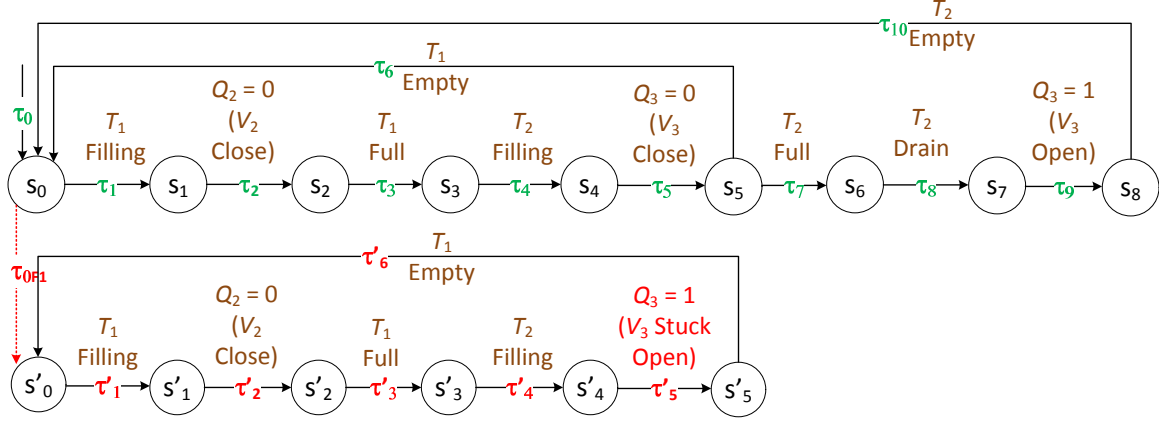


Figure 5.7: MIDES of the Two Tank System Shown in Fig. 5.6

s_0 . In Fig. 5.7, the transitions are not explicitly detailed as their six tuples, however, the corresponding event is shown. Table 5.2 illustrates the events corresponding to the sensor outputs and control commands. The transitions which are enabled by these events are shown in the Table 5.2. For explanation of the modeling we discuss the details of a normal G -transition (τ_1) and an F_i - G -transition (τ'_5).

τ_1 has the event T_1 Filling. When the sensor outputs for the tank T_1 are $-T_1$ Low = 1 and T_1 High = 0, the controller issues the command $CV_1 = 1$ which opens the valve V_1 . This allows flowing of the substance to T_1 and the flow sensor output $Q_1 = 1$. These sensor outputs and the controller command are represented by the event T_1 Filling that corresponds to the transition τ_1 .

From s_0 there is another transition τ_{0F1} which indicates the occurrence of a failure. Let us consider the F_i - G -transition τ'_5 which has the event V_3 Close associated with it. When the system is in state s'_4 (if F_i has occurred), the sensor outputs for the T_2 are $-T_2$ Low = 0 and T_2 High = 0, indicating that T_2 is filling and hence it must be ensured that the valve V_3 is closed so that the substance getting filled in tank T_2 does not drain out. Upon reading the sensor outputs, the controller issues the command to close the valve V_3 so that tank T_2 can be filled. However, because of failure F_1 , the valve V_3 remains 'stuck-open' and as the substance flows out of the tank T_2 , the sensor Q_3 outputs 1. So, in this case, despite the substance flowing from tank T_1 to tank T_2 , the level sensor for tank T_2 are $-T_2$ Low = 1 and T_2 High = 0, i.e., T_2 always remains at the lowest level. Due to stuck open fault of valve V_3 , eventually the tank T_1 is emptied and the system returns to the state s'_0 .

If the fault has occurred the controller maintains the command $CV_3 = 0$ perpetually because T_2 does not become full and the sensor output T_2 High = 1, which makes $CV_3 = 1$, never occurs. As a result the system moves from state s'_4 to s'_5 and eventually returns

Table 5.2: Transitions along with their representation. Events, sensor conditions, controller commands of the MIDES model of the two tank system shown in Fig. 5.7

Transition	What it Represents	Event	Sensor Conditions	Controller Commands
τ_0	All Tanks are Empty	Start	$T_1\text{Low} = 1, T_2\text{Low} = 1,$ $T_1\text{High} = 0, T_2\text{High} = 0,$ $Q_1 = 0, Q_2 = 0, Q_3 = 0.$	$CV_1 = 0, CV_2 = 0, CV_3 = 0.$
τ_1 & τ'_1	Tank T_1 Filling	$T_1\text{Filling}$	$T_1\text{Low} = 0, T_2\text{Low} = 1,$ $T_1\text{High} = 0, T_2\text{High} = 0,$ $Q_1 = 1, Q_2 = 0, Q_3 = 0.$	$CV_1 = 1, CV_2 = 0, CV_3 = 0.$
τ_2 & τ'_2	Close Valve V_2	$V_2\text{Close}$	$T_1\text{Low} = 0, T_2\text{Low} = 1,$ $T_1\text{High} = 0, T_2\text{High} = 0,$ $Q_1 = 1, Q_2 = 0, Q_3 = 0.$	$CV_1 = 1, CV_2 = 0, CV_3 = 0.$
τ_3 & τ'_3	Tank T_1 Full	$T_1\text{Full}$	$T_1\text{Low} = 0, T_2\text{Low} = 1,$ $T_1\text{High} = 1, T_2\text{High} = 0,$ $Q_1 = 0, Q_2 = 0, Q_3 = 0.$	$CV_1 = 0, CV_2 = 0, CV_3 = 0.$
τ_4 & τ'_4	Tank T_2 Filling	$T_2\text{Filling}$	$T_1\text{Low} = 0, T_2\text{Low} = 0,$ $T_1\text{High} = 1, T_2\text{High} = 0,$ $Q_1 = 0, Q_2 = 1, Q_3 = 0.$	$CV_1 = 0, CV_2 = 1, CV_3 = 0.$
τ_5	Close Valve V_3	$V_3\text{Close}$	$T_1\text{Low} = 0, T_2\text{Low} = 0,$ $T_1\text{High} = 1, T_2\text{High} = 0,$ $Q_1 = 0, Q_2 = 1, Q_3 = 0.$	$CV_1 = 0, CV_2 = 1, CV_3 = 0.$
τ_6 & τ'_6	Tank T_1 Empty	$T_1\text{Empty}$	$T_1\text{Low} = 1, T_2\text{Low} = 0,$ $T_1\text{High} = 0, T_2\text{High} = 0,$ $Q_1 = 0, Q_2 = 0, Q_3 = 0.$	$CV_1 = 0, CV_2 = 0, CV_3 = 0.$
τ_7	Tank T_2 Full	$T_2\text{Full}$	$T_1\text{Low} = 1, T_2\text{Low} = 0,$ $T_1\text{High} = 0, T_2\text{High} = 1,$ $Q_1 = 0, Q_2 = 0, Q_3 = 0.$	$CV_1 = 0, CV_2 = 0, CV_3 = 0.$
τ_8	Tank T_2 Drain	$T_2\text{Drain}$	$T_1\text{Low} = 1, T_2\text{Low} = 0,$ $T_1\text{High} = 0, T_2\text{High} = 0,$ $Q_1 = 0, Q_2 = 0, Q_3 = 1.$	$CV_1 = 0, CV_2 = 0, CV_3 = 1.$
τ_9	Open Valve V_3	$V_3\text{Open}$	$T_1\text{Low} = 1, T_2\text{Low} = 0,$ $T_1\text{High} = 0, T_2\text{High} = 0,$ $Q_1 = 0, Q_2 = 0, Q_3 = 1.$	$CV_1 = 0, CV_2 = 0, CV_3 = 1.$
τ_{10}	Tank T_2 Empty	$T_2\text{Empty}$	$T_1\text{Low} = 1, T_2\text{Low} = 1,$ $T_1\text{High} = 0, T_2\text{High} = 0,$ $Q_1 = 0, Q_2 = 0, Q_3 = 0.$	$CV_1 = 0, CV_2 = 0, CV_3 = 0.$
τ'_5	Close Valve V_3	$V_3\text{Close}$	$T_1\text{Low} = 0, T_2\text{Low} = 1,$ $T_1\text{High} = 1, T_2\text{High} = 0,$ $Q_1 = 0, Q_2 = 0, Q_3 = 1.$	$CV_1 = 0, CV_2 = 0, CV_3 = 1.$
τ_{0F1}	Failure Causing	Fault	$T_1\text{Low} = 1, T_2\text{Low} = 1,$ $T_1\text{High} = 0, T_2\text{High} = 0,$ $Q_1 = 0, Q_2 = 0, Q_3 = 0.$	$CV_1 = 0, CV_2 = 0, CV_3 = 0.$

to state s'_1 when tank T_1 becomes empty. On the other hand, if the system is normal, T_2 gets filled which makes T_1 empty and it is modeled by the transition τ_6 . So, in this case, after the substance flows from tank T_1 to tank T_2 , the level sensor for tank T_2 are – $T_2\text{Low}$

$= 0$ and $T_2\text{High} = 0$, i.e., T_2 is getting filled as the level sensor $T_2\text{Low} = 1$ changes to $T_2\text{Low} = 0$ indicating accumulation of filling of substance in tank T_2 from tank T_1 . This is in sharp contrast to the failure case where the level sensor for tank T_2 always showed $T_2\text{Low} = 1$ and remained at the lowest level. In a similar manner, referring to Table 5.2 and the discussion on the working of the two tank system, the whole modeling given in Fig. 5.7 can be explained.

In the two tank system under consideration, we have assumed that the volume of the tank T_2 is $h = 2$ times the volume of tank T_1 . This implies that after two iterations of draining of the substance from T_1 the tank T_2 gets full. So, from the MIDES model in Fig. 5.7 it can be observed that in order for T_2 to get full, the system moves in the trace containing transitions $\langle \tau_1, \tau_2, \tau_3, \tau_4, \tau_5, \tau_6 \rangle$ twice and during the third iteration the system takes the trace $\langle \tau_1, \tau_2, \tau_3, \tau_4, \tau_5, \tau_7, \tau_8, \tau_9, \tau_{10} \rangle$ which breaks out of the loop and the tank T_2 gets filled.

Now we discuss measurable/unmeasurable transitions of the model and consequently the equivalent states and transitions are identified. In this system all the sensor outputs are measurable and so are the controller commands. So any transition whose enabling event is based on the change in some sensor output or controller command, is measurable. For example, in case of τ_3 the event is $T_1\text{Full}$, whose corresponding change in sensor outputs are $T_1\text{Low} = 0$ (from 1), $T_1\text{High} = 1$ (from 0), $Q_1 = 0$ (from 1) and controller command is $CV_1 = 0$ (from 1). So τ_3 is a measurable transition. In a similar way it can be shown that all transitions except τ_{0F1} are measurable. τ_{0F1} is the failure causing transition and is unmeasurable because it is not caused by a change of any sensor output or controller command.

Two transitions are measurement equivalent if the corresponding changes in the sensor outputs and the controller commands are same. Events associated with equivalent transitions are also same. For example, transitions τ_3 and τ'_3 are measurement equivalent because they are caused by same changes in sensor outputs and controller commands i.e., $T_1\text{Low} = 0$, $T_1\text{High} = 1$, $Q_1 = 0$ and controller command is $CV_1 = 0$. Also the event associated with both these transitions is $T_1\text{Full}$. As per the Definition 46, $s_2Es'_2$ and $s_3Es'_3$, because the source states and also the destination states of equivalent transitions are equivalent. In a similar way it can be verified that $\tau_iE\tau'_i$, $1 \leq i \leq 4$. It may be noted that in case of F_i -transitions τ'_i , $1 \leq i \leq 4$ there is an equivalent normal transition e.g., $\tau_1E\tau'_1$. So, after the failure as long as the system moves through F_i -transitions τ'_i , $1 \leq i \leq 4$, the fault cannot be diagnosed because there is no transition that distinguishes the faulty behavior from the normal condition. To elaborate, F_i -transitions τ'_i , $1 \leq i \leq 4$ do not capture failure manifestation (in terms of distinguishing sensor outputs and controller commands) and hence cannot detect the fault.

Now let us consider the transitions τ_4 and τ'_5 . The sensor outputs and the controller command for the transition τ_4 are $T_2\text{Low} = 0$, $T_2\text{High} = 0$, $CV_3 = 0$ and $Q_3 = 0$. In case of the transition τ'_5 the sensor outputs and controller command are $T_2\text{Low} = 1$, $T_2\text{High} = 0$, $CV_3 = 0$ and $Q_3 = 1$. It may be noted that for both the transitions, the controller issues the command $CV_3 = 0$ after detecting that T_2 is getting filled (by sensor outputs $T_2\text{Low} = 0$, $T_2\text{High} = 0$). In case of τ_4 , as the system is normal the tank T_2 gets filled eventually. However, in case of τ'_5 , as the system is faulty, even when the controller issues the command $CV_3 = 0$ there is positive flow out of T_2 and the flow sensor $Q_3 = 1$. So transition τ'_5 captures the fault manifestation i.e., the valve V_3 remains open while tank T_2 is getting filled ($T_2\text{Low} = 0$, $T_2\text{High} = 0$) even after the controller issues the command $CV_3 = 0$. As F_i -transition τ'_5 captures failure manifestation its occurrence is required for detection of F_i .

5.4.5 Diagnosability

The objective of the failure diagnosis problem is to determine the occurrence of a failure F_i . If the event (σ) corresponding to τ_{F_i} is measurable, failure diagnosis is trivial. So the failure causing transitions are assumed to be unmeasurable. For such failure causing transitions, σ is unmeasurable. As σ is unmeasurable, there are no checks or assignment for model variables. As failures are assumed to be *permanent*, there is no transition from any state in x_{F_i} to any state in X_N . The event related to causing F_i is denoted as σ_{F_i} .

Informally, an DES G is diagnosable if it is always possible to determine the failure status of the states beyond a certain point along all the possible traces of G after the occurrence of a failure, using the sequence of measurements. A few terms are introduced before formally defining diagnosability.

Let $\psi(X_{F_i}) = \{s | s \in L_f(G) \text{ and } \text{final}(s) \in X_{F_i} \text{ and } s \text{ ends in a measurable transition} \}$.

Definition 52. F_i -Diagnosability: An DES model G (under a given measurement limitation) is said to be diagnosable for failure F_i iff the following holds.

$$(\exists n_j \in \mathbb{N})[\forall s \in \Psi(X_{F_i})](\forall t \in L_f(G)/s)[|t| \geq n_j \Rightarrow D] \quad (5.2)$$

where the condition D is $\forall y \in \{P^{-1}[P(st)]\}$, $\text{final}(y) \in X_{F_i}$

The above definition means the following. Let s be any finite prefix of a trace of G that ends in an F_i -state and let t be any sufficiently long continuation of s . Condition D then requires that every sequence of transitions, measurement indistinguishable with st , should end into an F_i -state. This implies that, along every continuation t of s , one can detect the occurrence of failure F_i with a finite delay, specifically in at most n_j transitions of the system

after s .

The fault diagnosis problem is to determine if the fault F_i has occurred within finite number n_{F_i} (where $n_{F_i} \in \mathbb{N}$) say, of transitions after the occurrence of the failure causing transition τ_{F_i} . Let us consider a trace of the MIDES model of the two tank system; $s = \langle \tau_0, \tau_{0F_1}, \tau'_1 \rangle$; obviously $s \in \Psi(X_{F_i})$. For diagnosing F_i , any sufficiently long but finite extension t of s of length n_{F_i} must ascertain that fault has occurred. In this case, if we extend $s = \langle \tau_0, \tau_{1F_i}, \tau'_1 \rangle$ as $t = \langle \tau'_2, \tau'_3, \tau'_4 \rangle$, we get $\exists y = \langle \tau_0, \tau_1, \tau_2, \tau_3, \tau_4 \rangle \in P^{-1}(P(st)) \wedge final(y) = x_1 \notin X_{F_i}$. In other words, as the F_i - G -trace $\langle \tau'_1, \tau'_2, \tau'_3, \tau'_4 \rangle$ is equivalent to $\langle \tau_1, \tau_2, \tau_3, \tau_4 \rangle$ (normal condition), so this F_i - G -trace cannot detect the fault. As already discussed, as none of the transitions involved in the F_i - G -trace under question captures failure manifestation, it is not helpful in fault detection.

In this example there is only one more way of extending s , namely, $t1$ is $\langle \tau'_1, \tau'_2, \tau'_3, \tau'_4, \tau'_5 \rangle$. It may be noted that $\exists y \in P^{-1}(P(st1))$ such that $final(y) \notin X_{F_i}$. So the fault is diagnosable. In other words, the transition τ'_5 captures failure manifestation. So the trace $st1$ detects the fault making the fault diagnosable.

5.4.6 MIDES Diagnoser Construction and Inconsistency Handling in MLDES vs MIDES Framework for the Two Tank System

The diagnoser is a directed graph represented by $O = \langle Z, A \rangle$; where Z is the set of diagnoser O -nodes, called O -nodes, and $A \subseteq Z \times Z$ is the set of diagnoser transitions, called O -transitions. Each O -node $z \in Z$ corresponds to a set of G -states representing the uncertainty about the actual state. Similarly, each O -transition $a \in A$ of the form $\langle z_i, z_f \rangle$ is a set of measurement equivalent transitions representing the uncertainty about the actual measurable transition that occurs. The *unmeasurable successor* (set) of a set Y of states is defined as $\mathcal{U}(Y) = \bigcup_{x \in Y} \{x^+ | \tau = \langle x, x^+ \rangle \in \mathfrak{S}_u\}$. The *unmeasurable reach* of a set Y of states, denoted as $\mathcal{U}^*(Y)$, is the reflexive-transitive closure of unmeasurable successors of Y .

Diagnoser Construction: The states in X_0 are partitioned into equivalent subsets denoted as $X_{01}, X_{02}, \dots, X_{0m}$. For all i , $1 \leq i \leq m$, an initial O -node z_{0i} is obtained as the unmeasurable reach of X_{0i} , i.e., $z_{0i} = \mathcal{U}^*(X_{0i})$. The set of all initial O -nodes is denoted as $Z_0 = z_{01} \cup \dots \cup z_{0m}$. The initial O -nodes capture the fact that the diagnoser can infer a set z_{0i} of possible initial system states (or their unmeasurable reach) by measuring the variables without waiting for the first measurable transition. Given any O -node z , the O -transitions emanating from z are obtained as follows. Let \mathfrak{S}_{mz} denote the set of measurable G -transitions from the states $x \in z$. Let A_z be the set of all equivalence classes of \mathfrak{S}_{mz} under

E. For each $a \in A_z$, a successor O -node z^+ of z such that $z^+ = final(a)$ can be created as follows. Let $z_a^+ = \{final(\tau) | \tau \in a\}$; then $z^+ = \mathcal{U}^*(z_a^+)$ and a is designated as: $\langle z, z^+ \rangle$. The set of the diagnoser transitions is augmented as: $A \leftarrow A \cup \{a\}$, and the set of O -nodes is augmented as: $Z \leftarrow Z \cup \{z^+\}$. Each $a \in A$ is an ordered pair $\langle z, z^+ \rangle$, where $z = initial(a)$ and $z^+ = final(a)$. Thus, each O -node contains equivalent states. The detailed algorithm for diagnoser construction is shown in Algorithm 4

Algorithm 4: Algorithm for construction of diagnoser O for an MIDES model G

Input: MIDES model G

Output: MIDES Diagnoser

```

1 Partition  $X_0$  into equivalent subsets  $X_{01}, X_{02}, \dots, X_{0m}$ 
2 for all  $i, 1 \leq i \leq m$  do
3   |  $z_{0i} = \mathcal{U}^*(X_{0i})$ 
4 end
5  $Z_0 \leftarrow z_{01} \cup \dots \cup z_{0m}$ 
6  $Z \leftarrow Z_0$ 
7  $A \leftarrow \phi$ 
8 for all  $z \in Z$  do
9   | /* Find the set of measurable  $G$ -transitions ( $\mathfrak{S}_{mz}$ ) outgoing from  $z$  */
9   |  $\mathfrak{S}_{mz} \leftarrow \{\tau | \tau \in \mathfrak{S}_m \wedge initial(\tau) \in z\}$ 
9   | /* Find the set of all measurement equivalent classes  $A_z$ , of  $\mathfrak{S}_{mz}$  */
10  | for all  $a \in A_z$  do
11  | |  $z_a^+ = \{final(\tau) | \tau \in a\}$ 
12  | |  $z^+ = \mathcal{U}^*(z_a^+)$ 
13  | |  $Z = Z \cup \{z^+\}$ 
14  | |  $A = A \cup \{a\}$ 
15  | end
16 end
    
```

Henceforth, we refer to states, transitions, and traces of G as G -states, G -transitions and G -traces, respectively. Similarly, for the diagnoser nodes and transitions, we use O -nodes, O -transitions and O -traces respectively. Now, we look into few definitions and properties related to diagnoser.

Definition 53. (Embedding of G -traces in O -traces): Given a O -trace $\gamma = \langle a_1, a_2, \dots, a_k \rangle$, a G -trace s , where $P(s) = \langle \tau_1, \tau_2, \dots, \tau_k \rangle$, is said to be embedded in γ , if $\tau_i \in a_i, 1 \leq i \leq k$. The set of all G -traces embedded in a O -trace γ is represented as $A_D(\gamma)$.

Property 4. If two traces $t, y \in A_D(\gamma)$, where t is F_i - G -trace and y is non- F_i - G -trace, then the O -nodes traversed by γ are F_i -uncertain.

Proof. The property also follows from the diagnoser construction. As any O -transition $a \in \gamma$ has an non- F_i - G -transition and a F_i - G -transition (which are equivalent), so source and

destination O -nodes of a are F_i -uncertain. □

Definition 54. F_i - O -node: An O -node, which contains an F_i - G state, is called an F_i - O -node, denoted as z_{F_i} . The set of all F_i - O -nodes is denoted as Z_{F_i} . In Fig. 5.8 the O -nodes z_0, \dots, z_5, z_9 are F_i - O -nodes as each O -node contains an F_i - G -state.

Definition 55. F_i -certain O -node and F_i -uncertain O -node: An F_i - O -node z is called an F_i -certain O -node if $z \subseteq X_{F_i}$. In Fig. 5.8 the O -node z_9 are F_i -certain O -node as it contains only failure G -states. An F_i - O -node which is not F_i -certain is called F_i -uncertain- O -node. In Fig. 5.8 the O -nodes z_0, \dots, z_5 are F_i -uncertain O -nodes as they contain both normal G -states as well as failure G -states.

In words, F_i -certain O -node comprises only F_i - G states, while F_i -uncertain O -node comprises some F_i - G states and some non F_i - G -states. So, if the diagnoser reaches any F_i -certain O -node failure is diagnosed. By Property 4 and Definition 53, if there is a O -trace γ which moves in F_i -uncertain O -nodes, there is a F_i - G -trace t which is embedded in γ . After failure, diagnoser moves in γ by virtue of t . However, as there is another non- F_i - G -trace y say, equivalent to t , fault cannot be diagnosed till γ is exited.

Definition 56. F_i - O -path (γ_{F_i}): A path of the diagnoser O is a sequence of O -transitions $\gamma = \langle a_1, a_2, \dots \rangle$, with the consecution property $initial(a_{i+1}) = final(a_i), i \geq 1$. An F_i - O -path γ is an O -path in which every O -node is an F_i - O -node.

Definition 57. F_i -uncertain cycle: An F_i -uncertain cycle is an F_i - O -cycle in which there is no F_i -certain O -node.

Definition 58. F_i -indeterminate cycle: An F_i -uncertain cycle γ in which the F_i -states contained in the O -nodes of γ form a cycle in G comprising transitions from γ , is called an F_i -indeterminate cycle. Consider a sequence $\langle x_1, x_2, x_3, \dots, x_k \rangle$ that corresponds to a normal cycle and measurement equivalent failure cycle $\langle x'_1, x'_2, x'_3, \dots, x'_k \rangle$. If the system is under normal conditions, the diagnoser moves into normal cycle and once a failure occurs it moves in the failure cycle. As both the normal and attack cycles are measurement equivalent, the normal and failure cycles are indistinguishable from one another. As a result of the presence of the indeterminate cycle it is not possible to predict whether the diagnoser is moving under normal or failure cycle leading to non-diagnosability. Thus, an F_i -indeterminate cycle is an F_i -uncertain cycle with the special property as stated below:

“There is also a cycle involving F_i -states of the composite model that corresponds to the F_i -uncertain diagnoser cycle.” In simple words, the existence of an F_i -indeterminate cycle in the diagnoser implies that there are at least two measurement indistinguishable

syntactic cycles in G , one comprising only non- F_i -states and the other comprising F_i -states. This implies that if the system moves in an F_i -indeterminate cycle, then the measurable variables are observed to be similar in both non- F_i and F_i conditions. Thus, if the diagnostic estimate moves along such an F_i -indeterminate cycle, then the fault F_i cannot be diagnosed, because, at each point in the cycle there exists uncertainty regarding the occurrence of F_i and as faults are assumed to be permanent, the system may not exit from such a cycle. The existence of an F_i -indeterminate cycle thwarts diagnosability. The equivalence between F_i -diagnosability and the absence of F_i -indeterminate cycles has been formally established for DES models [72].

The algorithm for the construction of the MIDES based diagnoser is exactly the same as that for the MLDES based diagnoser which is explained in Subsection 5.4.6. Just like MLDES diagnoser, the MIDES diagnoser takes into consideration the measurement equivalent transitions and states, the failure causing transitions and handles the unmeasurable transition by not using it for fault diagnosis. The principle difference between the MLDES framework and the proposed MIDES framework lies in the manner in which they handle the measurement inconsistency. Now we look into the few terminologies that are required only for the MIDES framework.

Definition 59. Incoming Transition Set (ITS): The ITS represents the set of all incoming O -transitions on the O -node z . The ITS of an O -node $z \in Z$ is defined as:

$$ITS(z) = \{\forall a \in A | final(a) = z\}.$$

Definition 60. Reachable O -node R_{z_i, z_j} : Given two O -nodes $z_i, z_j \in Z$, O -node z_j is said to be reachable from z_i if there exists an O -path $\gamma = \langle a_1, a_2, \dots, a_n \rangle$ such that $initial(a_1) = z_i$ and $final(a_n) = z_j$. If z_j is reachable from z_i then it is denoted as R_{z_i, z_j} .

Definition 61. Reachable O -node set RS_{z_i} : Given an O -node $z_i \in Z$ and the set of all diagnoser nodes $(z_1, z_2, \dots, z_n) \in Z$, the reachable O -node set contains all the O -node(s) that are reachable from z_i .

$$RS_{z_i} = \bigcup_{1 \leq j \leq n} \{z_j | R_{z_i, z_j}\}$$

Given an O -node z_i its RS_{z_i} can be calculated using Depth First Search (DFS) algorithm. Given an O -node z_i its $DFS(z_i)$ gives all the O -nodes that are reachable it.

Definition 62. Measurement Inconsistency Causing O -transition a_i by virtue of G -transition (τ_{ub}): Given an O -node z_{ub} and a G -transition $\tau_{ub} \in a_i$, such that $\forall a_i$ if $initial(a_i) = z_{ub}$ and $\tau_{ub} \notin a_i$ then a_i is said to be measurement inconsistency causing O -transition by virtue of G -transition τ_{ub} . In other words, an O -node z_{ub} may have many O -transitions a_i

emanating from it, but none of the G -transitions in a_i contain the G -transition τ_{ub} which is measured. If the diagnoser is at O -node z_{ub} and a measurement inconsistent O -transition a_i occurs by virtue of G -transition τ_{ub} then, the diagnoser cannot continue further fault diagnosis. z_{ub} is said to be measurement inconsistency causing O -node.

As shown in Fig. 5.8, if an O -transition sequence a_1, a_2, a_1 is observed by virtue of G -transition $\tau_1(\tau'_1), \tau_2(\tau'_2), \tau_1(\tau'_1)^2$, then the measurement inconsistency causing O -transition is a_1 caused by virtue of G -transition $\tau_1\tau'_1$ whereas the measurement inconsistency causing O -node is z_2 . This is because on observing O -transition a_1 by virtue of G -transitions $\tau_1(\tau'_1)$ the diagnoser reaches the O -node z_1 . At z_1 the O -transition is a_2 is observed by virtue of G -transition $\tau_2(\tau'_2)$ taking the diagnoser to the O -node z_2 . As none of the outgoing O -transitions from O -node z_2 has an G -transition $\tau_1(\tau'_1)$ in it, O -node z_2 is the measurement inconsistency causing O -node.

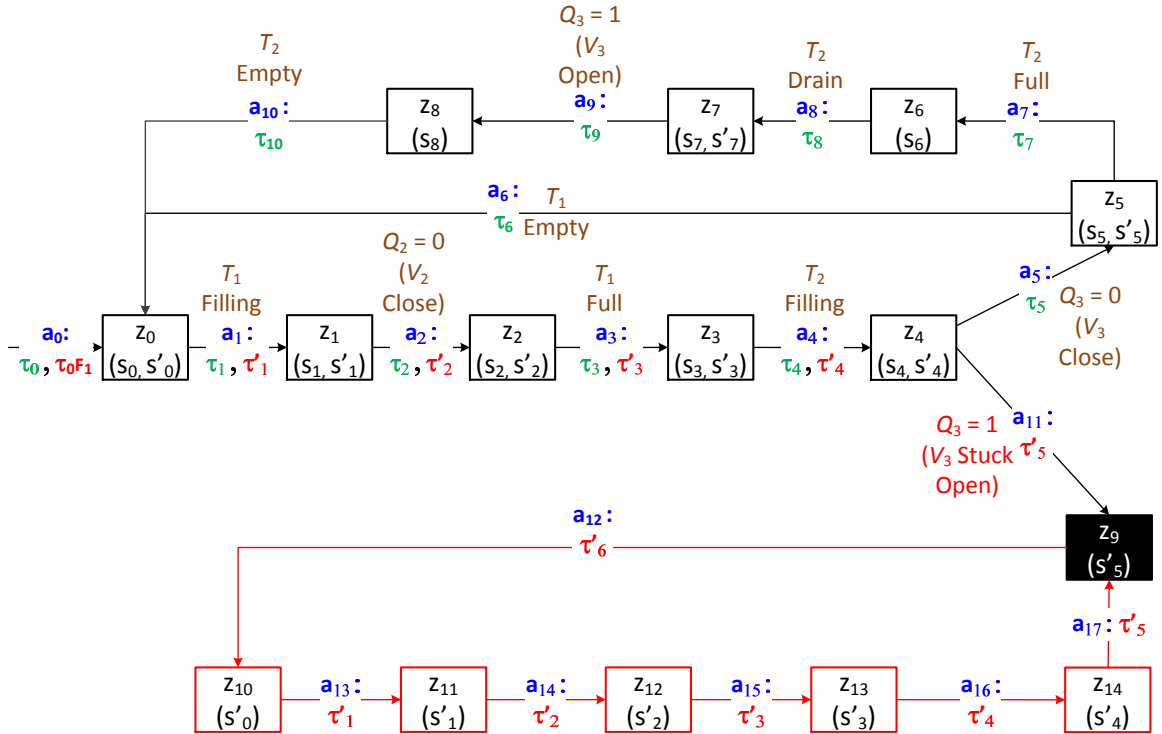


Figure 5.8: Case 1: MLDES diagnoser assuming no measurement inconsistent transition is observed

Inconsistency Handling: MLDES vs MIDES Framework

In order to explain the significance of the MIDES framework we now look into the fault diagnosis mechanism under measurement inconsistency. We first consider the scenario where

²As τ_1 and τ'_1 are measurement equivalent transitions, it cannot be ascertained whether the O -transition a_1 is observed by virtue of G -transition $\tau_1(\tau'_1)$. Similar case holds true for τ_2 and τ'_2 .

no measurement inconsistent transition occurs. Then we look into different approaches followed by MLDES based diagnoser to handle the measurement inconsistency. Following that we see how the proposed MIDES diagnoser offers a novel way of handling measurement inconsistency as compared to the philosophy adopted by the MLDES based diagnoser.

Case 1: MLDES Diagnoser – No measurement inconsistent transition observed The diagnoser shown in Fig. 5.8 is constructed using the philosophy proposed in [124]. As observed, the MLDES diagnoser shown in Fig. 5.8 contains no F_i -uncertain cycle, so no F_i -indeterminate cycle is present in the diagnoser. As the diagnoser does not contain any F_i -indeterminate cycle(s) the fault is diagnosable. As explained earlier, $s_0Es'_0, s_1Es'_1, s_2Es'_2, \dots, s_5Es'_5$ are the measurement equivalent states and $\tau_1E\tau'_1, \tau_2E\tau'_2, \dots, \tau_4E\tau'_4$ are the measurement equivalent transitions. Let us consider an O -trace $a_1, a_2, a_3, a_4, a_{11}$ by virtue of G -transitions $\tau_1(\tau'_1), \tau_2(\tau'_2), \tau_3(\tau'_3), \tau_4(\tau'_4), \tau'_5$. On observing O -transitions a_1, a_2, a_3, a_4 by virtue of G -transitions $\tau_1(\tau'_1), \tau_2(\tau'_2), \tau_3(\tau'_3), \tau_4(\tau'_4)$ (corresponding events: T_1 Filling, V_1 Close, T_1 Full, T_2 Filling) the diagnoser moves to O -node z_4 . At O -node z_4 the controller has already issued commands to open valve V_3 in order to drain out the liquid from tank T_2 . Since the command the open the valve V_3 is issued, the output of flowmeter should be $Q_3 = 1$ under normal scenarios. However, the output of flowmeter should be $Q_3 = 0$. Comparing the transitions τ_5 and τ'_5 it can be observed that these transitions are *not* measurement equivalent. τ_5 (τ'_5) denotes flow (no flow) through the pipe after the controller has issued the commands for opening the valve V_3 . On observing $Q_3 = 0$, the diagnoser moves to O -node z_9 by virtue of G -transition τ'_5 (O -transition a_{10}). O -node z_{10} is an F_i -certain O -node, so the occurrence of the fault is ascertained. As no measurement inconsistency is observed, both the MLDES and MIDES based diagnosers handle the given O -trace $a_1, a_2, a_3, a_4, a_{11}$ in exactly the same manner. Now we look into those cases where measurement inconsistency are observed.

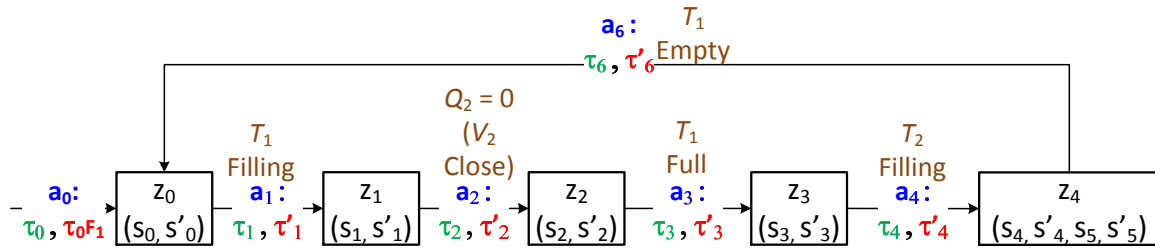


Figure 5.9: Case 2: MLDES diagnoser considering measurement inconsistent transition as unmeasurable.

Case 2: MLDES Diagnoser – Considering measurement inconsistent transition as unmeasurable: In this diagnoser shown in Fig. 5.9, let us assume that after the tank T_2 is full, the flow sensor (Q_3) cannot record the state of the flow because of measurement

inconsistency. Since measurement inconsistent transitions are assumed to be unmeasurable in this case, the model and diagnoser considers G -transitions τ_5, τ'_5 as permanently unmeasurable and hence not used for fault diagnosis. As G -transitions τ_5, τ'_5 are unmeasurable, the resultant O -node z_4 is composed of s_4, s'_4, s_5, s'_5 (s'_5 gets included because of unmeasurable reach of s'_4). As explained earlier, presence of F_i -indeterminate cycles leads to non-diagnosability. An F_i -indeterminate cycle requires two conditions to be satisfied: 1) Presence of F_i -uncertain cycle. 2) A faulty G -cycle within the F_i -uncertain cycle. The F_i -uncertain cycle is composed of the O -nodes $z_0, z_1, z_2, z_3, z_4, z_0$ and within the F_i -uncertain cycle, the faulty G -cycle is composed of the G -states $s'_0, s'_1, s'_2, s'_3, s'_4, s'_5$ making it an F_i -indeterminate cycle, leading to non-diagnosability. As a result, no fault diagnosis is possible in such a scenario. As it can be observed from Fig. 5.8, the transition τ'_5 is critical for fault diagnosis and since it is considered permanently unmeasurable because of measurement inconsistency the fault is rendered non-diagnosable. All future measurements of τ'_5 are never used for fault diagnosis thus, making a potential diagnosable system as non-diagnosable.

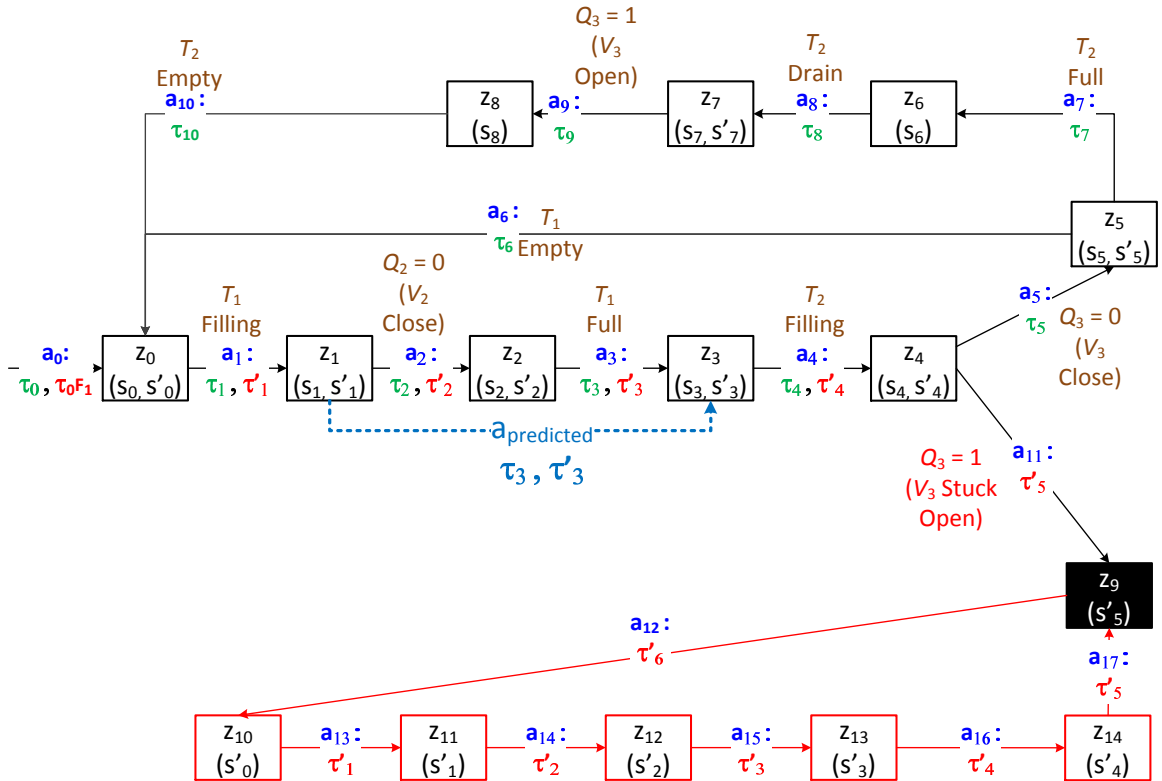


Figure 5.10: Case 3: MIDES diagnoser considering measurement inconsistent transition as measurable and tries to predict the possible O -node(s).

Case 3: MIDES Estimator Diagnoser – Considering measurement inconsistent transition as measurable and tries to predict the possible O -node(s)

Here, at O -node z_1 the diagnoser observes O -transition a_3 by virtue of G -transition $\tau_3(\tau'_3)$.

So the diagnoser comes to a halt. Now the proposed MIDES estimator diagnoser tries to predict the possible states the diagnoser could be in on observing the O -transition a_3 . The proposed MIDES estimator diagnoser predicts that the diagnoser would be in O -node z_3 (shown in dotted lines in Fig. 5.10) on observation of O -transition a_3 and starts fault diagnosis from z_3 . The detailed algorithm for the proposed MIDES estimator diagnoser is shown in Algorithm 5 and is explained next.

Algorithm 5: Estimator diagnoser for the MIDES framework

Input: z_{ub} : Measurement Inconsistent O -node, Measurement Inconsistent O -transition a_i by virtue of G -transition (τ_{ub}).

Output: Z_{ub} a union of O -node(s) z_1, z_2, \dots, z_n where $z_i (1 \leq i \leq n)$ is the possible O -node(s) the diagnoser is expected to be in when the measurement inconsistency occurs.

```

1  $Z_{ub} \leftarrow \phi$ 
2 foreach  $z \in RS_{z_{ub}}$  do
3   | if  $\tau_{ub} \in a_i$  such that  $a_i \in ITS(z)$  then
4   |   |  $Z_{ub} \leftarrow Z_{ub} \cup z$ 
5   | end
6 end
7 if  $\forall z \in Z_{ub}, z$  is  $F_i$ -certain then
8   | Occurrence of  $F_i$  is diagnosed. Exit
9 else if  $|Z_{ub}| == 1$  then
10  | Find the  $O$ -node  $z \in Z$  corresponding to  $z_{ub}$  and continue fault diagnosis with  $z$ 
    | as present  $O$ -node.
11 else
12  | Retain  $z_{ub}$  as it is and treat all future  $O$ -transition by virtue of  $G$ -transition  $\tau_{ub}$ 
    | in sequence as measurement inconsistent  $G$ -transition and goto Step 1.
13 end

```

Z_{ub} is initialized to null set (Line 1). Next, every O -node z that is reachable from O -node z_{ub} is calculated using $ITS(z)$ (Line 2). For every O -node z that is reachable from z_{ub} , its incoming transition set (Definition 59) is calculated (Line 3). It is possible that many O -nodes are reachable from z_{ub} whereas only few of those O -node(s) have an incoming O -transition a_i by virtue of the G -transition τ_{ub} in it. All those O -nodes that are reachable from z_{ub} and have an incoming O -transition a_i , by virtue of the G -transition τ_{ub} in it are stored in Z_{ub} (Line 4). The concept behind the incoming O -transition set and calculating the reachable O -node(s) is that, these O -nodes have an incoming O -transition containing the G -transition τ_{ub} and they represent the possible O -node(s) the diagnoser is expected to be in, on occurrence of the measurement inconsistent O -transition a_i . After all reachable O -node(s) and their incoming O -transition set are scanned, the resultant Z_{ub} is considered. If all the O -nodes z in Z_{ub} are F_i -certain (Line 7) then, fault F_i has surely occurred, as explained below. Z_{ub} represents the set of O -node(s) where the diagnoser is expected to

be in when the measurement inconsistency occurs. As all such O -node(s) are F_i -certain it implies that all the G -states in such nodes are faulty G -states. So F_i is considered diagnosed and the diagnosis procedure is complete. However, if some of the O -nodes in Z_{ub} are F_i -uncertain, then it is checked if Z_{ub} is a singleton set (Line 9). If yes, it is mapped directly to an O -node $z \in Z$ of the diagnoser and further diagnosis is carried out beginning from z (Line 10). If Z_{ub} contains multiple F_i -uncertain O -nodes (Line 11) the estimator diagnoser treats all future O -transitions by virtue of G -transitions $(\tau_1, \tau_2, \dots, \tau_j)$ in sequence as measurement inconsistent G -transition(s) and the process repeats (Line 12).

Using Algorithm 5, we look how MIDES estimator diagnoser handles the measurement inconsistent G -transition $\tau_3(\tau'_3)$. Here τ_{ub} is $\tau_3(\tau'_3)$ and z_{ub} is z_1 . We follow Algorithm 5 in a step wise manner for clarity. Z_{ub} is initialized to ϕ (Line 1). All O -nodes reachable from O -node z_1 are calculated using Definition 61 i.e., RS_{z_1} is $\{z_0, z_1, z_2, \dots, z_{15}\}$ (Line 2). For each of these O -nodes z its incoming transition set is calculated (Line 3). As a result, only those O -node(s) having an incoming O -transition a_i containing the G -transition $\tau_3(\tau'_3)$ are selected and stored in the set Z_{ub} . In this example, only the O -node z_3 satisfies the said criteria. So, the set Z_{ub} contains only z_3 (Line 4). However, the O -node z_3 is an F_i -uncertain O -node. Accordingly, the lines 7,8 of Algorithm 5 are skipped as it checks for the presence of only F_i -certain O -nodes. Z_{ub} consists of only single element (z_3) which can be mapped directly to the O -node $z_3 \in Z$ of the original diagnoser. Next, the diagnoser marks z_3 as its current O -node, measures the future G -transitions and continues the fault diagnosis starting from O -node z_3 (Line 9,10). As Z_{ub} consists of singleton O -node z_3 , lines 11, 12 of Algorithm 5 are skipped.

So by predicting the possible O -nodes on occurrence of measurement inconsistency (instead of assuming the event to be permanently unmeasurable), the MIDES framework handles the measurement inconsistency in an enhanced manner as compared to the MLDES framework.

Corollary 1. MIDES Diagnosability Condition: The MIDES diagnoser can diagnose a fault if the following two conditions hold: **1)** No F_i -indeterminate cycles. **2)** After any measurement inconsistency causing O -transition a_i by virtue of τ_{ub} is observed, the estimator diagnoser's prediction should result in a singleton O -node.

Proof: If the diagnoser contains F_i -indeterminate cycles then obviously the fault cannot be diagnosed. Once an inconsistency occurs the diagnoser can continue only when the estimator diagnoser's prediction results in a singleton O -node.

5.5 MIDES Model for Rogue DHCP Server Attack

The MIDES model G used to represent the rogue DHCP server under normal and attack scenarios is shown in Fig. 5.11 and is annotated with transition number τ_i and the event because of which the transition τ_i is fired. The transitions of the MIDES model G are explained in Table 5.4. States and transitions belonging to normal (attack) model are denoted by the non-primed (primed) notations. For simplicity of illustration, we assume that the attack initiates from the start state i.e., state s_0 . As already stated, the occurrence of attack is unmeasurable so the corresponding transition ($\tau_i F_i$) associated with the occurrence of attack is also unmeasurable. Our proposed MIDES based IDS works even if multiple genuine and rogue DHCP server exists in the network. However, for simplicity of illustration we consider that two genuine and one rogue DHCP server are present. The IDS maintains a whitelist of the IP and MAC addresses of both the genuine DHCP servers as well as IP-MAC mappings of the dummy clients. The attacker is assumed to spoof the IP and MAC address of the genuine DHCP server.

The various components of the MIDES model G are as follows:

$$X = \{s_0, s_1, s_2, s_3, s_4, s_5, s_6, s_7, s_8, s_9, s_{10}, s'_0, s'_1, s'_2, s'_3, s'_4, s'_5, s'_6, s'_7, s'_8, s'_9, s'_{10}, s'_{11}, s'_{12}, s'_{13}, s'_{14}, s'_{15}, s'_{16}, s'_{17}, s'_{18}\}$$

$$\mathfrak{S} = \{\tau_1, \tau_2, \tau_3, \tau_4, \tau_5, \tau_6, \tau_7, \tau_8, \tau_9, \tau_{10}, \tau_{11}, \tau_{12}, \tau_{13}, \tau_{14}, \tau'_1, \tau'_2, \tau'_3, \tau'_4, \tau'_5, \tau'_6, \tau'_7, \tau'_8, \tau'_9, \tau'_{10}, \tau'_{11}, \tau'_{12}, \tau'_{13}, \tau'_{14}, \tau'_{15}, \tau'_{16}, \tau'_{17}, \tau'_{18}, \tau'_{19}, \tau'_{20}, \tau'_{21}, \tau'_{22}, \tau'_{23}, \tau'_{24}, \tau'_{25}, \tau'_{26}, \tau'_{27}\}$$

$\Sigma = \{\text{DHCPDISCOVER, DHCPPOFFER, DHCPREQUEST, DHCPACK, DHCP-PROBE, DHCP-PROBE-RESPONSE-OFFER, DHCPRELEASE, DEAUTHENTICATION, ACKNOWLEDGMENT}\}$. Σ is used to model the events associated with the corresponding transitions. The DHCP Handler generates all these events as well as stores the information associated with every corresponding event triggered into the model variables like $ips, macs, id$ which are explained below.

$V = \{ips, macs, id\}$ is the set of model variables. The model variable $macs(ips)$ stores the MAC (IP) address of the frame and its domain is $\{xx : xx : xx : xx : xx : xx | x \in [0 - F]\}$ ($\{x.x.x.x|x \in [0 - 255]\}$). The id (Transaction IDentifier) is a random number generated by the client and is used by both client and DHCP server for syncing DHCP message exchange between them. The domain of transaction ID is hexadecimal.

Henceforth in the discussion, we use the short notations shown in Table 5.3. A combination of notations is used for representing the packet features, e.g., $DHCPDIS_{IPS}$ represents the source IP address of the DHCPDISCOVER frame. The subscript can be any one of the $IPS, IPD, MACS, MACD$, or $TRANS_ID$.

Table 5.3: Notations used in DES modeling for rogue DHCP server

Notation	Meaning	Notation	Meaning
IPS	Source IP Address	$DHCPOFR$	DHCPOFFER Frame
IPD	Destination IP Address	$DHCPREQ$	DHCPREQUEST Frame
$MACS$	Source MAC Address	$DHCPACK$	DHCPACK Frame
$MACD$	Destination MAC Address	$DHCPPRB$	DHCP Probe Frame
$DHCPDIS$	DHCPDISCOVER Frame	$DHCPPRBRES$	DHCP Probe Response Frame
$DHCPREL$	DHCPRELEASE Frame	$DEAUTH$	DEAUTHENTICATION Frame
ACK	acknowledgment Frame	$TRANS_ID$	Transaction ID of DHCP Frame.

—**Behavior Under Normal Conditions:** States $\{s_0, s_1, s_2, s_3, s_4, s_5, s_6, s_7, s_8, s_9, s_{10}\}$ and transitions $\{\tau_1, \tau_2, \tau_3, \tau_4, \tau_5, \tau_6, \tau_7, \tau_8, \tau_9, \tau_{10}, \tau_{11}, \tau_{12}, \tau_{13}, \tau_{14}\}$ represent the system under **normal** conditions.

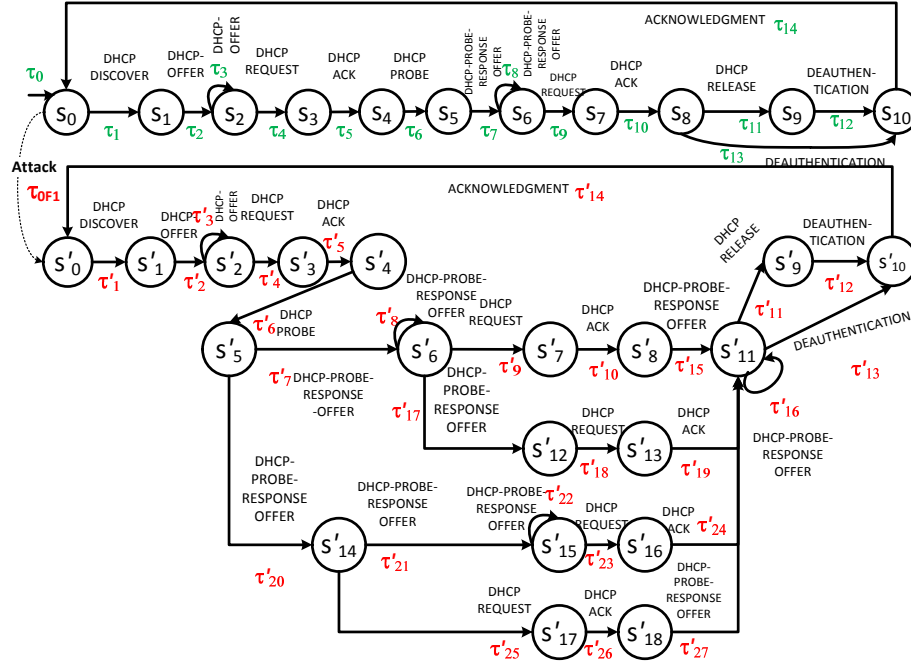


Figure 5.11: Normal and attack model in rogue DHCP server attack

- s_0 The model starts at state s_0 . At state s_0 , the client is about to send a DHCPDISCOVER frame to the DHCP server.
- $\tau_1(s_0 \rightarrow s_1)$: At state s_0 , the client sends a DHCPDISCOVER frame to the DHCP server and the model reaches state s_1 by traversing transition τ_1 . The “DHCP Handler” gets the “DHCPDISCOVER” frame and generates the “DHCPDISCOVER” event. The initial $(\tau_1) = s_0$, final $(\tau_1) = s_1$, $\sigma = \text{DHCPDISCOVER}$. As this is the first frame of the DHCP frame exchange, no checks are done; so $check(V) = \{--\}$ and $assign(V) = \{\mathbf{macs} \leftarrow \text{DHCPDIS}_{MACS}, \mathbf{id} \leftarrow \text{DHCPDIS}_{TRANS_ID}\}$. The model variables \mathbf{macs} and \mathbf{id}

are used to store the values of source MAC address and transaction ID of the DHCP message exchange, respectively. For example, $\mathbf{macs} \leftarrow DHCPDIS_{MACS}$ represents the assignment of SRC MAC address in the DHCPDISCOVER frame to model variable $macs$. If model variables (V) are not used it leads to state explosion problem as explained in previous chapters. The handler stores the information associated with each triggering event into the model variable.

- $\tau_2(s_1 \rightarrow s_2)$: After receiving the DHCPDISCOVER frame from the client the DHCP server replies with a DHCPOFFER frame. Event generated: “DHCPOFFER”. This is the first offer received by the client. Here $check(V) = \{ \mathbf{macs} \equiv DHCPOFR_{MACD}, \mathbf{id} \equiv DHCPOFR_{TRANS_ID} \}$. The transaction ID is used to sync DHCP four-way handshake. The check $macs \equiv DHCPOFR_{MACD}$ is done in order to ensure that the DHCPOFFER is for the same client that sent the DHCPDISCOVER in transition τ_1 . Hence the \mathbf{macs} is compared with the destination MAC address of the DHCPOFFER frame; the source and destination MAC of a request frame get reversed during a response frame. τ_3 is similar to τ_2 except that it represents the second DHCPOFFER to the client. For the subsequent transitions, the $check(V)$ and $assign(V)$ are similar to those explained

Table 5.4: Transition table for DES Model shown in Fig. 5.11. Assumption: 2 Genuine DHCP Servers and 1 Rogue DHCP Server

Transition	Initial State	Final State	Event	Check(V)	Assign(V)	Remarks
$\tau_1 (\tau'_1)$	$s_0 (s'_0)$	$s_1 (s'_1)$	DHCPDISCOVER	--	$\mathbf{macs} \leftarrow DHCPDIS_{MACS},$ $\mathbf{id} \leftarrow DHCPDIS_{TRANS_ID}$	Step 1 of four way DHCP handshake. DHCPDISCOVER
$\tau_2 (\tau'_2)$ $\tau_3 (\tau'_3)$	$s_1 (s'_1)$ $s_2 (s'_2)$	$s_2 (s'_2)$ $s_2 (s'_2)$	DHCPOFFER	$\mathbf{macs} \equiv DHCPOFR_{MACD},$ $\mathbf{id} \equiv DHCPOFR_{TRANS_ID}$	--	Step 2 of four way DHCP handshake. DHCPOFFER
$\tau_4 (\tau'_4)$	$s_2 (s'_2)$	$s_3 (s'_3)$	DHCPREQUEST	$\mathbf{macs} \equiv DHCPREQ_{MACS},$ $\mathbf{id} \equiv DHCPREQ_{TRANS_ID}$	--	Step 3 of four way DHCP handshake. DHCPREQUEST . (for DHCPOFFER of τ_2)
$\tau_5 (\tau'_5)$	$s_3 (s'_3)$	$s_4 (s'_4)$	DHCPACK	$\mathbf{macs} \equiv DHCPACK_{MACD},$ $\mathbf{id} \equiv DHCPACK_{TRANS_ID}$	--	Step 4 of four way DHCP handshake. DHCPACK . (for DHCPOFFER of τ_2)
$\tau_6 (\tau'_6)$	$s_4 (s'_4)$	$s_5 (s'_5)$	DHCP-PROBE	--	$\mathbf{ips} \leftarrow DHCPPRB_{IPS},$ $\mathbf{macs} \leftarrow DHCPPRB_{MACS},$ $\mathbf{id} \leftarrow DHCPPRB_{TRANS_ID}$	DHCP probe on behalf of dummy client (sent by IDS).
$\tau_7 (\tau'_7)$ $\tau_{21} (\tau'_{16})$ $\tau_{27} (\tau'_{22})$ $\tau_8 (\tau'_8)$	$s_5 (s'_5)$ $s'_{14} (s'_{11})$ $s'_{18} (s'_{15})$ $s_6 (s'_6)$	$s_6 (s'_6)$ $s'_{15} (s'_{11})$ $s'_{11} (s'_{15})$ $s_6 (s'_6)$	DHCP-PROBE-RESPONSE-OFFER	$\mathbf{macs} \equiv DHCPPRBRES_{MACD},$ $\mathbf{id} \equiv DHCPPRBRES_{TRANS_ID},$ $\mathbf{ips} \equiv DHCPPRBRES_{IPD},$	--	Pre-Configured IP obtained. Rogue DHCP server absent.
$\tau_9 (\tau'_9)$ $\tau'_{18} (\tau'_{23})$ τ_{25}	$s_6 (s'_6)$ $s'_{12} (s'_{15})$ s'_{14}	$s_7 (s'_7)$ $s'_{13} (s'_{16})$ s'_{17}	DHCPREQUEST	$\mathbf{macs} \equiv DHCPREQ_{MACS},$ $\mathbf{id} \equiv DHCPREQ_{TRANS_ID}$	--	DHCPREQUEST for DHCP-PROBE.
$\tau_{10} (\tau'_{10})$ $\tau'_{19} (\tau'_{24})$ τ_{26}	$s_7 (s'_7)$ $s'_{13} (s'_{16})$ s'_{17}	$s_8 (s'_8)$ $s'_{11} (s'_{11})$ s'_{18}	DHCPACK	$\mathbf{macs} \equiv DHCPACK_{MACD},$ $\mathbf{id} \equiv DHCPACK_{TRANS_ID}$	--	DHCPACK for DHCP-PROBE..
$\tau_{11} (\tau'_{11})$	$s_8 (s'_{11})$	$s_9 (s'_9)$	DHCPRELEASE	$\mathbf{macs} \equiv DHCPREL_{MACS}$	--	DHCPRELEASE
$\tau_{13} (\tau'_{13})$ $\tau_{12} (\tau'_{12})$	$s_8 (s'_{11})$ $s_9 (s'_9)$	$s_{10} (s'_{10})$ $s_{10} (s'_{10})$	DEAUTHENTICATION	$\mathbf{macs} \equiv DEAUTH_{MACS}$	--	DEAUTHENTICATION
$\tau_{14} (\tau'_{14})$	$s_{10} (s'_{10})$	$s_0 (s'_0)$	acknowledgment	$\mathbf{macs} \equiv ACK_{MACD}$	--	acknowledgment from the AP
τ'_{15} τ'_{17} τ_{20}	s'_8 s'_6 s'_5	s'_{11} s'_{12} s'_{14}	DHCP-PROBE-RESPONSE-OFFER	$\mathbf{macs} \equiv DHCPPRBRES_{MACD},$ $\mathbf{id} \equiv DHCPPRBRES_{TRANS_ID},$ $\mathbf{ips} \neq DHCPPRBRES_{IPD}$	--	Non Pre-Configured IP obtained. Rogue DHCP Server Present.

in transitions τ_1, τ_2 and can be referred from Table 5.4. Table 5.4 also has the *Remarks* column that explains the significance of the particular event observed.

- $\tau_4(s_2 \rightarrow s_3)$: At state s_2 , the client accepts one of the two offers it received. Event generated: “DHCPREQUEST”. On acceptance, the client sends a DHCPREQUEST frame to the DHCP server whose IP address is selected by the client.
- $\tau_5(s_3 \rightarrow s_4)$: The transition τ_4 is the DHCPACK frame sent by the DHCP server to the client. Event generated: “DHCPACK”. This confirms the mapping of the IP address of the client with the DHCP server along with a lease.
- $\tau_6(s_4 \rightarrow s_5)$: The transition sequence $\langle \tau_1, \tau_2, \tau_3, \tau_4 \rangle$ represents the four way DHCP handshake. In order to verify that the IP address assigned to the client is by the genuine DHCP server, the IDS broadcast the DHCP probe frame. Event generated: “DHCP-PROBE”. The DHCP probe is a DHCPDISCOVER frame with source MAC address set to the MAC address of the dummy client. Here: $check(V) = \{--\}$ and $assign(V) = \{ \mathbf{ips} \leftarrow DHCPPRB_{IPS}, \mathbf{macs} \leftarrow DHCPPRB_{MACS}, \mathbf{id} \leftarrow DHCPPRB_{TRANS_ID} \}$. Here **macs** stores the dummy client’s MAC address.
- $\tau_7(s_5 \rightarrow s_6)$: The transition τ_7 represents the DHCP probe response to the DHCP probe (τ_6) sent by the IDS. Event generated: “DHCP-PROBE-RESPONSE-OFFER”. The DHCP probe response is a DHCP OFFER frame that contains the IP address offered to the dummy client by the DHCP server. Here: $check(V) = \{ \mathbf{macs} \equiv DHCPPRBRES_{MACD}, \mathbf{id} \equiv DHCPPRBRES_{TRANS_ID}, \mathbf{ips} \equiv DHCPPRBRES_{IPD} \}$. Under normal circumstances, the IP address offered is the same as the one pre-configured at the DHCP server. In DHCP-PROBE-RESPONSE-OFFER, the offered IP address by the DHCP server is checked ($\mathbf{ips} \equiv DHCPPRBRES_{IPD}$) to ensure that the IP address assigned to the dummy client matches with the one that is pre-configured for it at the DHCP server. τ_8 is the second DHCP-PROBE-RESPONSE-OFFER similar to τ_7 .
- $\tau_9(s_6 \rightarrow s_7)$ and $\tau_{10}(s_7 \rightarrow s_8)$: The transitions τ_9 and τ_{10} represent the DHCPREQUEST and DHCPACK frames, respectively of the above DHCP probe response. Their explanation is similar to the transitions τ_4 and τ_5 explained earlier. The ‘DHCP Handler’ generates the “DHCPREQUEST” (τ_8) and “DHCPACK” (τ_9) event, respectively.
- $\tau_{11}(s_8 \rightarrow s_9)$: The transition τ_{11} represents the DHCPRELEASE frame. Event generated: “DHCPRELEASE”. A client sends a DHCPRELEASE frame when it wishes to no longer use the IP address assigned by the DHCP server.
- $\tau_{12}(s_9 \rightarrow s_{10})$ and $\tau_{13}(s_8 \rightarrow s_{10})$ The clients may directly send a deauthentication frame

to leave the network. Event generated: “DEAUTHENTICATION”. The transitions τ_{12}, τ_{13} represent the sending of deauthentication frame by the client.

- $\tau_{14}(s_{10} \rightarrow s_0)$: The AP sends an acknowledgment (ACK) frame to the client sending the deauthentication frame. The “DHCP Handler” generates the “Acknowledgment” event.

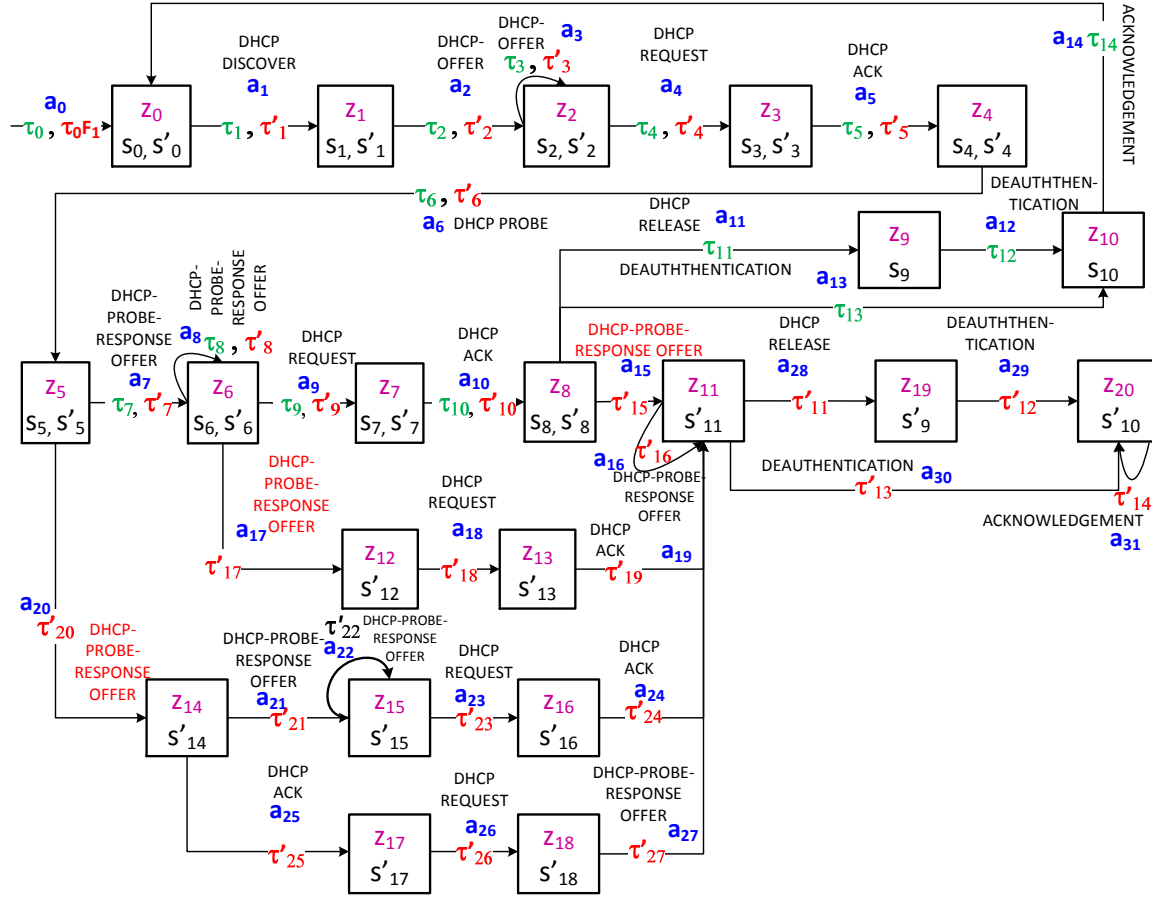


Figure 5.12: Diagnoser for rogue DHCP server attack

—**Behavior Under Attack Conditions:** States $\{s'_0, s'_1, s'_2, s'_3, s'_4, s'_5, s'_6, s'_7, s'_8, s'_9, s'_{10}, s'_{11}, s'_{12}, s'_{13}, s'_{14}, s'_{15}, s'_{16}, s'_{17}, s'_{18}\}$ and transitions $\{\tau'_1, \tau'_2, \tau'_3, \tau'_4, \tau'_5, \tau'_6, \tau'_7, \tau'_8, \tau'_9, \tau'_{10}, \tau'_{11}, \tau'_{12}, \tau'_{13}, \tau'_{14}, \tau'_{15}, \tau'_{16}, \tau'_{17}, \tau'_{18}, \tau'_{19}, \tau'_{20}, \tau'_{21}, \tau'_{22}, \tau'_{23}, \tau'_{24}, \tau'_{25}, \tau'_{26}, \tau'_{27}\}$ represent the system under **attack** conditions. For attack conditions we discuss only those states and transitions that differ from the normal scenario.

- $\tau'_{15}(s'_8 \rightarrow s'_{11})$, $\tau'_{17}(s'_6 \rightarrow s'_{12})$, and $\tau'_{20}(s'_5 \rightarrow s'_{14})$: The transitions τ'_{15} , τ'_{17} and τ'_{20} represents the “DHCP probe response” to the DHCP probe sent by the IDS. Event generated: “DHCP-PROBE-RESPONSE-OFFER”. Under attack conditions the DHCP-PROBE-RESPONSE-OFFER frame offers an IP address which is *different* than the one pre-configured at the DHCP server for the dummy client. Here $check(V) = \{ \mathbf{macs} \equiv DHCPPRBRES_{MACD},$

$\mathbf{id} \equiv DHCPRBRES_{TRANS_ID}$, $\mathbf{ips} \neq DHCPRBRES_{IPD}$ }. The check $\mathbf{ips} \neq DHCPRBRES_{IPD}$ signifies that the offered IP address to the dummy client *differs* from the one that is pre-configured for the dummy client.

Diagnoser construction for rogue DHCP server attack

Fig. 5.12 is the diagnoser for the MIDES model G shown in Fig. 5.11. In order for the diagnoser to detect the rogue DHCP server attack, the diagnoser should reach any one of the F_i -certain O -node(s) $z_{11}, z_{12}, z_{13}, z_{14}, z_{15}, z_{16}, z_{17}, z_{18}, z_{19}$ or z_{20} . However, if the diagnoser gets stuck in an F_i -indeterminate cycle before reaching any of the F_i -certain O -nodes it leads to non-diagnosability. On observing the MIDES diagnoser shown in Fig. 5.12, there are two cycles. a) Cycle 1 is composed of O -nodes $z_0, z_1, z_2, z_3, z_4, z_5, z_6, z_7, z_8, z_9, z_{10}, z_0$. However, this is an F_i -uncertain cycle and not an F_i -indeterminate cycle as there is no loop involving the failure transitions (i.e., F_i -transitions of cycle 1 $\tau'_1, \tau'_2, \tau'_3, \tau'_4, \tau'_5, \tau'_6, \tau'_7, \tau'_8, \tau'_9, \tau'_{10}$ does not form a cycle in G). b) Similar reasons hold for second F_i -uncertain cycle which is composed of O -nodes $z_0, z_1, z_2, z_3, z_4, z_5, z_6, z_7, z_8, z_{10}, z_0$. As the diagnoser does not have any F_i -indeterminate cycles, the fault is diagnosable (i.e., rogue DHCP server can be detected) even if the traditional MLDES framework is used and no measurement inconsistency is observed. However, if measurement inconsistency is observed, it may lead to non-diagnosability if MLDES framework is used. Now, we look at an example on how the proposed MIDES based IDS detects the rogue DHCP server attack if measurement inconsistent transition is observed.

5.5.1 An Example of Rogue DHCP Server Attack Detection Using MIDES Diagnoser

Let us assume that the sequence of frames observed is in the following order: DHCPDISCOVER, DHCPOFFER, DHCPOFFER, DHCPREQUEST, DHCPACK, DHCP-PROBE, DHCP-PROBE-RESPONSE-OFFER, DHCP-PROBE-RESPONSE-OFFER, DHCPREQUEST, DHCP-PROBE-RESPONSE-OFFER. On observing DHCPDISCOVER frame the diagnoser moves from O -node z_0 to z_1 via the G -transition $\tau_1(\tau'_1)$. As τ_1 and τ'_1 are measurement equivalent it cannot be ascertained at this point whether an attack has taken place or not. On observing the subsequent events, it can be noted that the diagnoser on observing the DHCPREQUEST frame reaches the O -node z_7 . Now the diagnoser observes the DHCP-PROBE-RESPONSE-OFFER frame which results in measurement inconsistency, as no outgoing transition from O -node z_7 consists of the DHCP-PROBE-RESPONSE-OFFER event (transition τ'_{15}). So the estimator diagnoser starts to predict the possible O -nodes that can be directly reached from z_7 using the 'Reach-

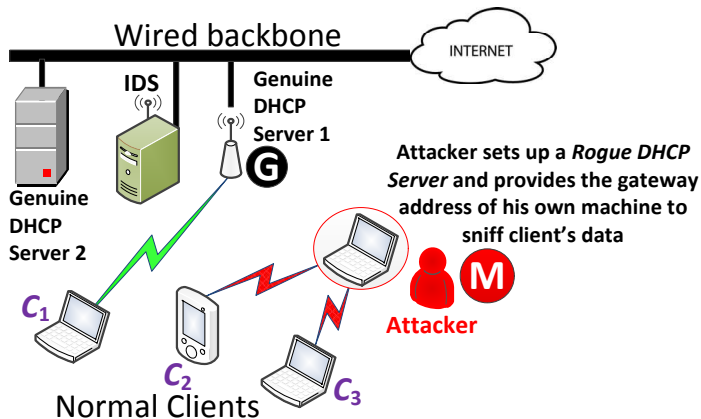


Figure 5.13: Experimental setup for rogue DHCP server attack

able O -node set RS_{z_i} defined in Definition 61. RS_{z_7} is: $(z_8, z_9, z_{10}, z_{11}, z_{19}, z_{20})$. For each O -node in RS_{z_7} , the incoming G -transition(s) are checked against the G -transition (τ'_{15}) . We observe that only the O -node z_{11} remains out of all the reachable O -node(s), that fulfills the criteria of reachability and has an incoming O -transition a_{15} caused by G -transition τ'_{15} . Now, the predicted O -node z_{11} can be mapped directly to the O -node $z_{11} \in Z$ of the original diagnoser. So, the diagnoser marks z_{11} as its current state and continues the fault diagnosis. As the O -node z_{11} traversed by the diagnoser is an F_i -certain O -node, the system is under faulty (attack) conditions. Thus, the proposed MIDES framework helps to detect the presence of rogue DHCP server even if measurement inconsistency occurs.

5.6 Results and Discussions

In this section we show the network test bed, the detection rate, accuracy and network load of the proposed IDS followed by the proof of the correctness.

5.6.1 Network Setup for Rogue DHCP Server Attack

The network setup for the rogue DHCP server attack is shown in Fig. 5.13. We denote C_1 as the client, G as the genuine AP with DHCP configured. As seen there are two DHCP servers, the first being the AP G itself and second one on the wired side. The rogue DHCP server is setup on a machine having Kali Linux 2.0 (x64) operating system with kernel 4.0 using the *isc-dhcp-server* package which provides a DHCP server environment. The IDS is located close to the genuine AP G so that frames traveling to and fro from the genuine AP are not lost. The IDS is implemented in *python* using the *scapy* library which possess both frame capturing and injection capabilities. The IDS runs on an Ubuntu 14.04 (x64)

machine having Wi-Fi connectivity. We have used smart-phones, laptops, and desktops equipped with wireless card as clients for testing the IDS.

5.6.2 Detection Rate and Accuracy of the Proposed MIDES Based IDS

The metrics used for measuring the performance of IDS are detection rate and accuracy. Detection Rate is defined as the number of attacks detected by the IDS to the total number of attacks actually present. $Detection\ Rate = TP / (TP + FN)$. Accuracy is the proportion of the total number of attacks that are correctly detected. $Accuracy = TP / (TP + FP)$. Here, TP is True Positive, FP is False Positive, and FN is False Negative. A TP is an instance, which is actually an attack and is classified as attack by the IDS. A $FP(FN)$ is a case when an IDS classifies a normal(attack) activity as attack(normal) activity.

Table 5.5: Detection rate statistics with and without the use of measurement inconsistent based IDS

Run #	Attack Instances launched	Instances detected using MLDES based IDS	Instances detected using MIDES based IDS	Undetected Cases using MIDES Based IDS	Detection Rate using MLDES	Detection Rate using MIDES	% Improvement
1	120	109	118	2	90.83	98.33	7.50
2	120	112	117	3	93.33	97.50	4.17
3	120	104	120	0	86.67	100.00	13.33
4	120	106	120	0	88.33	100.00	11.67
5	120	120	120	0	100.00	100.00	0.00
Average Improvement in detection rate because of Measurement Inconsistent based DES					91.83	99.17	7.33

Table 5.5 shows the detection rate of the IDS under MLDES and MIDES framework and the improvement observed because of the application of MIDES framework. In every run shown in Table 5.5, 120 instances of the DHCPDISCOVER messages are sent in presence of two genuine and one rogue DHCP server and their responses are recorded. As seen, the lowest detection rate observed using MLDES framework is mere 86.67% and the average detection rate during the 5 runs is 91.83%. In contrast to this, when the proposed MIDES framework is applied the average detection rate during the 5 runs increases to 99.17%. As explained earlier, Wi-Fi being a lossy medium, few frames might get lost in transit. The MLDES fails to detect the presence of rogue DHCP server in case few frame(s) are lost. But, the proposed MIDES based IDS has the ability to detect the rogue DHCP server even if few frame(s) are lost thereby leading to higher attack detection rate.

A point to be noted here is that, even after the application of the MIDES framework the IDS does not have a detection rate of 100% in all the cases. This is because if the key frames responsible for the detection of rogue DHCP server are lost, the MIDES based IDS is unable to detect the attack. Few cases arise when the set Z_{ub} contains more than one O -node which cannot be mapped to any singleton O -node of the diagnoser. This results in uncertainty.

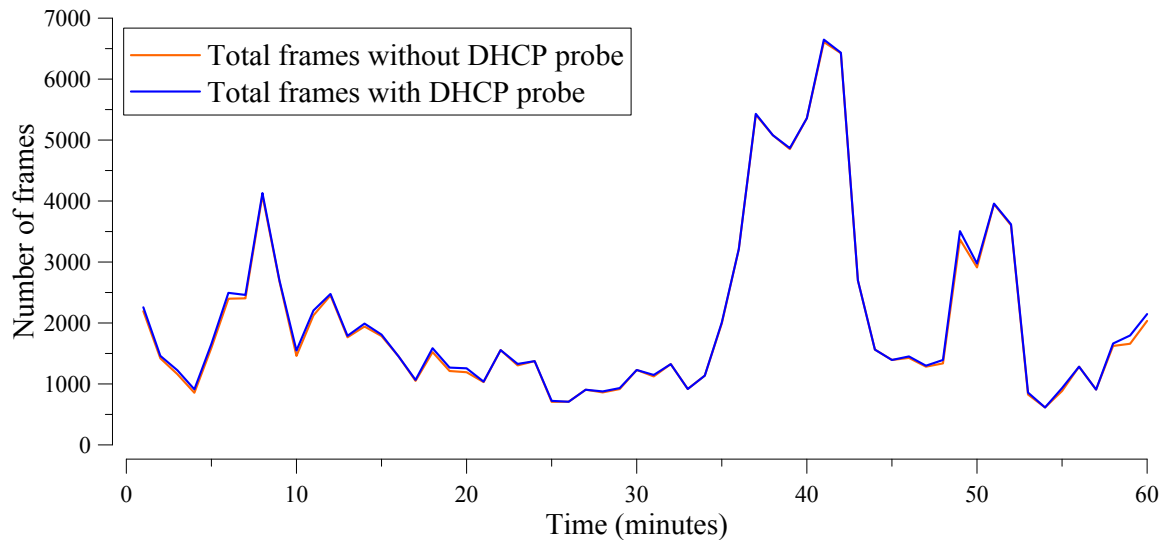


Figure 5.14: Network load with and without IDS

Capturing errors also results in lower detection rate. For example, if the IDS captures only one DHCP offer frame out of three possible offers and the captured frame belongs to the genuine DHCP server, the proposed IDS treats it as normal network activity. On the other hand, the accuracy touches 100% in all the runs. The IDS alerts for the presence of rogue DHCP server only when it receives a non-predefined IP address in response to a DHCP-PROBE. So, obviously there cannot be any false positives as the attacker does not have the IP-MAC mapping configured at the genuine DHCP server ensuring 100% accuracy. because, once the IDS receives a DHCP probe response containing a non-predefined IP address, the presence of rogue DHCP server is confirmed.

5.6.3 Network Load because of DHCP Probes

In Fig. 5.14 we show the number of frames seen in the network with and without the use of IDS. With the use of proposed IDS, DHCP probes are injected into the network as a part of the detection methodology. However, it can be seen in Fig. 5.14 that despite the injection of the DHCP probes into the network, the total frames seen in the network with and without the IDS are almost same. This signifies that traffic injection because of DHCP probes is low. Thus, it can be seen that the proposed MIDES based IDS detects the presence of rogue DHCP server effectively.

5.6.4 Correctness of the MIDES Diagnoser

The MIDES modeling helps us to formalize a given system and check for correctness and completeness [72]. In this section we show the correctness and completeness of the proposed scheme by considering all the exhaustive cases of the rogue DHCP server attack. For every case considered, we have shown that the proposed scheme successfully detects the presence of the rogue DHCP server attack. The proving of correctness and completeness by considering all the exhaustive cases helps to ascertain that the attacker does not escape from detection, thus making the detection scheme robust.

There are a number of ways in which the rogue DHCP server attack can be launched. In order to prove the correctness of the diagnoser shown in Fig. 5.12, we consider five possible cases based on the arrival of DHCP frames. We assume that two genuine and one rogue DHCP server are present.

1. *Attacker present and its offer is received after receiving two offers from the genuine DHCP server:* In this case, after receipt of multiple DHCPOFFERs the IDS sends a DHCP-PROBE. For the DHCP-PROBE, 3 offers are obtained. Here we assume that both the genuine DHCP server have already responded before the attacker replies with a DHCPOFFER. On obtaining two DHCP offers the diagnoser reaches O -node z_6 . Upon observing the third DHCP-PROBE-RESPONSE-OFFER, the MIDES diagnoser reaches the O -node z_{12} which is an F_i -certain (attack certain) O -node. So, the MIDES diagnoser correctly identifies the presence of attack.
2. *Attacker present and its offer is received before the two offers are sent from the genuine DHCP server:* This is similar to the case explained above. On observation of a DHCP-PROBE-RESPONSE-OFFER containing a non-pre-configured IP address, the diagnoser reaches the O -node z_{14} . As z_{14} is an F_i -certain O -node, the MIDES diagnoser correctly identifies the presence of the attack.
3. *Attacker present and its offer is received between the two offers are sent from the genuine DHCP server:* This is similar to the case explained above. On observation of a DHCP-PROBE-RESPONSE-OFFER containing a non-pre-configured IP address, the diagnoser reaches the O -node z_{12} . As z_{14} is an F_i -certain O -node, the MIDES diagnoser correctly identifies the presence of the attack.
4. *Attacker present but is passive:* Here, the attacker is present in the network, but only listens to the network traffic passively. No frame injection is done by the attacker. So, when two DHCPOFFERs are seen in the network and the DHCP probe is sent, only the reply from the genuine DHCP server is seen. Both the offers contain pre-configured IP

address. The O -trace traversed by the diagnoser is z_0, z_1, \dots, z_{10} none of which are F_i -certain (attack) O -node. So, the MIDES diagnoser reports correctly that the network is under normal conditions.

5. *Attacker absent*: Here, the attacker is not present in the network. This case is identical to Case 4.

So, all possible cases of arrival of DHCP frames are analyzed and the diagnoser which is implemented as an IDS engine correctly reports the network conditions in each of the case.

5.6.5 Discussion

Table 5.6 compares the various existing mitigation techniques for the rogue DHCP server attack. We have categorized the rogue DHCP server as simple and evil. In an evil (simple) rogue DHCP server attack the attacker spoofs (does not spoof) the IP and MAC address of the genuine DHCP server. The other features that we compare are the requirements of authentication, digital certificates, protocol changes and resource overhead. The remarks column of Table 5.6 describes the pros and cons of the techniques discussed.

Table 5.6: Comparison of existing mitigation solutions for Rogue DHCP Server attack

Method	Detects Simple Rogue DHCP Server	Detects Evil Rogue DHCP Server	Requires authentication	Requires Digital Certificate	Protocol Changes Required	Overhead	Remarks
DHCP Snooping [81]	N	N	N	N	N	N	Difficult to deploy. Requires Switch Configuration. Works on wired LAN.
Network Scan [82]	Y	N	N	N	N	High	Cannot detect the evil rogue DHCP server.
Authentication [83]	Y	Y	Y	Could be used	Y	High	Increase in resource overhead because of authentication
Digital Certificate [86, ?]	Y	Y	Y	Y	Y	High	Issues like certificate management, revocation, trust issues etc.
Proposed Scheme	Y	Y	N	N	N	Low	Easy to deploy. Free of Digital Certificates. Low resource overhead. Formally verifiable. No protocol modification required.

5.7 Conclusion

In this chapter, we proposed MIDES framework that can perform fault diagnosis even if measurement inconsistent transitions are observed. The traditional MLDES framework models inconsistency as permanently unmeasurable, thereby making fault diagnosis weak. The proposed MIDES estimator diagnoser is based on measurement inconsistency and predicts the possible system state by using the subsequent measured transitions, thereby improving the fault diagnosis. We have illustrated the efficacy of our proposed framework using a benchmark process of two-tank system. Further, the proposed MIDES framework is also used to develop an IDS for detection of the rogue DHCP server attack in Wi-Fi networks.

The proposed IDS detects the rogue DHCP server with high detection rate and accuracy as the lost frames are not considered permanently unmeasurable unlike MLDES. A slight increase in the network traffic is seen for the proposed IDS because of the injection of DHCP probes. However, given the improvement in attack detection rate and accuracy of the proposed IDS the slight increase in the network traffic induced because of probing is acceptable. Other major advantages of the proposed IDS is that it does not require any encryption algorithms, protocol modifications, or firmware upgrades either on the AP or on the clients and encompasses all the salient features of the MLDES framework. Although the proposed framework has been shown for rogue DHCP server attack, it can be applied to any system that contains factors which may lead to inconsistency.

The MIDES framework can also be used to detect all the previous attacks that have been discussed in Chapters 2-4. However, the MIDES framework needs to be adapted in accordance to the respective attack. For example, in PS-DoS attack the RTDES framework incorporates the timing related information in the model but assumes measurement inconsistency as permanently unmeasurable. If MIDES framework is used along with the RTDES framework, the resultant framework can take care of both the timing information in the DES model as well as deal with measurement inconsistency more efficiently. In this manner, MIDES framework can be applied to existing DES frameworks in order to provide more robust fault (attack) detection.



“You can’t hold firewalls and intrusion detection systems accountable. You can only hold people accountable.”

Daryl White,
U.S. Department of the Interior, Chief Information Officer

6

Conclusions and Future Work

The exponential growth of Wi-Fi networks across the globe has brought about a paradigm shift in the way humans communicate. An array of Wi-Fi Access Points (APs) are deployed at various locations from airports, libraries and shopping malls to coffee shops and hospitals, to provide Internet connectivity. Many of these APs are open and unsecured making them a soft target for attackers. An attacker present within the wireless range of a communicating client and AP can easily sniff their data exchange. An attacker can use this information to launch various attacks on the clients and the AP. In addition to this, the inherent protocol vulnerabilities that exist at the lower layers of the 802.11 protocol stack make it difficult to prevent various attacks.

An Intrusion Detection System (IDS) is deployed these days in most of the networks as the principal network security component. An IDS monitors the network for malicious activities and raises an alarm when it finds one. By raising an alarm, it provides an opportunity for the network administrator to take corrective steps so that the threat does not spread or inflict further damage. An IDS can be broadly classified as signature and anomaly-based depending on their approach to detect malicious activity. Signature-based IDS uses fix patterns (known as signatures) while anomaly-based IDS uses statistical values to detect presence of malicious activities. However, there are certain classes of known attacks like evil twin attack, Stealth Man-in-the-Middle (SMiTM) attack, power save Denial of Service (DoS) attack, rogue Dynamic Host Control Protocol (DHCP) attack etc. for which these IDSs cannot generate effective alarms. For these attacks signatures cannot be written because they do not change the semantics and sequence of network frames. Further, these attacks do not bring about a significant change in the behavior of the system. As a result, if anomaly-based IDS is used for detecting such attacks, it leads to generation of large number of false

alarms.

Existing methods to detect these attacks include patching client software, use of preshared keys, network wide scanning, encryption, use of digital certificates, proprietary hardware, upgrading software/hardware or modification in the 802.11 protocol. These techniques suffer from various drawbacks like expensive setup and deployment, scalability issues, change in protocol, difficulty in deploying to existing Wi-Fi networks, lacking formalism etc. Every attack poses its own set of characteristics and challenges, so the IDS needs to be tuned in appropriately.

Recently, with phenomenal growth in man made and highly complex dynamic systems, Discrete Event Systems (DES) has been widely used to model different aspects of these systems such as automation systems, computer systems, networks, communication systems, power plants and analog circuits, manufacturing systems, traffic systems etc. Failure Detection and Diagnosis (FDD) of DES has been widely used to determine if the system is working under normal or faulty condition.

6.1 Summary of Contribution of the Thesis

In this thesis, we have devised mechanism for detecting MAC layer attacks of the 802.11 Wi-Fi networks. We have adopted FDD theory of DES to detect the different MAC layer attacks. The individual contributions of each chapters through 2 to 5 are as follows:

Contributions of Chapter 2: An evil twin is a Rogue Access Point (RAP) setup by cloning the MAC address and the SSID (network name) of an existing AP. An evil twin is setup by an attacker to lure the clients into connecting to them. Once a client is connected, an attacker eavesdrops on its communication to steal confidential information. In this contribution we proposed a detection mechanism for evil twin using a DES based IDS. For detecting evil twin attack, the frame exchange between the client, genuine AP and the evil twin AP are analyzed and based on the frame features the presence of evil twin is ascertained. The IDS ensures that the attacker setting up the evil twin is caught the moment it sends a successful association request to the client. An attacker can tweak various frame features in order to escape detection, however the IDS is capable to detect all such instances of evil twin attack. The framework does not require protocol modifications, encryption or certificate management etc. Further, this being a software based approach which runs in one host and does not require any kind of software or hardware upgrading or software patching on the client/AP.

Contributions of Chapter 3: We propose the ASMiTM attack and an I²-DES based IDS

for its detection. In ASMiTM attack an attacker poisons the ARP cache of a victim in a Wi-Fi Protected Access II (WPA2) encrypted Wi-Fi network. ASMiTM attack cannot be detected by passively observing the frame exchange between the client, attacker and AP. In ASMiTM attack the genuinity of network traffic is verified by sending suitable ARP probe packets to the hosts and validating their responses. The ARP probes are normal ARP frames crafted with special parameters to determine if the attack has taken place or not.

For ASMiTM attack, deterministic diagnosis of states is not sufficient because of inherent uncertainties (because of increase in PACNUM value) in the ARP request frame by the attacker. So there are paths in the DES model which lead to uncertain states about the presence of an attack. To deal with this, I²-diagnosability framework has been adopted where empowering and indicator events are defined. Failure diagnosis is tested only on path(s) where a fault is followed by an empowering and indicator event. The I-diagnosis framework does not guarantee detection of ASMiTM attack as it does not check for the empowering event. The detection scheme is successfully validated on a testbed with differential probing rates and the results show the effectiveness of the proposed technique.

Contributions of Chapter 4: The 802.11 Wi-Fi standard provides power management feature that allow clients to enter into sleep state to preserve energy without any frame losses. In PS-DoS attack, the attacker exploits the vulnerability of the power save feature to retrieve the buffered frame(s) of the sleeping clients from the AP causing frame losses for the targeted client(s). In this contribution a novel scheme has been proposed which can detect the presence of PS-DoS attacker by injecting power save probes in the network and analyzing their responses. As compared to the evil twin and ASMiTM attack, the PS-DoS attack manifests itself with respect to timing information associated with the frame transmission. So, simply checking for the frame features of the null data frames do not help to detect the presence of PS-DoS attack. Accordingly an RTDES framework has been chosen for designing an IDS for PS-DoS attack as it can incorporate timing information in the DES model. The detection mechanism is verified on a test bed and results illustrated high detection rate and 100% accuracy with little increase in the network overhead because of power save probe injection.

Contributions of Chapter 5: In the above three contributions, DES modeling is designed assuming there are no frame losses. Wi-Fi being a lossy medium frame losses are not uncommon. Although the accuracy of our proposed IDSs stays at 100%, the detection rate varies because of frame losses. All the DES paradigms discussed earlier consider frame losses as permanently unmeasurable thereby affecting the detection rate. In the last contribution, we propose a new DES paradigm known as the MIDES which can perform attack detection even under frame losses.

For showing its practical utility we have developed a MIDES based detection mechanism for the rogue DHCP server attack in Wi-Fi network. The MIDES based IDS has an additional feature that it can detect the presence of rogue DHCP server even if few frames are missed by the IDS because of capturing errors. An attacker sets up a rogue DHCP server (software based DHCP server) by spoofing the IP and MAC address of the genuine DHCP server and sending fictitious IP address, DNS and gateway address (or a combination of these) to the client requesting DHCP services. By supplying wrong default gateway and DNS server address an attacker can re-direct client's traffic via its terminal thereby sniffing client's information, re-directing clients to phishing websites, install malware into the client's machine etc. The proposed IDS does not violate the standard DHCP because the only additional requirement is the DHCP probes, which are nothing but DHCP related frames. Experimental results illustrated high attack detection rate and 100% accuracy for rogue DHCP server attack. We also show that the proposed MIDES based IDS improves in terms of detection rate as compared to the traditional MLDES based IDS.

6.2 Scope of Future Work

The IDS mechanism presented in this thesis successfully detects attacks prevalent on the MAC layer of the 802.11 protocol. Various DES paradigms like RTDES, I², MLDES, MIDES have been used depending on the characteristics of the attack under consideration. The following are possible future research direction.

- A unified or an integrated DES framework may be developed to deal with attacks in different scenarios.
- The proposed IDS works strictly for 802.11 networks. Various other protocols that use wireless transmission like 802.15.4, 802.16, Bluetooth, NFC also consist of various security vulnerabilities. We hope to extend the DES frameworks in order to detect security attacks in these protocols.
- With the advances in technology, it is now possible to achieve gigabit speeds in Wi-Fi networks. The advent of 802.11 ac/ad etc. are now replacing traditional Wi-Fi standard like 802.11 b/g/n. Frame capturing and processing on such high speed networks remains a challenging task and needs to be further explored.
- The Internet of Things (IoT) is a promising technology and has found applications across various domains like smart homes, smart grids, health monitoring, machine-to-machine (M2M) communication, home and building automation etc. IoT uses wire-

6.2. Scope of Future Work

less communication as a major means of transmitting information. As much of the information transmitted is sensitive in nature, attacker can launch various attacks to hijack the information. A DES framework can be used to ensure protection from such malicious users under IoT environment.



Bibliography

- [1] Kali Linux. <http://www.kali.org/>.
- [2] BackBox Linux. <http://www.backbox.org/>.
- [3] Aircrack-ng Suite. <http://www.aircrack-ng.org/>, 2015.
- [4] Scapy - A powerful interactive packet manipulation program. <http://www.secdev.org/projects/scapy/>.
- [5] Airpwn - Tool for generic packet injection on an 802.11 network. <http://sourceforge.net/projects/airpwn/>.
- [6] AirJack - device driver for 802.11(a/b/g) raw frame injection and reception.
- [7] WifiCopper 802.11b Packet Injector. <http://nutsaboutnets.com/wificopper-802-11-packet-injector/>.
- [8] CERT. Attack Prevention Technology White Paper. http://www.cert.org/stats/cert_stats.html.
- [9] M. G. Gouda and C. T. Huang. CSI/FBI computer crime and security survey. *Computer Security Journal*, XV(2):20–51, 1999.
- [10] Michael Kennedy and Rossilawati Sulaiman. Following the Wi-Fi breadcrumbs: Network based mobile application privacy threats. In *International Conference on Electrical Engineering and Informatics (ICEEI)*, pages 265–270. IEEE, 2015.
- [11] Huaxin Li, Zheyu Xu, Haojin Zhu, Di Ma, Shuai Li, and Kai Xing. Demographics inference through Wi-Fi network traffic analysis. In *IEEE INFOCOM 2016-The 35th Annual IEEE International Conference on Computer Communications*, pages 1–9. IEEE, 2016.
- [12] S. Plosz, A. Farshad, M. Tauber, C. Lesjak, T. Rupprechter, and N. Pereira. Security vulnerabilities and risks in industrial usage of wireless communication. In *Proceedings of the 2014 IEEE Emerging Technology and Factory Automation (ETFA)*, pages 1–8, September 2014.

- [13] Rajeev Singh and Teek Parval Sharma. On the IEEE 802.11i Security: A Denial of Service Perspective. *Security and Communication Networks*, 8(7):1378–1407, 2015.
- [14] R. Heady, G. Lugar, M. Servilla, and A. Maccabe. The Architecture of a Network Level Intrusion Detection System. Technical report, Department of Computer Science, University of New Mexico, 1990.
- [15] M. Roesch. SNORT - Lightweight Intrusion Detection for Networks. In *USENIX System Administration Conference*, pages 229–238, 1999.
- [16] P. A. Porras and P. G. Neumann. EMERALD: Event Monitoring Enabling Responses to Anomalous Live Disturbances. In *National Information Systems Security Conference*, pages 1–13, 1997.
- [17] V. Chandol, A. Banerjee, and V. Kumar. Anomaly detection: A Survey. *ACM Computing Survey*, 41(3):1–58, 2009.
- [18] A. Patcha and J. Park. An Overview of Anomaly Detection Techniques: Existing Solutions and Latest Technological Trends. *Computer Networks*, 51(12):3448–3470, 2007.
- [19] Shreekant Gayaka and Bin Yao. Fault detection, identification and accommodation for an electro-hydraulic system: An adaptive robust approach. In *Proceedings of the 17th IFAC World Congress*, pages 13815–13820, 2008.
- [20] A Alaghi, N. Karimi, M. Sedghi, and Z. Navabi. Online NoC Switch Fault Detection and Diagnosis Using a High Level Fault Model. In *22nd IEEE International Symposium on Defect and Fault-Tolerance in VLSI Systems, DFT '07.*, pages 21–29, September 2007.
- [21] Luiz Fernando Gonçalves, Jefferson Luiz Bosa, Tiago Roberto Balen, Marcelo Soares Lubaszewski, Eduardo Luis Schneider, and Renato Ventura Henriques. Fault detection, diagnosis and prediction in electrical valves using self-organizing maps. *Journal of Electronic Testing: Theory and Applications*, 27(4):551–564, August 2011.
- [22] Seokin Hong and Soontae Kim. Lizard: Energy-efficient hard fault detection, diagnosis and isolation in the ALU. In *IEEE International Conference on Computer Design (ICCD)*, pages 342–349, October 2010.
- [23] Xiang Yu and Jin Jiang. Hybrid Fault-Tolerant Flight Control System Design Against Partial Actuator Failures. *IEEE Transactions on Control Systems Technology*, 20(4):871–886, July 2012.

- [24] Chen-Fu Chien, Chia-Yu Hsu, and Pei-Nong Chen. Semiconductor fault detection and classification for yield enhancement and manufacturing intelligence. *Flexible Services and Manufacturing Journal*, 25(3):367–388, 2013.
- [25] Sang-Jo Youk, Seung-Sun Yoo, Chang-Yong Lee, Jeong-Ho Kho, and Geuk Lee. Development of Fault Detection System in Air Handling Unit. In *International Conference on Convergence and Hybrid Information Technology*, pages 287–292, August 2008.
- [26] Z. Gao, C. Cecati, and S. X. Ding. A Survey of Fault Diagnosis and Fault-Tolerant Techniques 2014;Part I: Fault Diagnosis With Model-Based and Signal-Based Approaches. *IEEE Transactions on Industrial Electronics*, 62(6):3757–3767, June 2015.
- [27] N. Kanagawa and S. Takai. Verification and synthesis for failure diagnosis of discrete event systems subject to permanent sensor failures. In *Proceedings of the 2014 IEEE Emerging Technology and Factory Automation (ETFA)*, pages 1–8, September 2014.
- [28] Stephane Lafortune. Diagnosis of Discrete Event Systems. In *Encyclopedia of Systems and Control*, pages 1–10. Springer London, 2014.
- [29] J. Zaytoon and S. Lafortune. Overview of fault diagnosis methods for Discrete Event Systems. *Annual Reviews in Control*, 37(2):308–320, December 2013.
- [30] C. Mahulea, C. Seatzu, M.P. Cabasino, and M. Silva. Fault Diagnosis of Discrete-Event Systems Using Continuous Petri Nets. *IEEE Transactions on Systems, Man and Cybernetics, Part A: Systems and Humans*, 42(4):970–984, July 2012.
- [31] M.P. Fanti, AM. Mangini, and W. Ukovich. Fault Detection by Labeled Petri Nets in Centralized and Distributed Approaches. *IEEE Transactions on Automation Science and Engineering*, 10(2):392–404, April 2013.
- [32] D. Lefebvre. On-Line Fault Diagnosis With Partially Observed Petri Nets. *IEEE Transactions on Automatic Control*, 59(7):1919–1924, July 2014.
- [33] Baisi Liu, Mohamed Ghazel, and Armand Toguyéni. Diagnosis of Labeled Time Petri Nets Using Time Interval Splitting. *IFAC Proceedings Volumes*, 47(3):1784–1789, 2014.
- [34] Ming Chang, Wei Dong, Yindong Ji, and Lang Tong. On Fault Predictability in Stochastic Discrete Event Systems. *Asian Journal of Control*, 15(5):1458–1467, 2013.
- [35] J. Chen and R. Kumar. Failure Detection Framework for Stochastic Discrete Event Systems With Guaranteed Error Bounds. *IEEE Transactions on Automatic Control*, 60(6):1542–1553, June 2015.

- [36] R.H. Kwong and D.L. Yonge-Mallo. Fault Diagnosis in Discrete-Event Systems: Incomplete Models and Learning. *IEEE Transactions on Systems, Man, and Cybernetics Part B: Cybernetics*, 41(1):118–130, February 2011.
- [37] Jonathan S. Ostroff and W. Murry Wonham. A Framework for Real-time Discrete Event Control. *IEEE Transactions on Automatic Control*, 35(4):386–397, April 1990.
- [38] Jonathan S. Ostroff. Deciding Properties of Timed Transition Models. *IEEE Transactions on Parallel and Distributed Systems*, 1(2):170–183, April 1990.
- [39] Prodip Bhowal, Dipankar Sarkar, Siddhartha Mukhopadhyay, and Anupam Basu. Fault Diagnosis in Discrete Time Hybrid Systems - A Case Study. *Information Sciences*, 177(5):1290–1308, March 2007.
- [40] Abdellah Benzaouia, Mustapha Ouladsine, and Bouchra Ananou. Fault tolerant control for switching discrete-time systems with delays: An improved cone complementarity approach. *International Journal of Systems Science*, 45(10):2116–2126, 2014.
- [41] Neminath Hubballi, Santosh Biswas, S. Roopa, Ritesh Ratti, and Sukumar Nandi. LAN attack detection using Discrete Event Systems. *ISA Transactions*, 50(1):119–130, 2011.
- [42] FA Barbhuiya, Mayank Agarwal, Sanketh Purwar, Santosh Biswas, and Sukumar Nandi. Application of stochastic discrete event system framework for detection of induced low rate TCP attack. *ISA transactions*, 58:474–492, 2015.
- [43] Pradip K. Dubey and Jitesh Narayan Verma. Method And Apparatus For Detecting a Rogue Access Point in a Communication Network. <http://www.google.com/patents/US20120124665>, 2012.
- [44] Tired of Rogues: Solutions for Detecting and Eliminating Rogue Wireless Network, Air Defense Whitepaper. http://wirelessnetworks-asia.motorola.com/products/images/air_defense/downloads/White_Paper/Solutions_Detecting_Eliminating_Rogue.pdf, 2008.
- [45] AirWave Wireless Management Suite, Whitepaper, Aruba. <http://moonblinkwifi.com/files/airwave-solution-guide.pdf>, 2006.
- [46] A. Kumar and P. Paul. Security analysis and implementation of a simple method for prevention and detection against Evil Twin attack in IEEE 802.11 wireless LAN. In *2016 International Conference on Computational Techniques in Information and Communication Technologies (ICCTICT)*, pages 176–181, March 2016.

- [47] R. Beyah, S. Kangude, G. Yu, B. Strickland, and J. Copeland. Rogue access point detection using temporal traffic characteristics. In *IEEE Global Telecommunications Conference, GLOBECOM '04.*, volume 4, pages 2271–2275, November 2004.
- [48] P. Chumchu, T. Saelim, and C. Sriklauy. A new MAC address spoofing detection algorithm using PLCP header. In *International Conference on Information Networking (ICOIN)*, pages 48–53, January 2011.
- [49] Hao Han, Bo Sheng, C.C. Tan, Qun Li, and Sanglu Lu. A Timing-Based Scheme for Rogue AP Detection. *IEEE Transactions on Parallel and Distributed Systems*, 22(11):1912–1925, November 2011.
- [50] Chad D. Mano, Andrew Blaich, Qi Liao, Yingxin Jiang, David A. Cieslak, David C. Salyers, and Aaron Striegel. RIPPS: Rogue Identifying Packet Payload Slicer Detecting Unauthorized Wireless Hosts Through Network Traffic Conditioning. *ACM Transactions on Information Systems Security*, 11(2):2:1–2:23, May 2008.
- [51] Yimin Song, Chao Yang, and Guofei Gu. Who is peeping at your passwords at Starbucks?; To catch an evil twin access point. In *IEEE/IFIP International Conference on Dependable Systems and Networks (DSN)*, pages 323–332, July 2010.
- [52] Kuo-Fong Kao, Tau-Heng Yeo, Wai-Shuen Yong, and Hui-Hsuan Chen. A location-aware rogue AP detection system based on wireless packet sniffing of sensor APs. In *Proceedings of the 2011 ACM Symposium on Applied Computing, SAC '11*, pages 32–36, New York, USA, 2011. ACM.
- [53] Suman Jana and Sneha K. Kasera. On Fast and Accurate Detection of Unauthorized Wireless Access Points Using Clock Skews. *IEEE Transactions on Mobile Computing*, 9(3):449–462, March 2010.
- [54] Bhagyavati, Wayne C. Summers, and Anthony DeJoie. Wireless security techniques: An overview. In *Proceedings of the 1st Annual Conference on Information Security Curriculum Development, InfoSecCD '04*, pages 82–87, New York, USA, 2004.
- [55] Prakash Iyer, Victor Lortz, Lee Tapper, Roger Chandler, and Roxanne Gryder. Public WLAN Hotspot Deployment and Interworking. *Intel Technology Journal*, 7(3), 2003.
- [56] Ajah Ifeyinwa Angela. Evaluation of Enhanced Security Solutions in 802.11-Based Networks. *International Journal of Network Security & Its Applications*, 6(4):1–14, 2014.

- [57] Avinash Srinivasan and Lashidhar Chennupati. Robust Authentication of Public Access Points Using Digital Certificates—A Novel Approach. In *Cyberspace Safety and Security*, pages 153–164. Springer, 2012.
- [58] Kemal Bicakci and Bulent Tavli. Denial-of-Service attacks and countermeasures in IEEE 802.11 wireless networks. *Computer Standard and Interfaces*, 31(5):931–941, September 2009.
- [59] Dr Mirzoev, Stacey White, et al. The Role of Client Isolation in Protecting Wi-Fi Users from ARP Spoofing Attacks. *arXiv preprint arXiv:1404.2172*, 2014.
- [60] Sean Whalen. An Introduction to ARP Spoofing. http://rootsecure.net/content/downloads/pdf/arp_spoofing_intro.pdf, April 2001.
- [61] Md Sohail Ahmad. WPA TOO! *DEFCON*, 18:1–32, July 2010.
- [62] Survey: Insider attacks cause more damage than outside assault. <http://www.covertix.com/survey-insider-attacks-cause-more-damage-than-outside-assault/>, 2013.
- [63] Interesting Insider Threat Statistics. <http://www.cert.org/blogs/insider-threat/post.cfm?EntryID=60>.
- [64] Data Leakage Worldwide White Paper: The High Cost of Insider Threats . http://www.cisco.com/c/en/us/solutions/collateral/enterprise-networks/data-loss-prevention/white_paper_c11-506224.html.
- [65] Breaches Down, Insider Attacks Up, Verizon Business/Secret Service Study Says. <http://www.darkreading.com/attacks-breaches/breaches-down-insider-attacks-up-verizon-business-secret-service-study-says/d/d-id/1134067>.
- [66] Charles M Kozierok. *The TCP/IP guide: A comprehensive, illustrated Internet protocols reference*. No Starch Press, 2005.
- [67] Cisco Systems. Cisco Nexus 7000 Series NX-OS Security Configuration Guide, Release 4.1 Configuring Port Security. http://www.cisco.com/en/US/docs/switches/datacenter/sw/4_1/nx-os/security/configuration/guide/sec_portsec.pdf.
- [68] Arpwatch. <http://www.arpalert.org>.
- [69] Colasoft-Capsa. <http://www.colasoft.com>.

- [70] Mohamed G. Gouda and Chin-Tser Huang. A secure Address Resolution Protocol. *Computer Networks*, 41(1):57–71, 2003.
- [71] Wesam Lootah, William Enck, and Patrick McDaniel. TARP: Ticket-based Address Resolution Protocol. In *Annual Computer Security Applications Conference*, pages 106–116, 2005.
- [72] Meera Sampath, Raja Sengupta, Stephane Lafortune, Kasim Sinnamohideen, and Demosthenis C. Teneketzis. Diagnosability of Discrete-Event Systems. *IEEE Transactions on Automatic Control*, 40(9):1555–1575, September 1995.
- [73] John Bellardo and Stefan Savage. 802.11 Denial-of-Service Attacks: Real Vulnerabilities and Practical Solutions. In *Proceedings of the USENIX Security Symposium*, pages 15–28, August 2003.
- [74] Zaffar I. Qureshi, Baber Aslam, Athar Mohsin, and Yonus Javed. A solution to spoofed PS-Poll based Denial of Service attacks in IEEE 802.11 WLANs. In *Proceedings of the 11th WSEAS International Conference on Communications*, volume 11, pages 7–11, 2007.
- [75] Leandro Meiners. But...my station is awake! (Power Save Denial of Service in 802.11 Networks). http://corelabs.coresecurity.com/index.php?module=Wiki&action=view&type=publication&name=Wifi_Power_Save_DoS, September 2009.
- [76] Wenjun Gu, Zhimin Yang, Dong Xuan, Weijia Jia, and Can Que. Null Data Frame: A Double-Edged Sword in IEEE 802.11 WLANs. *IEEE Transactions on Parallel and Distributed Systems*, 21(7):897–910, 2010.
- [77] Daniel B. Faria and David R. Cheriton. Detecting identity-based attacks in wireless networks using signalprints. In *Proceedings of the 5th ACM workshop on Wireless security*, WiSe '06, pages 43–52, September 2006.
- [78] Babak Azimi-Sadjadi, Aggelos Kiayias, Alejandra Mercado, and Bulent Yener. Robust key generation from signal envelopes in wireless networks. In *Proceedings of the 14th ACM conference on Computer and Communications Security*, CCS '07, pages 401–410, 2007.
- [79] Yingying Chen, W. Trappe, and R.P. Martin. Detecting and Localizing Wireless Spoofing Attacks. In *Proceedings of the 4th Annual IEEE Conference on Sensor, Mesh and Ad Hoc Communications and Networks*, pages 193–202, 2007.

- [80] Santosh Biswas, Dipankar Sarkar, Prodip Bhowal, and Siddhartha Mukhopadhyay. Diagnosis of delay-deadline failures in real time Discrete Event Models. *ISA Transactions*, 46(4):569–582, 2007.
- [81] Cisco. DHCP Snooping. <http://www.cisco.com/c/en/us/td/docs/switches/lan/catalyst6500/ios/12-2SX/configuration/guide/book/snooDHCP.html>.
- [82] R. Spacil, J. Ikonen, and J. Porras. Forcing usage rules in public wireless LANs. In *Proceedings of 27th Annual IEEE Conference on Local Computer Networks*, pages 415–420. IEEE, 2002.
- [83] R. Droms. RFC 3118 - Dynamic Host Configuration Protocol. <https://tools.ietf.org/html/rfc3118>, June 2001.
- [84] R. Droms. RFC 2131 - Dynamic Host Configuration Protocol. <https://tools.ietf.org/html/rfc2131>, March 1997.
- [85] Dumitru Daniel Dinu and Mihai Togan. DHCP server authentication using digital certificates. In *10th International Conference on Communications (COMM)*, pages 1–6. IEEE, 2014.
- [86] Y. Xu, S. Manning, and M. Wong. An Authentication Method based on Certificate for DHCP. Technical report, DHC Internet Draft, September 2011.
- [87] Glenn Glazer, Cora Hussey, and Roy Shea. Certificate-Based Authentication for DHCP, 2003.
- [88] Jacques Demerjian and Ahmed Serhrouchni. DHCP authentication using certificates. In *Security and Protection in Information Processing Systems*, pages 457–472. Springer, 2004.
- [89] Kathryn De Graaf, John Liddy, Paul Raison, John C Scano, and Sanjay Wadhwa. Dynamic host configuration protocol (DHCP) authentication using challenge handshake authentication protocol (CHAP) challenge, October 2013. US Patent 8,555,347.
- [90] Ken Hornstein, Ted Lemon, Bernard Adoba, and Jonathan Trostle. DHCP Authentication Via Kerberos V. <https://tools.ietf.org/html/draft-hornstein-dhc-kerbauth-01>, October 2001.
- [91] J. Somers and Y. Kudo. System and method for protecting devices on dynamically configured network, December 2014. US Patent 8,910,282.

- [92] Pedro Garcia-Teodoro, J Diaz-Verdejo, Gabriel Maciá-Fernández, and Enrique Vázquez. Anomaly-based network intrusion detection: Techniques, systems and challenges. *Computers & Security*, 28(1):18–28, February 2009.
- [93] IEEE. Standard for Information technology-Telecommunications and information exchange between systems-Local and metropolitan area networks-Specific requirements - Part 11: Wireless LAN Medium Access Control (MAC) and Physical Layer (PHY) Specifications. *IEEE Std 802.11-2007 (Revision of IEEE Std 802.11-1999)*, pages C1–1184, December 2007.
- [94] Wei Wei, Kyoungwon Suh, Bing Wang, Yu Gu, J. Kurose, D. Towsley, and S. Jaiswal. Passive Online Detection of 802.11 Traffic Using Sequential Hypothesis Testing with TCP ACK-Pairs. *IEEE Transactions on Mobile Computing*, 8(3):398–412, March 2009.
- [95] K. Sui, Y. Zhao, D. Pei, and L. Zimu. How bad are the rogues' impact on enterprise 802.11 network performance? In *2015 IEEE Conference on Computer Communications (INFOCOM)*, pages 361–369, April 2015.
- [96] Min-Woo Park, Young-Hyun Choi, Jung-Ho Eom, and Tai-Myoung Chung. Dangerous Wi-Fi access point: Attacks to benign smartphone applications. *Personal and Ubiquitous Computing*, 18(6):1373–1386, 2014.
- [97] Liran Ma, Amin Y. Teymorian, Xiuzhen Cheng, and Min Song. RAP: Protecting commodity Wi-Fi networks from rogue access points. In *The Fourth International Conference on Heterogeneous Networking for Quality, Reliability, Security and Robustness Workshops, QSHINE '07*, pages 21:1–21:7, New York, USA, 2007. ACM.
- [98] Asaf Tzur, Ofer Amrani, and Avishai Wool. Direction Finding of rogue Wi-Fi access points using an off-the-shelf MIMO-OFDM receiver. *Physical Communication*, 17:149–164, 2015.
- [99] N. M. Ahmad, A. H. M. Amin, S. Kannan, M. F. Abdollah, and R. Yusof. A RSSI-based rogue access point detection framework for Wi-Fi hotspots. In *IEEE 2nd International Symposium on Telecommunication Technologies (ISTT)*, pages 104–109, November 2014.
- [100] Fu-Hau Hsu, Chuan-Sheng Wang, Yu-Liang Hsu, Yung-Pin Cheng, and Yu-Hsiang Hsneh. A client-side detection mechanism for evil twins. *Computers & Electrical Engineering*, pages 1–10, 2015.
- [101] Yu Hsiang Hsneh, Fu Hau Hsu, Shih Jen Chen, Yao Hsin Chen, Yan Ling Hwang, Chuan Sheng Wang, and Yu Liang Hsu. ET Detector: A Client-Based Solution to

- Detect an Evil Twin Access Point. In *Applied Mechanics and Materials*, volume 764, pages 900–904. Trans Tech Publ, 2015.
- [102] H. Mustafa and W. Xu. CETAD: Detecting evil twin access point attacks in wireless hotspots. In *IEEE Conference on Communications and Network Security (CNS)*, pages 238–246, October 2014.
- [103] Fabian Lanze, Andriy Panchenko, Ignacio Ponce-Alcaide, and Thomas Engel. Hacker’s toolbox: Detecting software-based 802.11 evil twin access points. In *12th Annual IEEE Consumer Communications and Networking Conference (CCNC)*, pages 225–232, 2015.
- [104] SungBae Kang, DaeHun Nyang, and KyungHee Lee. Evil-Twin Detection Scheme Using SVM with Multi-Factors. *The Journal of Korean Institute of Communications and Information Sciences*, 40(2):334–348, 2015.
- [105] Mayank Agarwal, Dileep Pasumarthi, Santosh Biswas, and Sukumar Nandi. Machine learning approach for detection of flooding DoS attacks in 802.11 networks and attacker localization. *International Journal of Machine Learning and Cybernetics*, pages 1–17, 2014.
- [106] Best Practices for Securing Your Wireless LAN - NLE, Whitepaper, AirMagnet, 2004. http://www.nle.com/literature/Airmagnet_WLAN_Security_Best_Practices.pdf.
- [107] R. Whelan, L. Van Wagenen, and R. Morris. System and method for detecting unauthorized wireless access points, July 2014. US Patent 8,787,576.
- [108] V.S.S. Sriram, G. Sahoo, and K.K. Agrawal. Detecting and eliminating Rogue Access Points in IEEE-802.11 WLAN - A multi-agent sourcing Methodology. In *IEEE 2nd International Conference on Advanced Computing (ICAA)*, pages 256–260, February 2010.
- [109] Mohan K Chirumamilla. Agent based Intrusion Detection and Response system for Wireless LANs. In *Proceedings of IEEE International Conference on Communications*, pages 492–496, 2003.
- [110] R. Shrestha and S. Y. Nam. Access point selection mechanism to circumvent rogue access points using voting-based query procedure. *IET Communications*, 8(16):2943–2951, 2014.

- [111] Paramvir Bahl, Ranveer Chandra, Jitendra Padhye, Lenin Ravindranath, Manpreet Singh, Alec Wolman, and Brian Zill. Enhancing the security of corporate Wi-Fi networks using DAIR. In *Proceedings of the 4th International Conference on Mobile Systems, Applications and Services, MobiSys '06*, pages 1–14, 2006.
- [112] Iluk Kim, Jungtaek Seo, Taeshik Shon, and Jongsub Moon. A novel approach to detection of mobile rogue access points. *Security and Communication Networks*, 7(10):1510–1516, 2014.
- [113] A. Aggarwal, E.T.L. Hardie, S.M. Das, R. Gupta, and A.F. Naguib. Detection of falsified wireless access points, June 2014. US Patent 8,750,267.
- [114] Fabian Lanze, Andriy Panchenko, Ignacio Ponce-Alcaide, and Thomas Engel. Undesired Relatives: Protection Mechanisms Against the Evil Twin Attack in IEEE 802.11. In *Proceedings of the 10th ACM Symposium on QoS and Security for Wireless and Mobile Networks*, pages 87–94, New York, USA, 2014.
- [115] Diogo Mónica and Carlos Ribeiro. WiFiHop - Mitigating the Evil twin attack through multi-hop detection. In *Proceedings of the 16th European Conference on Research in Computer Security, ESORICS'11*, pages 21–39, 2011.
- [116] Neha Agrawal and Shashikala Tapaswi. Wireless Rogue Access Point Detection Using Shadow Honeynet. *Wireless Personal Communications*, 83(1):551–570, 2015.
- [117] James Yu. Applying TCP Profiling to Detect Wireless Rogue Access Point. In *Proceedings of the International Conference on Wireless Networks (ICWN)*, pages 1–7. The Steering Committee of The World Congress in Computer Science, Computer Engineering and Applied Computing (WorldComp), 2014.
- [118] Tadayoshi Kohno, Andre Broido, and KC Claffy. Remote Physical Device Fingerprinting. In *Proceedings of the 2005 IEEE Symposium on Security and Privacy, SP '05*, pages 211–225, 2005.
- [119] Fabian Lanze, Andriy Panchenko, Benjamin Braatz, and Thomas Engel. Letting the puss in boots sweat: Detecting fake access points using dependency of clock skews on temperature. In *Proceedings of the 9th ACM symposium on Information, computer and communications security*, pages 3–14. ACM, 2014.
- [120] Sergey Bratus, Chrisil Arackaparambil, Anna Shubina, and Dartmouth College. Detection of Rogue APs Using Clock Skews: Does it Really Work? http://www.cs.dartmouth.edu/~cja/papers/toorcon11_ver6a.pdf, 2009.

- [121] B. Alotaibi and K. Elleithy. An empirical fingerprint framework to detect Rogue Access Points. In *Systems, Applications and Technology Conference (LISAT), 2015 IEEE Long Island*, pages 1–7, May 2015.
- [122] K. F. Kao, W. C. Chen, J. C. Chang, and H. T. Chu. An Accurate Fake Access Point Detection Method Based on Deviation of Beacon Time Interval. In *IEEE Eighth International Conference on Software Security and Reliability-Companion (SERE-C)*, pages 1–2, June 2014.
- [123] Kangsuk Chae, Jiawei Shao, Souhwan Jung, Changmoon Han, Seongsoo Bae, and Injang Jeong. A Scheme of Detection and Prevention Rogue AP using Comparison Security Condition of AP. *UACEE International Journal of Advances in Computer Networks and Its Security*, 2012.
- [124] Meera Sampath, Raja Sengupta, Stephane Lafortune, Kasim Sinnamohideen, and Demosthenis C. Teneketzis. Failure Diagnosis Using Discrete-Event Models. *IEEE Transactions on Control Systems Technology*, 4(2):105–124, 1996.
- [125] Christos G. Cassandras and Stephane Lafortune. *Introduction to Discrete Event Systems*. Springer-Verlag New York, Inc., Secaucus, NJ, USA, 2006.
- [126] K. Renganathan and VidhyaCharan Bhaskar. An observer based approach for achieving fault diagnosis and fault tolerant control of systems modeled as hybrid Petri nets. *ISA Transactions*, 50(3):443–453, 2011.
- [127] V. Kumar, S. Chakraborty, F.A. Barbhuiya, and S. Nandi. Detection of Stealth Man-in-the-Middle attack in Wireless LAN. In *2nd IEEE International Conference on Parallel Distributed and Grid Computing*, pages 290–295, December 2012.
- [128] S. Hashtrudi Zad, Raymond H. Kwong, and W. M. Wonham. Fault Diagnosis in Discrete-Event Systems: Framework and Model Reduction. *IEEE Transactions on Automatic Control*, 48(7):1199–1212, July 2003.
- [129] Santosh Biswas, Dipankar Sarkar, Siddhartha Mukhopadhyay, and Amit Patra. Fairness of Transitions in Diagnosability of Discrete Event Systems. *Discrete Event Dynamic Systems*, 20(3):349–376, September 2010.
- [130] S. Bavishi and E. Chong. Automated fault diagnosis using a discrete event systems framework. *IEEE International Symposium Intelligent Control*, pages 213–218, 1994.
- [131] G. Provan and Y.L. Chan. Model based diagnosis and control reconfiguration for Discrete Event Systems: An Integrated approach. In *38th IEEE Conference on CDC*, pages 1762–1768, Phoenix, 1998.

- [132] Understanding Wireless Isolation. <http://www.wirelessisolation.com>.
- [133] Security Watch A guide to Wireless Security. <https://technet.microsoft.com/en-us/magazine/958125c2-036f-4420-afc4-65dce49a83f1>.
- [134] DecaffeinatID: A Very Simple IDS / Log Watching App / ARPWatch For Windows. <http://www.irongeek.com/i.php?page=security/decaffeinatid-simple-ids-arpwatch-for-windows>.
- [135] Seung Yeob Nam, Sirojiddin Djuraev, and Minho Park. Collaborative approach to mitigating ARP poisoning-based Man-in-the-Middle attacks. *Computer Networks*, 57(18):3866–3884, 2013.
- [136] S.P. Abraham, G. Cherian, and J. Malinen. Systems and methods for broadcast WLAN messages with message authentication, November 2014.
- [137] Linux WPA/WPA2/IEEE 802.1X Supplicant. http://hostap.epitest.fi/wpa_supplicant/.
- [138] N.S. Dade and S.K. Lundsgaard. Detection of unauthorized changes to an address resolution protocol cache in a communication network, June 2012.
- [139] MadWifi. <http://madwifi-project.org/>.
- [140] R. Bansal, S. Tiwari, and D. Bansal. Non-cryptographic methods of MAC spoof detection in wireless LAN. In *16th IEEE International Conference on Networks*, pages 1–6, December 2008.
- [141] CWNP | Wireless LAN Security and IEEE 802.11w. http://www.cwnp.com/cwnp_wifi_blog/wireless-lan-security-and-ieee-802-11w/.
- [142] Joshua Wright. How 802.11w will improve wireless security. <http://www.networkworld.com/article/2312251/network-security/how-802-11w-will-improve-wireless-security.html>, May 2006.
- [143] R. Sekar, M. Bendre, D. Dhurjati, and P. Bollineni. A Fast Automaton-Based Method for Detecting Anomalous Program Behaviors. In *Proceedings of the 2001 IEEE Symposium on Security and Privacy*, SP '01, pages 144–155, 2001.
- [144] S.-J. Whittaker, M. Zulkernine, and K. Rudie. Towards Incorporating Discrete-Event Systems in Secure Software Development. In *Third International Conference on Availability, Reliability and Security, 2008. ARES 08.*, pages 1188–1195, March 2008.

- [145] H. Noura, D. Theilliol, and J.C. Ponsart A. Chamseddine. Application to a Three-tank System. *Fault-tolerant Control Systems*, pages 109–156, 2009.
- [146] BackTrack. <http://www.backtrack-linux.org/>.
- [147] Detecting Rogue DHCP Servers. <https://www.plixer.com/blog/detect-network-threats/detecting-rogue-dhcp-servers/>.
- [148] Osama S Younes. A Secure DHCP Protocol to Mitigate LAN Attacks. *Journal of Computer and Communications*, 4(1):39–50, 2016.
- [149] Mattias Krysander and Erik Frisk. Sensor placement for fault diagnosis. *IEEE Transactions on Systems, Man and Cybernetics, Part A: Systems and Humans*, 38(6):1398–1410, 2008.
- [150] H. Gao, T. Chen, and L. Wang. Robust fault detection with missing measurements. *International Journal of Control*, 81(5):804–819, 2008.
- [151] Xiao Lu, Linglong Wang, Haixia Wang, and Xianghua Wang. Kalman filtering for delayed singular systems with multiplicative noise. *IEEE/CAA Journal of Automatica Sinica*, 3(1):51–58, 2016.
- [152] Fanhua Shang, Yuanyuan Liu, James Cheng, and Hong Cheng. Robust Principal Component Analysis with Missing Data. In *Proceedings of the 23rd ACM International Conference on Conference on Information and Knowledge Management, CIKM '14*, pages 1149–1158, New York, USA, 2014. ACM.
- [153] Imtiaz S.A., S.L. Shah, and S. Narasimhan. Missing Data Treatment using Iterative PCA and Data Reconciliation. In *7th International Conference on Dynamics and Control of Process Systems*, 2004.
- [154] D. Daniel Dinu and M. Togan. DHCPAuth 2014; A DHCP message authentication module. In *IEEE 10th Jubilee International Symposium on Applied Computational Intelligence and Informatics (SACI)*, pages 405–410, May 2015.
- [155] James Weimer, Seyed Alireza Ahmadi, José Araujo, Francesca Madia Mele, Dario Papale, Iman Shames, Henrik Sandberg, and Karl Henrik Johansson. Active actuator fault detection and diagnostics in HVAC systems. In *Proceedings of the Fourth ACM Workshop on Embedded Sensing Systems for Energy-Efficiency in Buildings*, pages 107–114. ACM, 2012.



Vitae



Mayank Agarwal was born in Nasik, Maharashtra, India on 26th May, 1987. He completed his schooling from Vidya Vikasini English High School, Vasai Road in the year 2003. He did his Bachelor of Engineering (B.E.) degree from the Department of Information Technology at Sardar Patel Institute of Technology, Mumbai University, India in the year 2009. Following that, he joined as an assistant professor in the same department for a period of 18 months. He joined the Ph.D program at the Department of Computer Science and Engineering, Indian Institute of Technology Guwahati in the December 2010. Dr. Santosh Biswas and Prof. Sukumar Nandi were his PhD supervisors. He has received TCS Research Fellowship from TATA Consultancy Services, India for pursuing his PhD programme. His research interests include network and wireless security, network security and discrete event system modeling. He also has a Youtube channel - EasyVideoSeries (<https://youtube.com/EasyVideoSeries>) where he has more than 500 videos on Windows, Linux and Microsoft Office. He has mentored many inhouse projects at IITGuwahati which have been deployed for the benefit of the campus community.

Contact Information

Email : mayank.agl@iitg.ernet.in, mayank265@gmail.com

Web : <http://iitg.ernet.in/stud/mayank.agl/>
: <https://youtube.com/EasyVideoSeries/>

Address : Mayank Agarwal,
C/o Mr. Ajay Agarwal, 10 Shirish Apartment,
Jaitala Road, Nagpur 440022. Maharashtra, India

